UNIVERSITÉ DE NEUCHÂTEL

Plant Survival Graduate School
PhD Thesis

The Role of Palmitoylation in the Secretory Pathway of Plants

Ph.D. student: Stigliano Egidio

Supervisor: Professor Jean-Marc Neuhaus

UNIVERSITÉ DE NEUCHÂTEL

Faculté des sciences
Secrétariat-décanat de Faculté
Rue Emile-Argand 11
2000 Neuchâtel - Suisse
Tél: + 41 (0)32 718 2100
E-mail: secretariat.sciences@unine.ch

IMPRIMATUR POUR THESE DE DOCTORAT

La Faculté des sciences de l'Université de Neuchâtel autorise l'impression de la présente thèse soutenue par

Monsieur Egidio STIGLIANO

Titre:

"The role of palmitoylation in the secretory pathway of plants"

sur le rapport des membres du jury composé comme suit:

- Prof. Jean-Marc Neuhaus, Université de Neuchâtel, directeur de thèse
- Dr Giselbert Hinz, Université de Heidelberg, D
- Dr Guillaume Gouzerh, Université de Neuchâtel
- Dr Matthias Erb, Max Planck Institute, Iena, D

Neuchâtel, le 18 novembre 2014

Le Doyen, Prof. B. Colbois

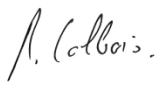

Acknowledgments

During these 4 years I was able to substantially increase my skills. But this long trip was primarily a human journey where I met people from all over the world. Languages and cultures that have changed me for the better ... I hope!

There are many people who would like to thank. Firstly I would like to thank Prof. Jean-Marc Neuhaus that gave me the chance to do Ph.D. in his laboratory.

Here I met two fantastic fellow travellers: Sanaa and Alessandro, with whom a fruitful collaboration and clear friendship was born.

A Special thanks to Guillaume and Sophie that through their wise counsel have made less arduous the path of the doctorate.

A warm thanks to Dr. Marc Creus with whom I shared office and apartment for a year. He is a person always full of advices and encouragements and to whom I will always be infinitely grateful.

Finally, one last thank to Dr. Di Sansebastiano: without him I would never have started this career. Big hugs to all friends of these years: Barbara, Chris, Erica, Giuseppe, Nicola, Giuseppe, Max, Fred, Anne-Flore (la petite Typhenn) ... and all those that I have forgotten in this short page, but I will never forget for the rest of my life.

TABLE OF CONTENTS

Abbreviations

ADP: Adenosine Diphosphate
AP: Adaptin Protein
ARF: ADP Ribosylation Factor
Bip: Binding immunoglobulin protein
BFA: Brefeldin A
BP-80: Binding Protein of 80 kDa
BSA: Biotin Switch Assay
CCV: Clathrin-Coated Vesicle
COPI: Coat Protein I
COPII: Coat Protein II
Ct-VSD: C-terminal Vacuolar Sorting Determinant
DIP: Dark-Induced Protein
DNA: Deoxyribonucleic Acid
DV: Dense Vesicle
EYFP: Enhanced Yellow Fluorescent Protein
ERAD: Endoplasmic Reticulum Associated Degradation
ERES: Endoplasmic Reticulum Export Site
ESCRT: Endosomal Sorting Complex Required for Transport
GDP: Guanosine Diphosphate
GEF: GTP Exchange Factor
GFP: Green Fluorescent Protein
GFP-Chi: Green Fluorescent Protein-chitinase vacuolar sorting determinant
Hsp: Heat Shock Protein
LV: Lytic Vacuole
MVB: Multivesicular Body
PA domain: Protein Associated domain
PAC: Precursor Accumulating Vesicle
Palm: palmitoylation
PM: Plasma Membrane
PSV: Protein Storage Vacuole
psVSD: Protein Structure dependent Vacuolar Sorting Determinant
PVC: Prevacuolar Compartment
Rab: Ras-related in Brain
RING: Really Interesting New Gene
RFP: Red Fluorescent Protein
RMR: Receptor-like Membrane Ring-H2
RNF13: RING Finger Protein 13
SNAP: Soluble NSF Attachment protein RNA: Ribonucleic Acid
SNARE: Soluble N-ethylmaleimide-sensitive Protein Attachment Protein Receptor
SP: Signal Peptide
SRP: Signal Recognition Particle
ssVSD: Sequence-specific Vacuolar Sorting Determinant
2BP: 2-Bromopalmitate
UPR: Unfolded Protein Response
VAMP: Vesicle Associated Membrane Protein
VSD: Vacuolar Sorting Determinant
VSR: Vacuolar Sorting Receptor

Summary

Keywords: RMR1, palmitoylation, Biotin Switch Assay, GFP-Chi, ERV pathway, GFP-Chi aggregation.

This study aimed to study an important eukaryotic post-translational modification, the S-palmitoylation. Until now, there was no study of palmitoylation in plant cell biology. In the first part of this study, we wanted to study the palmitoylation of the vacuolar receptor AtRMR1, as predicted *in silico*. We used a very innovative technique, the Biotin Switch Assay, which does not use radioactive palmitate, is much less time-consuming as it is possible to obtain results after three to four day. Another advantage for cell biology is that it allows the characterization of entire palmitoyl-proteomes. Yeast and neuronal palmitoyl-proteomes have indeed been recently characterized. The study of RMR1's palmitoylation revealed the first palmitoylated plant transmembrane protein. The palmitoylation of a small fraction of RMR1 at a higher molecular weight deserves further discussion.
In the second part of this thesis, I addressed the more general role of palmitoylation in the secretory pathway through the use of a potent palmitoylation inhibitor: 2BP. This study showed a specific action of the drug in TGN/post-TGN compartments. The drug affected the structural maintenance of macrovesicles of secretion. The macrovesicles of secretion have recently been characterized by cryo-fixation and by electron tomography. They are structures reminiscent of a bunch of grapes, where each grape is a secretory vesicle. They are associated with the building with TGN-rich secretory vesicles with a diameter of few tens of nanometers. These vesicles are particularly visible in tissues with a high growth rate, such as pollen tubes. 2BP drastically changed the state of aggregation of macrovesicles of secretion. In an imaged way, each grape was released and a diffuse fluorescence was observed. Palmitoylation is therefore important in the formation or stability of this important secretory structure. A possible extension of this work would be the isolation of palmitoylated proteins involved in this stabilization. In addition, palmitoylated Rabs were detected for the first time in a plant. The three plant Rabs for which I detected the effect of 2BP are located in post-Golgi compartments.

In a last part of the thesis, I decided to investigate the route of secretion of GFP-Chi, a vacuolar marker widely used in the lab that can be followed along the route of secretion. Apparent contradictions have been reported: a vacuolar sorting of this marker by the Golgi-TGN-PVC pathway or an independent-COPII trafficking that can bypass the classic route. Unexpectedly, when GFP-Chi was co-expressed with NtSar1H74L (a dominant-negative mutant blocking the ER-Golgi trafficking by preventing the formation of COPII vesicles), the reporter reached the vacuole. This suggests that the alternative pathway bypassing the Golgi can take place. I also detected the presence of a possible GFP-Chi dimer associated with the membrane fraction upon ultracentrifugation. The nature of this dimer of a soluble protein remains to be investigated although several cases of aggregation of soluble proteins have been reported in the literature (like β-amyloids presents in the of Alzheimer disease). Another matter of great interest is whether the dimer reaches the vacuole or is only transient intermediate during the transport to the vacuole.

1. Introduction

A notable function in all eukaryotic cells is to control the protein trafficking among different intracellular compartments and the plasma membrane. The efficiency of this trafficking is guaranteed by several classes of proteins and compartments, which cooperate among them in order to ensure the correct working of a global and widely conserved process which is named "trafficking".

It will highlight the different roles of proteins involved in cellular traffic with special emphasis on vacuolar trafficking and discuss the role of the ER in protein synthesis and above all the beginning of the route of secretion.

Then, I will continue with a structural description of the Golgi and proteins involved in ensuring the proper sorting to numerous post-Golgi organelles such as the Trans-Golgi Network (TGN), Prevacuolar compartment (PVC), and finally, with special emphasis, to the recycling endosome (RE) (and Rabs proteins involved therein), and vacuole (as one of the final station, with the plasma membrane, in protein and membrane trafficking).

A special mention will be given to describing two classes of vacuolar sorting receptors, RMRs and VSRs. Part of this research work will focus on RMR1 and its palmitoylation. Precise attention will also be given to soluble vacuolar markers and signals needed to address them to the vacuole.

We will then discuss the process of palmitoylation: mechanisms, functions and possible roles in polarized growth as pollen tubes and *Arabidopsis* roots.

Finally we will describe the use of various drugs that have become customary in the domain of the cell biology of plants as brefeldin A, wortmannin, concanamycin A, bafilomycin A, tyrphostins and, for the first time in plant cells, the 2-bromopalmitate (2BP), as a specific inhibitor of palmitoylation. I will highlight the possible use of 2BP as a specific inhibitor of Rab localized in the system for recycling and not others located in other compartment.

1.1 Endoplasmic Reticulum

In animal cells Endoplasmic Reticulum (ER) membranes typically constitute more than half of the total membranes. The ER is organized in a kind of net-like labyrinth of tubules and flattened saccules that spread throughout the cytosol. These tubules and saccules are connected with the nuclear envelope. The ER and the nuclear membrane enclose an internal

space called the ER lumen. The ER has a main role in lipid and protein synthesis and it is also an intracellular Ca^{2+} store, which is used for many intracellular processes such as signal transduction. Finally the ER is also the synthesis site of all transmembrane and soluble proteins for almost all cellular organelles.

As the ER has so many different functions, distinct regions have developed specialized structures. One of the most notable functions resides in rough ER. In fact, most proteins are inserted into the ER membrane before that their synthesis is complete. This process, called co-translation import, is different from the post-translational import of proteins by nuclei, peroxisomes, chloroplasts and mitochondria (Blobel and Dobberstein, 1975).

The rough ER has been named because of the presence of ribosomes coating the membrane and it differs from the smooth ER. Many cells have little smooth ER, but in certain specialized cells it is abundant and has very specific functions such as to synthesize steroids using cholesterol as precursor (Shibata, et al., 2006). Another function of the ER in most eukaryotic cells is to sequester Ca^{2+} from the cytoplasm. The release of Ca^{2+} into the cytosol is a response to many extracellular stimuli. Ca^{2+} is then captured by active pump transporters and stored in the ER lumen by a plethora of Ca^{2+} binding-proteins. Many studies have focused on the role of fatty acids, and more specifically palmitate, in initiating ER stress *in vitro* (Karaskov, et al., 2006; Laybutt, et al., 2007; Cunha, et al., 2008; Eizirik, et al., 2008) and *in vivo* (Laybutt, et al., 2007). For instance, long time treatment with palmitate, but not oleate, causes a morphological stretching of the ER, which could lead, in turn, to a stress response (Karaskov, et al., 2006). Because almost all eukaryotic proteins are synthesized by cytosolic ribosomes, those that have to be transported in other compartments have to pass by the membranes in an unfolded state and then refolded in the membranes of the final compartments. The ER membrane takes care of a single event of membrane insertion.

The ER has unique features among all the compartments of eukaryotic cells: it deals with folding and assembling of not only resident proteins but also proteins destined to other compartments.

Proteins synthesized in the ER are of two types: transmembrane proteins, which are only partially inserted into the ER membrane and water-soluble proteins, which are totally translocated and released into the ER lumen. These proteins, regardless of their final destination, are directed to the ER membrane by an N-terminal signal peptide, which initiates their translocation by a common mechanism. This mechanism uses two main components: a signal-recognition particle (SRP), which cycles between cytosol and ER membrane and

specifically recognizes the signal peptide and a SRP receptor localized in the ER. The N-terminal signal peptide is cleaved by a peptidase co-translationally while the polypeptide is entering into ER lumen (Vitale, et al., 1993). Studies carried out at the end of the 90's using fluorescent tagged proteins have demonstrated that the nascent polypeptide remains in an aqueous environment (Crowley, et al., 1993).

Therefore the current model for protein translocation and insertion into ER membrane includes a multi-protein complex, the translocon pore (Hamman, et al., 1998; Vitale and Denecke, 1999).

The Endoplasmic Reticulum is first station in the secretory pathway. Proteins travel starting from the ER, passing through the Golgi, to be delivered either to the plasma membrane or to the vacuole. This biosynthetic protein movement (or anterograde traffic) is counterbalanced by retrograde traffic. Pathways bypassing the Golgi also exist (Levanony, et al., 1992; Vitale and Raikhel, 1999).

The co-translational removal of the N-terminal signal peptide is essential for the correct folding of the nascent polypeptide. This function is taken by a class of chaperones globally termed signal peptidases (Figure 1-1, (Jackson and Blobel, 1980)).

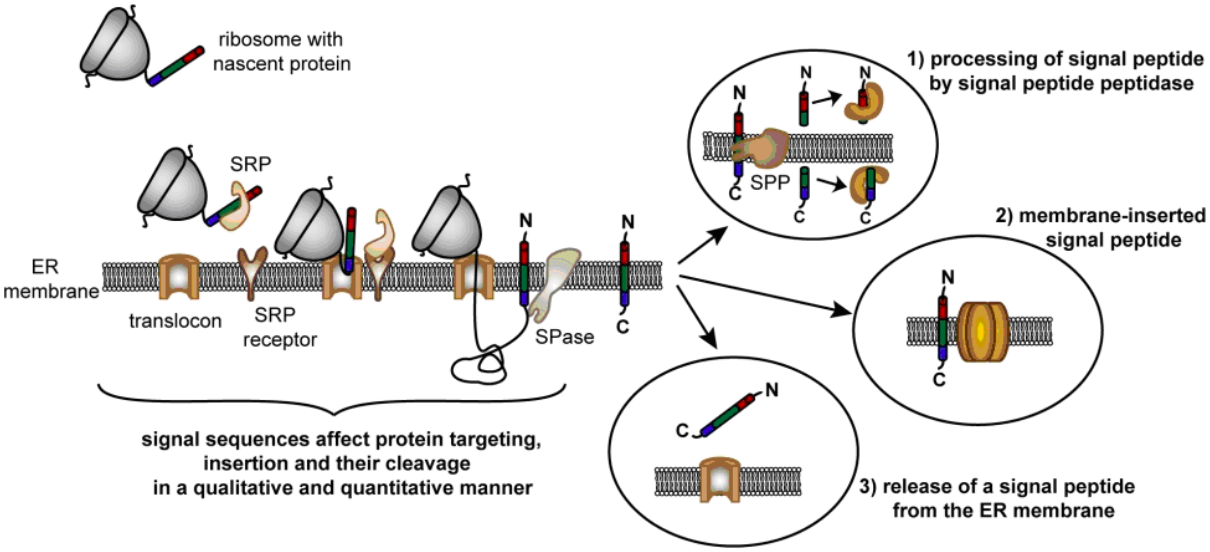

Figure 1-1: How proteins enter into the secretory pathway

N-terminal signal sequences allow targeting of nascent secretory and membrane proteins to the endoplasmic reticulum in a signal recognition particle (SRP)-dependent manner. Signal sequences have a tripartite structure, being composed of a hydrophobic core region (h-region) flanked by an n- and c-region. The latter contains the signal peptidase consensus cleavage site. Normally, signal sequences are cleaved off co-translationally; the resulting cleaved signal sequences are termed signal peptides. Signal sequences are extremely variable, both in their length and in their amino acid composition.

This variability suggests that ER targeting and the steps beyond, i.e. translocation, signal peptidase cleavage etc. are affected by the signal sequence. Secondly, this variability may account for additional functions, i.e. post-targeting functions. Some signal peptides are further processed by an intramembrane cleaving protease called signal peptide peptidase (SPP), and the resulting N-terminal signal peptide fragments are released into the cytosol. Alternatively, signal peptides remain membrane-inserted or are released from the ER membrane (picture taken from http://www.signalpeptide.de/).

1.1.1 HSPs (Heat Shock Proteins)

Loss of native and correct conformation leads to a deficiency of functional proteins but also to another problem for the cells: protein aggregation. In fact, under physiological conditions proteins might aggregate since the very first moment of their synthesis.

The crucial role of guaranteeing the correct folding and assembly has been elucidated in the last three decades with the discovery of molecular chaperones. These proteins are responsible for protein "quality control" (Hurtley and Helenius, 1989).

Chaperones are a large class of unrelated proteins, which take care correctly of non-covalent folding, and/or assembly of proteins, without being stable members of the final structure/s (Ellis, 1997; Liberek, et al., 2008). They are either constitutively expressed or induced under stress conditions, are indispensable for the cells and have been found in all living organisms. Many of these proteins are classified on the basis of their sequence homology and molecular weight (Gething, 1997): HSP (Heat- Shock Protein)110, HSP100, HSP90, HSP70, HSP60, HSP40, HSP10 and small HSP families.

Although these proteins are classified as inducible proteins not all of them are induced upon stress. Interactions with HSPs are responsible for *a*) maintaining chaperone partners in a folding-competent, folded or unfolded structures *b*) compartment localization, trafficking *c*) reducing the risk of protein aggregation and *d*) targeting unfolded or aggregated proteins to degradation compartments (vacuoles or proteasomes) for their removal from the cell.

1.2 Golgi apparatus

Due to its regular structure the Golgi apparatus (GA) was one of the first cell organelles to be discovered by the first light microscopists. Camillo Golgi described it for the first time in 1898, working in nerve cells of cats. It consists of flattened stacks and membrane-enclosed compartments, called *cisternae*. Generally each GA consists of four to six cisternae, but in some unicellular organism they can reach up to 60 cisternae. Each Golgi stack has a *cis* and a *trans*-face. The Golgi apparatus is the major site for the glycan synthesis, and also a site for the maturation and sorting of proteins previously synthesized in the ER. Proteins coming from the ER enter the *cis*-Golgi network (a tubular and cisternal structure) and then leave from the *trans*-Golgi Network (see later in the text for a more complete description), which might be described as a delivering station for vacuoles,

plasma membrane and chloroplasts (Villarejo, et al., 2005; Rose and Lee, 2010). Proteins destined to the Golgi, or beyond, are initially packaged into small COPII-coated vesicles. Membrane proteins are selectively and actively incorporated into these small vesicles (~50 nm). Many of these proteins display ER-exit signals in their cytosolic domain that are recognized by components of COPII complex. These components may also be cargo receptors selecting proteins for the GA, which are then recycled back to the ER. On the contrary, soluble proteins have exit signals that recognize portion of transmembrane proteins (Bannykh, et al., 1998; Lee, et al., 2004).

COPII coats have only four protein components: two internal cargo-receptors SEC23 and SEC23, and two external proteins, forming a dimer, SEC 31 and SEC13 (Stagg, et al., 2006; Stagg, et al., 2007; Stagg, et al., 2008). In Arabidopsis each of these COPII coat proteins has different isoforms: two for SEC13 and SEC31, five for SEC23 and four for SEC24 (Bassham Diane, et al., 2009). An important component of the COPII machinery is Sar1. The role of Sar1 was initially found in yeast as a suppressor of the mutation *sec12-1*, which blocks the trafficking between ER-Golgi (Nakano, et al., 1988; Andreeva, et al., 2000). Unlike other GTPases (Arfs, Rabs), Sar1 has no lipid moiety but it directly interacts with Sec12 for GTP/GDP exchange on Sar1. Sar1-GTP is responsible for the recruitment of all COPII components from the cytosol onto the nascent vesicles. Sec23 is responsible for the GTP hydrolysis, which is followed by the disassembly of the COPII coat before the vesicle fusion with the target membrane. Therefore, mutations in the GTP/GDP exchange domain of Sar1 would be predicted to block vesicles in the ER, while mutations in the GTPase activity domain would prevent the fusion of the vesicles (Oka and Nakano, 1994). *Arabidopsis* possesses three Sar1 isoforms, (Biermann, et al., 1996). Generation of mutants in functional domains of Sar1 were very useful tools to study the trafficking between ER and Golgi. In this study, I used the well-known dominant negative mutant, *Nt*Sar1H74L, with a mutation of the histidine 74, which is important for the coordination of one water molecule in the GTP-binding site. Co-expression of Sar1H74L with ERD2-GFP (a *cis*-Golgi marker), drastically blocks the marker in the ER (Andreeva, et al., 2000). The *At*Sar1H74L also works as a dominant-negative mutant, blocking the vacuolar marker sporamin-GFP in the ER (Takeuchi, et al., 2000).

In contrast to COPII vesicles, COPI vesicles are responsible for the retrograde traffic to the ER and within the Golgi (Lee, et al., 2004).

The COPI coat is composed of two subcomplexes F-COP and B-COP, which together form the coatomer (Stagg, et al., 2007). F-COP has four subunits: β-COP, γ-COP, δ-COP, and ζ-

COP. They interact with specific domains in the cytosolic tail of receptor or cargo proteins.
B-COP is composed of three subunits: α-COP, β'-COP, ε-COP. The latter group of proteins might be considered analogous, at least structurally to the clathrin triskelion (see below) and they are assembled onto the outer surface of the vesicles. Exception for γ-COP and δ-COP, plants encode different isoforms of the COP subunits, suggesting that different COPI vesicles might co-exist in plant cells. A first study (Donohoe, et al., 2007) postulated the presence of two different pools of COPI vesicles, COPI-a (derived from *cis-cisternae*) and COPI-b (derived from *trans-cisternae*), based only on a difference in coat thickness. Although the co-existence of two different pools of COPI vesicles is fascinating more studies are needed to confirm the initial observation.
Another class of vesicles ensures trafficking in post-Golgi compartments: clathrin-coated vesicles.
Clathrin consists of three heavy chains of 192Kda each, bound to three 30Kda light chains. This complex is called triskelion based on its three-legged appearance when observed by negative staining or rotary shadowing (Ungewickell and Branton, 1981; Kirchhausen, et al., 1986; Schmid, 1997). Each molecule of triskelion represents the unit of the coating budding vesicle made of, essentially, pentagon and hexagon. The second major constitutive element are the adaptins (APs), firstly identified because of their ability to favour clathrin assembling in physiological conditions (Keen, 1990). In animals, as in plants, we may identify four AP complexes, AP1, AP2, AP3 and AP4. They are structurally similar, being constituted of two distinct large 100kDa subunits, two medium size subunits (47-50kDa) and one small subunit (17-19kDa).
Clathrin-coated vesicles, in plants, have been mainly localized at the PM and at the cell plate and over-expression of dominant-negative mutant subunits interferes with the recycling of the auxin carriers PIN1 and PIN2 (Dhonukshe, et al., 2007; Hinz, et al., 2007; Richter, et al., 2009).
The Trans-Golgi Network (TGN) represents a necessary step for proteins, destined to the vacuole. For example, CLV3 is principally accumulated in the vacuole rather than in the extracellular space when it is fused to vacuolar sorting signal (VSS, see later in the text) (Rojo, et al., 2002). The VSS of soluble cargo proteins is recognized by specific vacuolar sorting receptors (VSRs or RMRs: see next in the text) and carried to prevacuolar compartment (PVC)/multi vesicular body (MVB) to be released.

1.2.1 Retromer complex

Retrograde traffic from MVB/PVC to TGN also exists and is mediated by the *retromer complex* (Oliviusson, et al., 2006; Collins, 2008; Collins, et al., 2008). In animals and yeasts, the retromer is composed of two complexes: a larger one made of Vps26p, Vps29p and Vps35p and a smaller one made of two members of the sorting nexin family (Seaman, et al., 1998; Haft, et al., 2000; Schellmann and Pimpl, 2009). The larger retromer complex is involved in cargo recognition, as Vps35 interacts with the cytosolic domains of Vps10p, MPR and VSR1 (Nothwehr, et al., 2000; Arighi, et al., 2004; Oliviusson, et al., 2006; Collins, 2008) (Figure 1-3).

Sorting nexins can curve the membrane via their BAR (Bin, amphiphysin, Rvs) domain

In plants the exact composition of the retromer has not been fully understood. *Arabidopsis* genome contains three genes for VPS35, two for VPS26, only one for VPS29 and three for VPS5 (AtSNX1, 2a and 2b) (Vanoosthuyse, et al., 2003; Oliviusson, et al., 2006; Jaillais, et al., 2007). VPS35 and VPS26 (Oliviusson, et al., 2006) have been positively identified in 90nm vesicles. Additionally, in KO mutants for VPS29 or in double KO mutant for VPS35 (*vps35b-1/vps35c-1*), missorting of storage proteins toward apoplast was shown in *Arabidopsis* seeds maybe due to an impairment in recycling of the receptors (Shimada, et al., 2006; Yamazaki, et al., 2008).

Regarding SNX1, it was shown that is required to maintain intracellular level of auxin carrier PIN2, which it is drastically reduced in *snx1* mutant (Kleine-Vehn, et al., 2008). All these findings taken together, support the involvement of plant retromer in processes of endosomal transport (Schellmann and Pimpl, 2009).

VPS35, VPS29 and VPS26 were found at the PVC/ late endosome compartment (LEC) (Oliviusson, et al., 2006), while SNX1 were identified in different endosomal compartments: BFA-induced compartment (Robinson, et al., 2008a), wortmannin-sensitive organelles (PVC/LEC, (Tse, et al., 2004)). SNX1 co-localizes with VPS35 and PI(3)P-sensor FYVE-YFP (a typical PI(3)P binding domain) (Vermeer, et al., 2006; Kleine-Vehn, et al., 2008). SNX2a is associated, by its PX domain, to the TGN and PVC, strongly suggesting that it might cycle between these compartments (Phan, et al., 2008). This model assumes that the interaction between receptor (all these studies were performed using the elective VSR1) and cargo occurs in the TGN. However, a convincing example of an interaction receptor-cargo occurring in the ER was already available in literature: PV72 (a VSR1/BP80 related protein expressed in pumpkin seeds) included in large vesicles budding off from the ER upon having bound the 2S albumin (Hara-Nishimura, et al., 1998).

Supporting the idea that receptor-cargo interaction might occur in the ER, it was convincingly shown that the interaction between aleurain and BP80 occurs in the ER (Niemes, et al., 2010a). At the TGN the interaction is lost and the receptor can recycle back to the ER or to an early Golgi compartment by the retromer complex (Niemes, et al., 2010b). The authors also discuss on previous localization results for GFP-BP80, widely used as PVC marker. In fact its presence at the PVC might reflect an aberrant accumulation of the reporter due to the deletion of whole ligand-binding domain, and is probably destined to the vacuole for degradation. Ultimately the movement of vacuolar cargo, previously released at the TGN, continue to the lytic vacuole in a receptor-independent manner, maybe by maturation of TGN into PVC and finally fusion with the tonoplast. The current model is proposed in Figure1-2.

Furthermore, the plant TGN has been recently described as functional equivalent of the animal early endosomes, as indicated by its rapid labelling of the FM4-64 (Dettmer, et al., 2006).

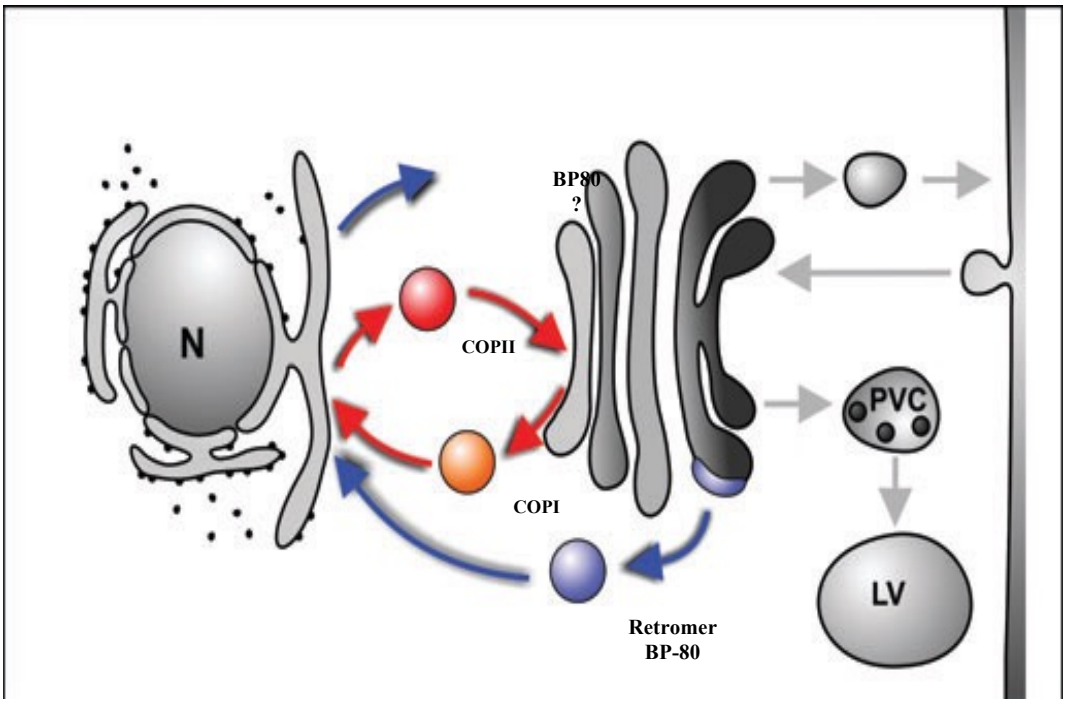

Figure 1-2: Receptor mediated sorting and recycling in plants.
Secretory pathway begins in the ER where VSR recognizes the cargo for exit from ER (it is not known what type of vesicles used) and reaches the TGN where they dissociate. The receptor can recycle back to the ER while the cargo continues to PVC and then, by organelle fusion, vacuole (Niemes, et al., 2010a).

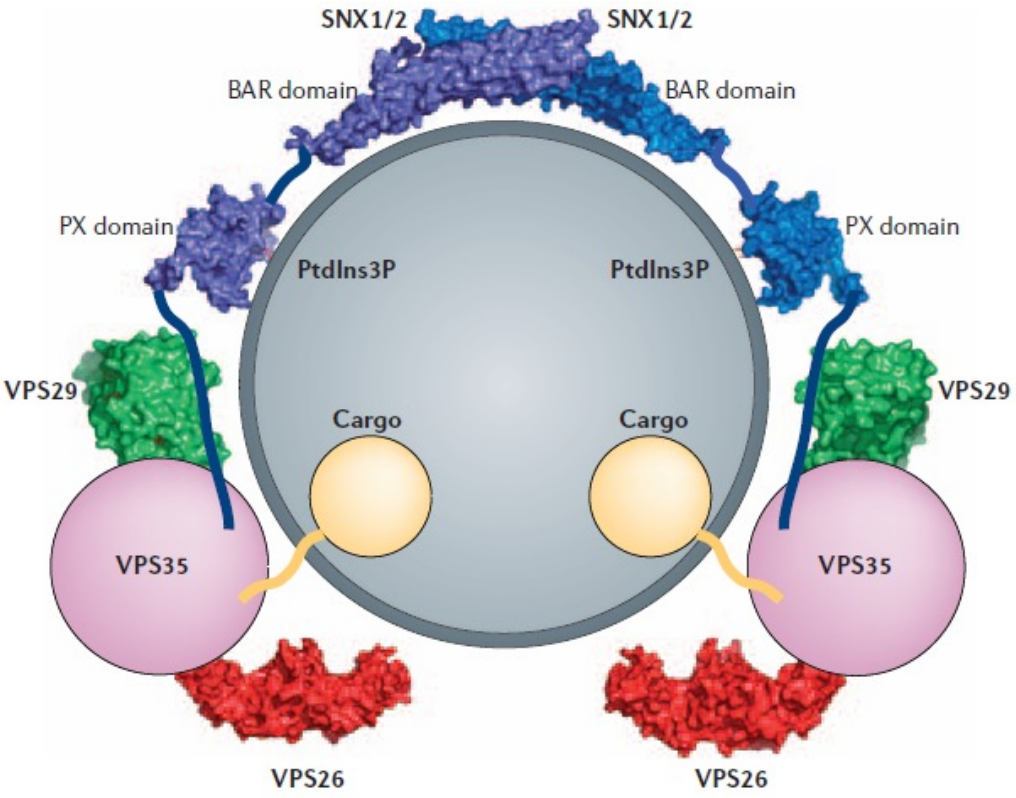

Figure 1-3: Assembling of Retromer Complex
Retromer is a multi-subunit complex that mediates the retrograde transport of acidic hydrolase receptors between endosomes and the *trans*-Golgi network (TGN). The subunits of *Saccharomyces cerevisiae* retromer are named vacuolar protein sorting-5 (Vps5), Vps17, Vps26, Vps29 and Vps35, whereas those of the human retromer are named sorting nexin-1 (SNX1), SNX2, VPS26, VPS29 and VPS35.
Genetic and biochemical analyses have shown that both the *S. cerevisiae* Vps35 and human VPS35 proteins interact with the cytosolic domains of retrograde cargo proteins (Vps10) (Nothwehr, et al., 2000) and the cation-independent mannose 6-phosphate receptor (Nothwehr, et al., 2000; Arighi, et al., 2004). Vps26, Vps29 and Vps35 in *S. cerevisiae* (or VPS26, VPS29 and VPS35 in mammals) form a subcomplex (Seaman, et al., 1998; Haft, et al., 2000) that might be responsible for cargo recognition and regulatory functions.
The figure shows a working model for the assembly and function of mammalian retromer. In this model, SNX1/2 subcomplexes are recruited onto endosomal membranes. The VPS26–VPS29–VPS35 subcomplex is then recruited through interactions with the N termini of SNX1 and SNX2. Once in place, VPS35 captures retrograde cargo proteins in 'retromer-coated' membrane domains.(picture taken from (Bonifacino and Rojas, 2006))

1.3 ESCRT complex

The ESCRT complex is involved in responsible for sorting of transmembrane proteins tagged with an ubiquitin moiety into the intraluminal vesicles of MVB (Figure1-4). These vesicles will be released into the vacuolar lumen for degradation. ESCRT is divided in 4 complexes (ESCRT0-III) that are transiently associated with the endosomes and act sequentially for the inward pushing of membrane into the MVB (Babst, 2005; Babst, 2006). Disassembly of the ESCRT complex is an energy-dependent mechanism involving the AAA-ATPase Vps4, belonging to the ESCRTIII complex (Lata, et al., 2008). In plants the best characterized Vps4

homolog is SKD1 (Haas, et al., 2007). It has an ATPase activity regulated by LIP5, homolog of Vta1p (which is always associated with ESCRTIII).

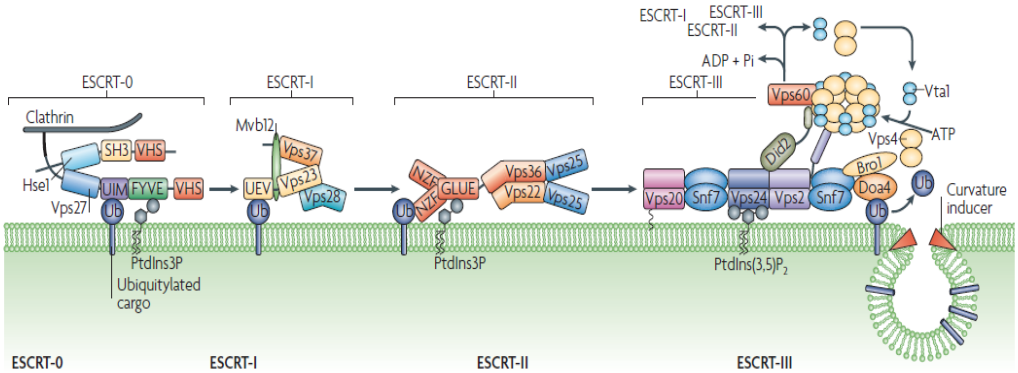

ESCRT-0

S. cerevisiae	Mammalian
Vps27	HRS (HGS)
Hse1	STAM1, STAM2

ESCRT-I

S. cerevisiae	Mammalian
Vps23	VPS23 (TSG101)
Vps28	VPS28
Vps37	VPS37A, B, C, D
Mvb12	?

ATPase complex

S. cerevisiae	Mammalian
Vps4	VPS4A and VPS4B (SKD1)
Vta1	LIP5

ESCRT-II

S. cerevisiae	Mammalian
Vps22	VPS22 (EAP30, SNF8)
Vps25	VPS25 (EAP20)
Vps36	VPS36 (EAP45)

Accessory

S. cerevisiae	Mammalian
Bro1	ALIX (AIP1, PDCD6IP)
Doa4	UBPY?
?	AMSH

ESCRT-III

S. cerevisiae	Mammalian
Vps2	VPS2A, B (CHMP2A, B)
Vps24	VPS24 (CHMP3)
Snf7	SNF7-1, -2, -3 (CHMP4A, B, C)
Vps20	VPS20 (CHMP6)
Did2	CHMP1A, B
Vps60	CHMP5
-	CHMP7

Figure 1-4: Assembling of the ESCRT complex
The four ESCRTS complexes are recruited to endosomes by their interactions with membranes, clathrin, and ubiquitin and with each other. Features of both yeast and mammalian pathways are included. Lipid recognition of either phosphatidylinositol-3-phosphate (PtdIns3P) by the FYVE domain of Vps27 (ESCRT-0) or the GLUE domain of Vps36 (ESCRT-II), or PtdIns(3,5)P2 by Vps24 (ESCRT-III) might contribute to the early or late endosomal localization of the components (BOX 3). All of the ESCRTs except ESCRT-III recognize and bind the ubiquitinated cargo, either through an ubiquitin-interacting motif (UIM) (ESCRT-0), an ubiquitin E2 variant (UEV) domain (ESCRT-I) or the GLUE domain of Vps36 (ESCRT-II). ESCRT-III orchestrates the last steps in the pathway in which ubiquitin is removed by a de-ubiquitinase (degradation of alpha-4 (Doa4)), and the complexes are disassembled by the AAA+ ATPase Vps4. Budding away from the cytosol is depicted as being facilitated by a curvature-inducing factor that could flex the membrane by being localized to the neck of the budding vesicle. The ESCRT components might facilitate the recruitment of such curvature-inducing factors or the concentration of inverted cone shaped components in the endosomal membrane, such as lysobisphosphatidic acid (LBPA) (with the caveat that yeast does not produce LBPA), and non-cargo transmembrane proteins that have bulky glycans on the luminal side of the membrane, such as tetraspannins. Did2, Vps2 and Vps60 are shown interacting with the Vps4–Vta1 complex. The bottom panels list ESCRT subunits and accessory proteins from Saccharomyces cerevisiae and their mammalian homologues. AMSH, associated molecule with the SH3 domain of STAM; CHMP, charged multivesicular body (MVB) proteins; SH3, Src-homology-3; STAM, signal transducing adaptor molecule; UBPY, ubiquitin-specific protease Y (Williams and Urbe, 2007).

1.4 Vacuole structure and functions

A peculiar intracellular structure in plant cells is the vacuole. Essentially it is a large endomembrane compartment delimited by a specific membrane called *tonoplast*.

It acts as a buffering compartment containing many different inorganic and organic compounds but it serves also as a protein storage compartment to be used during germination. These properties differentiate the vacuole from its animal counterpart, the lysosome, which has exclusively degradative functions (Zouhar, et al., 2009).

Plant cells may contain at least two vacuoles, (Frigerio, Hinz et al. 2008): a lytic vacuole (LV) and a protein storage vacuole (PSV). In addition to PSV and LV other examples of co-existing vacuoles have been reported. In fact, during leaf senescence there may be *de novo* formation of a senescence-associated vacuole (SAV). This vacuole is characterized by a higher cysteine-protease activity and a lower pH than a LV (Otegui, et al., 2005) .

The tonoplast lipid composition has been characterized in different species: *Acer pseudoplatanus* cell cultured cells (Tavernier, et al., 1993), *Mesembryanthemum crystallinum* leaf (Duperon, P., J. P. Allais, et al. (1992). Duperon, Allais, et al. 1992), red beet root (Marty and Branton, 1980), mung bean seedling (Yoshida, et al., 1986), oat primary leaf (Verhoek, Haas et al. 1983). It shows a very different composition in lipids and sterols and in any case the lipids/sterols ratio is different from that of the plasma membrane.

A special mention to plant aquaporins. Aquaporins facilitate the transport of water across a lipid bilayer in an osmotic-dependent manner and they accomplish an indispensable physiological role in all the organisms (Maurel, 1997; Chrispeels, et al., 1999; Kjellbom, et al., 1999; Tyerman, et al., 1999).

Plant aquaporins have unique characteristics. They show a high multiplicity of homologs being represented with 35 isoforms in *Arabidopsis* and in rice (Johanson, et al., 2001; Quigley, et al., 2002; Sakurai, et al., 2005; Maurel, et al., 2008).

They are distinguished in four sub-groups: PIPs (Plasmalemma Intrinsic Proteins, with two distinct phylogenetic subgroups PIP1 and PIP2 and 13 isoforms in Arabidopsis), TIPs (Tonoplast Intrinsic Proteins, 10 homologs in *Arabidopsis*) (Johanson, et al., 2001; Quigley, et al., 2002). The third group includes the nodulin-26-like intrinsic proteins (NIPs), which are localized in the peribacteroid membrane of N_2-fixing symbiotic root nodules. *Arabidopsis* encodes 9 isoforms (Wallace, et al., 2006). The fourth group comprises SIPs proteins (Small basic Intrinsic Proteins) with 3 homologs in *Arabidopsis* (Johanson, et al., 2001; Ishikawa, et al., 2005) and residing in the ER. This classification is obviously based on the localization of plant aquaporins, which is unique. Firstly, TIPs participate at rapid osmotic equilibrium between cytosol and vacuolar lumen (Coury, et al., 1999) and although they enter into the secretory pathway, it is thought that TIPs acquire their function only at their final destination.

Secondly, TIPs are highly expressed in land plants (*A.thaliana*, mung bean, radish) (Johnson, et al., 1989; Maeshima, 1992; Marty-Mazars, et al., 1995), with few exceptions. The TIP content is relatively low in tobacco suspension cells (Matsuoka, et al., 1997) while it is extremely low in crassulacean acid metabolism plants (Maeshima, et al., 1994).

Thirdly, many members of the two subgroups are present on both membranes hypothesizing a

possible cooperation of the two subgroups in keeping the osmotic pressure. *A.thaliana* contains 23 isoforms of aquaporins (Weig, et al., 1997). The sequence identity of amino acids between TIPs and PIPs is less than 40%. TIPs are 23-26 kDa proteins and are smaller than PIPs, which are 30kDa.

The vacuole might be considered as one of the final compartments (along with the plasma membrane) along the secretory pathway. Most soluble proteins are incorporated into the lumen of the vacuole in an inactive form and are then processed to an active form by Vacuolar Processing Enzymes (VPEs) (Hara-Nishimura, et al., 1991).

It has been demonstrated that the delivery of soluble protein precursors to the PSV is mediated by dense vesicles, with a density of 1,24g/cm^3 in maturing pumpkin and castor been seeds (Hara-Nishimura, et al., 1985; Fukasawa, et al., 1988). Due to this unique feature, these vesicles have been labelled as precursors-accumulating (PAC) vesicles. Isolation of these vesicles has revealed the presence of protein precursors of 11S globulin and 2S albumin. PACs are 300-400 nm vesicles forming directly from the ER and are labelled by a type I membrane protein, PV72 (Hara-Nishimura, et al., 1998; Shimada, et al., 2002; Watanabe, et al., 2002; Shimada, et al., 2003a). PV72 is related to *Arabidopsis* homologue VSR1 (Shimada, et al., 2003a). Trafficking to the PSV is also ensured by smaller vesicles, ~ 150nm, called dense vesicles (DVs). These vesicles formed onto the cis-Golgi, are carried through the Golgi and released at TGN and they do not have any protein coat (Hohl, et al., 1996; Hillmer, et al., 2001). Isolation of DVs demonstrated the absence of γ-COP and of BP-80/VSR1 (Hinz, et al., 1999).

In tobacco seeds of DIP (Dark Intrinsic Protein) organelles has been detected, which are labelled by RMR1 (Jiang, et al., 2000).

Processing of vacuolar proteins sorted to the lytic vacuole in green tissues has been largely investigated in *Arabidopsis*, which encodes three VPEs: βVPE is specific for seeds (and therefore, the promoter is silent in vegetative tissues); αVPE and γVPE are specific for vegetative organs. These enzymes are responsible for the processing of soluble proteins in the lytic vacuole and are transported by AP1/clathrin coated vesicles (Jürgens, 2004).

The sorting of soluble proteins to vacuoles is ensured by three different so-called Vacuolar Sorting Determinants (VSD).

One type was identified in the N-terminal propeptides of prosporamin and proaleurain, and were initially termed NTPP; the second type was found in the C-terminal propeptide of barley lectin and of tobacco chitinase, and labelled as CTPP; the third one, mainly described for seed storage proteins, termed internal determinants (Chrispeels and Raikhel, 1992; Nakamura and

Hayashi, 1993; Neuhaus and Rogers, 1998). The NTPP propeptide requires a conserved sequence, recognized by a sorting receptor, and can work for other proteins, which are normally not sorted, to the vacuole.

Therefore, I will refer to the NTPPs as "sequence -specific VSD" (ssVSD); similarly, CTPPs will be reported as "C-terminal VSD". Internal determinants of storage proteins have been very difficult to identify and no amino-acid sequence has been reported to be important for a correct sorting. Probably, a main role for correct targeting is accomplished by the three-dimensional structure of the proteins. Therefore, this third class of proteins will be designated as "physical structure VSD" (psVSD) (Di Sansebastiano, et al., 1998).

1.4.1 Sequence- specific Vacuolar sorting Determinants (ssVSD)

One of the first ssVSD to be characterized was found in the sporamin of sweet potato tubers (Maeshima, et al., 1985). After cleavage of the signal peptide, as indeed happens for all proteins entering the secretory pathway, prosporamin has a 16 amino acids propeptide (HSRFNPIRLPTTHEPA) at the N-terminus which determines the correct sorting to the vacuole where it is removed and sporamin assumes its active conformation (Matsuoka, Matsumoto et al. 1990). Deleting the propeptide led to a full secretion of sporamin in the apoplast, demonstrating that these amino acids are essential for a correct vacuolar sorting (Matsuoka and Nakamura, 1991; Neuhaus and Rogers, 1998).

A single point mutation, Asn-26 to Gly, reduced by about 40% the delivery to the central vacuole, while another mutation, Ile-28 to Gly, caused a total secretion of the vacuolar protease (Matsuoka and Nakamura, 1992). The sporamin ssVSD works also efficiently when placed at the C-terminus, demonstrating that it is the specific sequence that is important for a correct and efficient delivering to the vacuole and not the position of the propeptide (Koide, et al., 1997).

Barley aleurain, a cysteine protease, closely related to mammalian cathepsin L, is efficiently sorted to the central vacuole. It is synthesized as pro-protein and sorted in a post-Golgi compartment. It has been localized in vacuoles by immunoelectron microscopy in aleurone cells, a compartment physically different form PSV (Holwerda, et al., 1990; Neuhaus and Rogers, 1998). Barley aleurain has an N-terminal propeptide, which contains the vacuolar sorting determinant. If this part was also partially removed, the mutated form of aleurain was secreted, while an exchange with the C-terminal pro-peptide of a secreted protease it caused its efficient vacuolar retention. These data clearly showed that this N-terminal extension of proaleurain, SSSSFADSNPIRPVTDRAAST, is an efficient VSD (Holwerda, et al.,

1992).This N-terminal extension is highly conserved among all the aleurains found in monocotyledons and dicotyledons. Furthermore, comparison between sporamin VSD and aleurain VSD demonstrated the presence of a conserved and central NPIR motif that was critical for correct protein sorting (Ahmed, et al., 2000).

1.4.2 C-terminal Vacuolar Sorting Determinants (CtVSD)

The presence of a C-terminal pro-peptide in soluble vacuolar protein has been a first clue for Ct-VSD. Accordingly to the literature only few C-terminal amino acids of few proteins have been identified as involved in vacuolar sorting. These are: barley lectin (Dombrovski, et al., 1993) a chitinase , a glucanase and an osmotin from tobacco (Neuhaus, et al., 1991; Sticher, et al., 1992; Melchers, et al., 1993), 2S albumin storage protein from Brazil nut (Saalbach, et al., 1991) and pea (Higgins, et al., 1986).

Fusion of the C-terminal pro-peptide of tobacco chitinase to several reporters (glucuronidase and GFP) demonstrated that the propeptide GLLVDTM is necessary and sufficient for vacuolar targeting. Contrarily to ssVSD, no motif is indispensable for vacuolar sorting and different amino-acid substitution led to a different efficiency of delivering to the vacuole. However, there is a way to abolish totally vacuolar sorting of barley lectin: addition of 1 or 2 Gly caused a total secretion of the reporter to medium (Dombrowski, et al., 1993). For few other proteins it has been possible to describe a blockage of sorting by adding two extra Gly residues: an ER retention signal H/KDEL and peroxisomal targeting for PTS1. A possible explanation for a possible interactions between Ct-VSD proteins and their vacuolar receptor involves the last 20-30 amino-acids that confers a three-dimensional structure for a correct folding of the full length which is then recognized by the receptors (Fedorov and Baldwin, 1997).

Interestingly, use of Brefeldin A (see later in the text) on suspension of tobacco protoplasts transfected with the reporter RGUS-Chi (Sansebastiano, et al., 2007) caused about 50% of the retention and not almost 100% of secretion such as for the wortmannin (see later in the text). This might suggest the existence of two different pathways for the chitinase: a classical one passing through the Golgi and an escape pathway in which soluble cargoes appear to exit the ER and to be delivered to the lytic vacuole in green tissues, although little is known about proteins involved in this pathway.

1.4.3 Physical-structure Vacuolar sorting determinant (psVSD)

This is a third class of heterogeneous proteins sorted to the vacuole for which it is not possible to assert that a pro-peptide, albeit present, is a sufficient signal for the sorting.
In this new class of proteins we may include vicilin-like proteins and legumin-like proteins that accumulate into dense vesicles at trans-side of Golgi and are then sorted to the vacuole without the help of CCVs (Hinz, et al., 1999). Although phytohemagglutinin (PHA) has been one the first vacuolar markers, it is still unknown where its sorting determinant resides.
A study on legumin indicated that the sorting information might involve several elements of sequences, indicating a role of the structure (Saalbach, et al., 1991).
Another possible sorting mechanism would be protein aggregation (Vitale and Chrispeels, 1992). The existence of this mechanism has already been shown for animal cell proteins, where it is caused by a lowered pH (Castle, et al., 1997).
In plant cells it is very interesting to note that the precursor of pea legumin isolated from ER and Golgi showed a higher affinity to membranes than the mature form. Determinants for aggregation would involve hydrophobic regions on the surface of the regions formed by the folding of the structure (Hinz, et al., 1997).

1.5 Brief and general description of the animal and yeast endomembrane systems

Many differences can be highlighted between sorting of hydrolases in mammalian cells and in plants.
In mammalian cells the major pathway for diverting soluble hydrolases, to the lysosome (corresponding to the lytic vacuole for plant cells), rather than to the plasma membrane, implicates that they are marked by the addition of mannose 6-phosphate (Traub and Kornfeld, 1997; Lemmon and Traub, 2000).
So far, two different mannose 6- phosphate receptors (MPR) have been identified by their ability to bind M6P: the 46kDa cation dependent MPR, and the 300 kDa calcium independent receptor (Kornfeld, 1992). Including the delivery to the lysosome, the cation-independent receptors have been involved in also in recycling of insulin-like growth factor receptor (Ghosh, et al., 2003a; Ghosh, et al., 2003b; Ghosh and Kornfeld, 2003). MPR exit from the TGN by clathrin-coated vesicles containing the AP-1 adaptor (Figure 1-5).
In *Saccharomyces cerevisiae* the prevailing pathway to the vacuole is constituted by several

vacuolar hydrolases, such as carboxypeptidase Y (CPY) and membrane proteins such as carboxypeptidase S (Conibear and Stevens, 1998). Sorting of CPY is mediated by the sorting receptor Vps10p, which gathers cargoes at the TGN for delivery to the PVC/endosome and then recycles back to the TGN. In this case clathrin and AP-1 are not important for sorting of CPY In fact, yeast with multiple deletions of APs gene is still able to efficiently sort CPY to the vacuole (Huang, et al., 1999; Yeung, et al., 1999). It is proposed that other protein might compensate their role: GGA (Golgi-localizing, gamma adaptin ear homology domain, Arf binding) proteins (Boman, et al., 2000; Dell'Angelica, et al., 2000). In yeast, *gga1*and *gga2*knock-outs partially abolish sorting of CPY and show a high fragmented vacuole (Dell'Angelica, et al., 2000; Hirst, et al., 2000).

In yeast protein delivery by TGN vesicles to the endosome/prevacuole is defined by different classes of proteins, which include Ypt51p/Vps21p Rab like-GTPase, Vac1p/Pep7p containing a FYVE domain that binds to phosphatidylinositol 3 -phosphate, Vps45p, Pep12p (Conibear and Stevens, 1998; Corvera, et al., 1999; Waters and Pfeffer, 1999; Wurmser, et al., 1999). Similarly, but in an opposite direction, a retrograde traffic to the TGN takes place. In both yeast and animals, Shiga toxin fragment or chimeric protein fused with the cytosolic tail of the TGN resident protein TGN38, are both transported straight to the TGN via early/recycling endosomes (Ghosh, et al., 1998; Mallard, et al., 1998), while furin and MPR are recycled back to the Golgi from the late endosomes (Hirst, et al., 1998b; Mallet and Maxfield, 1999). However MPR and furin can recycle to the TGN from the plasma membrane following a pathway, which involves early sorting endosomes and then late endosomes (Mallet and Maxfield, 1999). MPR needs Rab7 to traffic from early to late endosome before arriving to the TGN (Hirst, et al., 1998a; Press, et al., 1998). Subsequently, a set of retrieval phenotypes were isolated in yeast, identifying a new complex that coats vesicles is termed retromer (Seaman, et al., 1998). This complex is composed of two sub-complexes: the first including Vps35p, Vps29p, Vps26p and Pep8p and the second one including Vps5p and Vps17p. Vps5p is homologs to the mammalian proteins sorting nexin1 and 2 (SNX1 and SNX2). SNX1 and SNX2 bind to the luminal domain of different receptor tyrosine kinase for internalization them (Kurten, et al., 1996; Haft, et al., 1998).

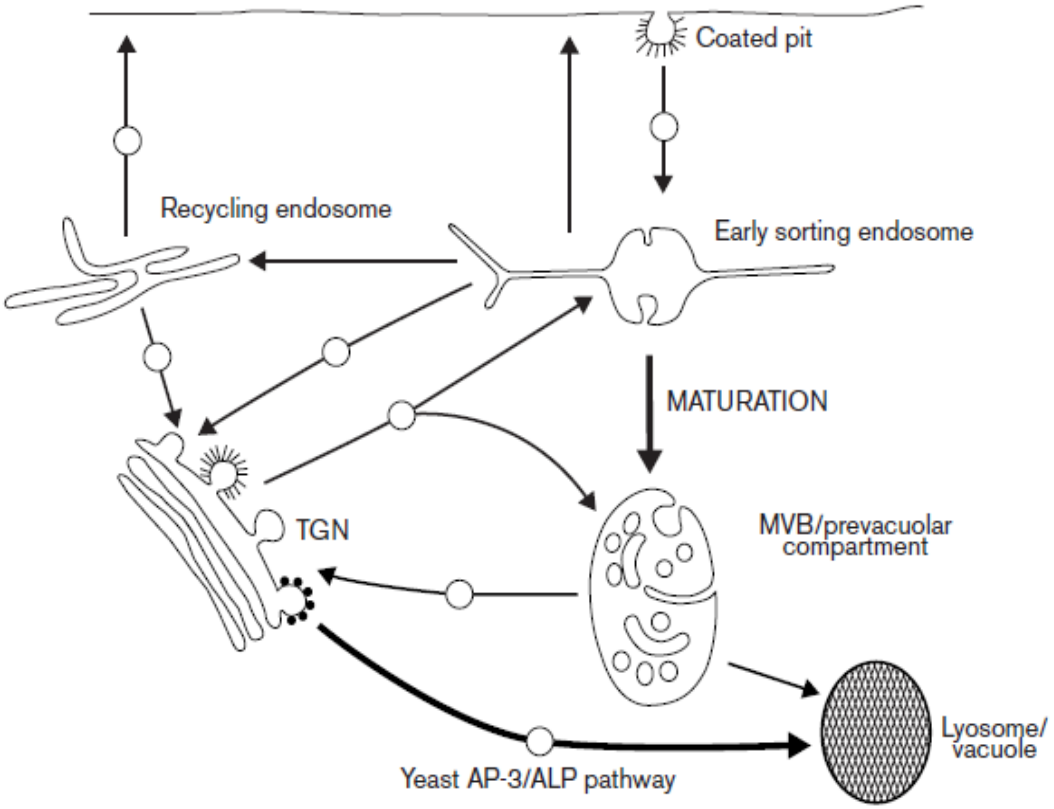

Figure 1-5: Scheme of the endocytic system in yeast and non-polarized cells
The arrows indicate the major trafficking routes through the endocytic system, with spheres indicating transport steps involving known or surmised vesicular intermediates. The bifurcation in traffic flow from the TGN to both the early sorting endosome and to the MVB reflects the maturation process that underlies MVB formation. Initially, multiple fusion events involving vesicles from both the cell surface and the TGN deliver material to a newly forming early sorting endosome. Recycling components (e.g. transferrin receptors) are sorted into the tubular extensions of the structure, which contain the bulk of the membrane of the early sorting endosome, en route to the tubular recycling endosome or to the cell surface for direct recycling. Over time, the sorting endosome loses the capacity to fuse with PM-derived vesicles, but not with vesicles from the TGN. The radiating tubules are replaced by extensive internal membrane invaginations as the maturing endosome moves toward the centre of the cell along microtubules. The available data indicate that in yeast, CPY (not shown) is delivered to a more mature prevacuolar compartment, whereas in animal cells, MPRs may preferentially enter the endocytic pathway at the early sorting endosome. Nevertheless, recent evidence suggests there is a pathway from the TGN to an early endosome in yeast as well and that recycling to the TGN may take place from either the early endosome or prevacuole, similar to animal cells. In yeast, current information supports the direct delivery of ALP to the vacuole in an AP-3- dependent process, although there is presently no evidence for a similar direct route to the lysosome in animal cells (Lemmon and Traub, 2000) .

1.6 Actin microfilaments and microtubules

Actin polymerizes into filaments that offers myriads of advantages to the cells. Actin is necessary for the survival of the cells: it guarantees internal mechanical support, tracks for the for delivering of intracellular components and driving force for cell movements (Martin and Chang, 2006). Under physiological conditions actin polymerizes into long and stable filaments. Beginning of actin polymerization is slow because small oligomers are unstable,

but once the filaments have been synthesized, polymerization is almost completed (Thomas, et al., 2009). Actin polymerization is polar because all the subunits are added in the same directions.

All eukaryotic cells have more than 100 accessory proteins involved in maintaining a pool of actin monomers, initiating the polymerization, and regulating the assembly and the turnover of the monomers and filaments and cross-linking filaments into a very dense network or bundles. Genes for many of these accessory proteins were inserted 1 billion years ago on the phylogenetic tree: amoebas, fungi and animals share many of the molecular mechanism which regulate actin formation and functions (Vidali, et al., 2009).

Plants lost almost 200 genes required for the assembly of cilia and flagella which are responsible for the cell movement in animals (Vitha, et al., 2000). In budding yeast cells actin filaments are responsible for transferring almost all organelles and secretory vesicles to the daughter cell before cell division. Filaments assemble at sites of plasma membrane internalization in budding and fission yeast (Jackson and Casanova, 2000). In these sides "actin patches" assemble *de novo* and provide force to internalize endocytic vesicles from the outer environment, and then disassemble in a process self-limited by space and time. Many, maybe all, eukaryotic cells use actin filaments to transport organelles.

Fission yeast (Mathur and Hulskamp, 2002) and plant cells (Marc, 1997; Mathur and Hulskamp, 2002) mainly depend on formin to assemble polarized actin cables for transport in polarized cells. In the last years a critical step towards the comprehension of plant actin cytoskeleton was an overview of the highly organization of actin filaments, and above all of the extreme dynamics of actin filaments (Nebenfuhr, et al., 2002). Imaging of plant actin cytoskeletons has not been an easy challenge since all classical fixation and embedding methods result in a poor preservation of actin filaments (Geldner, 2004). Moreover, the slow penetration of chemical fixatives, which is enhanced in higher plants by a rigid cell wall, was suspected to provoke artefacts of actin rearrangements (Richter, et al., 2007). Therefore, cryofixation methods have been developed in order to improve chemical fixation procedures. These techniques guarantee a better preservation of structures (Teh and Moore, 2007).

Elevated calcium concentration leads to fragmentation of F-actin microfilaments (MFs) and to depolymerisation of microtubules (MTs).

MFs are involved in vesicle delivering to the target membranes. Basically, they are distributed along the longitudinal axis of the pollen tubes and are almost absent in the apical zone, forming a transverse actin band which is not in tight contact with the apical dome, although very recent studied the presence of few actin filaments in the this area.

MTs are the next component of cytoskeleton. They are involved in several cellular processes such as mitosis, cytokinesis and vesicular transport. They are polymers composed of α and β heterodimers. Studies in animals and yeast have already shed light on their fast dynamics, their association with other factors and biogenesis. It is the organization between all these events which regulates the spatial organization of microtubules and their ability to respond to specific cellular requirements (Tse, et al., 2006).

Genes involved in microtubules biogenesis have been identified in a group of embryo-lethal mutants: *TFC-A (KIESEL), TFC-C (PORCINO), TFC-D (CHAMPIGNON), TFC-E, ARL2 (TITAN5)* (Dettmer, et al., 2006). All these mutants show a defective cortical microtubule array.

Extension of a given MT is finely tuned by polymerization and depolymerisation rates at its ends. In animals, this is ensured by the presence of microtubule-organizing centres, which it is not well defined in plants. Therefore, rapid and efficient spatial reorganization of MTs still remains one of the fascinating mechanism areas in plant cell research.

Stabilization of microtubules is another important mechanism. A putative microtubule stabilizer has been identified in the gene microtubules organization1 (mor1). This gene encodes a homologue of the TOGp-XMAP215 class of very conserved proteins. This mutant is characterized by a very high disorder in the cortical microtubules at high temperature.

1.7 Brief overview of the most common traffic inhibitors in plant cells

1.7.1 Brefeldin A (BFA)

BFA is a macrocyclic lactone that inhibits the activity of ARF GTPases through the interaction with their associated GEFs (Tse, et al., 2004). BFA has been described as an inhibitor of secretion (Satiat-Jeunemaitre and Hawes, 1992; Driouich, et al., 1993) or endocytosis (Grebe, et al., 2003). This depends upon where different BFA-sensitive Arf-GEFs are located, whether early Golgi (Osherov, et al., 1993; Posner, et al., 1994) or post-Golgi (Geldner, et al., 2003).

For instance in BY-2 cells, ER-to-Golgi traffic is inhibited at 10 μ/ml (Jaillais, et al., 2006; Jaillais, et al., 2008) even if it is not possible to detect any morphological changes in Golgi structures (Tse, et al., 2004). In other cells, at same concentration, it is already possible to observe morphological changes in Golgi apparatus (Geldner, et al., 2001; Grebe, et al., 2002; Boonsirichai, et al., 2003; Geldner, et al., 2003; Grebe, et al., 2003; Takano, et al., 2005;

Geldner, et al., 2007). One of the preferred systems in plant cells to study the role of the BFA is the *Arabidopsis* root. Here, the TGN marker VHA-a1 is present in the core of BFA compartments while the remaining of the Golgi stacks are located on the surface of the structure, as monitored by the heterologous Golgi marker sialyl transferase (Satiat-Jeunemaitre and Hawes, 1992).

The proton-pump is required is not only required for the formation of BFA compartments but also for the transport of FM4-64 to TGN/LE and in the end to the tonoplast (Baluska, et al., 2002).

Also the post-Golgi Arf-GNOM accumulates in the core of the structure (Vanhaesebroeck, et al., 2001; Knight and Shokat, 2007), while PVC/MVB markers (ARA7 and BP80) are not observed in the core of BFA compartments, as verified by different technical approaches. However, it has also been asserted (Welters, et al., 1994) that MVB enter into the BFA compartments as seen by the formation of BP80 and AtSNX-1 containing aggregates, although it has been also been demonstrated that the formation of PVC/MVB aggregates at high BFA concentrations (50-100μgmL^{-1}) do not represent BFA compartments (Baggiolini, et al., 1987), meant as PM proteins that recycle between PM and TGN (Arcaro and Wymann, 1993).

Indeed, BFA compartments are mainly filled by cell wall polysaccharides (Wymann, et al., 1996) suggesting an accumulation of secretory vesicles rather than endocytic compartments(Vlahos, et al., 1994).

1.7.2 Wortmannin

Wortmannin is a fungal metabolite that was originally described as a potent inhibitor of the respiratory burst in neutrophils and monocytes (Das, et al., 2005).

Phosphatidylinositol 3-kinase (PI3K) is the target of wortmannin (Welters, et al., 1994; Dasilva, et al., 2005). PI3K is activated by receptor tyrosine kinase at PM to produce the lipid second messenger phosphatydilinositol-3,4,5-trisphosphate (PIP_3) (Sadhu, et al., 2003). PIP_3, in turn, recruits and activate downstream different proteins containing lipid-binding domains. These effectors are: I) protein kinases that promote cell growth, survival and proliferation, such as Akt1, PDK1 (phosphoinositide dependent kinase1) and Tec family kinase; II) GAPs (GTPase-Activating Protein, see earlier in the text) and GEFs (Guanine nucleotide-Exchange Factors, see earlier in the text), essentially involved in membrane trafficking; III) scaffold proteins that nucleate and assemble signalling complexes.

In plants, PI3K is also important for development and signalling (Knight, et al., 2006), although less information is available.

PI3K binds wortmannin and the interaction involves the Lys^{833} within the ATP binding site of PI3K (Tse, et al., 2004; Jaillais, et al., 2006; Oliviusson, et al., 2006; Jaillais, et al., 2008; Silady, et al., 2008; Wang, et al., 2009). Synthesis of another of PI3K inhibitor LY294002 was later reported (Lam, et al., 2007; Wang, et al., 2009).

Both inhibitors show little selectivity within the PI3Ks family members and their structures give little information how to design more selective drugs, which would have a big therapeutic potential.

IC87114 was the first selective inhibitor of one of the PI3K members (Lam, et al., 2007). This inhibitor inhibits p110δ with very high affinity (mid-nanomolar concentrations) and shows between 100-1000 fold selectivity between p110δ and the other members of the family (p110α, p110β, p110γ) (Tse, et al., 2004; Miao, et al., 2006; Delhaize, et al., 2007; Miao, et al., 2008).

No data is available about the use of IC87114 in plant cells.

In plants PI3K homologs have been described (Jaillais, et al., 2006; Miao, et al., 2006; Jaillais, et al., 2008; Robinson, et al., 2008a; Robinson, et al., 2008b) and wortmannin has been demonstrated to be an efficient inhibitor of protein trafficking to the plant vacuole (Wang, et al., 2007). In cells treated with wortmannin the PVC dilates as it can be seen with VSR or ARA7 tagged fluorescent proteins resulting in fluorescent ring-structures (Gazit, et al., 1993; Osherov, et al., 1993). This effect, which can be used as a tool for the identification of PVCs (Posner, et al., 1994), is rapid as it can be visualized 15 minutes after the application of the drug. It can be interpreted as a TGN fusion with the PVC, contributing to the enlargement of the PVC (Kovalenko, et al., 1994). It seems that the wortmannin-induced enlargement of the PVC is a general observation since it has been highlighted in BY-2 cells, *Arabidopsis* and *rice* (Yaish, et al., 1988; Shechter, et al., 1989), root cells of *Arabidopsis*, tobacco, pea and mung bean (Umezawa, et al., 1986) germinating mung bean seeds (Yaish, et al., 1988; Gazit, et al., 1989; Levitzki and Mishani, 2006).

1.7.3 Tyrphostins

Research on the development of PTKs (Protein Tyrosine Kinase) started after finding, in the early 80s, that natural compounds, such as quercetin, erbstatin, genistein and lavendustin inhibit the activities of PTKs such as $pp60^{src}$ and EGFR. Even if these substances have

showed low affinity, selectivity or poor potency, they have been very useful in order to develop new synthetic compounds with a more potent inhibitory activity: tyrphostins.
The activity of itaconic acid (Holen, et al., 1995; Austin and Shields, 1996) along with the erbstatin (Ortiz-Zapater, et al., 2006) triggered the research for the synthesis of these new compounds. The structure of these new compounds has been used as base for a vast number of compounds, many of which showed a very high specificity for PTKs and insignificant inhibition of Ser/Thr kinase (Dhonukshe, et al., 2007).
Tyrphostins are classified in 1) competitive for the substrate and non-competitive for the ATP (ATP competitive, (Robinson, et al., 2004; Robinson, et al., 2008a)), 2) bisubstrate-competitive (Robinson, et al., 2008a) and 3) mixed competitive (Reichardt, et al., 2007). Further investigations led to synthesis' of cyclic tyrphostins (Drose and Altendorf, 1997).
In mammalian cells it has been highlighted that they can inhibit endocytosis towards the TGN (Dettmer, et al., 2006). Two articles supported tyrphostins A23 as useful tool to study endocytosis in plants: I) the internalization of the hTfR expressed in *Arabidopsis* protoplast is inhibited by tyrphostin A23 (Dettmer, et al., 2006); II) tyrphostin A23 was reported to inhibit the internalization of PIN2, but not of FM4-64 in *Arabidopsis* roots, especially preventing its accumulation in BFA compartments (Dettmer, et al., 2005).
Tyrphostin A23 seems to have different effects on different subcellular compartments: *Arabidopsis* roots pre-treated with tyrphostin A23 are unable to form BFA compartments, and do not form cell plate formation (Robinson, et al., 2008a). This demonstrates that tyrphostin A23 acts at level of the Golgi, as Golgi based secretion is required for the formation of BFA-compartments and cytokinesis (Higgins, 1992).

1.7.4 *Bafilomycins and Concanamycins*

ATPases can be distinguished on the base of their transport mechanism, their sensitivity to specific inhibitors and their quaternary structures (Bowman, et al., 1988). An initial classification has been made by Pedersen and Carafoli (Pedersen and Carafoli, 1987), who introduced the terms P-type, V-type and F-type ATPases.
P-type ATPases pass through a phosphorylated transitional stage; F-type ATPases are mostly involved in ATP synthesis (they are also named F-ATP synthase); V-type ATPases are genetically related to F-types but function only in proton pumping. Later, it came also clear that ATP binding cassette (ABC) transporters (or traffic ATPases) had to be added to this classification. ABC transporters are involved in uptake or efflux of a huge variety of solutes

by hydrolysing ATP (Umata, et al., 1990; Tapper and Sundler, 1995). The use of specific inhibitors has increased our comprehension of the function and role of these important proteins.

Ortho-vanadate is a well-known inhibitor for P-ATPases, while venturicidin inhibits F-ATPases. Dicyclohexylcarbodiimide (DCCD), NO_3^-, N-ethylmaleimide (NEM) and 7-chloro 4-nitrobenz-2-oxa-1,3-diazole (NBD-Cl) were only inhibitors for the V-ATPases, although DCCD has been shown to inhibit also F-ATPases. The discovery of new antibiotics, bafilomycins, as high affinity inhibitors of V-ATPases (Nadler, et al., 1998), led to a rapid analysis of V-ATPases.

Bafilomycins and concanamycins are closely related compounds which belong to the group of unusual macrolides (Omura, 1984) which are characterized by a 10-to-48-membered macrocyclic lactone and are produced in bacteria. Together with highly related unsaturated macrolides produced in *Streptomyces* strains, they form the group of plecomacrolides.

Even before the discovery of bafilomycins and concanamycins as inhibitors of the proton-pumps V-ATPases, it was well established that these proteins actively pump protons into the lumen of different eukaryotic compartments such as lysosomes, endosomes and vacuoles in plant cells (Viotti, et al., 2010). To study the role of acidification in these compartments, many acidotropic permeant bases have been extensively used. These bases accumulate in the lumen of acidic compartments in the protonated form, raising the pH. However, their accumulation causes osmotic swelling (also called vacuolation), and, therefore, pleiotropic effects cannot be excluded.

Bafilomycins can specifically inhibit vacuolar ATPases without causing vacuolation in animal cells (Sasse, et al., 2003; Menche, et al., 2007). On the contrary, in plant cells both concanamycin A and bafilomycin A (two macrolides), lead to massive vacuolation of the Golgi apparatus (Sasse, et al., 2003). Analogous observations can be drawn in *Arabidopsis* roots treated with concanamycin A in which it is possible to observe changes in Golgi morphology and aggregations of vesicles (Huss, et al., 2005).The same effects are visible in *vha* mutant cells (Huss, et al., 2005).

Concanamycin A blocks the trafficking of newly synthesized proteins to the PM and the transport of FM4-64 from the TGN to the tonoplast (Huss, et al., 2005).

The role of Concanamycin A in the maintenance of structure and morphology of the TGN was recently studied. The authors showed by electron microscopy that the number of Golgi cisternae increased and there was no more spatial difference between the Golgi and the TGN. In addition, VHA-a1 and SYP61 were no longer detectable only at the level of the TGN, but

also in the Golgi cisternae, indicating that the V-ATPase was important for the identity of the TGN (Boyd, et al., 2001).

Research of new inhibitors for V-ATPases proteins has allowed identifying macrolactone archazolid compounds, which are produced by the myxobacteria *Archangium gephyra* and *Cystobacter violaceus* (Erickson, 1997; Kunze, et al., 1998; McKee, et al., 1998; Kim, et al., 1999; Huss, et al., 2005). This new class of inhibitors is characterized by a macrocyclic lactone ring with a thiazole side chain.

A deeper analysis in cells has revealed that archazolids led to the formation of vacuole in the ER, which is typical for V-ATPases inhibitors in animal cells (Boyd, et al., 2001). Moreover, archazolids also prevents the acidification of lysosomes, reinforcing the idea that these compounds were specific for V-ATPases (Boyd, et al., 2001). When archazolids were tested on preparations of Na^+/K^+-ATPases and mitochondrial F-ATPases, they appeared to exclusively target V-ATPases with IC_{50} values in the nanomolar range (Huss and Wieczorek, 2009). Even if archazolid is one of newest inhibitors for V-ATPases, part of its binding site has already been identified (Gagliardi, et al., 1998).

Another class of natural inhibitors of V-ATPases is the benzolactone enamides. These compounds are extracted from either marine macroorganisms such as the sponge *Haliclona* sp. or the tunicate *Aplidium lobatum* or from microorganisms such as *Pseudomonas* sp and the myxobacterium *Chondromyces* sp. The benzolactone enamides extracted from the tunicate are believed to be part of the metabolism of microbial symbionts (Gagliardi, et al., 1998).

In vitro and *in vivo* tests have showed that all these substances exhibited IC_{50} in the nanomolar range (Pali, et al., 2004; Dixon, et al., 2008) and all revealed an inhibitory pattern similar to that of the plecomacrolides (Webb, et al., 2000).

One of the most amazing features of the benzolactone enamides is that they do not have inhibitory activity against V-ATPases form fungal sources. Salicylihalamides, lobatamides, oximidines showed an inhibitory effect on preparations of purified vacuolar membranes from *N. crassa* and *S. Cerevisiae* (Webb, et al., 2000; Percherancier, et al., 2001; El-Husseini, et al., 2002; Chen, et al., 2003; Drisdel and Green, 2004; Drisdel, et al., 2004; Chenette, et al., 2005), and apicularen with preparations of vacuolar membrane from *S .cerevisiae* (Chase and Tubbs, 1972; Coleman, et al., 1992). In conclusion, benzolactone enamides are the first class of inhibitors of V-ATPases, which, for unknown reasons, are able to discriminate between V-ATPases from different species. Another important feature, yet to be deciphered, is the binding site for the benzolactone enamides.

Studies on bafilomycin structure led to the identification of several key structural elements for

biological activity (Coleman, et al., 1992). This allowed developing and synthesizing structurally simpler V-ATPases inhibitors (Brandes, et al., 1995a; Bastie, et al., 2000). The most efficient inhibitor, with an IC_{50} of 30 $nmol^{-1}$ was (2Z,4E)-5-(5,6-dichloro-2-indolyl)-2-methoxy-N-(1,2,2,6,6-pentamethylpiperidin-4-yl)-2,4-pentadienamide, also referred as INDOLO (Webb, et al., 2000). With a spin-labelled derivatives of INDOLO, it was possible to demonstrate a strong interaction between the transmembrane domain of subunit c of the V-ATPase and the INDOLO (DeJesus and Bizzozero, 2002).

1.7.5 2Bromopalmitate (2BP)

A method that has gained increasing popularity among researchers in the last years is to treat cells with 2BP, a non-metabolizable palmitic acid analogue that prevents palmitoylation (Remizov, et al., 2003; Schnell, et al., 2007) as verified for at least 2 dozen of palmitoylated protein including Src families kinases, Rho family proteins, H-Ras, PSD-95, the transmembrane Nicotinic α7 receptor and CCR5 (Gwiazda, et al., 2009). Once inside the cell, 2BP is rapidly converted to 2BP-CoA. As 2BP is very similar to palmitate, it is not surprising that this drug has multiple effects on different cellular processes: it inhibits carnitine palmitoyl transferase1 and in turn, prevents fatty acid β-oxidation (Resh, 2006a; Resh, 2006b).

2BP inhibits also other enzymes of triacylglycerol biosynthesis, fatty acid CoA ligase and Glycerol-3-phosphate acyl transferase (Coleman, et al., 1992). Effects on NADPH cytochrome c reductase and glucose-6- phosphatase have also been reported. Moreover, in pre-adipocytes, 2BP causes gene expression and differentiation via activation of peroxisome proliferator-activated receptors (Brandes, et al., 1995b; Bastie, et al., 2000). Therefore, close attention is required when using this drug due to its pleiotropic effects. All these data were obtained by studies on animal cell systems; so far, no information is available about the effects on plant cells systems. The inhibition of the palmitoylation process through the 2BP is still not understood: other palmitate analogues, such as 2-hydroxypalmitate, 16-hydroxypalmitate and palmitoleic acid have no effect on palmitoylation of Src family kinase Fyn (Webb, et al., 2000). Perhaps, the high electro-negativity of bromide stabilizes the complex of PAT with 2BP. In support of this thesis, it has been observed that the 2-fluoropalmitate (fluoride has a highest electro-negativity) inhibits palmitoylation in brain cells by competing with palmitate uptake (this phenomenon has not been observed for 2BP) (DeJesus and Bizzozero, 2002) . Recently, it was shown palmitate elicits intracellular

Ca^{2+}rodent islets and some β cell line (Remizov, et al., 2003; Schnell, et al., 2007).

In contrary, when cells were incubated with 2-bromopalmitate (2BP), a non-metabolizable analogue of palmitate, Ca^{2+}release in the cytosol was attenuated, but not fully abolished**.** 2BP is esterified to 2BP-CoA but cannot undergo β-oxidation and also prevents other fatty acids to be β-oxidised by blocking carnitine palmitoyl transferase1, which transports long-chain free fatty acids into the mitochondria (Resh, 2006b) .

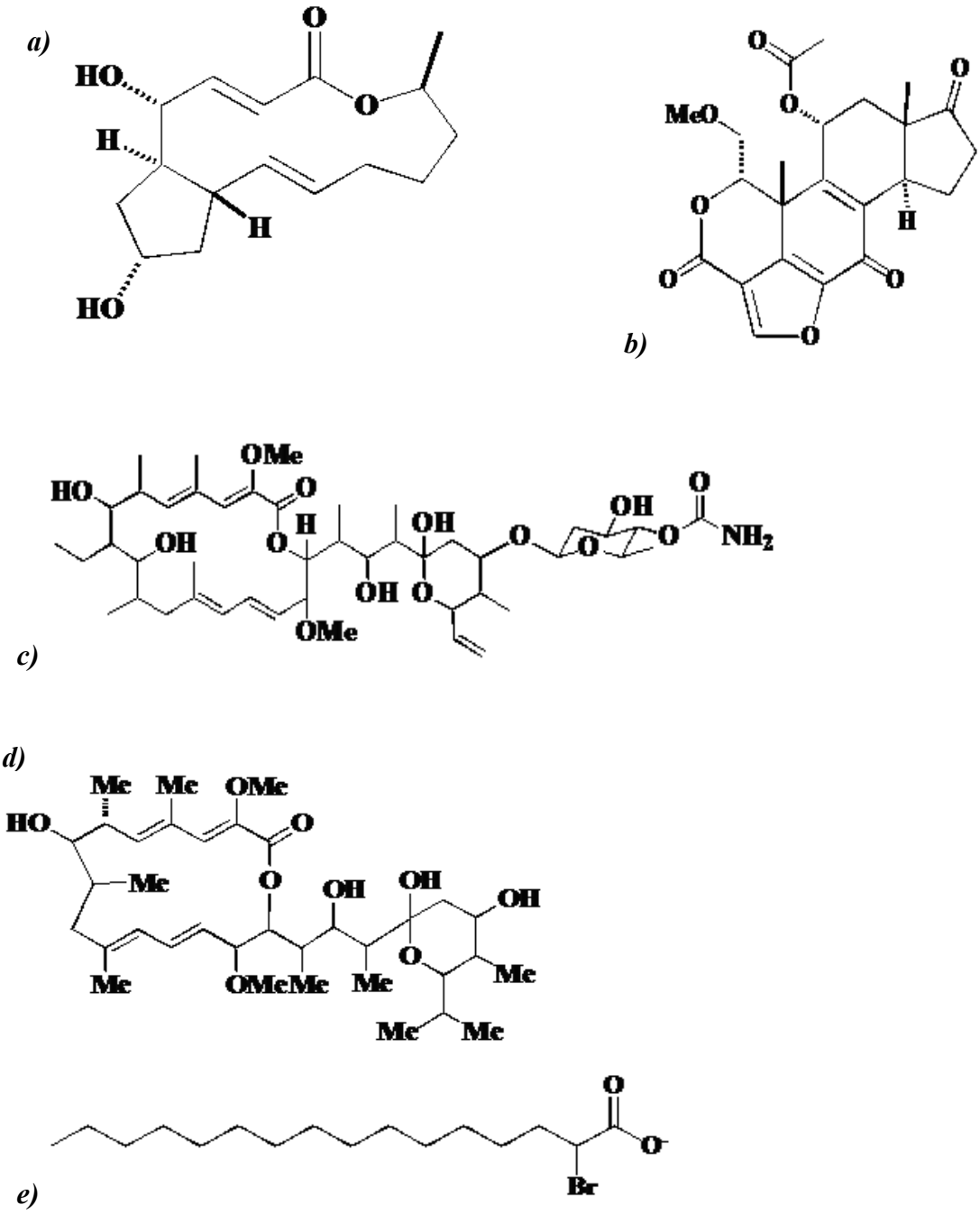

Figure 1-6: Main inhibitors in plant cell trafficking
Molecular structure of a) Brefeldin A, b) wortmannin, c) concanamycin A, d) Bafilomycin A, e) 2-Bromopalmitate. Structures have been designed by ChemBioDraw ultra software.

2. Palmitoylation of AtRMR1

2.1 Vacuolar Sorting Receptors (VSRs)

One of the first transmembrane receptors involved in vacuolar sorting was identified in pea and was named BP80 ((Kirsch, et al., 1994; Hadlington and Denecke, 2000), or VSR1 (Vacuolar Sorting Receptor, (Shimada, et al., 2003a) or *At*ELP1 (Epidermal growth factor like protein, (Ahmed, et al., 1997).

The complete sequencing of the *A.thaliana* genome highlighted the presence of seven different isoforms.

This receptor was identified because it was able to recognize and to bind the NPIR motif of aleurain. It has no homologues in other eukaryotic organisms than plants (Kirsch, et al., 1996; Paris, et al., 1997; Ahmed, et al., 2000). Knock-out plants lacking the gene VSR1 are still able to transport the aleurain precursor to the lytic vacuole (Shimada, et al., 2003a). In the same plants, 12S globulin and 2S albumin storage proteins were secreted into the extracellular space (Shimada, et al., 2003b)(. These results strongly suggest that VSR1 works as vacuolar receptor for storage proteins delivered to PSV in embryos and for cysteine-protease in vegetative tissues. A study of gene expression and phenotype in VSR3-silenced plants (Avila, et al., 2008) indicated its importance in the function of guard cells, but its role in vacuolar sorting remains unknown. In order to elucidate the role of each VSR receptor, vacuolar sorting should be studied in knockout plants for each *VSR*. To validate the effective role of the members of VSRs, Zouhar et al. have shown that only VSR1,3 and 4 are effectively involved in vacuolar sorting of VAC2 (a translational fusion of the extracellular ligand CLAVATA3 to the VSD from barley lectin driven by the 35S promoter, (Rojo, et al., 2002)) in vegetative tissues and of 12S and 2S globulins in seeds (Zouhar, et al., 2010).

VSRs are type I integral proteins composed in the luminal side of the membrane of a Protease-Associated (PA) domain, an extended VSR region, and, preceding the 23 amino-acid transmembrane domain, three repeats of an epidermal growth factor motif (Watanabe, et al., 2004) (Figure 2-2b). The PA domain is responsible for cargo binding, while the EGF repeats are supposed to stabilize the receptor-cargo association (Cao et al., 2000). Although this idea is widely accepted in the literature, the role of PA domain in proteases and sorting receptors remained somewhat elusive (Luo and Hofmann, 2001). A clearer role came to light when the

X-ray structure of the ectodomain of the transferrin receptor was solved (Lawrence, et al., 1999). This study showed that the PA domain acts as a lid that covers the active site of the protease. The PA domain in BP-80 is important for the binding of various ligands, suggesting a more general role in cargo binding (Cao, et al., 2000). So far, two different ligands have been identified: aleurain (a protease) and sporamin (a protease inhibitor) (Ahmed, et al., 2000).

The very short cytosolic C-terminus contains a tyrosine motif (YXXL), interacting with the μA adaptin and thus responsible for the incorporation into CCV for its exit from the TGN to the PVC/MVB (Happel, et al., 2004; daSilva, et al., 2006).

Very recently, VSR1 was proposed to undergo a homomeric interaction. The authors demonstrated by mutation of a very short region of the cytosolic tail spanning 9 amino-acids, that it was responsible for the formation of a high molecular weight complex (~200 KDa) and that the mutant was dominant-negative, interfering with endogenous VSR1 in the complex formation. This mutant (C2A) also caused the secretion of the two vacuolar markers Aleu-GFP and Spo-GFP (Kim, et al., 2010). However, the mutated region includes also the tyrosine of the Tyr motif, which is critical for the binding to the μA adaptin, and therefore, inclusion in CCV. The same mutant further includes the IM dipeptide (see below) important for VSR1 recycling to the TGN. In conclusion, the author support the idea that homomeric interaction is critical for binding to the adaptor complex and in turn to efficiently recruit clathrin at the TGN.

A new trafficking signal was also identified for BP-80/VSR1, the dipeptide $Ile^{608}Met^{609}$ in the cytosolic tail which is involved in two different trafficking steps: 1) recycling from the PVC and TGN and 2) endocytosis described as alternative pathway (Saint-Jean, et al., 2010). The importance of the cytosolic tail (and above all of a YXXL motif) in proper sorting is well established as VSR1 lacking the cytosolic domain is trapped in the Golgi (Brandizzi, et al., 2002). In the main pathway the authors argue that the receptor recognizes the cargo in the TGN (in strong discrepancy with Niemes et al., 2010) and exits thanks to its interaction with the μA adaptin-containing complex. Following the fusion of vesicles with the PVC, the receptor releases the ligand and recycles back to the TGN, probably by an interaction between the dipeptide and the retromer complex.

The alternative endocytic pathway is used to recover ligands from the apoplast. The receptor binds its ligand and traffics to the early endosome using the IM dipeptide, part of a EXXXIM dileucine motif and perhaps the Tyr motif. The latter process is sensitive to BFA (Figure 2-1).

As can be seen from this description, we still cannot get a clear picture of VSR1 trafficking. Several models have been proposed and, the discrepancies are evident for recycling, either to the TGN (as in the classical view) or to the ER (as proposed by Niemes et al. 2010). Only this last work takes into account several members of the retromer complex showing, albeit in a heterologous system, that VSR recycling effectively begins at the TGN.

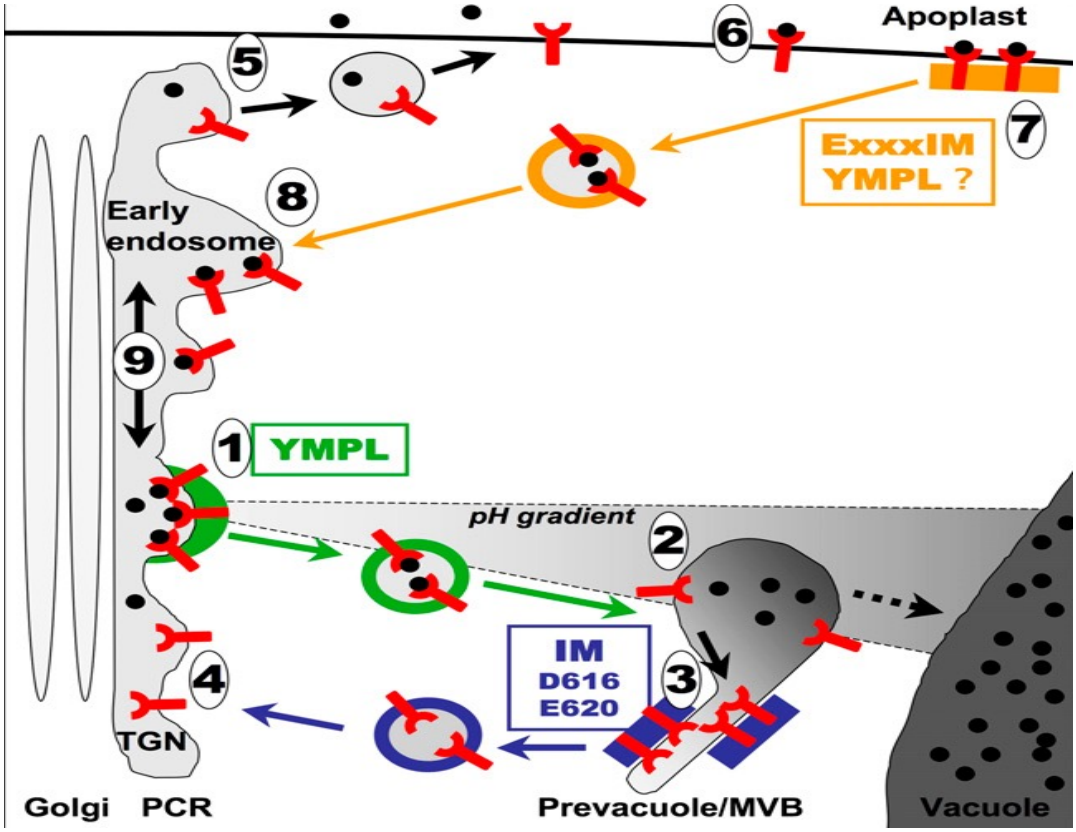

Figure 2-1: Different pathways and roles for the vacuolar sorting receptor BP80
The receptor BP80 can use two different pathways: a major one (green and blue arrows) or an alternative pathway (black and orange arrows). In the major pathway, BP80 recognizes the ligand (black circle) at the level of the TGN. The exit from the TGN (1) requires the tyrosine motif through its interaction with μA-adaptin containing complex (green box and vesicle coat). After fusion of the vesicle to the prevacuole (2), the receptor releases its ligand, possibly due to a pH decrease. The free receptor is then segregated out of the ligand release area (3) most likely by interaction of the IM motif with a retrieval complex (blue box). The free receptor is packed in coated vesicles (vesicle with blue coat) back to the TGN where fusion (4) may require VPS45. The final steps for ligand transport to the vacuole (dashed arrow) do not require BP80 but instead are believed to be maturation processes of the prevacuole/MVB that eventually fuses with the vacuole. The alternative pathway serves to recover ligands from the apoplast. The free receptor but also free ligand can exit the TGN (5; black arrows) to reach the plasma membrane by a BFA-sensitive process. At the plasma membrane, the receptor binds a ligand (6) and is endocytosed using the IM dipeptide as part of a dileucine-like motif ExxxIM, probably involving also the Tyr motif The endocytosis signal should interact (7) with the retrieval complex (orange box and vesicle coat). Fusion of the vesicle with the early endosome (8) leads to release the receptor-ligand where the complex can diffuse into the membrane (9) and may enter the main pathway thanks to the Tyr motif (1) (Saint-Jean, et al., 2010).

2.2 RMRs

A new family of putative receptors, named RMRs (luminal Receptor homology domain, trans Membrane domain and RING-H2 motif in the cytoplasmic tail(Jiang, et al., 2000), was identified by its homology to the PA domain of the VSR proteins (Jiang, et al., 2000).

This new family of receptors shows the following structural organization: an N-terminal signal peptide, a PA domain involved in cargo-binding (a general description is made in 1.4.1), a TM domain, a RING-H2 domain involved in protein-protein interactions and a Serine Rich domain (SRD) (Figure 2-2a).

RING domains are cysteine-rich zinc-binding domains and mediate protein degradation by poly-ubiquitination to proteins substrates (Borden, 2000; Freemont, 2000; Jackson, et al., 2000; Joazeiro and Weissman, 2000). They contain a Cys3 His Cys4 domain, which binds two zinc cations.

Poly-ubiquitinated substrates are degraded by 26S proteasome pathway (Pickart, 2001; Glickman and Ciechanover, 2002). The ubiquitin-proteasome pathway is composed by E1 enzyme (or ubiquitin activating enzyme), then by E2 enzymes (or conjugating enzymes) and finally by E3 enzymes (or ubiquitin ligase). Ubiquitin ligases have a RING, a PHD (Plant Homeodomain) or a HECT domain (to E6AP COOH terminus).

The RING-H2 domain is a subset of the RING domains in which the cysteines at position 5 is replaced with histidine (Figure 2.3). RING-H2 domains are specific for ubiquitin ligase targeting.

The last domain of the cytosolic tail of RMR1 is named serine-rich domain (SRD) and has no clear functions, but is probably involved in protein interactions and in post-translation regulation by phosphorylation on serines (Briknarova, et al., 2005).

Arabidopsis encodes six different RMRs isoforms, distinct in their predicted molecular weight (between 34kDa and 48kDa), their good homology of the N-terminal (around 41%) but their larger diversity of the C-terminal. Here we use the following nomenclature for the six RMRs members (Neuhaus and Paris, 2005):

At1g71980	JR702 / RMR1
At5g66160	JR700/RMR2
At1g22670	T22J18/RMR3
At4g09560	CAB78079/RMR4
Atg135630	RMR5
§At1g35625	RMR6

Observation of ubiquitination activity of proteins having classical RING domains (see below) shows the uniqueness of RING-H2 domains in E3-ligase function. Furthermore, RING-H2 proteins can function outside of the ubiquitin pathway (Kentsis & Borden, 2000).

A preliminary study (Park, et al., 2007) showed an *in vitro* interaction between the CtVSD of tobacco chitinase and luminal domain of RMR1. Consistent with this finding, the authors showed also that a default secretion of GFP-Chi in protoplasts was abolished by the co-expression of a mutated fusion protein, RMR-BP80 (RMR luminal domain-BP80 transmembrane domain/cytoplasmic tail) and that the vacuolar reporter was mainly found in an enriched vacuolar fraction. Moreover, both the chimera and the reporter were localized in the vacuole. These data show a clear involvement of the RMR1 receptor with the GFP-Chi pathway, although more proofs are needed, in order to elucidate the interaction between cargo and receptor (Silady, et al., 2008).

Preliminary bioinformatics studies of RMR1 evidenced a high potential of post-translational modification such as phosphorylation (above all in Serine Rich domain) and palmitoylation.

a)

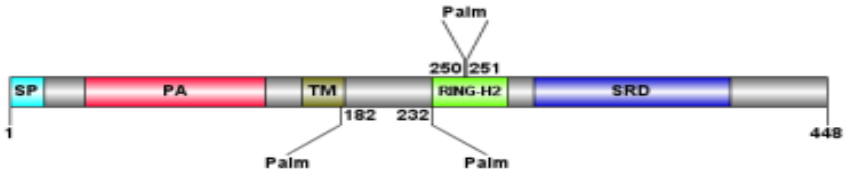

b)

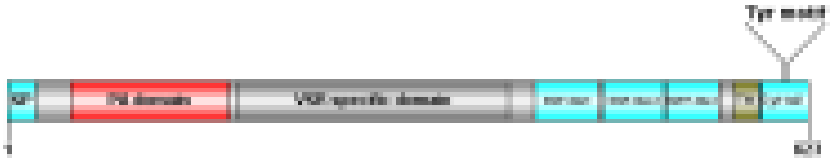

Figure 2-2: Scheme of RMR1 and BP80 domains

Schematic representation of a) RMR1 and b) VSR1.SP: Signal Peptide. PA domain: Protease Associated domain, involved in binding of cargo. TM: Transmembrane domain. RING-H2 domain: Really Interesting New Gene. SRD: Serine Rich Domain. Palm: predicted S-acylated site.

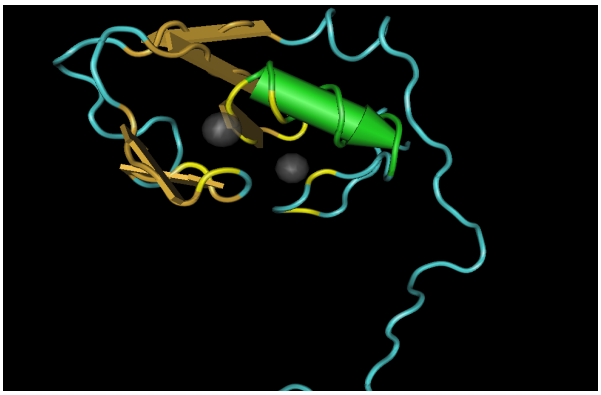

Figure 2-3: Structure of Praja1
Consensus sequence for the RING-H2 domain: C-X2-C-X(9-39)-C-X(1-3)-H-X(2-3)-(N/C/H)-X2-C-X(4-48)C-X2-C. NMR structure of chain A of the Zinc finger domain of E3 ubiquitin-protein ligase Praja-1 from *Homo sapiens*. The protein has 52% of identity with the RING-H2 domain of RMR1. Parenthetical numbers refer to spacing; X indicates any residue, residues involved in the coordination on Zn^{2+} ions are in yellow.

2.3 Preliminary analysis of RMR1 palmitoylation

Preliminary bio-informatics studies show a high palmitoylation probability for RMR1 (table 2-1). Even though the cysteines in position 12 and 16 have a high score, they will not be considered because they are located in the signal peptide. Cysteines in position 232 and 250 will not be taken initially into account because they are involved in the formation of the RING-H2 domain, although a palmitoylation cannot be totally excluded.

Position	Peptide	Score	Cut-off	Type
12	…LYVCTVS…	2,609	1,000	Type III: Others
16	…TVSCLAS…	3,287	1,000	Type III: Others
182	…LATCFFV…	1,165	1,000	Type III: Others
232	…AFTCAIC…	0,917	0,800	Type II: -CXXC-
250	…LLPCCHK…	1,703	1,700	Type I: -CC-
251	…LPCCHKF…	1.359	1,000	Type I: -CC-
448	…LPDC*	1,930	1,000	Type III: Others

Table2-1: Prediction of palmitoylation sites in *At*RMR1.
The first two cysteines, in position 12 and 16, although have a very high probability to be palmitoylated, are located in the signal peptide and therefore they are lost after cleavage.
The cysteine in position 182 is at end of the trans-membrane domain, the cysteines in position 232, 250and 251 are in the RING-H2 domain, and C-terminal cysteine is in the Serine-Rich domain.

2.4 Investigation of a role of palmitoylation in anchoring to membrane microdomains

S-acylation is known to be involved in different processes such as anchoring to membrane

microdomains (Smotrys and Linder, 2004), protein stability by preventing ubiquitination (Valdez-Taubas and Pelham, 2005), sorting to an endosomal compartment (Subramanian, et al., 2006) and localisation (Webb, et al., 2000).

Initially, I tested, whether palmitoylation could affect the affinity to membrane microdomains. For this purpose I used a solubilisation assay with different detergents and with or without 2-Bromopalmitate (2BP, a potent inhibitor of S-palmitoylation).

Surprisingly the major part of RMR1 was found in the supernatant after centrifugation at 100.000g for 1h (Figure 2-4). Only a small amount of protein could be found in the microsomal fraction (about 7%). Solubilisation assays and band quantification were performed and results are summarised in Figure 2-5. No clear information could be derived from these experiments, even though we could notice a different solubility of RMR1 with different detergents, which strongly suggests an association with membrane microdomains.

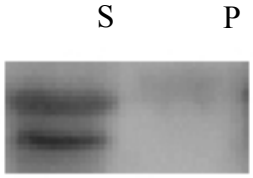

Figure 2-4: Western blot of supernatant and pellet fractions from Arabidopsis leaves.
Upon centrifugation at 100'000g for 1 h RMR1 was mainly (~ 93%) detected in the soluble fraction. We always detected two bands the upper band being ~ 15-20 kDa heavier than the lower band.

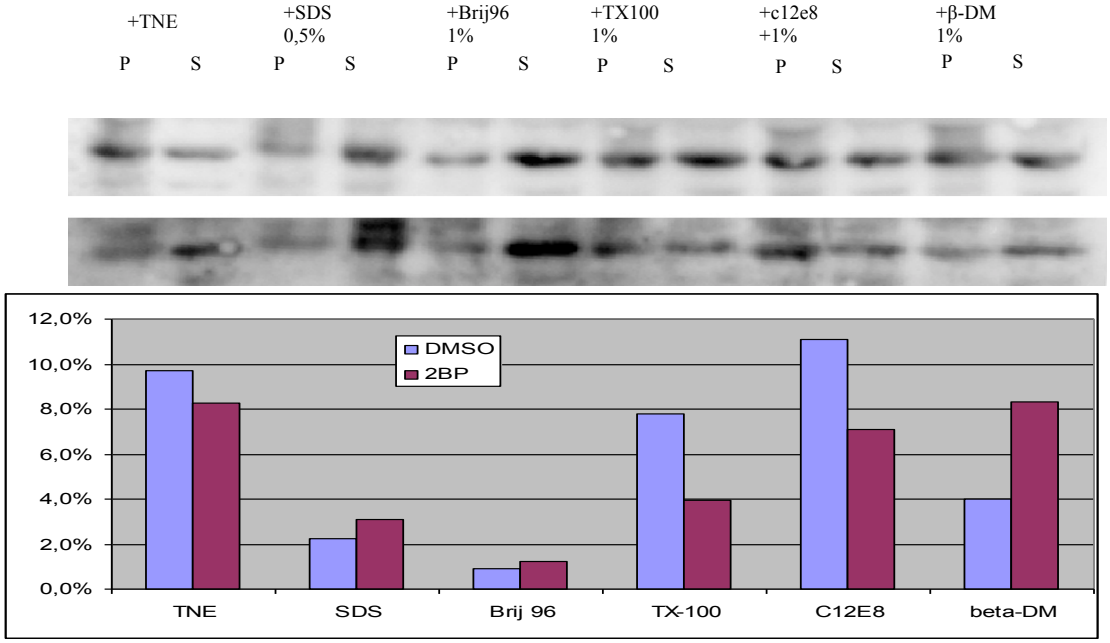

Figure 2-5: Solubilisation of RMR1 by different detergents.
Arabidopsis leaves were treated O.N. with 2BP, a strong inhibitor of palmitoylation or with DMSO as control. Total extracts were solubilised with different detergents. Soluble and membrane-bound proteins were separated by ultracentrifugation at 100'000g for 1h.
Extracts were analysed by western blot using anti-RMR1 antibody. Blots were quantified by ImageJ as shown in the bottom graph. TNE=Tris-NaCl-EDTA, no detergent control; SDS=Sodium Dodecyl Sulphate; TX-100= Triton X-100; C12E8= Octaethylene glycol monododecyl ether; beta-DM= n-Dodecyl-beta-D-Maltoside

2.5 Localisation of RMR1 is affected by 2BP

The next step was to verify if inhibiting palmitoylation by 2BP would change the localisation of RMR1 as detected by fractionation in a sucrose gradient. Indeed treatment of *A. thaliana* protoplasts with 2BP caused the appearance of RMR1 in new fractions not observed in the untreated sample (Figure 2-6 a, d).

The markers used for this assay, BiP (Figure 2-6c,f), which labels the ER (Denecke, et al., 1991) and γ-TIP (Figure 2-6 b, e), which labels the tonoplast (Maurel, et al., 1993), were not affected by 2BP, demonstrating that the drug does not unspecifically affect the localization or alter the general membrane organization.

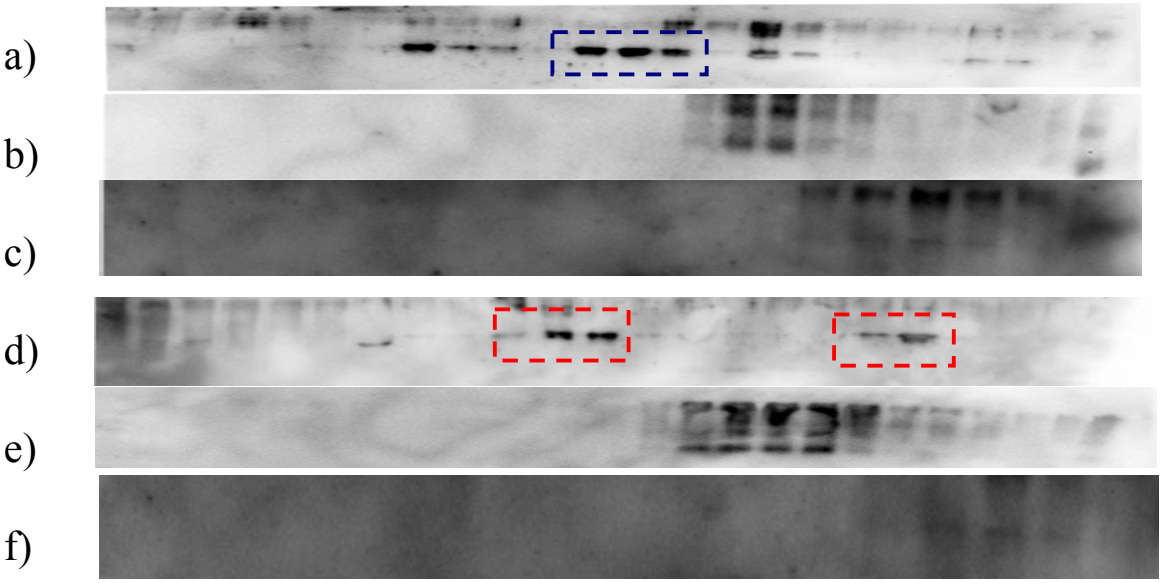

Figure 2-6: Cell fractionation on a sucrose density gradient after treatment with 2BP.
Palmitoylation was inhibited over night in protoplasts from 4 weeks-old Arabidopsis plants with 2BP (a-c) or DMSO (d-f) and then fractionated in a sucrose gradient and analysed on a western blot using antibodies for RMR1 (a, d), the vacuolar marker γ-TIP (b, e), or the ER marker BiP (c, e)

In order to confirm this mislocalisation a RMR1-YFP fusion protein was generated and transiently expressed in *Nicotiana benthamiana* leaves. RMR1-YFP perfectly colocalized with the TGN marker SYP61 (Alessandro Occhialini thesis, personal communication).

No strong effect of 2BP was detected, although the typical TGN dots appeared smaller in the 2BP-treated samples. This was confirmed by a statistical analysis of dot sizes by the Watershed Counting3D software (Gniadek and Warren, 2007), which allows to measure organelle volumes also in presence of inhomogeneous backgrounds. This analysis (Figure 2-7) indicated the presence of two populations with different sizes in the DMSO-treated sample but of a single peak for the 2BP-treated sample. This difference was statistically significant.

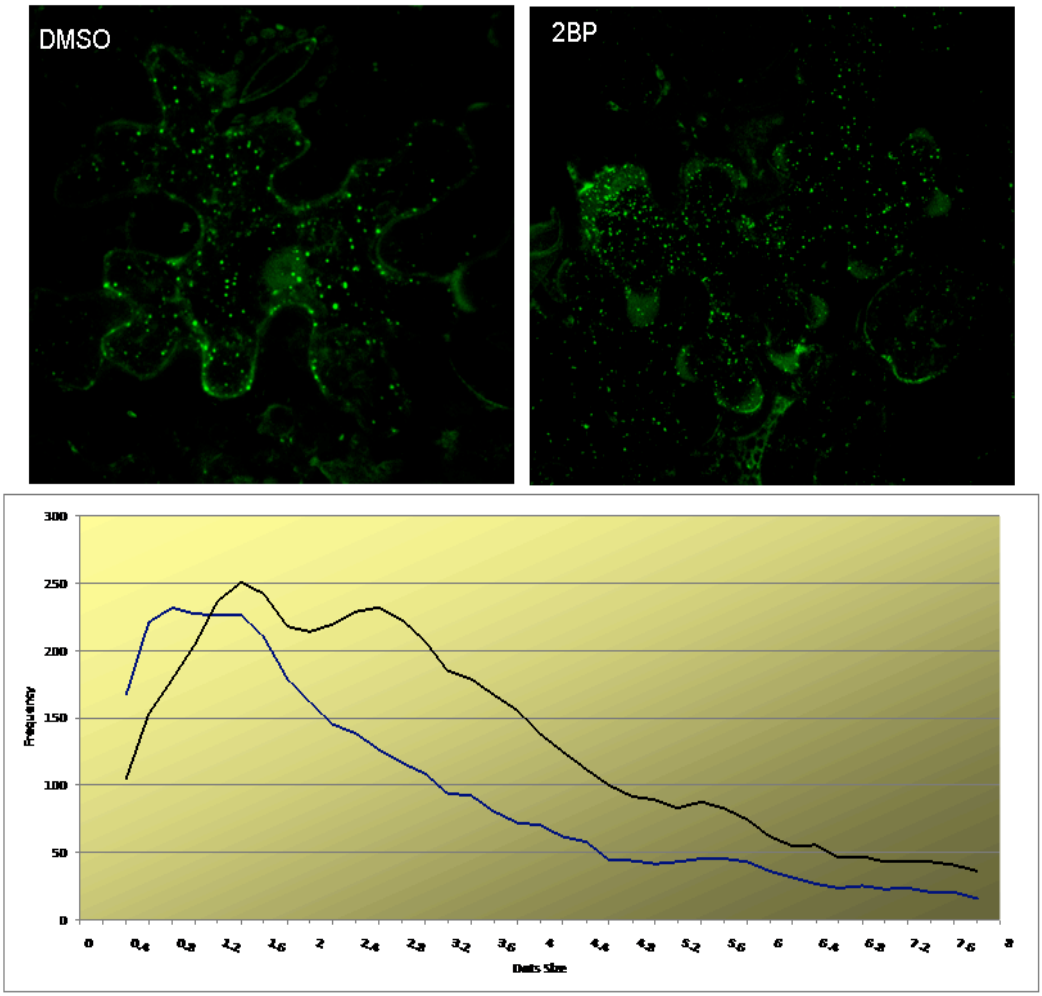

Figure 2-7: Effect of 2BP on the intracellular localisation of RMR1-YFP in epidermal cells of agro-infiltrated *N. benthamiana* leaves.

Twenty independent image stacks (ten for each treatment) of almost 20 µm thickness (from the top of the cell to the nucleus) from three independent experiments were collected on the confocal microscope using a 63x objective and were analysed with the Watershed Counting 3D software (Gniadek and Warren, 2007). A) RMR1-YFP+ DMSO; B) RMR1YFP+2BP

C) Size distribution of dots collected in groups of 0.2 voxels

Mutant versions of RMR1-YFP were generated in order to identify the palmitoylated cysteines. A triple mutant RMR1C1C3C4YFP was first analysed, where the cysteines in positions 182 (C1), 250 (C3) and 251 (C4) were mutated to alanines.

RMR1-YFP and the triple mutant were expressed together with an RFP-labelled RMR1. Any difference in localisation with RMR1-RFP was detected neither for the wild type nor for the triple mutant (Figure 2-8).

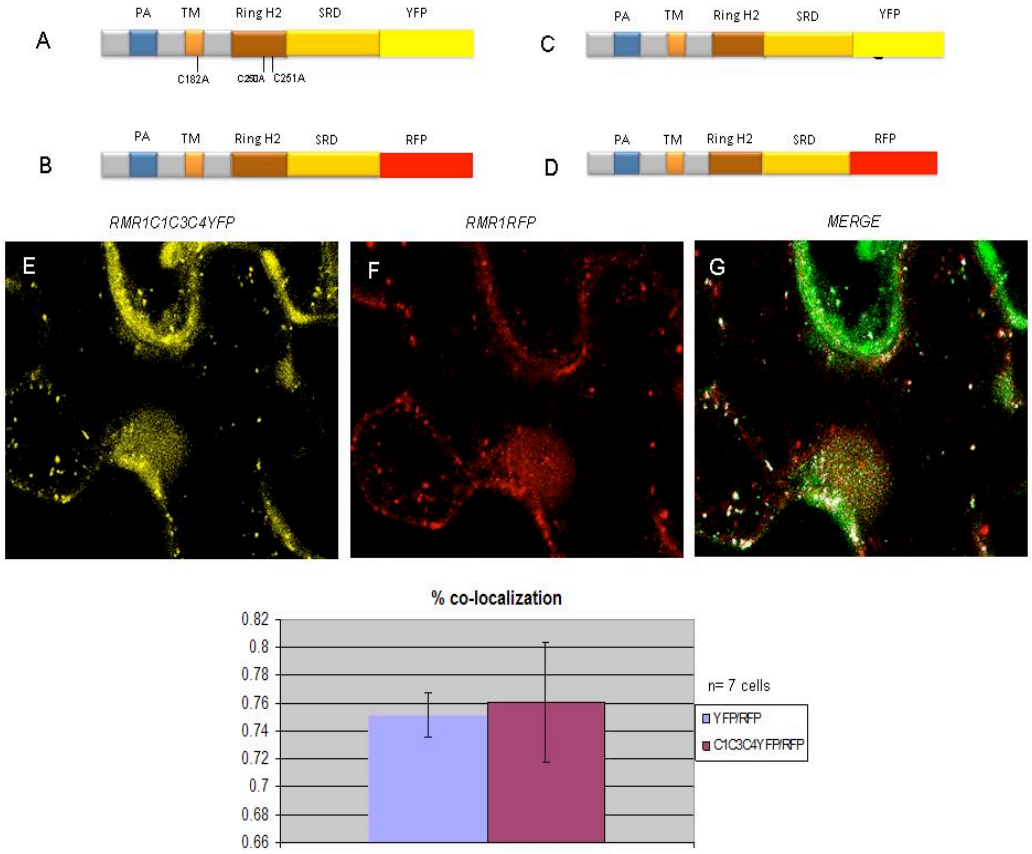

Figure 2-8: Effects of mutations in three cysteines susceptible to be palmitoylated
A) A triple Cys to Ala mutant of RMR1 was fused to YFP (RMR1C1C3C4YFP)
B, D) Wild type RMR1 was fused to RFP (RMR1RFP)
C) Wild type RMR1 was fused to YFP (RMR1YFP)
E) The pattern of the triple mutant (A)
F) The pattern of RMR1RFP (B)
G) The merged images.
G) Quantification of the colocalization between A and B (blue) and between C and B (violet). Seven different cells from three independent experiments were analysed by the ImageJ Manders coefficient plug-in.

2.6 Biotin Switch Assay of Palmitoylation

Until recently the only detection method for palmitoylation of proteins used radio-labelled ^{3}H-palmitoyl-CoA. This technique is expensive, hazardous (due to the radioactive material) and time-consuming, typically requiring up to six weeks exposure for the autoradiography.

The biotin switch assay (Figure 2-9) was first described in 2006 (Drisdel, et al., 2006) and recently adapted to plants by Hemsley et al., (2008).

In the first step all free cysteines are blocked by NEM (N-Ethylmaleimide, Figure 2-9, 1). The second step (Figure 2-9, 2) is an incubation with hydroxylamine (Hyd) at neutral pH,

which cuts all thioester bonds. The third step (Figure 2-9, 3) is the labelling of liberated cysteines with a biotinylation reagent (BMCC and HPDP were the first to be synthesized, Figure 2-10). In the negative control without hydroxylamine treatment, no biotinylation should occur as no free sulfhydryls were generated.

In the fourth step (Figure 2-9, 4) biotinylated proteins are selectively retained by a streptavidin column, due to the strong affinity between biotin and streptavidin. After elution (E Hyd+ and E Hyd-) proteins are separated by SDS-PAGE and then analysed by western blotting (Figure 2-9, 5). Following biotinylation a sample of each reaction is retained as a column loading control (C Hyd+ and C Hyd-).

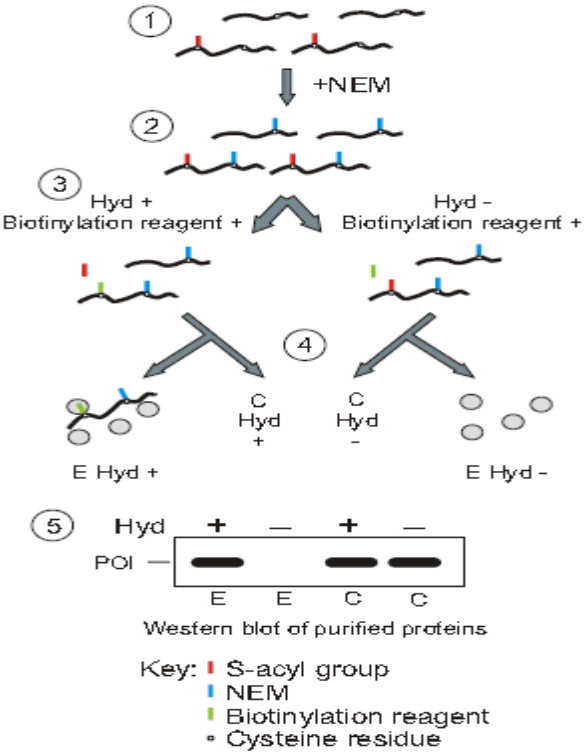

Figure 2-9: Biotin switch assay for palmitoylation

Cell extracts are treated with *N*-ethylmaleimide (NEM) to block free Cys residues (2). Half of the sample is then treated with hydroxylamine to remove palmitates from Cys residues, whereas the other half is the control sample. Both samples are then treated with the Cys-biotinylating reagent BMCC (1-biotinamido-4-(4′-(maleimidoethyl-cyclohexane)-carboxamido) butane) (3). Following biotinylation a sample of each reaction is removed to act as a column loading control (4). Biotinylated proteins are captured on a streptavidin column and eluted. Proteins eluates (E Hyd+ and E Hyd-) and loading controls (C Hyd+ and C Hyd) are then analysed by western blotting.

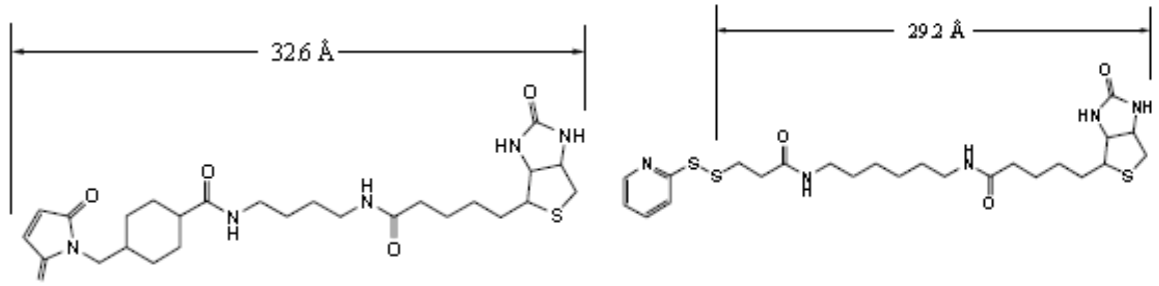

A) **B)**

Figure 2-10: Cysteine biotinylation reagents
(A) BMCC (1-biotinamido-4-(4′-(maleimidoethyl-cyclohexane)-carboxamido) butane). (B) HPDP (N-[6-(Biotinamido)hexyl]-3´-(2´-pyridyldithio)propionamide). BMCC has a maleimide group while HPDP has a pyridyldithiol group. Both groups react with -SH groups to form a stable disulfide bond with a thiol group of a cysteine. The main difference between the two reagents is in the possibility to cleave the disulphide bond formed by HPDB with the protein by a reducing agent such as 2-mercaptethanol.

We performed this assay for *At*RMR as described above. We could observe two different forms of RMR1 (Figure 2-11). Only the upper band is biotinylated and represents a small percentage of RMR1, if compared to the lower band. The upper band, approximately at double of the molecular weight, is much less if compared with the band at the expected molecular weight (around 50Kda). This might reflect a transient palmitoylation of RMR1.

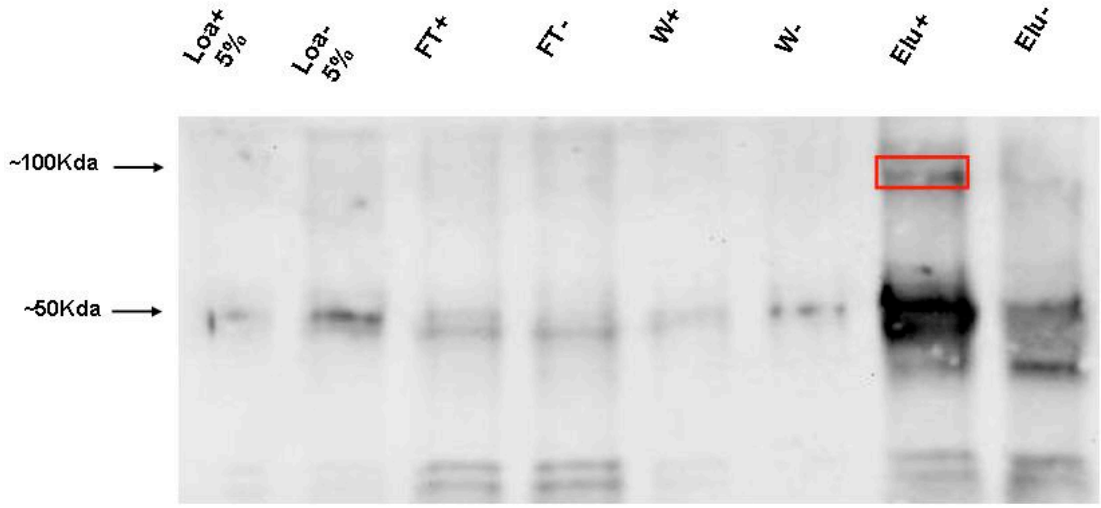

Figure 2-11: Biotin switch assay for AtRMR1
This experiment, led on one month old Arabidopsis leaves, shows clearly RMR1 palmitoylation, but with a complex pattern. Indeed, it is possible observe two distinct bands in the loading (either with Hydroxylamine or without) and only one in the purification.

2.7 Stability of the triple cysteine mutant

The triple cysteine mutation did not significantly mislocalise RMR1. Would it change its stability? Leaves from *Nicotiana benthamiana* were agroinfiltrated with the triple cysteine mutant-YFP fusion or with the wild type RMR-YFP fusion. Protein extracts obtained at different time points after infiltration were separated by SDS-PAGE, blotted and probed with anti-GFP antibody. We detected proteins with MW between 50 and 150 kDa. The highest band was present at 48h of expression in agroinfiltrated leaves with both the wild type construct and the triple cysteine mutant. However, at 72h of expression, this band was strongly reduced or completely gone. Bands at 50Kda represent a truncated form of the protein and do not show big quantitative differences (Figure 2-12).

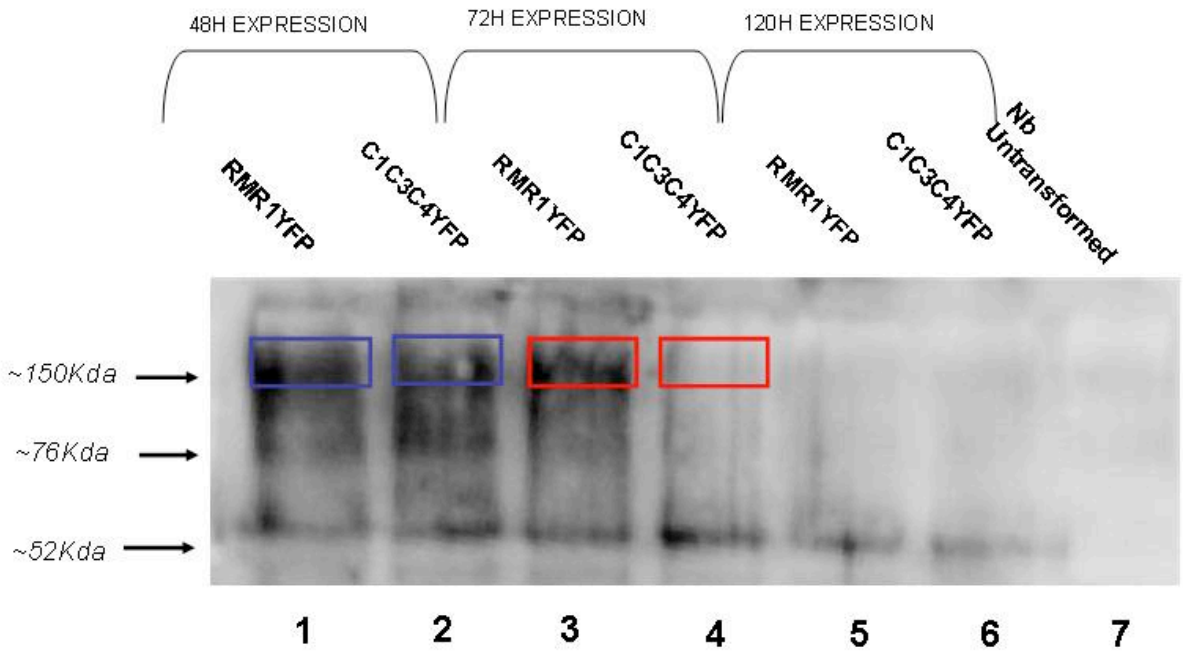

Figure 2-12: Stability of the triple cysteine mutant
Total extract from *N. benthamiana* leaves agroinfiltrated with RMR1YFP and RMR1C1C3C4YFP were obtained at different time points and analysed by western blotting using an anti-GFP antibody. Apparent molecular weights are also showed on the right. Lanes 1 3 and 5: leaves agroinfiltrated with RMR1YFP; lanes 2, 4 and 6: leaves agroinfiltrated with RMR1C1C3C4YFP. Lane 7: non-infiltrated leaves. Samples were collected after 48h (lanes 1 and 2), 72h (lanes 3 and 4) and 120h (lanes 5 and 6)

2.8 Phosphorylation of RMR1

Preliminary bioinformatics studies highlighted the presence of high number of potentially phosphorylated serines (but also threonines and tyrosines) phosphorylated (Table 2-2). As is clear from the photo 2-10, a large number of putative sites to be phosphorylated is located in the C-terminal region of RMR1 and in particular its Serine-Rich domain. To verify the presence of a large number of phosphorylated amino acid residues, we incubated an extract of total proteins of Arabidopsis leaves in the presence or absence of CIP (Calf Intestinal phosphatase). The Western blot is shown in Figure 2-14. Since the difference between the highest bandwidth and lowest is around 15-17 kDa, we deduce that RMR1 is subject to a high phosphorylation. The phosphorylation of such a large number of residue remains to be elucidated.

A) Serine predictions

Name	Pos	Context v	Score	Pred
Sequence	15	VCTVSCLAS	0.007	.
Sequence	19	SCLASSKVI	0.137	.
Sequence	20	CLASSKVIL	0.024	.
Sequence	32	NITLSFDDI	0.923	*S*
Sequence	43	NFAPSVKGT	0.994	*S*
Sequence	72	KPEQSSNET	0.882	*S*
Sequence	73	PEQSSNETS	0.966	*S*
Sequence	77	SNETSPFVL	0.446	.
Sequence	88	RGGCSFEEK	0.820	*S*
Sequence	122	MAGNSGGIR	0.008	.
Sequence	156	WLIPSFENS	0.066	.
Sequence	160	SFENSAWSI	0.013	.
Sequence	163	NSAWSIMAV	0.114	.
Sequence	168	IMAVSFISL	0.062	.
Sequence	171	VSFISLLAM	0.007	.
Sequence	176	LLAMSAVLA	0.036	.
Sequence	195	RRRTSRSSR	0.997	*S*
Sequence	197	RTSRSSRVR	0.968	*S*
Sequence	198	TSRSSRVRE	0.998	*S*
Sequence	207	FHGMSRRLV	0.077	.
Sequence	216	KAMPSLIFS	0.047	.
Sequence	220	SLIFSSFHE	0.054	.
Sequence	221	LIFSSFHED	0.072	.
Sequence	261	ACVDSWLTS	0.009	.
Sequence	265	SWLTSWRTF	0.693	*S*
Sequence	280	DARTSTGEP	0.998	*S*
Sequence	287	EPPASESTP	0.798	*S*
Sequence	289	PASESTPLL	0.020	.
Sequence	294	TPLLSSAAS	0.144	.
Sequence	295	PLLSSAASS	0.139	.
Sequence	298	SSAASSFTS	0.221	.
Sequence	299	SAASSFTSS	0.927	*S*
Sequence	302	SSFTSSSLH	0.329	.
Sequence	303	SFTSSSLHS	0.115	.
Sequence	304	FTSSSLHSS	0.590	*S*

Sequence	307	SSLHSSVRS	0.986	*S*
Sequence	308	SLHSSVRSS	0.961	*S*
Sequence	311	SSVRSSALL	0.009	.
Sequence	312	SVRSSALLI	0.637	*S*
Sequence	319	LIGPSLGSL	0.017	.
Sequence	322	PSLGSLPTS	0.014	.
Sequence	326	SLPTSISFS	0.965	*S*
Sequence	328	PTSISFSPA	0.022	.
Sequence	330	SISFSPAYA	0.881	*S*
Sequence	335	PAYASSSYI	0.184	.
Sequence	336	AYASSSYIR	0.004	.
Sequence	337	YASSSYIRQ	0.968	*S*
Sequence	342	YIRQSFQSS	0.843	*S*
Sequence	345	QSFQSSSNR	0.903	*S*
Sequence	346	SFQSSSNRR	0.094	.
Sequence	347	FQSSSNRRS	0.956	*S*
Sequence	351	SNRRSPPIS	0.991	*S*
Sequence	355	SPPISVSRS	0.994	*S*
Sequence	357	PISVSRSSV	0.270	.
Sequence	359	SVSRSSVDL	0.996	*S*
Sequence	360	VSRSSVDLR	0.925	*S*
Sequence	369	QQAASPSPS	0.995	*S*
Sequence	371	AASPSPSPS	0.587	*S*
Sequence	373	SPSPSPSQR	0.955	*S*
Sequence	375	SPSPSQRSY	0.957	*S*
Sequence	378	PSQRSYISH	0.929	*S*
Sequence	381	RSYISHMAS	0.628	*S*
Sequence	385	SHMASPQSL	0.726	*S*
Sequence	388	ASPQSLGYP	0.246	.
Sequence	395	YPTISPFNT	0.969	*S*
Sequence	403	TRYMSPYRP	0.997	*S*
Sequence	408	PYRPSPSNA	0.991	*S*
Sequence	410	RPSPSNASP	0.045	.
Sequence	413	PSNASPAMA	0.811	*S*
Sequence	419	AMAGSSNYP	0.005	.
Sequence	420	MAGSSNYPL	0.012	.
Sequence	430	PLRYSESAG	0.917	*S*
Sequence	432	RYSESAGTF	0.005	.
Sequence	437	AGTFSPYAS	0.943	*S*
Sequence	441	SPYASANSL	0.167	.
Sequence	444	ASANSLPDC	0.668	*S*

B) Threonine predictions

Name	Pos	Context v	Score	Pred
Sequence	13	LYVCTVSCL	0.023	.
Sequence	30	RNNITLSFD	0.009	.
Sequence	47	SVKGTGEIG	0.027	.
Sequence	76	SSNETSPFV	0.027	.
Sequence	114	EDRGTLIAM	0.090	.
Sequence	133	AVFVTKETG	0.016	.
Sequence	136	VTKETGEVL	0.239	.
Sequence	149	GFPDTKVWL	0.760	*T*
Sequence	181	AVLATCFFV	0.009	.
Sequence	194	IRRRTSRSS	0.994	*T*
Sequence	227	HEDNTTAFT	0.211	.
Sequence	228	EDNTTAFTC	0.013	.
Sequence	231	TTAFTCAIC	0.009	.
Sequence	240	LEDYTVGDK	0.095	.
Sequence	264	DSWLTSWRT	0.845	*T*
Sequence	268	TSWRTFCPV	0.209	.

Sequence	279	RDARTSTGE	0.304	.
Sequence	281	ARTSTGEPP	0.755	*T*
Sequence	290	ASESTPLLS	0.421	.
Sequence	301	ASSFTSSSL	0.040	.
Sequence	325	GSLPTSISF	0.050	.
Sequence	393	LGYPTISPF	0.255	.
Sequence	399	SPFNTRYMS	0.551	*T*
Sequence	435	ESAGTFSPY	0.240	.

C) Tyrosine predictions

Name	Pos	Context	Score	Pred
Sequence	10	VLLLYVCTV	0.053	.
Sequence	54	IGVVYVAEP	0.108	.
Sequence	107	AAIIYDNED	0.417	.
Sequence	143	VLKEYAGFP	0.042	.
Sequence	239	CLEDYTVGD	0.770	*Y*
Sequence	333	FSPAYASSS	0.950	*Y*
Sequence	338	ASSSYIRQS	0.396	.
Sequence	379	SQRSYISHM	0.552	*Y*
Sequence	391	QSLGYPTIS	0.203	.
Sequence	401	FNTRYMSPY	0.964	*Y*
Sequence	405	YMSPYRPSP	0.426	.
Sequence	422	GSSNYPLNP	0.176	.
Sequence	429	NPLRYSESA	0.434	.
Sequence	439	TFSPYASAN	0.658	*Y*

Table2- 2: Prediction of phosphorylated sites in RMR1

In A) List of all possible phosphorylated serines in RMR1 with a score >0.8 (*S*); in B) List of all possible phosphorylated threonines in RMR1 with a score >0.8 (*T*) in C) list of all possible phosphorylated tyrosines in RMR1 with a score >0.8 (*Y*)

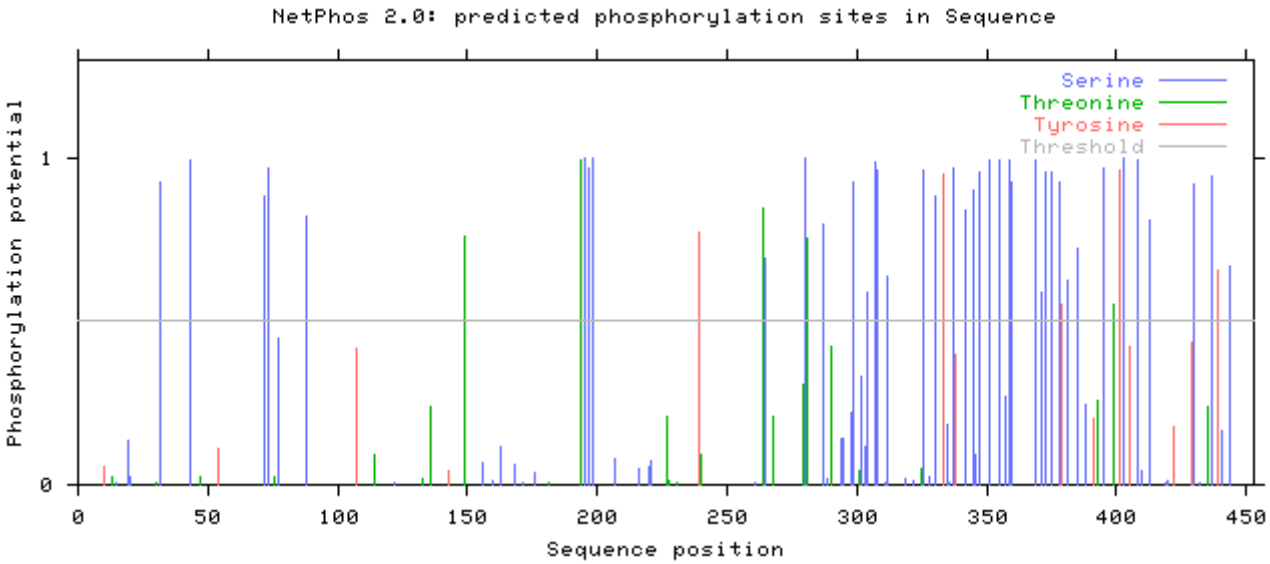

Figure 2-13: Prediction of phosphorylated sites in RMR1

Scheme of prediction phosphorylation sites in RMR1 realized by NetPhos 2.0. PA domain sequence position: 43-151; TM domain sequence position:162-184; RING-H2 domain sequence position: 232-274; SRD sequence position: 287-443

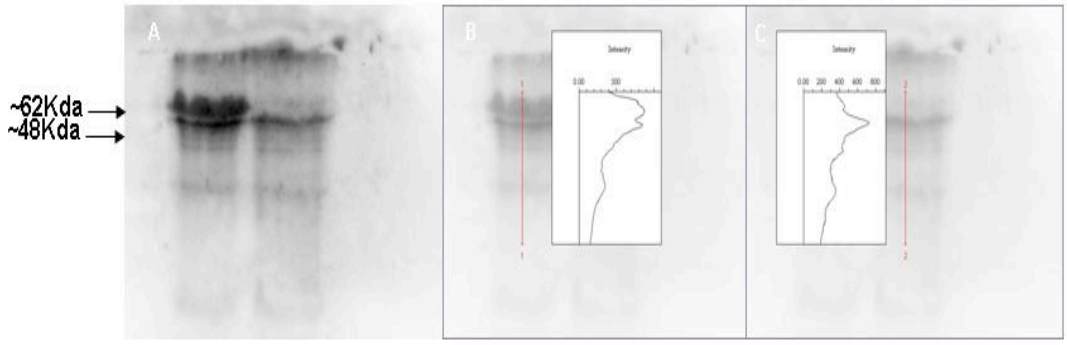

Figure 2-14: CIP assay for RMR1
Total protein extract from *A.thaliana* leaves were extracted and incubate in Tris-HCl EDTA TX100 0.5% sucrose buffer pH 7.5 for 1h at 37 C. First lane: Total extract plus CIP, Second lane: Total extract minus CIP. In A overexposed membrane. In B&C analysis of intensity of the bands revealed by the GelDoc Biorad. In B&C are represented not overexposed membranes for not going out of scale during the reading.

2.9 Discussion

Preliminary *in silico* analyses (table 2-1) had shown a possible palmitoylation of the vacuolar sorting receptor *At*RMR1. In order to verify the effective palmitoylation of *At*RMR1, we used a new technique, the biotin switch assay (Drisdel, et al., 2006; Hemsley, et al., 2008; Hemsley and Grierson, 2008; Hemsley, 2009). This technique has several advantages compared to the classical use of radiolabelled palmitate: it is less expensive, less hazardous (no radioactive material), and less time-consuming (normally 3-4 days are sufficient to detect a palmitoylated protein).

This method allowed detecting a palmitoylated protein corresponding to a higher molecular weight band of about 100Kda (Figure 2-11). This might be a either a dimer or a RMR1 stably associated with another protein partner. However, in both cases it must be assumed that the inter-polypeptide bond could not be reduced by β-mercaptoethanol. Several examples of such stably associated higher molecular weight complexes have been reported (Joazeiro, et al., 1999; Chen, et al., 2000; Leverson, et al., 2000; Miller, et al., 2006) . The protein c-cbl is a 120 KDa protein that contains a RING finger domain, like RMR1. The two proteins do not show any significant similarity over the entire protein sequence, but the two RING finger domains are quite similar, having a 31% of identity. c-abl can recognize the platelet-derived growth factor receptor (Miyake, et al., 1998) by its SH2 domain and in turn, catalyse its

ubiquitination. Normally this complex (formed by c-abl and the platelet derived growth factor) are stable bound and not–reducible by the β-mercaptoethanol A similar mechanism might be involved also for RMR1.

In RMR1 homologs the cytosolic serine-rich domain was demonstrated to be important for protein-protein interactions (Briknarová, et al., 2005), the RING-H2 domain could catalyse the ubiquitination of target protein/s. Further analyses, including immunoprecipitation of RMR1 are needed in order to elucidate the nature of this high molecular weight form.

In order to characterize the role of palmitoylation for RMR1, a C-terminal YFP fusion construct was expressed in *N. benthamiana* leaves. Leaves were then treated with 2-bromopalmitate, a well-known inhibitor of palmitoylation. Treated and untreated samples did not differ much, although in the treated sample dots looked somewhat smaller. To quantify this difference, confocal stacks from 20 different cells were analysed by the software Watershed 3D counting, which allows analysing confocal stacks with a non-uniform background. This last feature was very useful since transient expression in *Nicotiana* very often gives a non-uniform background because of the free fluorescent marker. This analysis confirmed that in the control samples the fluorescence was associated with two different sizes of dots, while in 2BP-treated samples there was a single size of dots. This change in localisation was also confirmed by sucrose gradient fractionation. In control *Arabidopsis thaliana* protoplasts, *At*RMR1 was also associated with two different groups of fractions at different sucrose densities. On the contrary, 2BP-treated protoplasts *At*RMR1 was shifted in the gradient with a major peak at density different from the peaks in the control samples.

I next wanted to identify the cysteine(s) needed for palmitoylation. The first tested cysteine was C182, which is located at the border between the transmembrane domain and the cytosolic tail. Many proteins have indeed been found to be palmitoylated at this border (Levental, et al., 2010a). Since any change in mislocalisation was possible to detect if changing all the TMD (Alessandro Occhialini thesis, personal communication), I began to test the triple mutant C1C3C4 (C182, C250 and C251 mutated to alanine, also as YFP fusion). This mutant also did not show any significant change in localisation (Figure 2-8), although some punctate structure associable with the mutant form does not show co-localization with the wild type fusion protein). This might be explained either by a different number of the Agrobacteria infecting the cells in the transient assay, and therefore to a different numbers of proteins present in the cells and, ultimately, to a different rate of accumulation in the final compartment, or to a different rate of accumulation between the triple mutant and mutant form. However, further analysis by immunoblot showed that the high molecular weight band

at ~150Kda (Figure 2-12) (comparable with the wild type form a ~100Kda observed in BSA, Figure 2-11) mostly disappeared after 72h of expression for the mutant, but much less for the wild type. Global expression level at longer incubation times was low for both wild type and mutant constructs. This indicates that this triple mutant affects the stability of the fusion protein. This could be due to the Cys250 (C3), which is involved in Zn^{2+} coordination. Its mutation might be responsible for the reduced stability of the protein. Only the cysteine in position 232 (C2) needs to be checked with the triple cysteine mutant in order to determine definitely if all the four cysteines may be responsible for the change in localization. Single mutations have been rejected from the study of RMR1 localization since deletion of the RING-H2 and/or the Serine-Rich domain, trans-membrane domain and PA domain does not change the localization of the protein (Alessandro Occhialini thesis, personal communication). In conclusion the mislocalisation observed in Figure2-6 and 2-7 might be due either to a cumulative effect of the four predicted cysteines or to a side effect of the drug on some protein partner/s.

A similar complex SDS-PAGE pattern is observable for one of the few animal RMR homologs: RNF13 (Bocock, et al., 2009). RNF13 has a similar domain organization with a luminal PA domain, a transmembrane domain, and a cytosolic tail with a RING-H2 domain and a serine-rich domain. RNF13 is an endosome-associated protein with an E3-ligase activity catalysed by its RING-H2 domain. The wild type form is barely detectable by western blotting (like RMR1), but it becomes more visible and at a higher molecular weight once cells are incubated with either MG132 or epoxomycin (proteasome inhibitors). The pattern consists of a heterologous group of proteins at 80Kda, a second group of proteins at 45 KDa and one protein band at 36Kda. The expected molecular weight for RNF13 is ~45Kda. In immunoprecipitation assays the authors showed that the N-terminal domain of RNF13, such as the C-terminal domain, is released TM domain around the middle of the protein. Any information is available about protease/s involved in this process and in which compartment this proteolytic process occurs. This protein is also modified by acquiring carbohydrate modification. This work shows extensive post-translation modifications of RNF13.

Finally, RMR1 shows also a high degree of phosphorylation as shown in Figure 2-14. In order to elucidate the role of each putative residue involved in the phosphorylation a high-throughput proteomic analysis needs to be performed. In conclusion, RMR1, like its closest human homolog RNF13, shows a complex post-translation modification (including palmitoylation, phosphorylation and proteolytic cleavages), which needs to be further clarified.

3. Role of palmitoylation in the secretory pathway

3.1 Introduction

Palmitoylation is a general post-translation modification in all eukaryotic cells. In animal cells, where its role has been intensely investigated and debated, it fulfils different roles: protein stability and localization, rearrangement of protein structure within a lipid bilayer, promotion of protein binding. In contrast, very little is known about the role of palmitoylation in plant cells. In the previous chapter we have described that *At*RMR1 may well be palmitoylated, but that preventing its palmitoylation by mutating its putative modified cysteines did not affect its localisation. However, the specific palmitoylation inhibitor 2-bromopalmitate (2BP) affected the localisation of *At*RMR1, an effect that is probably indirect. This chapter investigates the effect of 2BP inhibiting tip growth in two model systems: *Nicotiana benthamiana* pollen tubes and *Physcomitrella patens* protonema.

3.2 S-PALMITOYLATION

S-Palmitoylation of cysteines in proteins is a pervasive post-translational modification occurring in all eukaryotic cells. The acyl donor is palmitoyl-CoA (Pal-CoA), a 16 carbons fatty acid and the major product from cellular fatty acid synthesis. The ionized thiolate side chain of cysteine residues is the most reactive side chain in proteins. This acyl transfer is a transthiolation (Figure 3-2) and is a reversible reaction, in contrast to protein N-myristoylation and N-farnesylation (which both produce an acyl amide, Figure 3-1), which is a high-energy bond. However, when the palmitoylation occurs at an N-terminal cysteine, a thioester intermediate is formed, followed by a rearrangement to a stable amide linkage. This N-palmitoylation is not reversible (Linder and Deschenes, 2007) (Pepinsky, et al., 1998). In the following, palmitoylation will refer to S-acylation, not to N-palmitoylation.

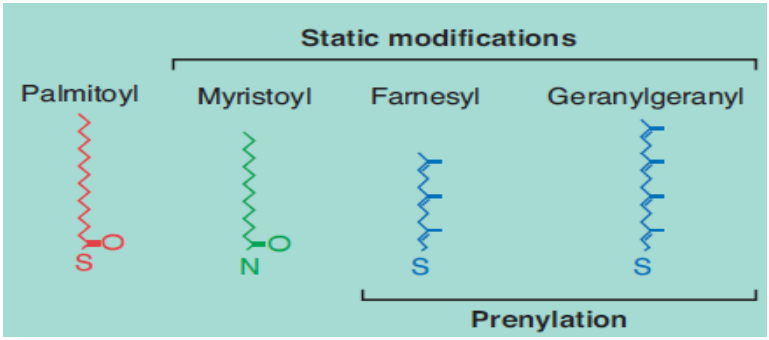

Figure 3-1: Possible lipidations in eukaryotic cells
Protein lipid modification by myristoyl moiety (C_{14}), farnesyl (C_{15}) or geranylgeranyl (C_{20}) are static modifications and therefore are not responsible for cycling of Ras superfamily proteins ((Conibear and Davis, 2010).

3.2.1 Mechanism of protein palmitoylation by Palmitoyl Acyl Transferases (PATs)

S-acylation is catalysed by membrane-bound S-acyl transferases (Roth, et al., 2002) (Figure 3-3).

In yeast and mammals PATs are highly compartmentalized (Ohno, et al., 2006), being found in most cellular compartments, although mechanisms and/or signals which sort these proteins are unknown (Hemsley and Grierson, 2008). Palmitoyl transfer to the target protein requires a previous membrane association, which can be favoured by prenylation, myristoylation or protein-protein interactions. This may help to determine PAT specificity by limiting the number of its targets (Hemsley and Grierson, 2008). Although this interpretation has been verified for many small GTPases, it is not true for membrane proteins or tail-anchored proteins (e.g. Tlg1), which have been found only S-acylated. Once the substrate is S-acylated, it remains attached to the membrane, which does not hinder its trafficking between different intracellular compartments (Adjobo-Hermans, et al., 2006; Zeng, et al., 2007).

It has been shown that the DHHC (Asp-His-His-Cys)-motif domain in the catalytic enzyme is responsible for S-acylation (Lobo, et al., 2002; Roth, et al., 2002). The first two DHHC proteins were identified in yeast: Erf2p and Akr1p. Both are polytopic membrane proteins with four predicted transmembrane domains. Erf2p recruits Erf4p at the ER (Zhao, et al., 2002) and both have a specific palmitoylation activity *in vivo* on farnesylated Ras2 (Lobo, et al., 2002). Mutations in the DHHC box of Erf2p interfere with palmitoylation of Ras2 *in vitro* and *in vivo*. The other identified DHHC protein Akr1p is necessary for the correct targeting of

two casein kinase homologues (Yck1-2p) to the plasma membrane (Feng and Davis, 2000; Dietrich and Ungermann, 2004).

Akr1p was shown to add at the Golgi palmitate to Yck2p, which is then transported to the plasma membrane via vesicles (Roth, et al., 2002; Babu, et al., 2004). Purified Akr1p can palmitoylate both Yck2p and itself. Self-palmitoylation is an independent process and occurs even if the substrate Yck2p is absent from the reaction medium. Mutations in the DHHC box abolish both self-palmitoylation and palmitoylation of Yck2p. Surprisingly, the process is somehow accelerated in the presence of ATP, although neither Akr1p nor Yck2p have any nucleotide-binding domain which could explain this acceleration (Davis, et al., 2001).

PATs have been classified in three categories: ankyrin repeat-containing (Roth, et al., 2002; Huang, et al., 2004; Hemsley, et al., 2005), heterodimeric (Lobo, et al., 2002; Swarthout, et al., 2005) and monomeric PATs (Keller, et al., 2004). Although ankyrin repeats have been involved in protein-protein interactions, no functional link has been found with S-acylation. The *Arabidopsis* genome encodes 23 putative PATs but only one with an ankyrin repeat, TIP1. *tip1* KO plants have a reduced cell size, a reduced pollen tube growth rate and cell polarity defects, showing that this PAT has an important role in the plant (Schiefelbein, et al., 1993; Ryan, et al., 1998; Hemsley, et al., 2005).

However, as briefly mentioned above, palmitoylation can occur spontaneously *in vitro* without the help of any enzyme (Duncan and Gilman, 1996; Veit, et al., 1998; Bijlmakers and Marsh, 2003; Smotrys and Linder, 2004) and auto-palmitoylation occurs at the same cysteines as in the *in vivo* enzymatic reaction, even if at a slower rate (Leventis, et al., 1997; Bano, et al., 1998). This plethora of data supporting auto-palmitoylation has led to speculate that enzymes may be unnecessary for the palmitoyl transfer (Bizzozero, et al., 2001). In support of this idea, Bizzozero and colleagues have found that, under appropriate conditions, the activation energy required for the uncatalysed palmitoyl transfer onto a synthetic peptide is lower than for the enzymatic reaction (Bharadwaj and Bizzozero, 1995). Therefore, auto-acylation can occur spontaneously. The basic step in either self or trans palmitoylation is the formation of the thiolate anion, as only the anion can act as a nucleophile on the thioester bond in Palm-CoA (Figure 3-2).

If auto-acylation is necessary for the S-acylation (trans-acylation), this raises two questions: how spontaneous is the transfer of palmitate and at which level is it controlled. The pK of the sulfhydryl group of cysteine is 8.5, which makes the formation of the thiolate less improbable at the neutral intracellular pH. However, in a protein the pK_a can be reduced by up to six pH units (Mossner, et al., 2000) by amino acids with an acidic side chain, making the reaction

highly probable. The dependence of thiolate formation on the position in a protein can also explain that auto-acylation has the same target cysteines as *in vivo* S-acylation (O'Brien and Colwell, 1987; Quesnel and Silvius, 1994; Bharadwaj and Bizzozero, 1995; Schroeder, et al., 1996; Schroeder, et al., 1997). The auto-acylation can also be stimulated by protein-protein interactions that can change the pK_a of a target cysteine. Indeed, acylation of SNAP-25 is almost 100 times more efficient when it is bound to the SNARE syntaxin1a (Veit, 2000).

Another possible level of control of spontaneous acylation is the availability of Palm-CoA in the cell. In all organisms, Palm-CoA is buffered by acyl-CoA binding protein, which maintains the intracellular concentration of free Palm-CoA within a low nanomolar range (Faergeman and Knudsen, 1997). This buffering may be critical to prevent uncontrolled reactions.

In this context, it is remarkable that no kinetics has been presented either for Erf2p or for Akr1p and that the only data supporting an enzymatic activity are the mutations of the DHHC sequence, which demonstrate that these amino acids are indispensable for the formation of the thioester intermediate (Lobo et al. 2002, Roth et al. 2002).

Recently the spatial organization of the palmitoylation machinery has been analysed in mammalian cells (Rocks, et al., 2010). The authors, using a very original biochemical approach, revealed that palmitoylation occurs in the Golgi and that this organelle contributes to the directionality of the palmitoylation for proteins that enter into the secretory pathway and are delivered to the plasma membrane. Moreover, the authors propose a model for the selectivity of palmitoylation. In fact, they assert that any protein can be palmitoylated if it has an accessible thiol group with a transient access to the Golgi membrane. This might be given by a myristoyl or prenyl moiety, a transmembrane domain or by Golgi-associated protein partners. This leads to a very important question: While in yeast PATs are localized in different endomembrane compartments (Ohno, et al., 2006; Hou, et al., 2009), why are all 25 mammalian PATs but one localized in the Golgi (Noritake, et al., 2009), if just one or a few enzymes would be sufficient? The authors propose that this abundance of PATs in the Golgi might improve the efficiency of the whole process. However, it could be that some PATs have other biological functions than palmitoylation, like yeast Swi1p, which is involved in polarized secretion (Dighe and Kozminski, 2008).

Until a few years ago, there was no reliable algorithm predicting S-Acylation from protein sequences. Now, new software gives an answer with a good confidence degree: http://csspalm.biocuckoo.org/

3.2.2 Palmitoylation and raft localization

Several studies have indicated that palmitoylated proteins selectively accumulate in cholesterol- and sphingolipid-rich lipid rafts (Waheed and Jones, 2002). Lipid rafts are liquid-ordered membrane micro-domains and are mainly localized in plasma membranes, but can also be found in internal membrane compartments such as Golgi and TGN (Fullekrug and Simons, 2004). The lipid rafts in TGN are implicated in sorting to the apical plasma membrane in epithelial cells and neurons, while basolateral sorting depends on short amino acid sequences present in cytosolic domains of proteins (Keller and Simons, 1997; Fullekrug and Simons, 2004). Little information is available on the presence of lipid rafts in other compartments than the PM, although it is known that proteins localized in lipid rafts acquire their detergent resistance in the TGN (Levental, et al., 2010a).

The model mainly developed for animal cells asserts that rafts can ferry protein cargoes to specific membrane destinations, or that they act as a platform on which proteins can assemble to form complexes. These lipid rafts are also named Detergent-Insoluble Membranes (DIM) or Detergent-Resistant Membranes (DRM) as they are insoluble in Triton X-100 at 4 °C. A recent analysis on palmitoylated proteins in neurons suggested that this process occurs as a ubiquitous post-translational modification. Indeed the list of palmitoylated proteins involved in presynaptic and\or postsynaptic trafficking is long: Synaptotagmin-1, synaptobrevin-2, SNAP-25, GAD-65, PSD95, etc. (Hess, et al., 1992; Solimena, et al., 1994; Nakata, et al., 1998; Topinka and Bredt, 1998; Veit, 2000; Fukata and Fukata, 2010).

Different roles for S-acylation are the regulation of protein-protein interactions and the regulation of transmembrane domain length (see Figure 3-4).

S-acylation promotes and increases membrane affinity of proteins which otherwise have a weak affinity (such as Ras superfamily proteins). Following S-acylation proteins are trapped and they approach each other promoting membrane clusters (Figure 3-4a).

S-acylation may mask the binding site for other partners or to the contrary increase the proximity of a protein-binding domain to another membrane protein, enhancing the probability of productive interactions. In addition to these direct effects protein, palmitoylation may indirectly regulate protein-protein interactions by spatially coupling or segregating proteins within lipid microdomains. (Figure 3-4b)

Palmitoylation may enhance hydrophobic matching between a transmembrane domain and the lipid bilayer. This can happen when there is a discrepancy between the bilayer thickness and

the length of the TM domain. This discrepancy is energetically unfavourable and can lead the protein aggregation (Lam, et al., 2006) or to ubiquitination (Valdez-Taubas and Pelham, 2005). S-acylation can thus promote the lateral movement of the protein towards membrane microdomains (Figure 3-4c).

Palmitoylation can also relieve hydrophobic mismatch by altering the tilt of transmembrane helices within the bilayer (Kandasamy and Larson, 2006). Indeed, palmitoylation of hydrophobic membrane-spanning peptides was suggested to modify peptide orientation in lipid vesicles (Joseph and Nagaraj, 1995) (Figure 3-4d).

Moreover, S-Acylation can drastically affect the localisation of several proteins. ROP10 (AtRac8, a small membrane GTPase) is localised at PM when it S-acylated (Lavy et al. 2002). When palmitoylation is inhibited by 2Br-Palmitate, ROP10 is mainly localised in the cytosol (like in Figure 3-4a). Examples of palmitoylated proteins are depicted in Figure 3-5.

In contrast to palmitoylation, very little is known about depalmitoylation. Apt1 (Acyl protein thioesterase1) is a cytosolic protein that was identified because it removed *in vitro* a palmitoyl moiety from proteins such as H-Ras, Gα subunits and endothelial nitric oxide synthase and enhanced the rate of palmitate turnover when these proteins were overexpressed in cells (Duncan and Gilman, 1998; Duncan and Gilman, 2002; Prescott, et al., 2009). Apt1 is clearly active against different targets, there is no further investigation of its specificity or range of substrates. As not all palmitoylated proteins undergo dynamic palmitoylation cycles, Apt1 could be the factor determining $t_{1/2}$ of palmitoylation. Proteins that are not substrates of Apt1 would remain palmitoylated until they are finally degraded.

Sensitivity to Apt1 might be due directly to the protein sequence around the palmitoylated cysteine(s). Alternatively, sensitivity might be indirectly due to the intracellular localization or to the protein-protein interactions of target proteins. A third possibility is that Apt1 just appears to be the only thioesterase identified so far. However there is no proof that Apt1 is a general protein thioesterase (Prescott, et al., 2009). After all, gene knockout of Apt1 gene in *Saccharomyces cerevisiae* caused no growth defects and/or any remarkable phenotype (Duncan and Gilman, 2002).

Depalmitoylation is also important for protein degradation. In this regard, two lysosomal thioesterases have been identified: Ppt1 and Ppt2 (for Protein palmitoyl thioesterase) (Camp and Hofmann, 1993; Camp, et al., 1994; Verkruyse and Hofmann, 1996). These two enzymes have very different substrates: Ppt1 is active on palmitoylated proteins while Ppt2 is active on Palm-CoA (Camp and Hofmann, 1993; Camp, et al., 1994; Soyombo and Hofmann, 1997).

Thus, it is evident that more research is required to elucidate the role of thioesterification in

cell: specific thioesterase inhibitors will be useful tools to clarify open questions on the function of Apt1 (Deck, et al., 2005; Biel, et al., 2006).

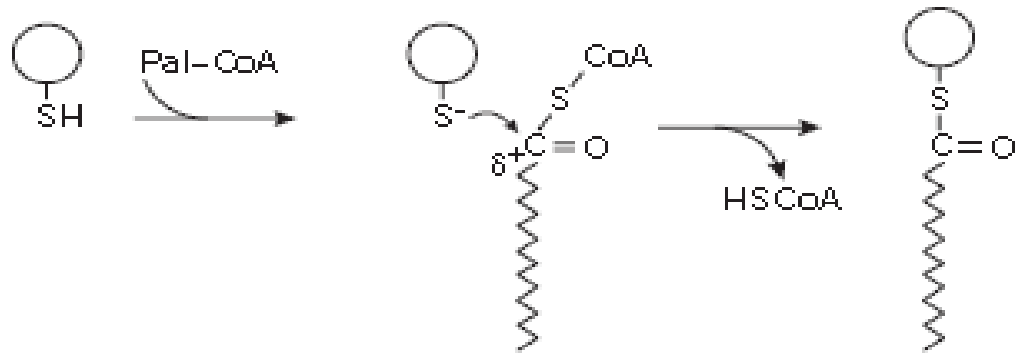

Figure 3-2: Mechanism of palmitoylation
A basic representation of protein palmitoylation. The sulfhydryl group is deprotonated to form a thiolate. The thioester bound is formed by a nucleophilic attack of the thiolate on the carboxylate of the palmitate, resulting in a palmitoylated protein (Dietrich and Ungermann, 2004)

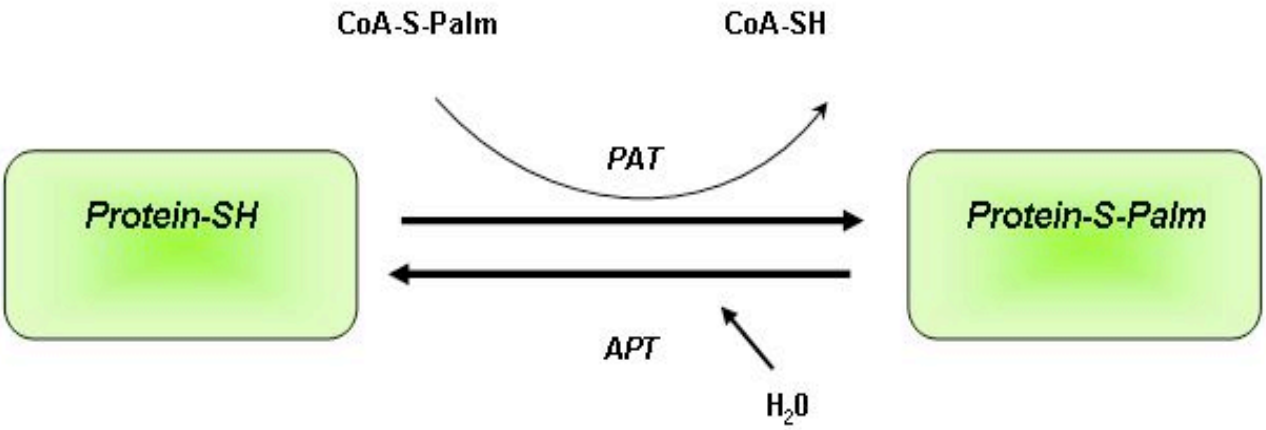

Figure 3-3: Palmitoylation is a reversible reaction
Palmitate is transferred from palmitoyl–CoA (Co-S-Palm) to a thiolate residue onto a target protein (protein–SH) by a protein acyltransferase (PAT), and the palmitate remains attached to the protein throughout its lifetime (Protein-S-Palm). Palmitate can be removed by an acylprotein thioesterase (APT) in presence of water.

3.3 About other lipid post-translation modifications: N-myristoylation, S-isoprenylation and addition of GPI (Glycosyl Phosphatidylinositol) anchors

N-myristoylation is another important lipid modification that occurs co-translationally in eukaryotic cells at N-terminal glycines of proteins (McLaughlin and Aderem, 1995; Resh, 1999). The addition of myristate ($C_{14:0}$) is catalysed by N-myristoyltransferase (NMT). In

some cases small amounts of C_{12}, $C_{14:1}$ or $C_{14:2}$ are also transferred by NMT, but their donor acyl-CoAs are normally at low concentrations in the cell and heterogeneous transfers are rare. The specificity of NMT for myristoyl-CoA and for the Gly at N-terminal has been resolved by X-ray structure (Johnson, et al., 1994; Farazi, et al., 2001).

Because all eukaryotic proteins have an N-terminal methionine, the target proteins have a consensus N-terminal sequence MGXXXS/T. Before myristoylation, the peptide bond between Met1-Gly2 has to be hydrolysed by methionine aminopeptidase (MAP), which also acts cotranslationally, liberating the N-terminal Gly.

In myristoylated and palmitoylated proteins (e.g. GAP-43), palmitoylation occurs later than myristoylation.

In plants N-myristoylation is estimated to concern almost 2% of all proteins (Meinnel and Giglione, 2008).

The *Arabidopsis* genome encodes two NMT isoforms, AtNMT1 and AtNMT2 (Boisson, et al., 2003). Studies on knockout mutant lines have shown that AtNMT1 is the main protein involved in protein myristoylation and especially in development at shoot apical meristem. Different approaches have led to identify the subunit β of kinase complex SnRK1 (SNF1-related protein kinase) as one of the major target of AtNMT1 (Pierre, et al., 2007).

The third type of post-translational lipidation is the addition of isoprenyl groups (C_{15}, farnesyl and C_{20}, geranylgeranyl) to cysteine residues at the C-termini of proteins.

Farnesylation was discovered first in sex pheromones from jelly fungi, in yeast mating type *a* factor, in Ras proteins and in nuclear dynamin (Glomset, et al., 1990; Zhang and Casey, 1996). General interest for these post-translation modifications rose when it became clear that Ras superfamily proteins (Ras, Rho, Rac, Arf but not Ran, see below) are prenylated, generally with the C_{20} prenyl chain. Further investigations have estimated that 2% of eukaryotic proteins are prenylated (Nalivaeva and Turner, 2001) and 150 substrates have been identified (mainly in humans) (Roskoski, 2003).

According to their prenylation, Ras superfamily members can be divided into two groups. One group has the C-terminus consensus sequence CaaX. When X is small (Ala, Ser or Met) the Cys is farnesylated as in Ras itself. When X is a terminal Leu, as in Rac and RhoA, the protein is geranylgeranylated (Pereira-Leal, et al., 2001). The reaction is catalysed by a farnesyltransferase or a geranylgeranyltransferase I (GGT-I), respectively.

The second group of Ras superfamily members has two C-terminal cysteines as XXCC, CCXX, CXCX or CCXX. Both cysteines are prenylated by geranylgeranyltransferase II

(GGT-II).

Like other protein lipidations, prenylation increases membrane association even though it does not provide a stable and lasting association. Subsequent palmitoylation at the nearest cysteines increases membrane affinity. Alternatively, a cluster of basic amino acids may help to stabilize the membrane association (Walsh, 2006).

Many proteins on the cell surface of lower and higher eukaryotes have GPI (Glycosylphosphatidylinositol) anchors attaching them to the outer layer of the plasma membrane (Englund, 1993; Udenfriend and Kodukula, 1995) (Mayor and Riezman, 2004). The GPI anchor includes a phospholipid (phosphatidylinositol) coupled to a tetrasaccharide chain ending with a phosphoethanolamine. In a transamidation reaction the protein to be anchored functions as the acyl donor, resulting in breaking a peptide bond near the C-terminus of the protein and in the formation of a new amide bond with the ethanolamine-glycolipid anchor. GPI-anchored proteins have their moiety attached in the lumen of the ER, where the anchor has been previously assembled, and the GPI-anchored protein is then transported to the cell surface. Once the protein arrives at the cell surface, it can be released by proteolytic cleavage catalysed by a phospholipase C in bacteria and phospholipase C and D in eukaryotes. Nascent proteins have a C-terminal GPI attachment signal of about 10 amino acids (with a DAA motif), which is replaced by the GPI anchor (Meyer, et al., 2000).

In animal cells different proteins are GPI-anchored, e.g. the prion protein (Rudd, et al., 1999), the folate receptor, and hydrolytic enzymes such as 5'-nucleotidase. Trypanosomatids can have their whole surface covered by one type of GPI-anchored protein which gives resistance against the immune system of the infected host (Englund, 1993). In the *Arabidopsis* thaliana genome, 187 GPI-anchored proteins have been predicted (Eisenhaber, et al., 2003).

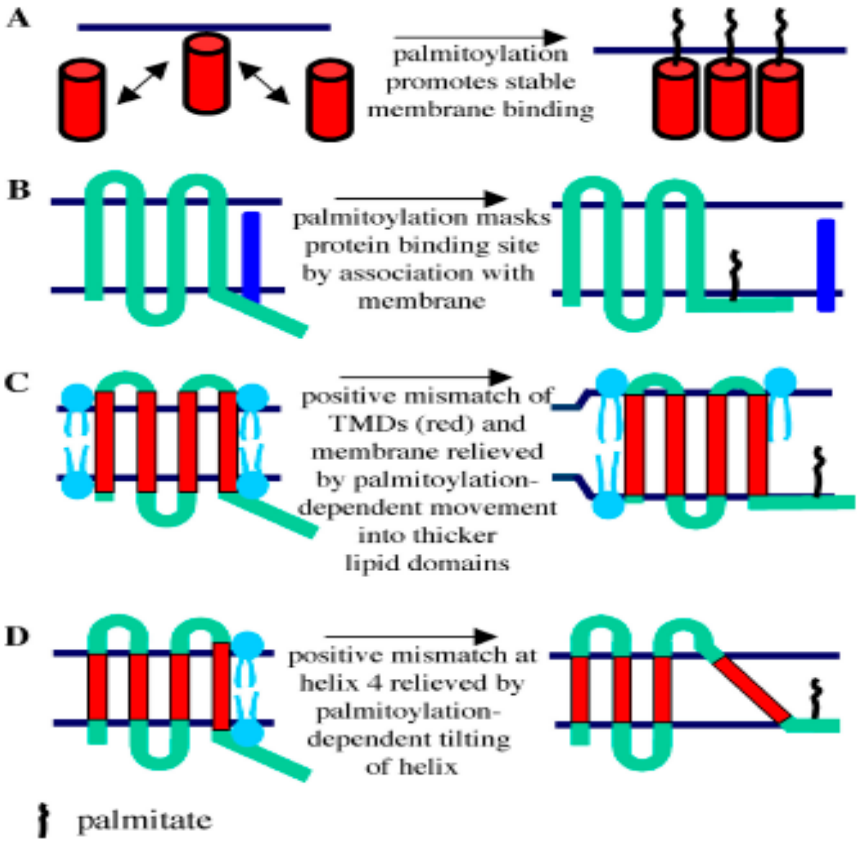

Figure 3-4: Possible roles of palmitoylation

(A) Membrane "trapping" by S-acylation. The Figure shows a protein with a relatively weak membrane affinity (such as either farnesylated Ras or S-acylated Rab) undergoing dynamic exchange between the cytosol and membrane. Palmitoylation traps the protein at the membrane by increasing its hydrophobic anchor. (B) Illustration of a potential mechanism whereby palmitoylation of a cysteine residue masks a protein binding site by pulling it into close proximity to the membrane. One possible outcome would be that the palmitoylated protein is now free to traffic to a distinct membrane compartment. (C) Model depicts palmitoylation modifying the lateral distribution of a protein within the membrane. In this instance, the association with thicker membrane domains relieves a hydrophobic mismatch between the hydrophobic part of transmembrane helices (shown in red) and the original membrane domain. The stabilization of the hydrophobic segments may directly allow the protein to traffic, for example, by preventing aggregation, or, alternatively, the association of the protein with distinct membrane domains might drive subsequent sorting. TMD, transmembrane domain. (D) Hydrophobic mismatch of helix 4 is relieved by palmitoylation, which in this instance changes the tilt of the transmembrane domain. This modified membrane association of the protein may facilitate trafficking (Greaves and Chamberlain, 2007).

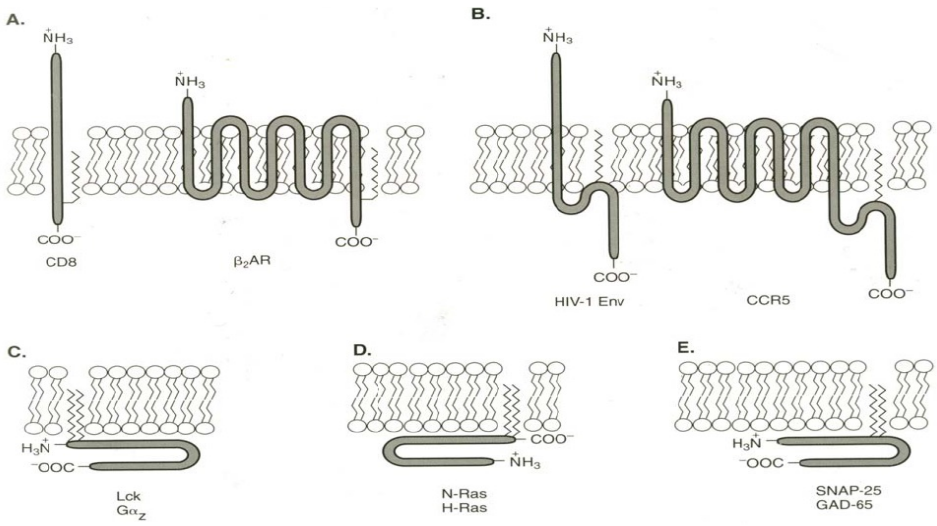

Figure 3-5: Examples of palmitoylated proteins.
In this picture are shown integral membrane protein, from single transmembrane proteins as THE CD8 α-subunit (a) to the seven TM β_2-adrenergic receptor (β_2AR) that get S-acylated near TM/cytosol boundary (a). Hiv-Env and CCR5 get S-acylated at cysteines distal from TM/Cytosol boundary (b). Figure C shows two cytosolic proteins examples that are both N-myristoylated and S-acylated in the N-terminal region. Figure D shows a dual lipid modification, S-acylation and prenylation at the N-terminus of N-Ras and H-Ras. Figure E shows two cytosolic proteins where the bis-S-acylation occurs in the central domains of SNAP-25 and GAD-65 (Glutamate Decarboxylase).

3.4 Small GTPases and polar growth

Tip growth is a form of polarised growth of living cells that results in an extended cylindrical cell with a dome-shaped tip at which the growth activity takes place.

Tip growth occurs in algae (e.g., *Acetabularia acetabulum*), fungi (hyphae) and plants (e.g. root hairs, pollen tubes and *Physcomitrella patens* filaments).

Pollen tube development depends on the activity of small GTPases. These proteins are molecular switches cycling between an active state, in which they bind GTP, to an inactive state in which they are GDP-bound. Structural and functional analysis of the members of this superfamily has highlighted five different families: Ras, Rab, Rho, Arf and Ran (Kahn, et al., 1992; Vernoud, et al., 2003). Ras GTPases control cell proliferation in yeast and mammalian cells. Rho GTPases and Ras (Rivero and Somesh, 2002) regulate actin remodelling and signal transduction pathway in association with the MAP kinase pathway (Figure 3-6).

In mammalian and fungal cells Rho homologs regulate cell polarity and influence cell morphogenesis (Arellano, et al., 1999). Because members of this family have shown unique features in *Arabidopsis*, plants Rho have been named ROP. *Arabidopsis* genome encodes 11

ROP GTPases (Figure 3-9). Three of them, AtRop1, AtRop3, and AtRop5 are mainly expressed in pollen tubes and might have a redundant function. They can also fulfil other roles such as controlling tip growth by modelling the net of F-actin and regulating the influx of calcium (Li, et al., 1999; Fu, et al., 2001).

Recently, Hwang et al. (Hwang, et al., 2010) showed that over-expression of AtRop1 caused an enlargement of the pollen's apical region and a decrease of tube length due to a membrane depolarization. The fine regulation of AtRop1 activity and the inhibition of its lateral diffusion from the very tip of pollen tubes are maintained by interactions with RhoGDI and RhoGAP. One of the first links between palmitoylation and members of the Ras super-family proteins was found for AtROP6 (Sorek, et al., 2007). The authors showed that it was activated (in the GTP-bound state) only when associated with DRM and this occurred only when the protein was modified with palmitic or stearic acid. The same authors (Sorek, et al., 2010) later showed that two conserved cysteines in the G-domain, C21 and C156 were palmitoylated. Based on structure comparison, they showed that the first cysteine is sufficiently exposed to the aqueous environment to be palmitoylated, while C156 needs a conformational change to be palmitoylated. Moreover, the double cysteine mutation interfered with the uptake of the endocytic tracer FM4-64, with the polar growth in *Arabidopsis* root hairs and caused a redistribution of reactive oxygen species (ROS).

In animal systems, Rho and Rac are described as key regulators of polar growth of epithelial cells acting downstream of polar complexes, Par6/aPKC/Par3, Dlg/Lgl/scribble, Crumbs/PALS1/PATJ (Gibson and Perrimon, 2003; Jaffe and Hall, 2005). Neuronal morphogenesis requires the specific action of polar complexes, and particularly of Par6/aPKC/Par3. If hippocampal neurons are plated in culture, they are able to form axons even without cell-cell contacts. Inactivation of one of the members of this complex leads to zero or multiple axons (Schwamborn and Puschel, 2004). Rho GTPases may control vesicular trafficking and microtubules rearrangement, which is particularly important in the polar organization of epithelial and neurons cells (Musch, 2004).

ROPs have regulatory proteins called RopGAPs and RopGDI (see later in the text). Three RhoGDI homologs are encoded in the *Arabidopsis* genome. AtRhoGDIs are expressed in all tissues and have been shown to interact specifically with AtROP4 and AtROP6 GTPases (Bischoff, et al., 2000). RopGAP4 is involved in the reaction to oxygen deprivation as revealed by a *ropgap4* knockout mutant (Baxter-Burrell, et al., 2002).

The Rab GTPases participate in different steps of the secretory pathway. They are the largest

family of this super-family in *Arabidopsis*, being represented by 57 members (Figure 3-8). In yeast and mammalian systems, Rabs members have been widely studied and found to be highly compartmentalized, which seems to hold also for plant cells (Stenmark and Olkkonen, 2001; Vernoud, et al., 2003). Some Rabs have a C-terminal cysteine residue in a consensus sequence for post-translational modifications such as prenylation and/or (less frequently) palmitoylation. Although no difference could be detected in their lipidation (prenylation or palmitoylation) signal, few palmitoylated Rabs have been discovered: Ypt1 in yeast (Molenaar, et al., 1988) and Ara6 in *Arabidopsis* (Ueda, et al., 2001) and little information is available on their role. The Biotin Switch Assay (see 2-4) used to characterize the palmitoyl-proteome of rat neurones (Kang, et al., 2008b) and of yeast (Roth, et al., 2006) detected palmitoylated Rabs, but provided no information on their function.

Yeast Protein Transport proteins (Ypt), the Rabs of yeast, are localized throughout the secretory pathway: in the endoplasmic reticulum, the Golgi apparatus, the Trans-Golgi Network, prevacuolar compartments and the vacuole.

In humans and yeast there is a high correlation between sequence and function in membrane trafficking: Rabs sharing a high similarity to yeast Ypt counterpart act in compartments with related functions (Huber, et al., 1993). In mammalian cells and yeast, they also control trafficking between ER and Golgi (Salminen and Novick, 1987; Goud, et al., 1988).

Arabidopsis expresses five Rab GTPases with high similarities with corresponding mammalian and yeast isoforms involved in polarized trafficking. They belong to the AtRabE subfamily: AtRabE1a-e. In yeast, Sec4p, a RabE homolog, controls the membrane trafficking towards the daughter cell bud site. A study in tomato (*Solanum lycopersicon*) showed an interaction between the avirulence factor avrPto from *Pseudomonas* and members of the RabE subfamily (Bogdanove and Martin, 2000). In a very interesting discussion, the authors postulated that they might regulate the polarized secretion of antimicrobial compounds or components in response to pathogen attacks.

The 26 distinct AtRabA represents the largest Rab subfamily in *Arabidopsis*. RabAs regulate the trafficking between post-Golgi compartments and the PM or the vacuole. In mammals Rab11a and Rab11b were found in recycling endosomes (Calhoun, et al., 1998; Duman, et al., 1999), and Rab11a is fundamental for exit of internalized proteins from apical recycling endosomes (Nagano, et al., 1995).

It is not known, whether all these RabAs have different functions or are partially redundant. In pea (*Pisum sativum*) Pra2 is constitutively expressed and localized in Golgi and possibly in

endosomal compartments, while Pra3 is up-regulated in the zone of stem elongation of dark-grown seedlings (Inaba, et al., 2002) and appeared to localize in TGN and/or PVC. Rab11a from tomato was also examined. It localized at the TGN in *N. tabacum* protoplasts and generation of a dominant negative mutant interfered with the secretion of secRGUS (Rehman, et al., 2008). In *Arabidopsis* root tips RabA2 and RabA3 are involved in trafficking to the PM as well as to the phragmoplast (Chow, et al., 2008). Their dominant-negative mutants disrupted cell division indicating that they are both involved in the formation of newly cell wall. Dominant-negative RabA2a also targeted to the cell periphery during interphase and might be involved in post-Golgi trafficking to the PM (Chow, et al., 2008).

Therefore, many members of RabA seem to play a major role in secretion to the cell wall and could play a pivot role in regulating growth by modification of the cell walls (Lycett, 2008).

In a general view, it is proposed that RABA subfamily regulates trafficking of hemicellulose, integral cell wall proteins, cellulose synthase complex (Vernoud, et al., 2003) from post-Golgi compartments and might reflect the high degree of complexity of plant cell wall.

The physiological control of these GTP-binding proteins occurs via accessory proteins called RabGEFs (Rab Guanine nucleotide Exchange Factors) and RabGAPs (Rab GTPase Activating Proteins). Binding to the target membrane and subsequent activation of Rabs is realized by RabGEFs catalysing the conversion of the Rab-GDP to the Rab-GTP state (Figure 3-7). The *Arabidopsis* genome encodes two sequences with a certain similarity to Vps9p in yeast and Rabex-5 in mammalian (RabGEFs homologs), named AtVPS9A and AtVPS9B (Vernoud, et al., 2003).

In an opposite function to RabGEFs, RabGAPs (Gyp in yeast) inactivate Rab GTPases by accelerating their slow intrinsic GTPase activity (Figure 3-7). The *Arabidopsis* genome encodes at least 20 AtGYP proteins with some or all “catalytic core” present in well characterized RabGAPs.

Arfs (ADP-ribosylation factors) were identified by their capacity to stimulate the ADP-ribosyltransferase activity of cholera toxin (Moss and Vaughan, 1998). Arf GTPases have been classified in two subgroups: the Arf proper and the Arl (Arf-like) GTPases, which show a significant similarity (40%-60%) to Arf but cannot stimulate the activity of cholera toxin nor complement S. cerevisiae *arf* mutants. *Arabidopsis* encodes 21 Arf and Arl (Figure 3-10) (Vernoud, et al., 2003). Arfs plays a fundamental role in vesicle trafficking in all eukaryotic cells. Arf GTPases are responsible for the recruitment of proteins coats in COP-I and clathrin vesicles, whilst Sar1 GTPases are involved in the recruitment of COP-II coat.

Brief description about isoforms and functions of *At*Sar1s are presented elsewhere in the text (1.2). Six of them belong to Arl subgroup. Very little is known about the role of these proteins. Mutations in the gene *At*ARLC1, result in a dramatic alteration in mitosis and cell cycle in developing seeds (McElver, et al., 2000). Contrary to Rabs and ROPs, which are palmitoylated and/or prenylated, Arfs are myristoylated at their N-terminus showing a weak membrane association (Franco, et al., 1995).

Arf GTPases also have interacting proteins, which are named GAPs and GEFs. Sec7p is an ArfGAP of yeast. A 200 amino acids Sec7 domain present in all Arf GEFs catalyses the replacement of GDP by GTP. In *Arabidopsis* eight proteins containing a Sec7 domain have been found, the best characterized being GNOM, which was identified in a mutant screen for embryo-lethal mutations (Mayer, et al., 1991). *Arabidopsis gnom* knockout mutants disrupt the polarized localization of the auxin carrier PIN1 implicating GNOM in PIN1 trafficking (Steinmann, et al., 1999; Geldner, et al., 2003).

Arabidopsis encodes 15 proteins containing an ArfGAP domain (AGD). According to the phylogenetic analysis presented by Vernoud et al. (2003), they have been grouped into four distinct classes. The first class (AtAGD1-4) is a novel plant-specific family containing a pleckstrin homology (PH) domain and two or three ankyrin repeat domains. The PH domain suggests that these proteins might participate in phospholipid signalling as PH domains bind phosphoinositide (Lemmon, et al., 2002). Class 2 AGDs (AtAGD5-10) contain the AGD domain at their N-terminus and no domain can be recognized in the rest of the proteins. Class 3 AGDs (AtAGD11-13) share a C2 domain in the centre of the protein. C2 can bind a wide range of ligands such as phospholipids and phosphoinositides in a calcium-dependent manner (Sutton, et al., 1995; Essen, et al., 1996; Shao, et al., 1997). Class 4 AGDs (AtAGD14-15) the AGD domain comprises almost all the open reading frame of these two proteins. The presence of a potentially transmembrane α-helix in AtAGD14 suggests a more permanent membrane anchoring.

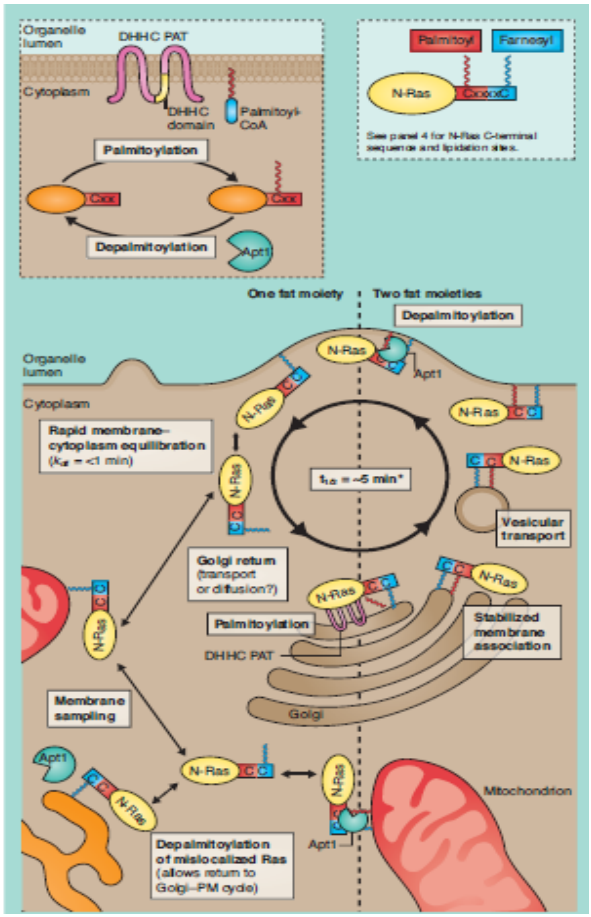

Figure 3-6: General description of palmitoylation-depalmitoylation cycle for Ras proteins.

As already discussed, palmitoylation can occur at C-terminal of any Ras super-family member. Palmitoylation occurs by DHHC enzyme (see text for a more detailed discussion), generally at the Golgi. On the contrary depalmitoylation occur at the target membrane allowing the recycling of the proteins. Generally, this cycle takes no longer that 5 minutes indicating a high level of regulation of all the classes of enzymes involved in the process. The image depicts the palmitoylation-depalmitoylation cycle in animal cells, highlighting also a vast complexity, which involves other organelles, such as mitochondria. Any information is available concerning Ras associated with mitochondria or plastids in plant cells (pictures taken from (Conibear and Davis, 2010))

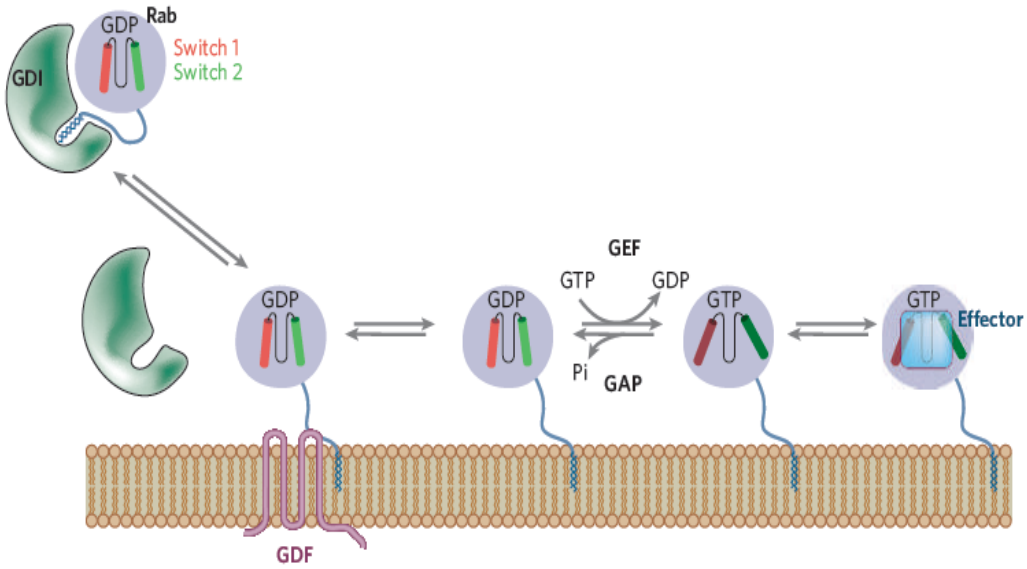

Figure 3-7: Cycle of Rab GTPases.
Rab–GDP forms a complex in the cytosol with GDI. GDF displaces GDI from Rab–GDP, and its C-terminal prenyl groups anchor the Rab at the membrane. There, a GEF activates the Rab by exchange of GDP for GTP. This induces a conformational change in the switch 1 and 2 regions of the GTPase (indicated here by a change in colour) that enables the Rab–GTP to bind to its effectors. A GAP stimulates the hydrolysis of GTP and the Rab is retrieved by GDI to the cytosol once again (not shown) (Behnia and Munro, 2005)

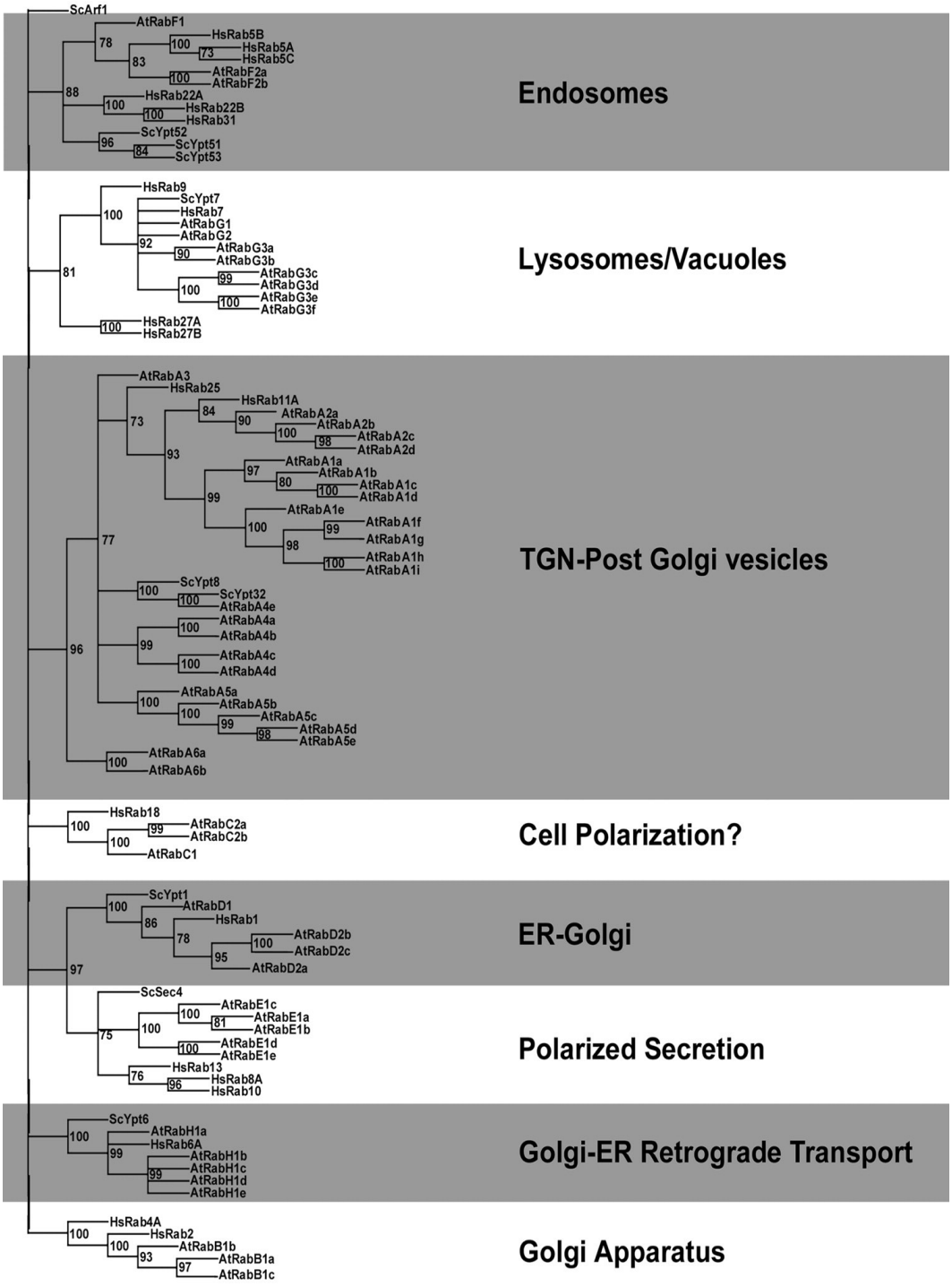

Figure 3-8: The Rab GTPase family of *Arabidopsis Homo and Yeast*
The Rab GTPases tree of *Arabidopsis*. Labels on the right represent putative sub-cellular localization. Picture taken from (Vernoud, et al., 2003).

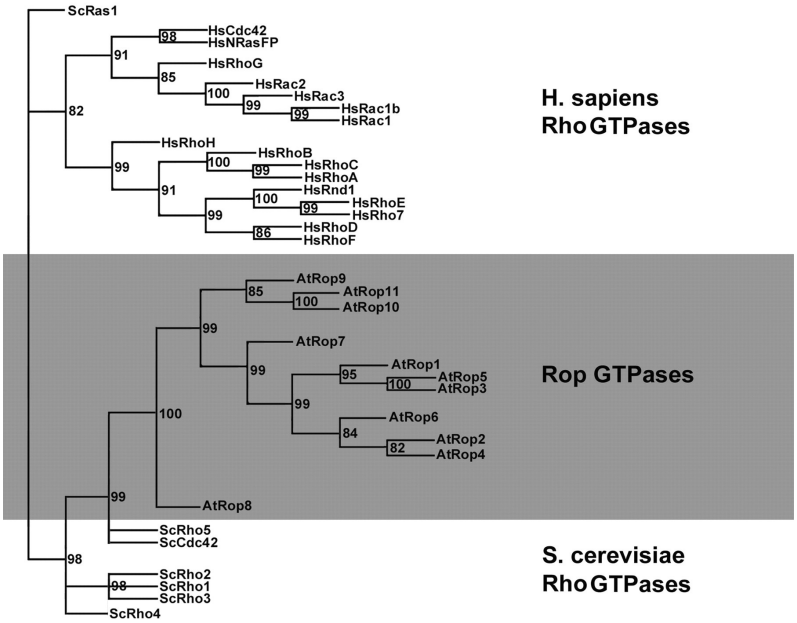

Figure 3-9: The Rop GTPase family of *Arabidopsis Homo and Yeast*
The Rho-family GTPases tree of *Arabidopsis*. Rops clearly represent a distinct subfamily from animal homologs. Picture taken from (Vernoud, et al., 2003).

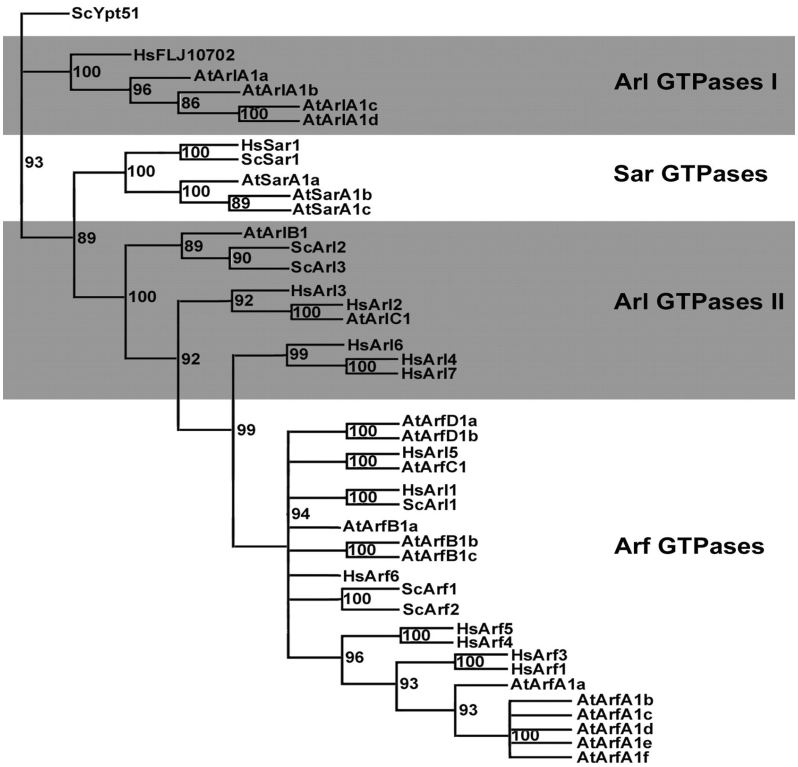

Figure 3-10: The Arf GTPase family of *Arabidopsis Homo and Yeast*
The Arf GTPases family tree of *Arabidopsis*. Picture taken from (Vernoud, et al., 2003) .

3.5 The cytoskeleton is not affected by 2BP

In order to investigate the role of palmitoylation in the general membrane organization in plant cells, 2-bromopalmitate (2BP) was used in combination with different intracellular markers on different plants species and tissues. To demonstrate the treatment efficacy we chose a plasma membrane marker with known palmitoylation.

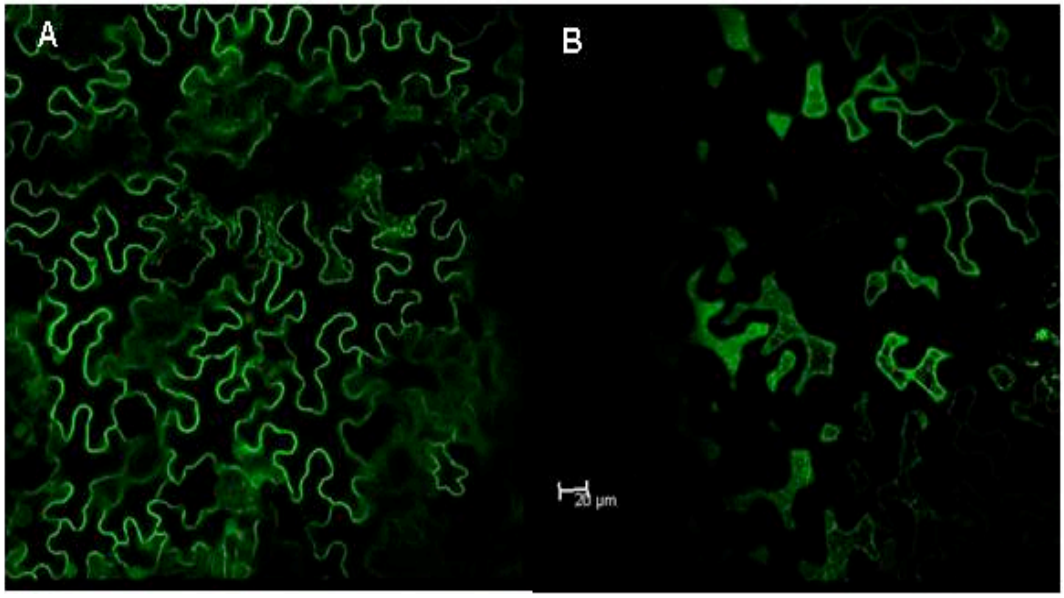

Figure 3-11: Agroinfiltrated N.benthamiana leaves expressing palmitoylated GFP-Rac8
Transient expression of the positive control GFP-Rac8.

Rac8 (also called *At*Rop10) is a small GTPase of the ROP family, which is predicted to be palmitoylated at a C-terminal consensus sequence like many small GTPases (Figure 3-11). Rac8 shuttles between the plasma membrane (to which it attaches via its C-terminal palmitoyl moiety) and the cytosol (Lavy, et al., 2002). Different papers (Li, et al., 1999; Zheng and Yang, 2000; Fu, et al., 2001; Szumlanski and Nielsen, 2009) have shown a tight correlation between actin remodelling and ROP activity in tip-growing cells. In order to study the organization of actin in plant cells, we used a GFP protein fused in frame to the F-actin-binding domain of mouse talin. This fusion protein has been extensively used to visualize actin *in vivo* (Kost, et al., 1998). Transient expression of GFP-Talin in *N. benthamiana* epidermal cells treated with 2BP revealed no significant difference in the general distribution of the fusion protein (Figure 3-12 C-D).

Similar experiments were performed with the fluorescent microtubule-associated reporter protein MBD-RFP (Crowell, et al., 2009) on agroinfiltrated *N.benthamiana* leaves, also revealing no effect of 2BP (Figure 3-12 A-B)

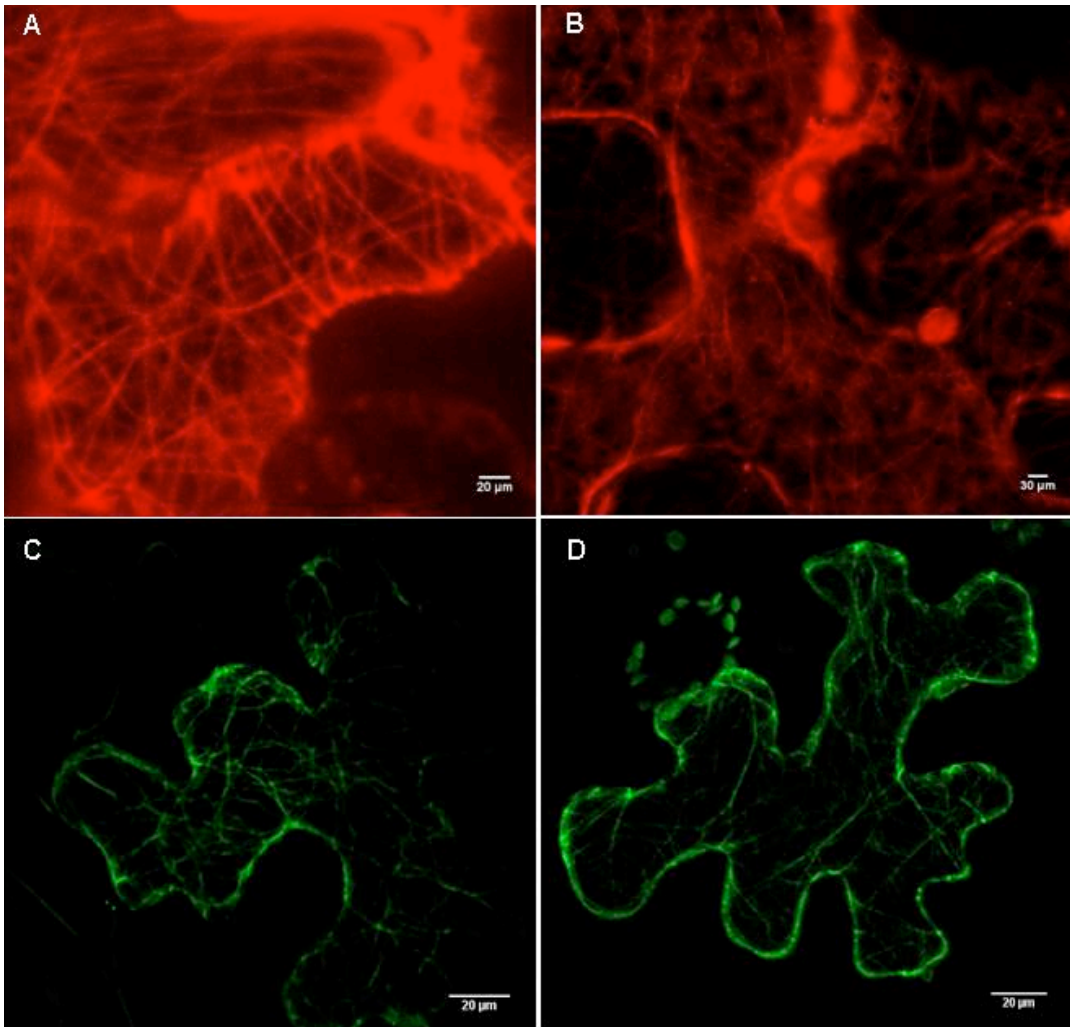

Figure 3-12: No effects of 2BP treatment on the microtubules or microfilaments in *N. benthamiana.*

(A and B) Transient expression of MBD-RFP and treatment with DMSO (A) or 1mM 2BP (B)

(C and D) Transient expression of GFP-talin and treatment with DMSO (C) or 1mM 2BP (D)

The same observation was made for a *P. patens* line with an inducible GFP-talin gene, treated with different concentrations of 2BP. In particular, the apical pole, i.e. the growing region of the apical tip characterized by thick actin interconnections (Finka, et al., 2007) (Figure 3-13 A-B), was not affected by the drug . Moreover, *P. patens* protoplasts also showed similar actin patterns with or without 2BP (Figure 3-14).

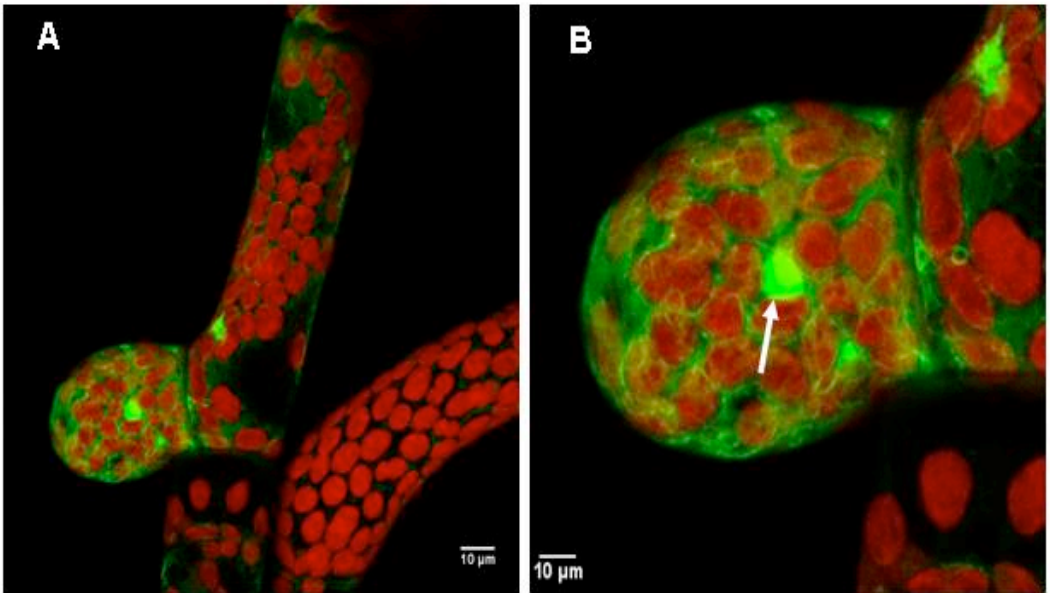

Figure 3-13: No effect of 2BP on the microfilaments of moss protonema apical cells
P. patens expressing a heat inducible GFP-Talin. (A and B) 2BP treatment. (C and D) DMSO treatment for 24-36h. Arrows in (A) shows actin accumulation at the pole of cellular division.

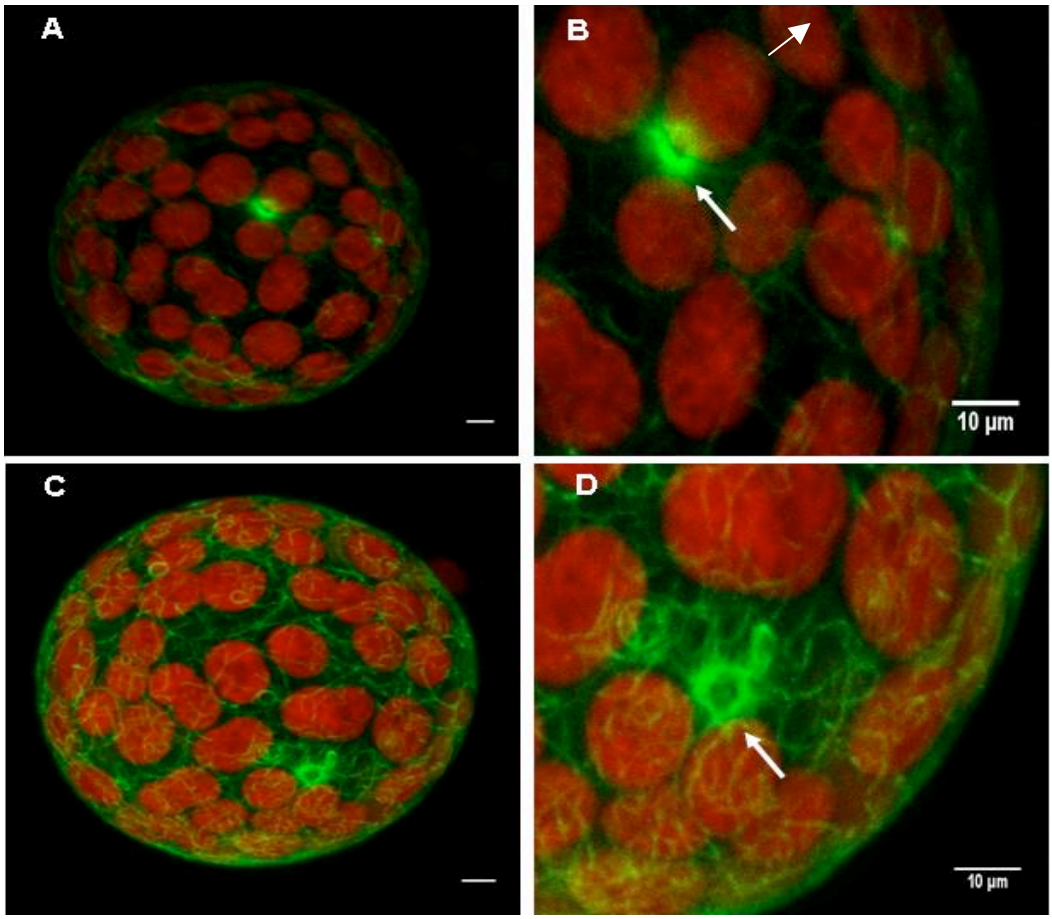

Figure 3-14: No effect of 2BP on the microfilaments of moss protoplasts
P. patens protoplasts expressing heat inducible GFP-Talin. (A and B) DMSO treatment ON. (C and D) 2BP treatment ON. Arrows point to actin accumulations representing the pole of cellular division. (B and D) magnification of the squared area in (A and C). In (A and C) scale bar is 5 µm.

P. patens stably expressing a GFP-tubulin fusion protein (Hiwatashi, et al., 2008) did not show any effect upon treatment with 2BP (Figure 3-15 C-D.). Finally, the formation of the mitotic spindle was also not affected (Figure 3-16).

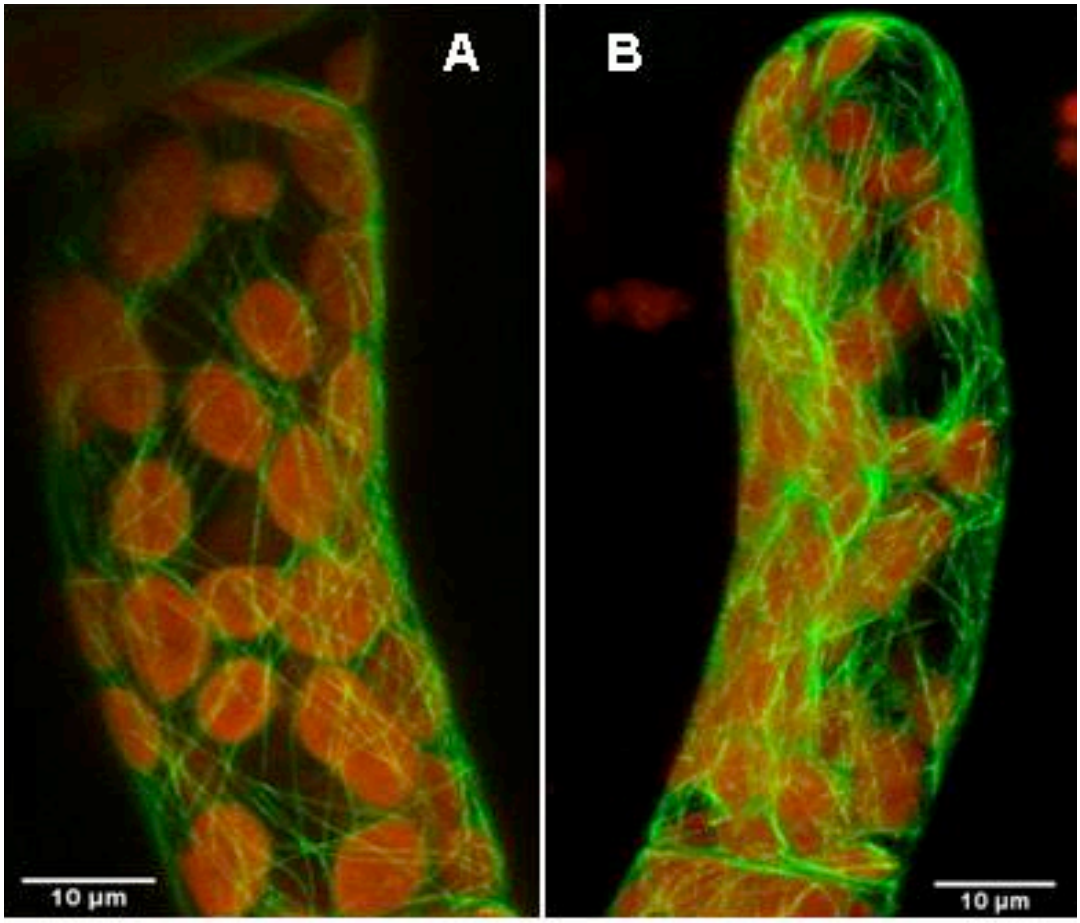

Figure 3-15: No effect of 2BP on the microtubules in moss
P. patens stably expressing GFP-Tubulin were treated with 1mM 2BP for 24 36h. (A) water controls. (B) 2BP treatment.

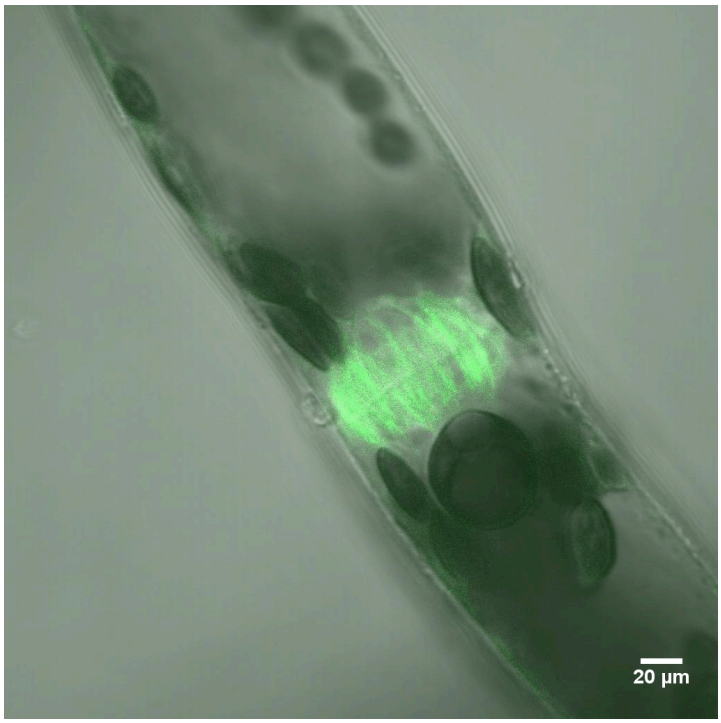

Figure 3-16: No effect of 2BP on the mitotic spindle of moss

Even though palmitoylation of tubulin has been largely debated for different organisms (Caron, 1997; Rosenbaum, 2000; Westermann and Weber, 2003), no solid evidence was given for an effect of this modification on tubulin localization. Interestingly, in animal cells acetylated microtubules have been found to be associated with Golgi membranes and to participate in the formation of the centrosome (Chabin-Brion, et al., 2001).

3.6 Inhibition of apical growth

Apical growth is only occurring in specific cells with mostly unidirectional growth. In plant cells, only three types of cells elongate by tip growth: root hairs, pollen tubes and moss protonema. Upon treatment with 2BP *P. patens* protonema (i.e. chloronema and caulonema) cells unexpectedly showed a very clear effect: apical growth was inhibited resulting in cubic-shaped cells (Figure 3-17).

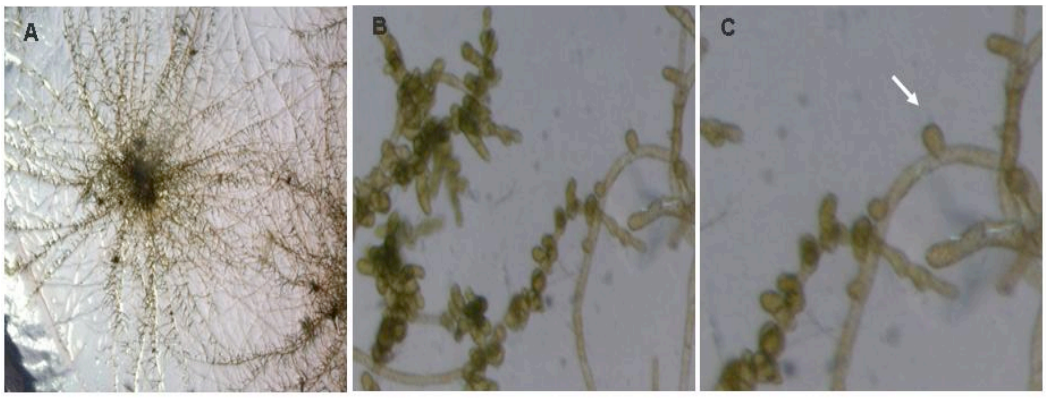

Figure 3-17: Effect of 2BP treatment on moss growth
Young colonies of *P. patens* were incubated for 48-72h with 1mM 2BP. A) DMSO Control; B) 1mM 2BP; C) magnification of the squared area in B

In order to confirm the effect of 2BP on apical growth, *N. benthamiana* pollen grains were also treated. Incubation of pollen grains with increasing 2BP concentrations (starting from 0.04 mM and doubling the concentration up to 1 mM) showed that inhibition of germination was dose-dependent. 50% of inhibition was observed at a concentration between 0.5mM and 1mM (Figure 3-18, arrow).

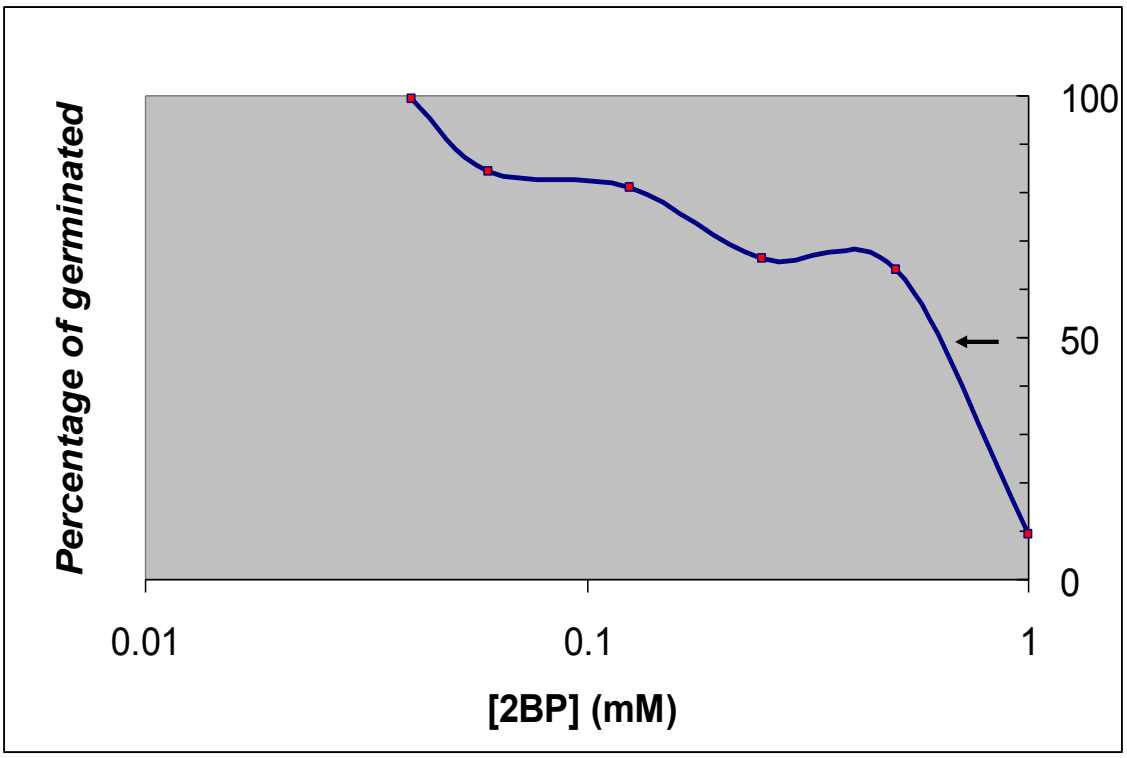

Figure 3-18: Inhibition of pollen germination by 2BP
Pollen grains were germinated for 2h with 2BP at different concentrations. Germinated pollen grains were counted on an inverted microscope with a 10x objective and the percentage germination was normalized to 100% for the DMSO-containing sample,. Pollen tubes were considered germinated when the length of the tube was longer than the diameter of the grain (Wang, et al., 2005)The Figure represents the sum of the three independent experiment. For each independent experiment a chi-square test was performed showing a highly significant inhibition ($P<0.001$). 50% inhibition was obtained at a concentration between 0.5mM and 1mM (arrow).

The highest 2BP concentration used in the germination assay was then used to test the drug in an elongation assay of pollen tubes (Figure 3-19). Pollen tube germination was initiated for 2h. At this time point the average elongation speed (calculated between 1h and 5h) was constant higher for pollen tubes incubated over night (~0.03mm/h- versus ~0.01mm/h). Therefore, all the elongation assays were performed in this range of time. When pollen tubes were incubated with 2BP a statistically significant shortening was detected (~28%).

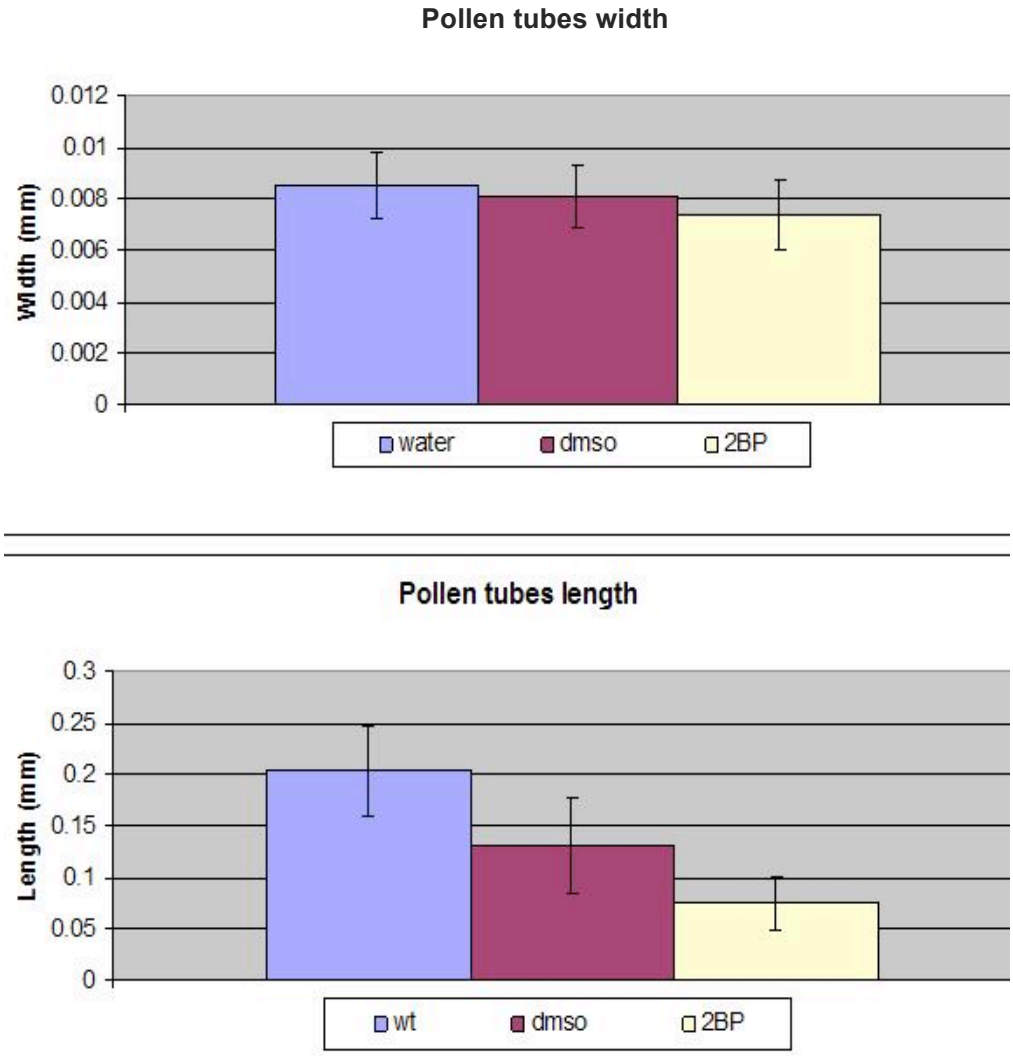

Figure 3-19: Effect of 2BP on pollen tube elongation
Pollen tubes in the elongation phase (3h after germination) were incubated with 1mM 2BP for 90-120 minutes. They were photographed on an inverted microscope with a 40x objective. The length and width of the pollen tube were calculated using ImageJ. Data were collected from three independent experiments. The star indicates a statistically significant difference ($P<0.05$; $t<0.05$). In each experiment 30-40 cells were counted for each treatment.

In order to elucidate the relationship between palmitoylation and endocytosis, pollen tubes were first treated with 2BP and then incubated with the endocytic tracer FM4-64. Short time observations were performed, and the general uptake of the tracer was not affected (including the labelling of the plasma membrane), nor was the formation of the reverse cone (Figure 3-20). In contrast, the formation of "macrovesicles of secretion" (Zonia and Munnik, 2008) was drastically changed. In other publications these structures were described as late endosomes (Wang, et al., 2005) or TGN (Dettmer, et al., 2006). Upon 2BP treatment, they tended to disappear giving a diffuse fluorescence, which did not accumulate in specific intracellular compartments (Figure 3-21).

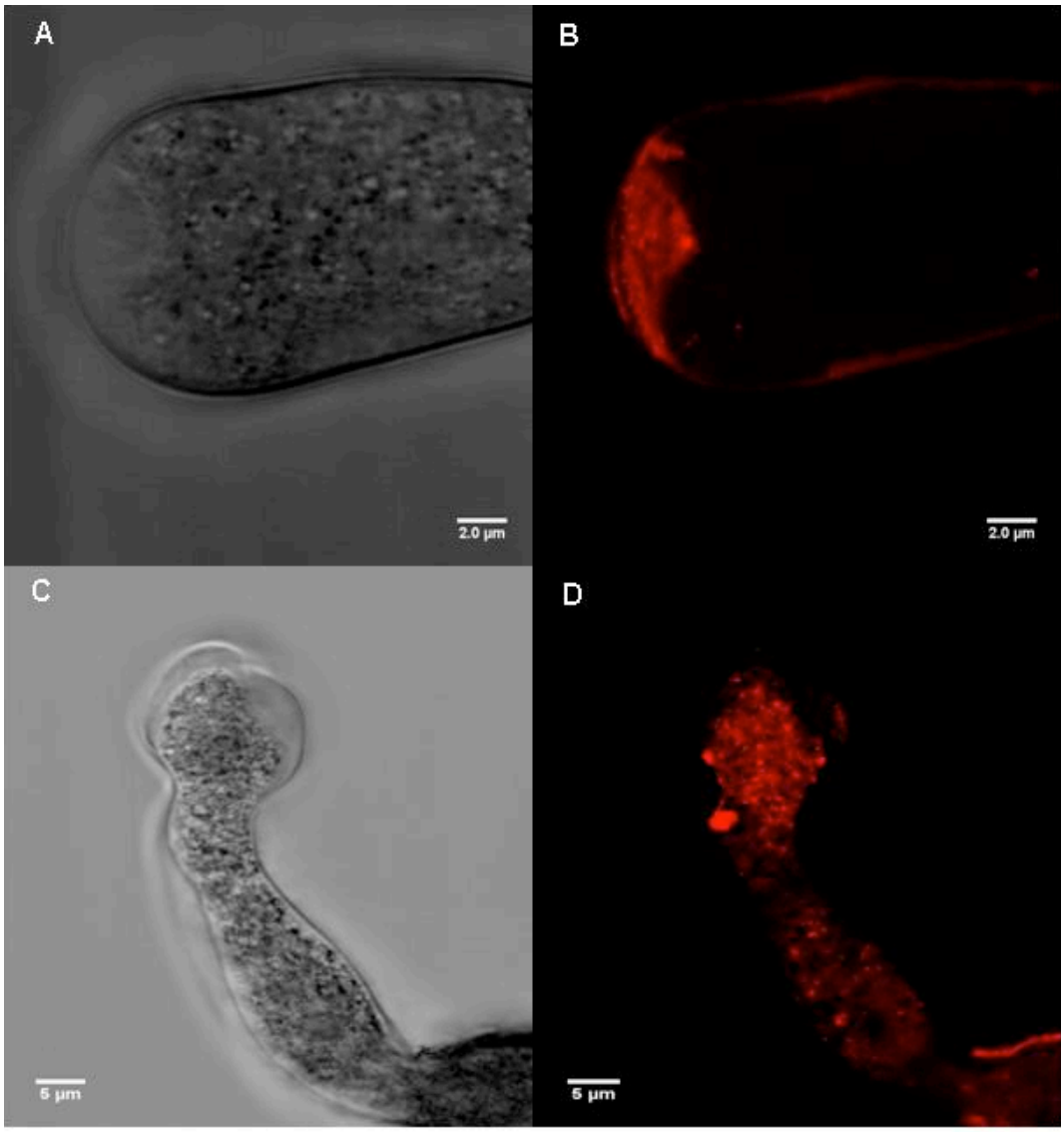

Figure 3-20: Immediate effect of 2BP treatment on pollen tube tip growth.
N. benthamiana Pollen tubes were incubated with DMSO (A-B) or 1mM 2BP (C-D) for 5min . A and C: bright field, B and D: FM4-64 labelling, revealing the "reversed cone" in the control (D) and its absence in the treated pollen (B).

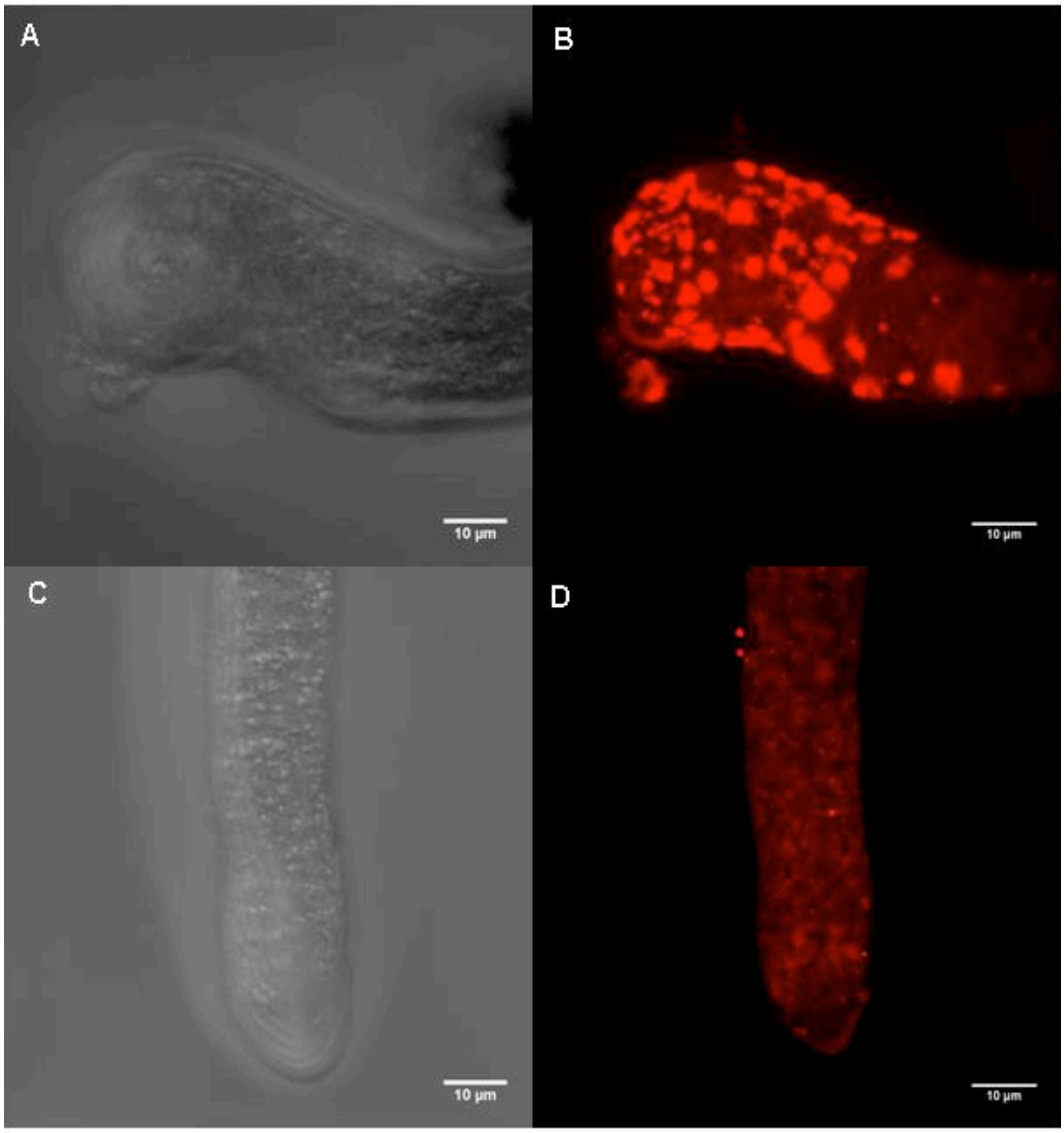

Figure 3-21: Later effects of 2BP treatment on pollen tubes tip growth
N.benthamiana Pollen tubes were incubated with DMSO (A-B) or 1mM 2BP (C-D) for 2 hours A and C: bright field, B and D: FM4-64 labelling. FM4-64 labelling reveals macrovesicles of secretion in the control, which totally disappeared after 2BP treatment, leaving a diffuse cytoplasmic fluorescence.

Ultrastructural analysis by Scanning Electron Microscopy (SEM) also showed defects in cell wall remodelling, with the formation of 2 µm swellings on the outer surface of the pollen tube, particularly evident on the sidewalls (Figure 3-22). Sidewalls are the largest sites of exocytosis (not only in terms of extension but also in terms of activity) as demonstrated by Zonia et al., (2008) and swellings were absent at the very tip of the cells.

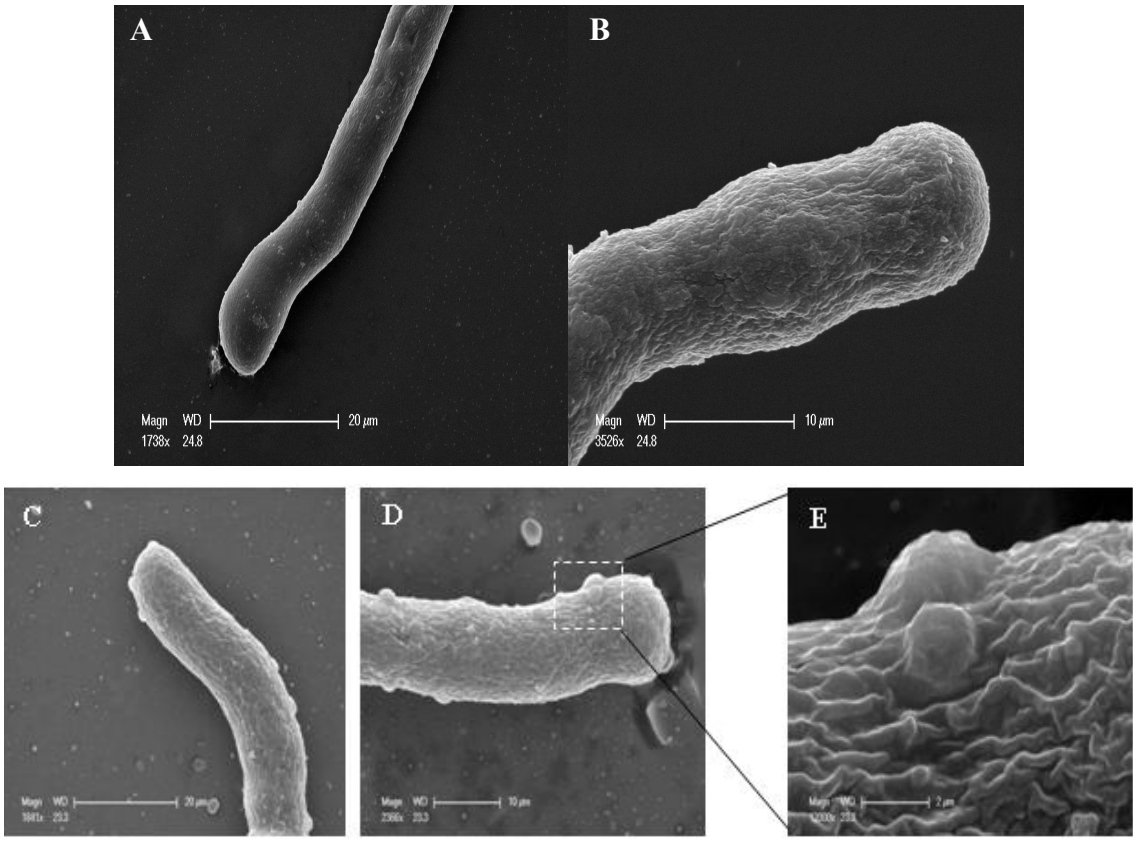

Figure 3-22: Effects of 2BP on N. benthamiana pollen tubes
Pollen tubes in elongating phase were incubated with or without 2BP and fixed with glutaraldehyde/OsO_4. Samples were analysed in a scanning electron microscope. A-B samples treated with 1% DMSO, in C-D samples treated with 1mM 2BP. E) higher magnification of the squared area in d.

3.7 Effects of 2BP on the localisation or markers of the secretory system

The effects of 2BP were also analysed using fluorescent protein markers for various compartments of the secretory pathway: p6-RFP (ER), Erd2-YFP (*cis*-Golgi), Venus-Syp61 (TGN) and GFP-Chi (vacuole).

The ER and *cis*-Golgi markers revealed no pattern changes (Figure 3-23 A-D). In contrast, the TGN marker Venus-Syp61 showed alteration of its localization and the formation of round structures (Figure 3-23 E-F). Since Syp61 itself is not predicted to be palmitoylated,, this mislocalisation is probably due to a indirect effect via SYP41, a binding partner of SYP61 (Zouhar, et al., 2009). Indeed, SYP41 is predicted to be palmitoylated and therefore the inhibition of SYP41 palmitoylation by 2BP is expected to affect the localization of SYP61and of VTI12, the third component of this SNARE complex.

Although trafficking to the vacuole via the TGN should be drastically affected by the

impairment of the ternary SYP61-SYP41-VTI12 complex, it is not completely abolished since the vacuolar reporter GFP-Chi reaches the vacuole in agroinfiltrated *N. benthamiana* leaves even in presence of 2BP (Figure 3-23 G-H). As discussed in the next chapter, GFP-Chi has two pathways to reach the vacuole from the ER: either via the Golgi and the TGN or bypassing these compartments and directly reaching the vacuole. The first pathway is probably dominant, but if it is blocked by 2BP affecting the TGN the other pathway can take over. A similar effect is also shown in the next chapter.

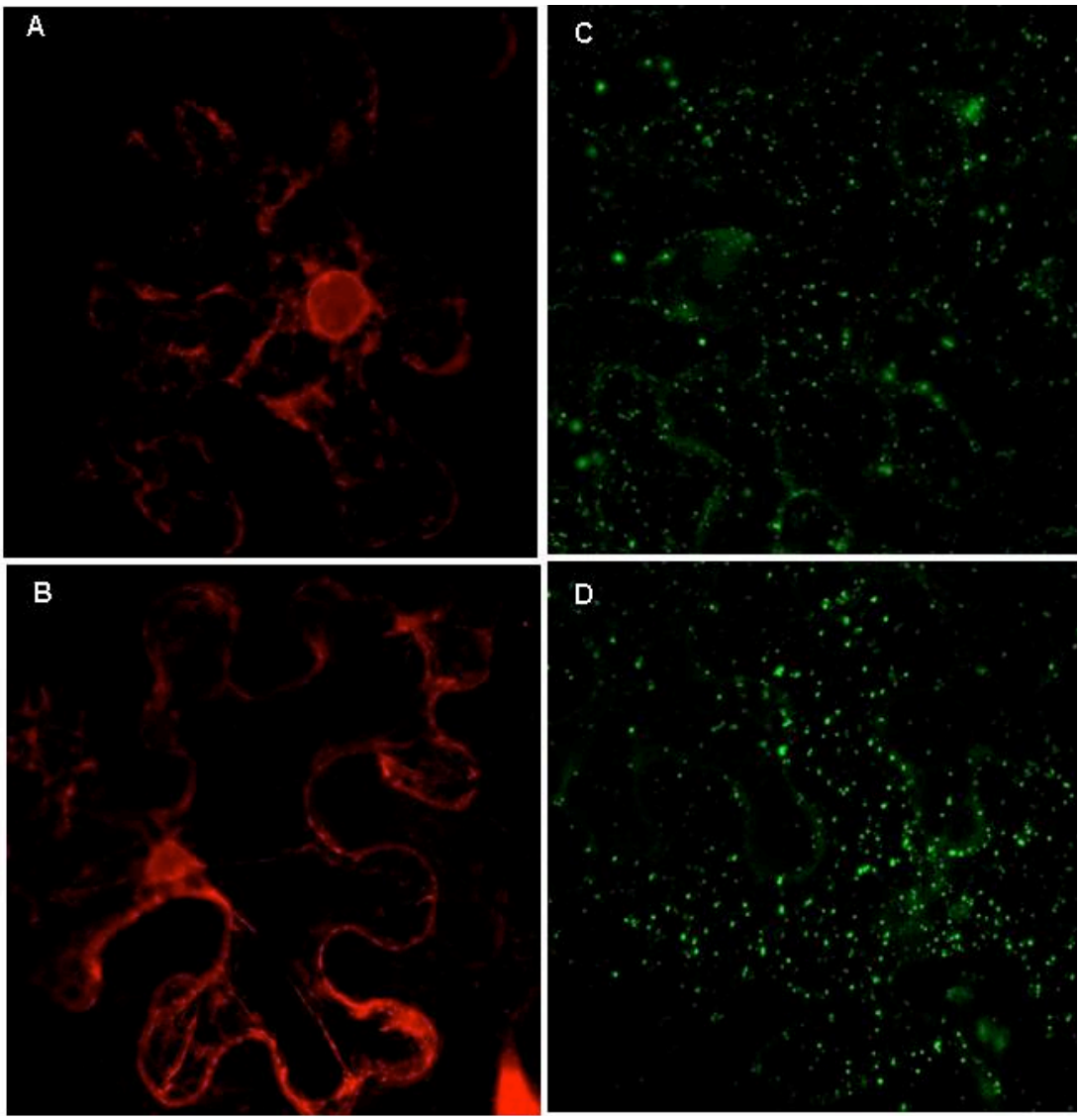

Figure continue

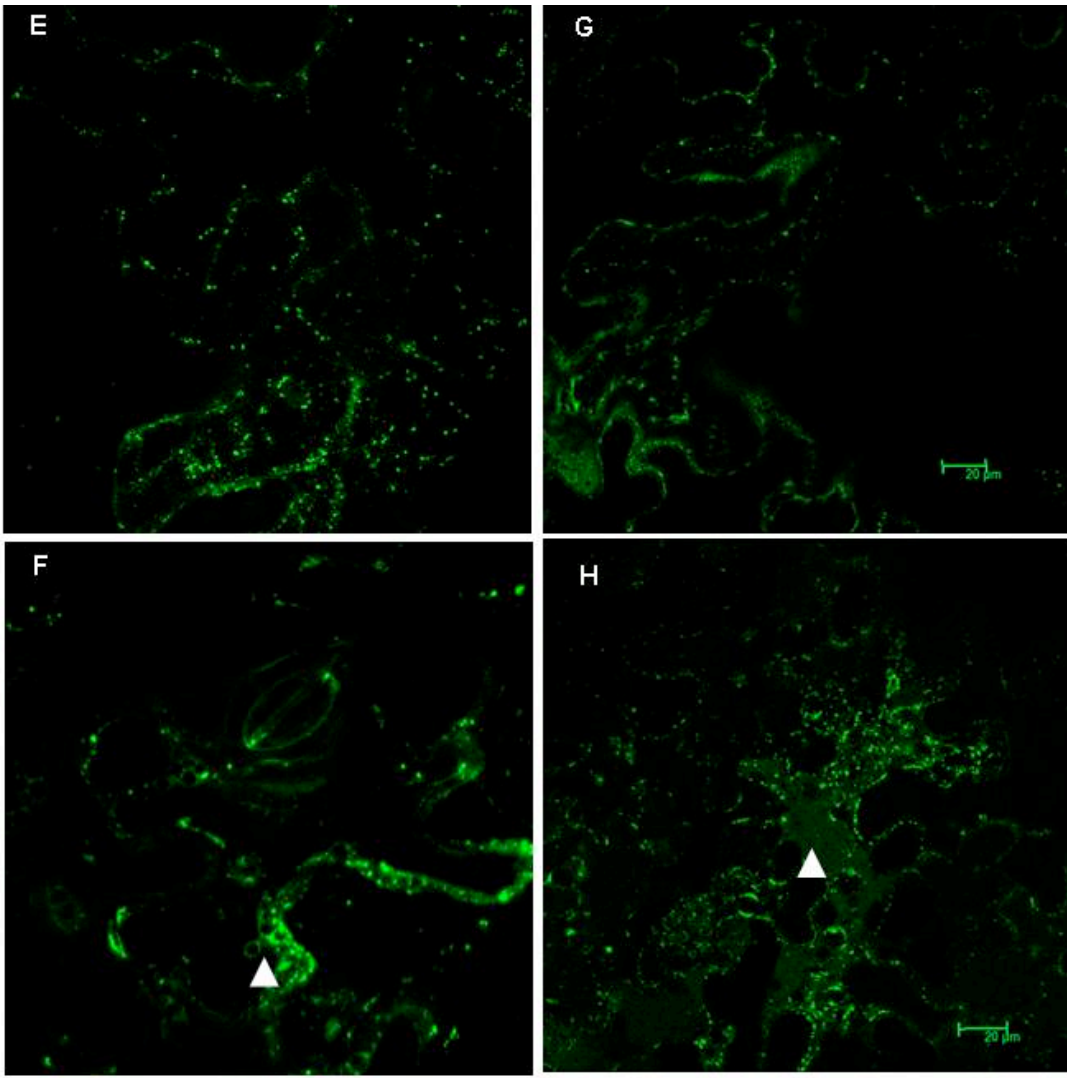

Figure 3-23: Effects of 2BP on markers of the secretory pathway in agroinfiltrated leaves.
N.benthamiana leaves were agroinfiltrated with different intracellular markers in combination with either DMSO (control, A-C-E-F) or 2BP (B-D-F-H). A&B ER marker p6-RFP, C&D *cis*-Golgi marker ERD2-YFP, E&F TGN marker Venus-SYP61, G&H vacuolar marker GFP-Chi. Arrowheads indicate mislocalisation of the reporter. Scale bars=20µm

3.8 Interference of 2BP with the localization of Rab GTPases

Rabs are important regulators of membrane trafficking in all eukaryotic systems (Zerial and McBride, 2001; Linder and Deschenes, 2007). Since these proteins shuttle between the cytosol, in a GDP-bound form, and a membrane, in a GTP-bound form, they have not been considered good candidates as markers for intracellular compartments (Zerial and McBride, 2001; Pfeffer, 2003; Mayorga and Campoy, 2010). However, effects of dominant negative Rab mutants have been observed for RabA2a, which showed a block of cytokinesis in

Arabidopsis roots.

In *Arabidopsis* RabA2a and its closest homolog RabA3b showed a partial colocalization with the TGN marker VHA-a1 and were associated with the endocytic pathway. The authors thus identified a new compartment similar to an early endosome (Chow, et al., 2008). Two other Rab proteins, RabH1b and Rab1H1c, were also characterized. Both localized at the Golgi and in the cytosol and their activation/inactivation state was important for their localization. In contrast to RabH1c, RabH1b also labelled a not yet identified compartment, without colocalization with RabH1c or any other Golgi marker. No effect was found when potentially dominant-negative mutants of these two isoforms were expressed (Johansen, et al., 2009).

It is known from the characterization of the palmitoyl proteome in neural cells that Rabs can be also palmitoylated, not only prenylated, as was believed before. This study revealed for the first time that Rabs belonging to the groups 3a, 10, 1b, 2, 2b, 5, 7, 14 are palmitoylated, although the modified forms are much less abundant than the non-modified forms (Kang, et al., 2008a). This study revealed for the first time that Rabs can also be palmitoylated, not only prenylated, as was believed before.

In this study, we investigated the possible role of the palmitoylation for all Rab markers available as Wave lines (Geldner, et al., 2009) (table 3-1).

Wave number	Name	At number	Assignment localisation	Localisation Ref.	Remarks
Wave 2Y	RabF2b (ARA7)	At4g19640	Late endosome/ prevacuolar compartment	(Rutherford and Moore 2002), (Nielsen 2009)	extensive experimental evidence for localization to multi-vesicular bodies and function in trafficking to vacuole
Wave 3Y	RabC1	At1g43890	Post Golgi/ endosomal		No experimental data found
Wave 5Y	RabG3f	At3g18820	Late endosome /vacuole	(Rutherford and Moore 2002; Carter, et al. 2004)	Homologs identified in vacuolar proteome
Wave 7Y	RabF2a (Rha1)	At5g45130	Late endosome/ prevacuolar compartment	(Rutherford and Moore 2002), (Nielsen 2009), (Carter, et al. 2004)	extensive experimental data for localization to multi-vesicular bodies and function in trafficking to vacuole
Wave 11Y	RabG3c	At3g16100	late endosome/vacuole	(Rutherford and Moore 2002), (Carter, et al. 2004)	Homologs identified in vacuolar proteome
Wave 24Y	RabA5d	At2g31680	Endosomal/ recycling endosome	(Choi and Roberts 2007)	
Wave 25Y	RabD1	At3g11730	Post-Golgi/endosomal	(Sanderfoot, et al. 2000, Uemura, et al. 2004)	similar to Wave29 and 33
Wave 27Y	RabE1d	At5g03520	Post-Golgi/endosomal	(Sanderfoot, et al. 2000, Uemura, et al. 2004, Conchon, et al. 1999)	different from reported Golgi localisation by transient expression in tobacco cells
Wave 29Y	RabD2a	At1g02130	Golgi/endosomal	(Rutherford and Moore 2002)	broad localisation, clearly extending beyond Golgi into endosomal compartments
Wave 33Y	RabD2b	At5g47200	Golgi/endosomal	(Rutherford and Moore 2002)	Broad localisation, clearly extending beyond Golgi into endosomal compartments
Wave 34Y	RabA1e	At4g18430	Endosomal/Recycling endosome	(Choi and Roberts 2007; Chow, et al. 2008)	Also strong cell plate localisation, data not shown
Wave 129Y	RabA1g	At3g15060	Endosomal/ Recycling endosome	(Choi and Roberts 2007; Chow, et al. 2008)	Also strong cell plate localisation, data not shown

Table 3-1: List of Wave lines used in this study in combination with 2BP.
Table modified from (Geldner, et al., 2009).

Many of these proteins are predicted to be palmitoylated based on a consensus sequence at their C-terminus (table 3-2).

Name	Prediction of palmitoylation	Palmitoylated peptide
RabF2b (ARA7) At4g19640	C198: 3.79 C199: 5.26	…SSS**CC**A*
RabC1 At1g43890	C209: 3.54 C210: 3.35	…SSY**CC**SS *
RabG3f At3g18820	C204: 1.52 C206: 2.15	…STG**C**E**C***
RabF2a (Rha1) At5g45130	C198: 3.70 C199: 5.76	…SSS**CC**A*
RabG3c At3g16100	C204: 1.47 C206: 1.99	…STG**C**E**C***
RabA5d At2g31680	C215: 3.04 C216: 3.59	…GFS**CC**SS*
RabD1 At3g11730	C202: 2.82 C203: 2.64	…NGG**CC**GQ*
RabE1d At5g03520	C202: 2.71 C203: 3.26	…KSA**CC**SY*
RabD2a At1g02130	C200: 3.93 C201: 4.12	…KNG**CC**ST*
RabD2b At5g47200	C199: 3.04 C200: 3.04	…QSG**CC**SS*
RabA1e At4g18430	C214: 3.14 C215: 3.51	…SSG**CC**SG*
RabA1g At3g15060	C214: 3.60 C215: 4.03	…KVG**CC**SS*

Table 3-2: Prediction of palmitoylation using CSS-palm 2.0 software.
In the second column a prediction value for palmitoylation is given for bolded cysteines (setting the software at the highest threshold).

As expected, not all analysed Rabs showed a clear mislocalisation upon treatment with 2BP, indicating that not all of them are palmitoylated (Figure 3-24). The main effect was detected for RabA5d (fluorescence very weak), RabE1d and RabA1a (Figure 3-24, squared pictures).

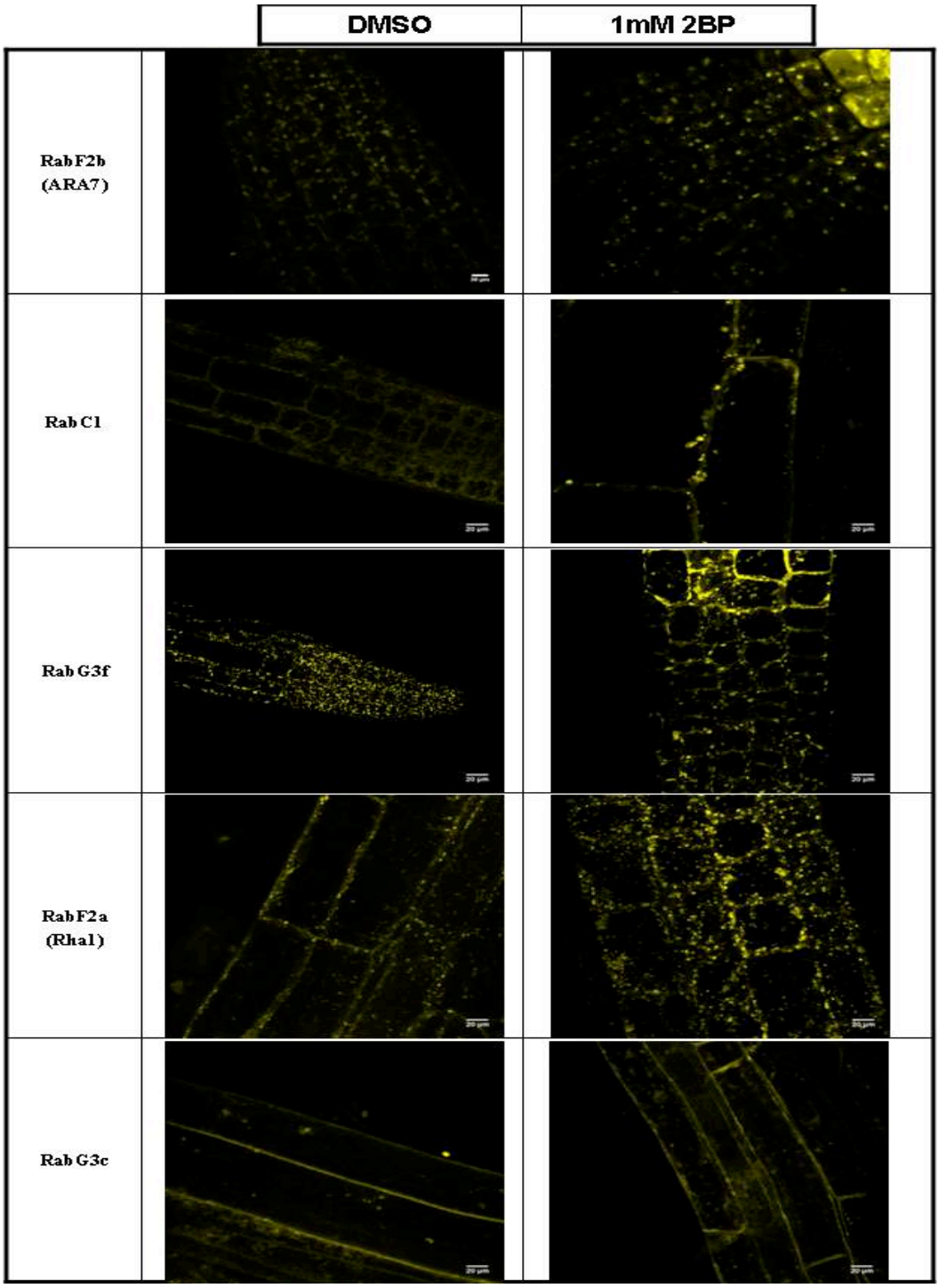
DMSO
1mM 2BP
RabF2b (ARA7)
RabC1
RabG3f
RabF2a (Rha1)
RabG3c

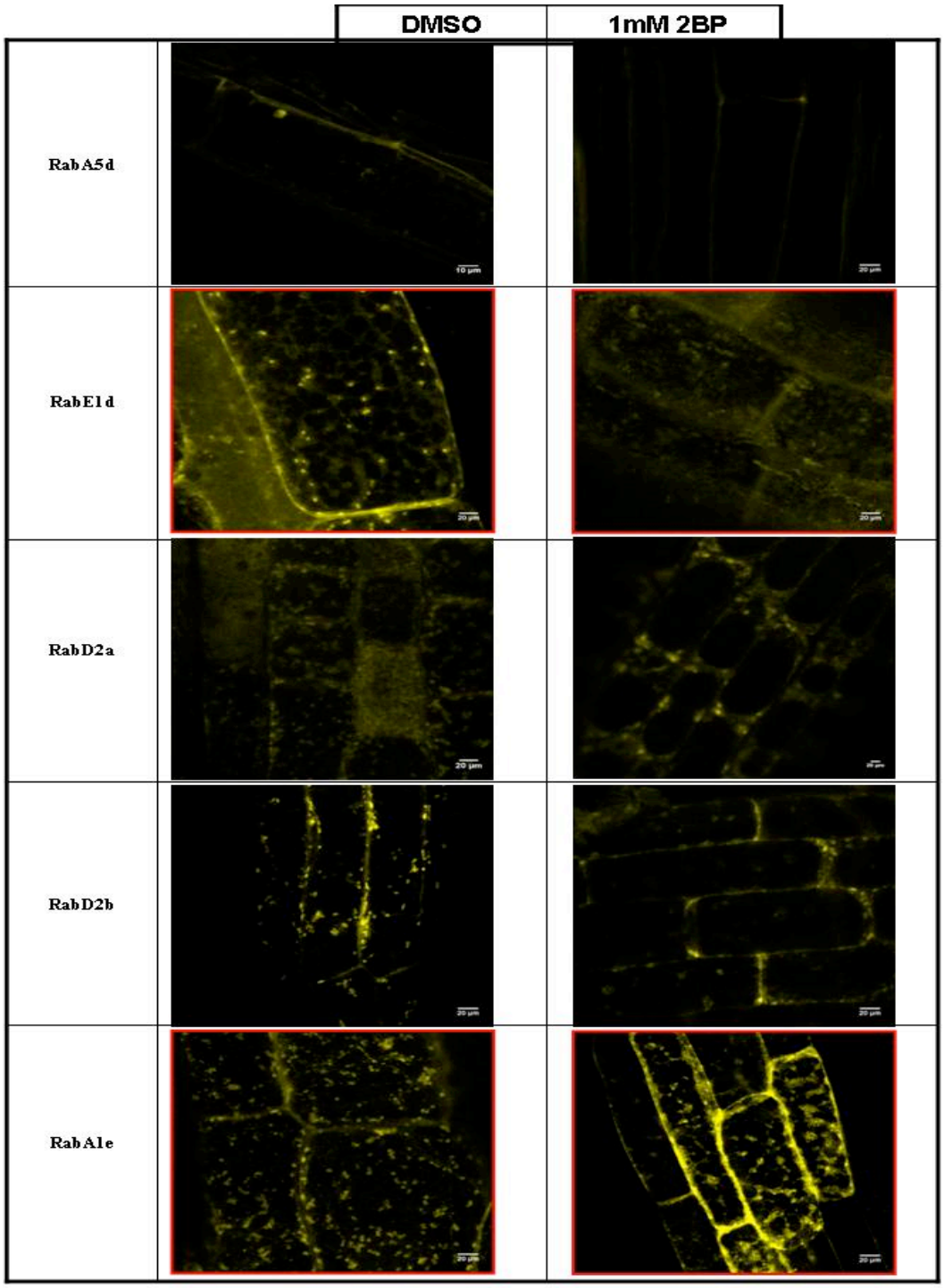

Figure 3-24: Effect of 2BP on Wave lines expressing different fluorescent Rab reporters
Confocal sections of 3-4 weeks old *Arabidopsis thaliana* roots incubated with liquid MS +/- 2BP and observed. Incubation time is 30 min.

Members of the RabA subgroups are thought to be involved in cell wall remodelling (Lycett, 2008) and in *Arabidopsis* roots treated with 2BP they showed a peripheral, probably cytosolic localisation.

The RabE1d isoform associated with an endosomal recycling system, likely in a polarized

growth, also mislocalised in the treated samples. Moreover, the untreated samples show a cytosolic pattern, with the typical strands. The 2BP treated samples always keep the cytosolic labelling, a diffuse fluorescence increased. This might be induced by increasing free YFP or losing its association with the endosomes (Figure 3-25).

In particular, RabA1a showed the expected punctuate pattern associated with endosomal recycling and in 2BP-treated samples the localization was clearly shifted to a cytosolic pattern, visible particularly in cytosolic strands and by empty structures externally labelled by the fluorescent fusion protein (Figure 3-26). Similar observations were made for RabA5d, which showed a peripheral pattern upon 2BP treatment (Figure 3-24).

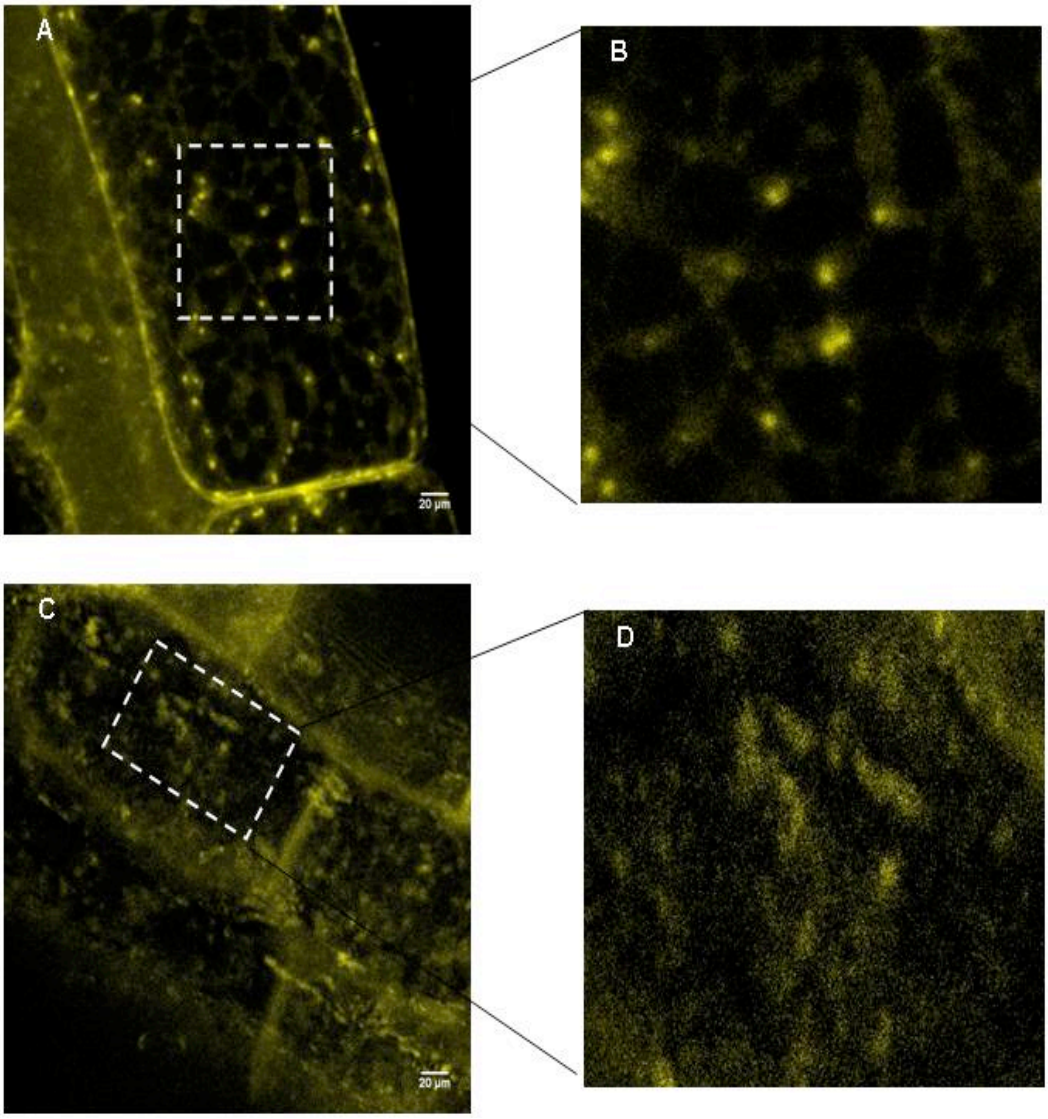

Figure 3-25: Effects of 2BP on *A. thaliana* roots expressing RabE1d fusion proteins (magnification of squared pictures in Figure 14).
Magnification of the pattern represented in Figure 14. *A.thaliana* roots incubated with MS plus DMSO (A-B) and plus 2BP (C-D). C&D are the magnification of the squared area in A&B respectively.

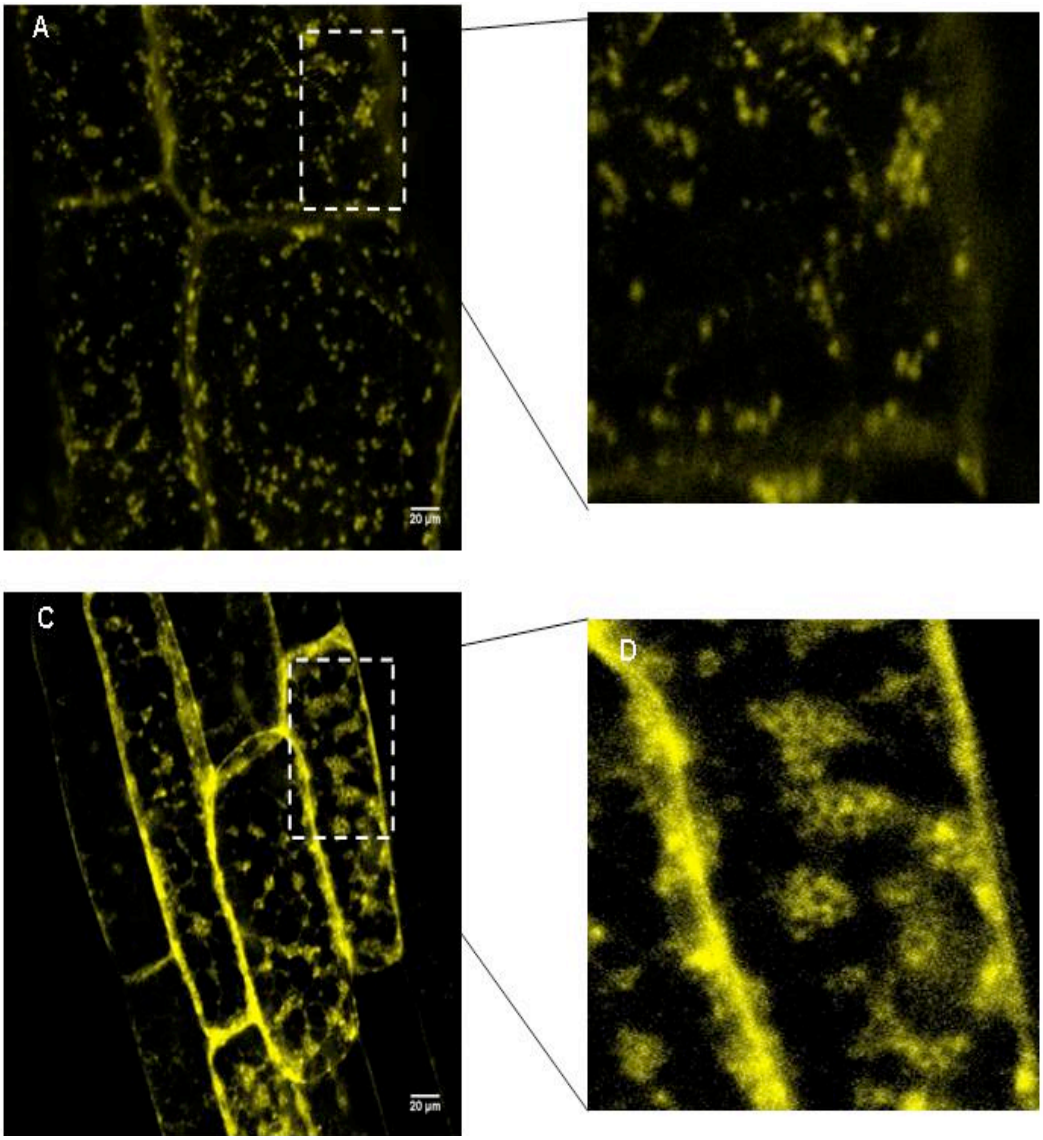

Figure 3-26: Effects of 2BP on *A. thaliana* roots expressing RabA1e fusion proteins (magnification of squared pictures in Figure 14)
Magnification of the pattern represented in Figure 14. *A. thaliana* roots incubated with MS plus DMSO (A-B) and plus 2BP (C-D). C&D are the magnification of the squared area in A&B respectively.

None of the other tested Rabs were affected by the drug in their localization. No fluorescence could be detected for the Wave line w25y and w129y (table 3-1).

Furthermore, FM4-64 incorporation was not affected by 2BP since it was clearly visible in *A. thaliana* roots expressing RabA1e at level of the cell plate (Figure 3-27).

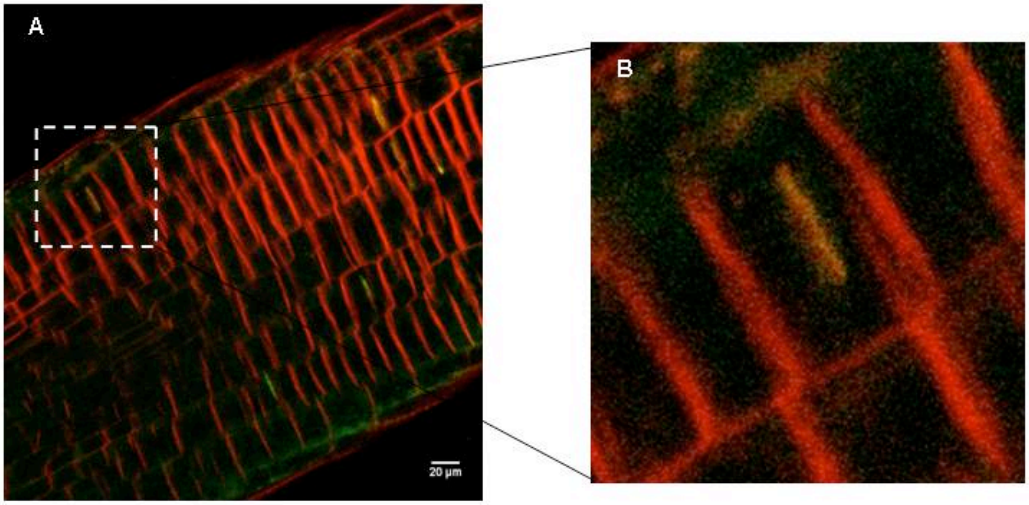

Figure 3-27: 2BP does not affect the formation of the cell plate
A. thaliana roots expressing RabA1e fusion protein in combination with FM4-64 incubated with liquid MS plus 2BP still reveals a strong cell plate labelling. In B magnification of the squared area on A.

3.9 Ultrastructural analysis in A.thaliana roots

In order to exclude any mislocalisation due to general, or local, membrane disorganization, freezing-freeze substitution fixation coupled to electron microscopy was performed on *A.thaliana* root tips treated with 2BP. In comparison with control plantlets, the 2BP treatment had no detectable effects (Figure 3-28). All the compartments had their well-known structure, suggesting that the drug does not alter their membrane organization. In some cells a slight swelling of the ER could be observed, but it was not a general and reproducible effect (Figure 3-28). This swelling could be due to the over-accumulation of misfolded proteins. This finding suggests that the mislocalisation of RabA5d, RabA1e and RabE1d is not due to global and unspecific membrane disorganization.

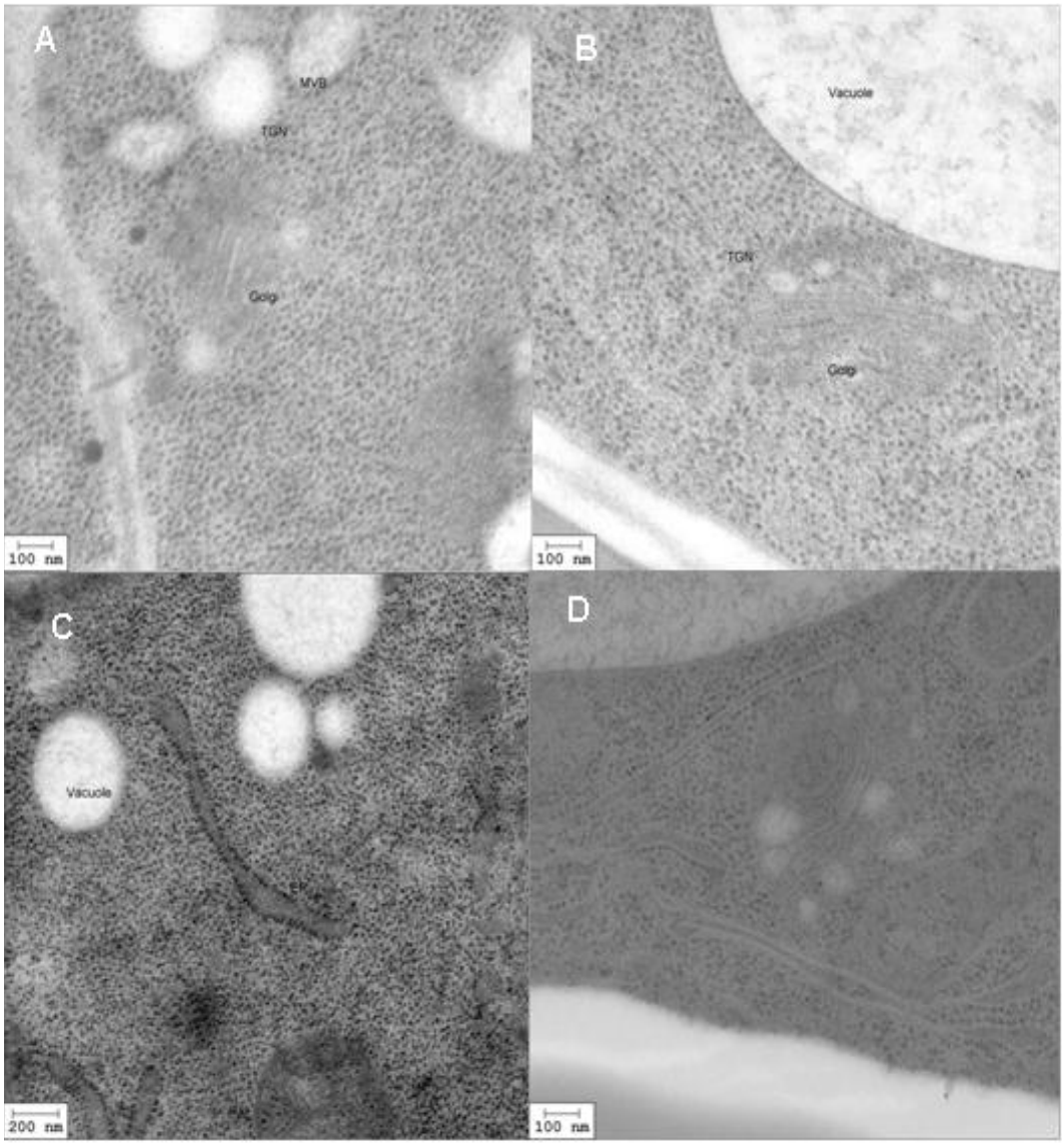

Figure 3-28: No difference in global membrane organization of *A. thaliana* root tips is detectable upon treatment with 2BP
In A, B and C 3-4 weeks old plantlets were incubated in liquid MS plus 2BP (in D plus DMSO). Roots were treated for a freeze-freezing substitution method and 30-80nm slices were analysed in a JEM 1400 transmission electron microscope operating at 80Kv.

3.10 Discussion

The aim of this work is to determine which specific intracellular compartment is affected by the palmitoylation inhibitor 2-Bromopalmitate. Palmitoylation is a general and pervasive post-translational modification occurring in all eukaryotic cells and the only reversible lipid modification. According to the literature many proteins are palmitoylated (Levental, et al., 2010a; Levental, et al., 2010b), and they have different functions such as promoting membrane anchoring and/or association with protein partners. The role of palmitoylation in

plants trafficking is far from being elucidated.

This work aims to shed light on specific functions of palmitoylation on secretion, in contrast to the overall role of palmitoylation. In order to investigate the hypothesis that palmitoylation could affect the structure of intracellular compartments, different intracellular markers were used in combination with 2BP. No particular shifts in localization were detected, except for the vacuolar marker GFP-Chi and for the TGN marker SYP61 (Figure 3-23 G-H and E-F, respectively).

GFP-Chi is a marker which can be followed through the secretory pathway during transient expression in *N. benthamiana* leaves (Sansebastiano, et al., 1998). In Arabidopsis plants stably expressing GFP-Chi, the central vacuole is strongly labelled and only in juvenile tissues is it possible to distinguish small compartments defined as "neutral vacuoles". Therefore, transient expression allowed following the fate of this vacuolar marker, from a punctate pattern to a central vacuole labelling within 60-72h. Upon 2BP treatment GFP-Chi accumulated faster in the central vacuole, the reason for which is not clear. Possibly, the vacuolar sorting receptor for the reporter was impaired and this led to an accumulation in the lytic vacuole by activation of an alternative pathway (an ER-Vacuole pathway). However, this finding clearly demonstrates that the drug does not affect vacuole biogenesis *per se*, *e.g.* by fragmentation of the tonoplast.

For the TGN marker SYP61, *in silico* analysis showed no putative site of palmitoylation. Therefore, the effect observed is likely due to a "side-effect" on SYP41, a partner of SYP61 and VTI12 in the ternary complex required for the delivery of soluble markers to the vacuole (Zouhar, et al., 2009), as SYP41 is predicted to be palmitoylated.

We chose to concentrate on apical growth, in which the secretory pathway can be well studied. We chose two systems with well-studied properties, the elongating pollen tube and the moss protonema.

The 2BP dose-response curve was determined with *Nicotiana benthamiana* pollen grains. A dramatic germination inhibition was observed at 1mM 2BP (Figure 3-18), which was then used as working concentration.

Further investigation highlighted a clear inhibition by 2BP of the apical growth in the two systems, *Physcomitrella patens* protonema (Figure 3-17) and *N. benthamiana* pollen tubes (Figure 3-18; 3-19). This inhibition was not due to cell death, as mitotic spindles were observed in moss (Figure 3-16).

This inhibition of apical growth was initially thought to be associated with cytoskeleton remodelling, as many small GTPases belonging to ROPs subgroups are involved in this process (Gu, et al., 2004; Gu, et al., 2005). However, no particular change in cytoskeleton organization was observed in *N.benthamiana* leaves, neither for microtubules nor for microfilaments (Figure 3-12). Furthermore, in moss we could still detect the apical star of actin, showing that the new growing site was not abolished by 2BP (Figures 3-15). This finding excludes a large number of proteins involved in cytoskeleton remodelling, like dyneins (Cai, et al., 1997; Moscatelli, et al., 1998; Romagnoli, et al., 2003) and kinesins (Cai, et al., 2000) .

With the endocytic tracer dye FM4-64 it was still possible to highlight after short time incubation an endosomal recycling activity, in both treated and untreated samples (Figure 3-10). In pollen tubes an enormous flux of newly synthesized membrane on the lateral walls of the pollen tube has to be recycled. Indeed the main exocytosis sites are the lateral shanks of the pollen tube at ~6-10µm from the very tip (Zonia and Munnik, 2008; Zonia and Munnik, 2009).

Starting from the very tip, it was possible to detect the typical "reversed cone" in the untreated, as well as in the treated pollen tube. There also still was endocytosis as the tracer uniformly labelled endocytic compartments. This shows that 2BP does not interfere with this crucial activity. Moreover this area is also less optically-dense than the rest of the surrounding cytoplasm, showing that the recycling area is not involved in the transport of cell-wall components and/or PM (Figure 3-10). Labelling of pollen tubes by FM4-64 revealed after 2h 2BP treatment a clear perturbation of macro-vesicles of secretion (Zonia and Munnik, 2008) or TGN/endosomes (Wang, et al., 2005) compared to untreated pollen tubes (Figure 3-21B).

In the latter samples, it was possible to observe the presence of structures strongly labelled by the dye, while in the treated samples the fluorescence was diffuse and almost no such structures were visible (Figure 3-21 D).

Further ultra-structural analysis by scanning electron microscopy also pointed to defective cell wall remodelling at the shank of pollen tubes (Figure 3-28). In the treated samples we observed there the formation of bubble-like structures, which were absent in the untreated samples. This area has been widely studied and is currently considered as the main exocytosis site in pollen tubes. This model differs from the old model which pointed out a general defect: continuous cell wall remodelling in a very small region from the tip (3-5 um) implies a huge exo- and endocytosis activity and a high production of cell wall remodelling enzymes, with a

high-cost consuming for the cell. Moreover, the cell wall is thinner at the tip than along the rest of the pollen tube. In fact, the apical hemisphere is mainly composed of pectins and with a remarkable absence of cellulose. The sub-apical region and lateral shanks, on the contrary, are covered by an inner cell wall composed also of cellulose and callose that is positioned underneath the outer (or also called primary) cell wall (Cole and Fowler, 2006). This demonstrates the existence of differently regulated membrane delivery between the sub-apical/lateral shank and tip region.

Zonia and Munnik (2008) described three active regions of endomembrane trafficking in pollen tubes: 1) an endocytic recycling region at the very tip of the cell. This finding is in agreement with other studies revealing that the very tip of pollen tubes is an active endocytic area recycling excess plasma membrane and with a high Ca^{2+} influx (Camacho and Malho, 2003). 2) An exocytic sub-apical region (3-10 um from the apex. This exocytosis involves two classes of large vesicles (400 and 650 nm) .3) another endocytic region along the lateral shank of the tube. The endocytosis in this region is mediated by larger vesicles (~700 nm) suggesting that clathrin-coated vesicles might be involved in this process. Electron microscopy experiments on cryo-fixed tobacco pollen tubes are also in agreement with this model showing that the region between 6 and 18 μm from the tip is enriched in clathrin coated vesicles (Derksen, et al., 1995) Furthermore, two distinct endocytosis pathways, including one mediated by clathrin-coated vesicles, were reported for pollen tubes using charged nanogold particles (Moscatelli, et al., 2007).

Camacho and Malho (2003) also demonstrated a clear relationship between tip growth and GTP-dependent activities. Incubating pollen tubes with the non-hydrolysable analogue GDPβS (which locks small GTPases in an inactive form), the average length of the pollen tube was considerably decreased (-30%). Incubation of pollen tubes with 2BP reduced the average length to a very similar degree (-28%). It known from literature that depalmitoylation leads to an inactive GDP-bound state of some small GTPase (Rocks, et al., 2005; Levental, et al., 2010a). 2BP appears to mimic the effect of GDPβS in reducing the elongation of pollen tubes by also inhibiting the function of small GTPases.

A recent systems model describes vesicle trafficking during pollen tube growth (Kato, et al., 2010). In this model the author could restrict the number of important key proteins to a few families of proteins including Rabs. We decided to investigate a possible role of Rabs in palmitoyl-dependent processes and therefore chose to examine the effect of 2BP on different Rab-Wave reporter lines (Geldner, et al., 2009). As expected, not all Wave lines expressing

Rab-fluorescent protein fusions were affected by 2BP after a short time incubation (30 minutes) as only three members belonging to RabA (RabA5D and RabA1e) and RabE (RabE1D) subgroups were mislocalised (Figure 3-24). RabAs are generally described as being involved in endosomal recycling activity (Geldner, et al., 2009), although more extensive analysis showed also a possible involvement at the Golgi level (Pinheiro, et al., 2009). A more complete description of their functions, including the role of various post-translational modifications, needs to be performed. Endosomal recycling is however not affected in *N.benthamiana* pollen tubes since the typical reversed cone is present after a very short treatment. On the contrary, a clear mislocalisation is visible in *A.thaliana* roots. For both RabA1e and RabA5D (although the latter's fluorescence was very weak, Figure 3-24) a cytosolic pattern was induced by the 2BP treatment and for RabA1e (Figure 3-26) also the formation of empty structures surrounded by the fluorescent protein, probably still associated to the TGN/endosome. RabA1e also still strongly labelled the cell plate, a transient membrane compartment that is formed by the fusion of vesicles and eventually becomes the plasma membrane and cell-wall between the daughter cells (Jürgens, 2005). Generally, cytosolic patterns of Rab proteins are associated with an inactive state.

Less is known about RabE1d, which seems to be involved in polarized endosome-dependent processes (Vernoud, et al., 2003). RabE1d shows a typical punctuate structure with also a weak cytosolic labelling. In the untreated samples, on the contrary, the punctuate structures disappeared giving way to a diffuse, probably cytosolic fluorescence and to unstructured compartments (Figure 3-25).

The other Wave lines tested in this study did not show any significant difference (Figure 3-24).

To demonstrate that the observed mislocalisations were not due to a general membrane disruption in the endomembrane system, ultrastructural analysis on *A.thaliana* root tips was performed. No change was observed and therefore the mislocalisation of the three Rabs is probably a direct effect of 2BP on these proteins.

Two articles (Toyooka, et al., 2009b; Kang, et al., 2011) have shown the existence of vesicle clusters similar in size (~400 nm) to the macrovesicles of secretion described by Zonia et al., (2008). In these articles the authors demonstrate the existence of clusters of secretory vesicles, which are initially associated with the Golgi and then mature in free TGN. Here the two models diverge: Toyooka et al. assert that whole clusters are involved in exocytosis and fuse to the plasma membrane, whereas Kang et al. demonstrate that single secretory vesicles fuse with the plasma membrane. These three articles, in conclusion, have identified main actors

involved in secretion at the plasma membrane. These structures, clearly visible in pollen tubes using the endocytic tracer FM4-64 (Figure 3-21), disappear in presence of 2BP. This is likely due to the breakdown of the macrovesicles of secretion (or free TGN or vesicle clusters), shifting the balance towards the presence of free secretory vesicles. These vesicles are very small (average ~70 nm) and cannot be resolved by regular confocal laser scanning microscopy, which has a resolution of ~200 nm in the x and y-axes and 500-800 nm in z-axis (Jakobs, 2006). Our data demonstrate the inhibition by 2BP, and therefore the importance of palmitoylation, in the process of secretion by interfering with the formation of macrovesicles of secretion. Moreover, three palmitoylated proteins (RabA5d, RabA1a, and RabE1d) have been identified by this study as good candidate targets of 2BP. No information is available for the role of these RabA proteins in the secretory pathway. No phenotype of single KO mutants has been reported, but there is a possible redundancy among the 26 members of this subclass. Neither has any KO mutant or dominant-negative mutant been reported so far.

Regarding the RabE subclass (five members including RabE1d) an interaction was demonstrated between GTP-bound RabEs and PIP5K2 (Camacho, et al., 2009). RabE subclass members were found to localise in Golgi via a nucleotide- and lipid-dependent mechanism in *Arabidopsis* root tips and to the plasma membrane in *Arabidopsis* leaves, strongly suggesting a role in trafficking (Zheng, et al., 2005). A dominant-negative mutant (RabE1d S29N, locked in the GDP-bound state) was mainly cytosolic. The diffuse and inhomogeneous pattern observed in this work for RabE1d (Figure 3-25), suggesting a cytosolic localization in presence of 2BP, can effectively be due to its depalmitoylated, and hence inactive, GDP-bound state (Camacho, et al., 2009).

These findings open new approaches to study Rab-dependent polarized secretion. A special attention will be focussed on the role of palmitoylation. New Rab mutants will be needed lacking the palmitoylation sites.

More generally the functions of palmitoyl transferases (PAT) and acyl protein thioesterases (APT) will be need to be addressed. A first step here will be the characterization of the palmitoyl-proteome of Arabidopsis to better decipher the various roles of this important post-translational modification and in particular in polarized secretion.

4. The vacuolar marker GFP-Chi can bypass the ER- Golgi route and reach the vacuole.

4.1 Introduction

During the last years our laboratory has developed and characterized two vacuolar reporters: a GFP fusion in frame with the C-terminal Vacuolar Sorting Determinant (VSD) of tobacco chitinase (GFP-Chi) and a N-terminal fusion in frame with the sequence-specific VSD of the cysteine protease barley Aleurain (Aleu-GFP). These fusion proteins allowed the identification of two different vacuoles: a non-acidic vacuole labelled by the GFP-Chi and an acidic vacuole labelled by Aleu-GFP (Fluckiger, et al., 2003). Furthermore, each reporter has independent routes to arrive to the vacuole since Aleu-GFP interacts to VSR-1 and labels the central vacuole while it is unknown the vacuolar receptor of the chitinase and labels small vacuoles with a clear ER labelling. The Arabidopsis aleurain was found to bind to VSR-1 (Ahmed, et al., 2000) although it was recently shown that VSR4 also might participate to the vacuolar trafficking demonstrating a certain functional redundancy among vacuolar sorting receptors (Zouhar, et al., 2010).

Several studies have addressed the pathway of the GFP-Chi to vacuoles. It has been argued very convincingly that the GFP-Chi follows the classical pathway passing through Golgi-TGN-PVC, involving *At*VPS45 (Zouhar, et al., 2009) and VTI12 (Sanmartin, et al., 2007) and reaching finally the central large vacuole. On the other hand, it was also highlighted that GFP-Chi could bypass the Golgi-TGN-PVC route: incubation of Arabidopsis roots expressing GFP-Chi with BFA did not dramatically alter the typical punctate GFP-Chi pattern, while Aleu-GFP targeting was inhibited (Poustka, et al., 2007).

As Zouhar et al (2009) asserted in their discussion it was still possible to detect a faint fluorescence in GFP-Chi plants crossed with VPS45-silenced plants, meaning " that less fusion protein was reaching the vacuole " while the majority was effectively secreted into the apoplast. Similar observations were also made by Sanmartin et al. (2007) in GFP-Chi plants crossed with a *vti12* null allele. These observations are very interesting and represented the starting point of this work, based on the hypothesis that GFP-Chi might reach the central

vacuole by an alternative pathway bypassing the Golgi-TGN-PVC route.

Other typical ctVSD proteins, the 7S and 2S globulins, are delivered to the Protein Storage Vacuole bypassing the classical route in maturing pumpkin seeds, as revealed by electron microscopy (Hara-Nishimura, et al., 1998). This trafficking is achieved by PAC vesicles (Precursor Accumulating Vesicles) in which storage proteins aggregate.

Although functionally similar compartments were also described in leaf tissues of three plant species (Park, et al., 2004a), no evidence for the existence of a direct ER-Vacuole (ERV) pathway was provided.

In order to verify the existence of such an alternative pathway for the transport of GFP-Chi to vacuoles, we decided to block the traffic via the Golgi using *Nt*Sa1H74L (Andreeva, et al., 2000), which blocks the COPII vesicle-mediated anterograde transport from ER to Golgi (Barlowe, et al., 1993; Takeuchi, et al., 1998; Takeuchi, et al., 2000).

4.2 Blocking the ER-Golgi trafficking does not retain the vacuolar reporter GFP-Chi in the ER

GFP-Chi can be considered a slow vacuolar reporter, in contrast to Aleu-GFP (Di Sansebastiano, et al., 2001) and other vacuolar markers. Indeed, in a transient expression assay RFP-AFVY, targeted to the vacuole by the Ct-VSD of bean phaseolin (REF) is very quickly accumulating in the vacuole, while most GFP-Chi is still in the ER after 24-36h infection (Figure 4-1), and only labels some large central vacuoles after 48h (Figure 4-2).

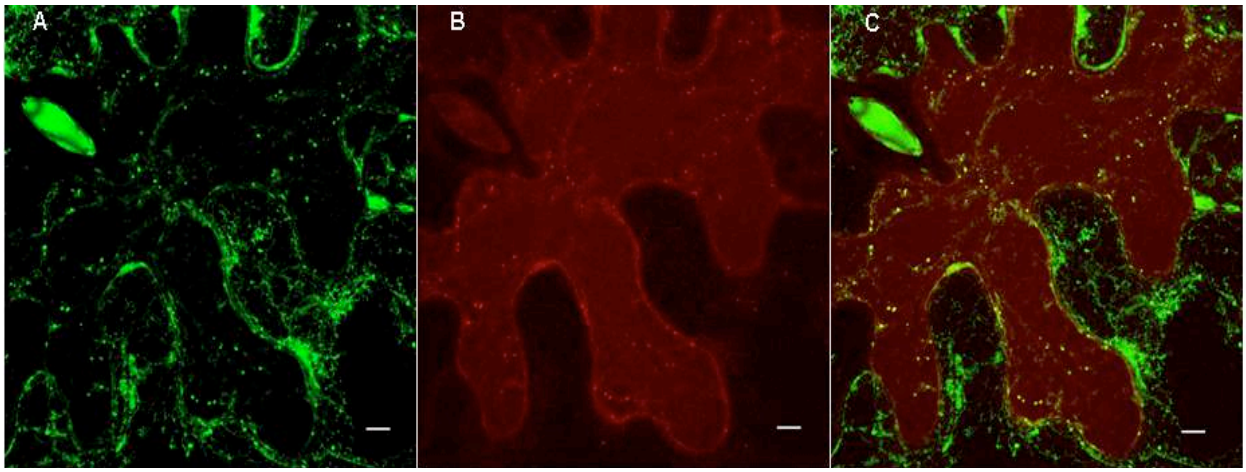

Figure 4-1: GFP-Chi does not colocalize with RFP-AFVY at 36h of expression
Agroinfiltrated *N. benthamiana* leaf expressing both A) GFP-Chi and B) RFP-AFVY; C) merged image. Scale bar is 20 µm

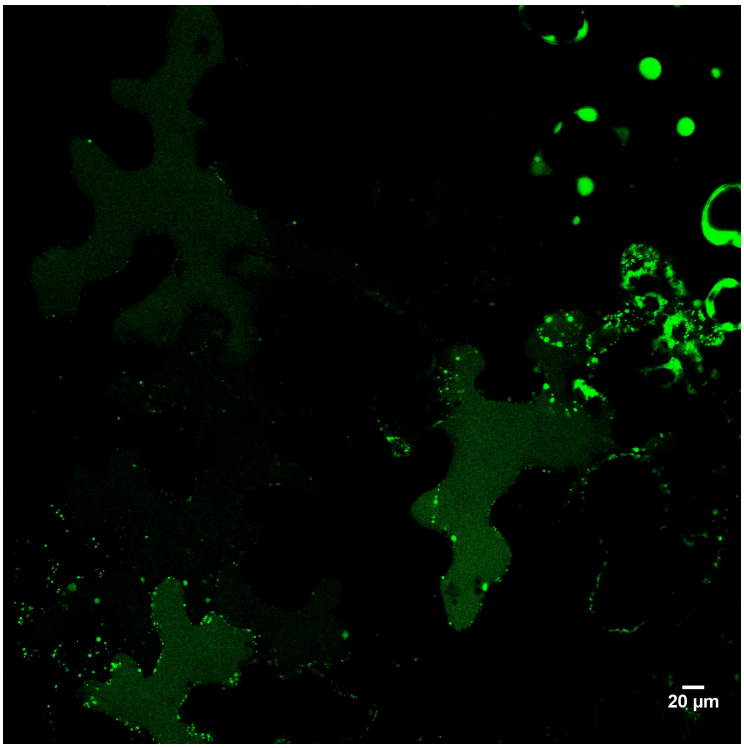

Figure 4-2: GFP-Chi also reaches the central vacuole when trafficking via the Golgi is inhibited
Agroinfiltrated *N.benthamiana* leaf expressing the vacuolar reporter GFP-Chi and the dominant negative mutant NtSar1H74L.

The dominant-negative mutant of Sar1, NtSar1H74L has been shown to block the ER-Golgi trafficking by interfering with the COPII-vesicle mediated transport (Andreeva, et al., 2000). Unexpectedly, GFP-Chi even more strongly labelled the lumen of the central vacuole in co-agroinfiltration experiments with *Nt*Sar1H74L. In fact it increased rather than decreased the vacuolar labelling (Figure 4-3).

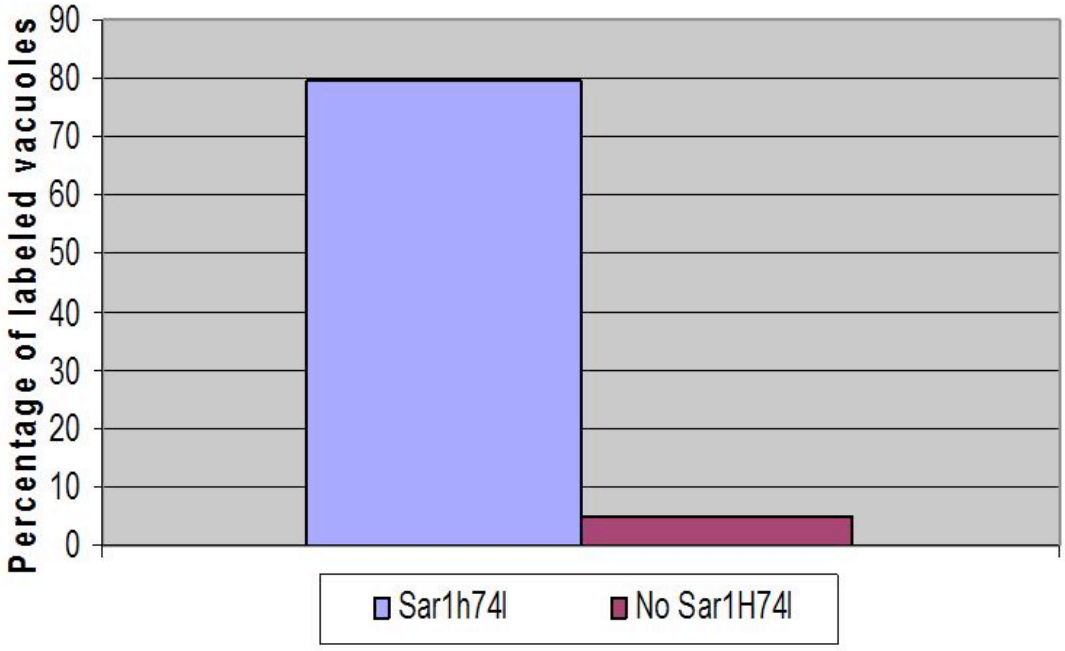

Figure 4-3: GFP-Chi labelling of the central vacuole in presence or absence of Sar1H74L
Epidermal cells, with or without vacuolar labelling, were counted on leaves expressing GFP-Chi with or without *Nt*Sar1H74L. The graph presents data from three independent experiments. Number of cells: 135 for "No Sar1H74L" and 57 for "Sar1H74L"

In addition to this vacuolar pattern, 10-20 µm round structures incorporating smaller vesicles were also labelled by the soluble vacuolar reporter and the Golgi marker Gonst1-RFP (Baldwin, et al., 2001), used as a control to verify the effective collapse of Golgi apparatus. These structures showed a strong fluorescence associated to membranes and a high co-localization (Figure 4-4)

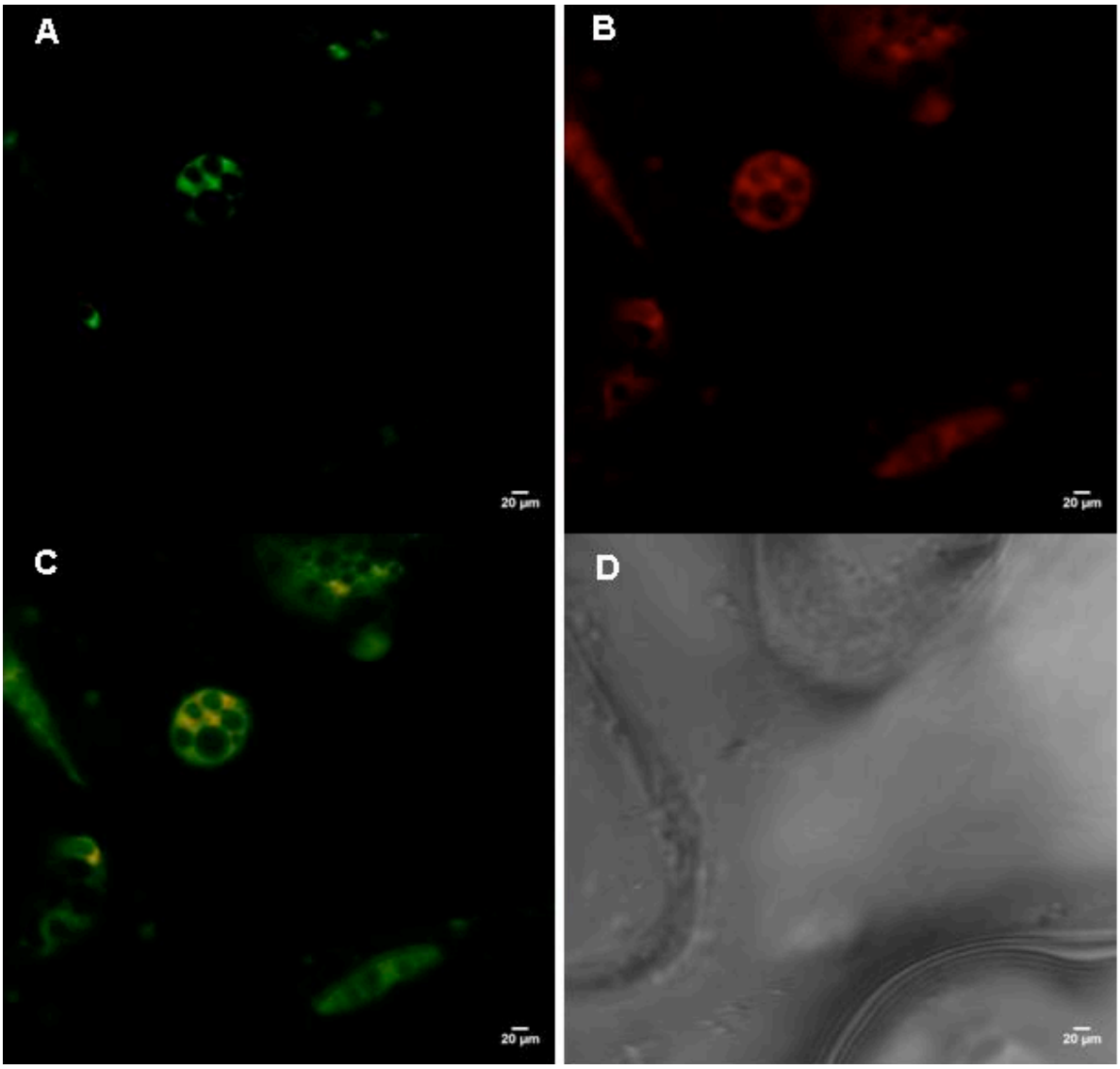

Figure 4-4: Presence of large multivesicular aggregates in cells expressing GFP-Chi and Gonst1-RFP in presence of Sar1H74L
N. benthamiana agroinfiltrated leaves expressing A) GFP-Chi; B) Gonst1-RFP; C) Merge; D) bright field

while in cells not transformed with Sar1H74L cells, the two signals were well separated (Figure 4-1).

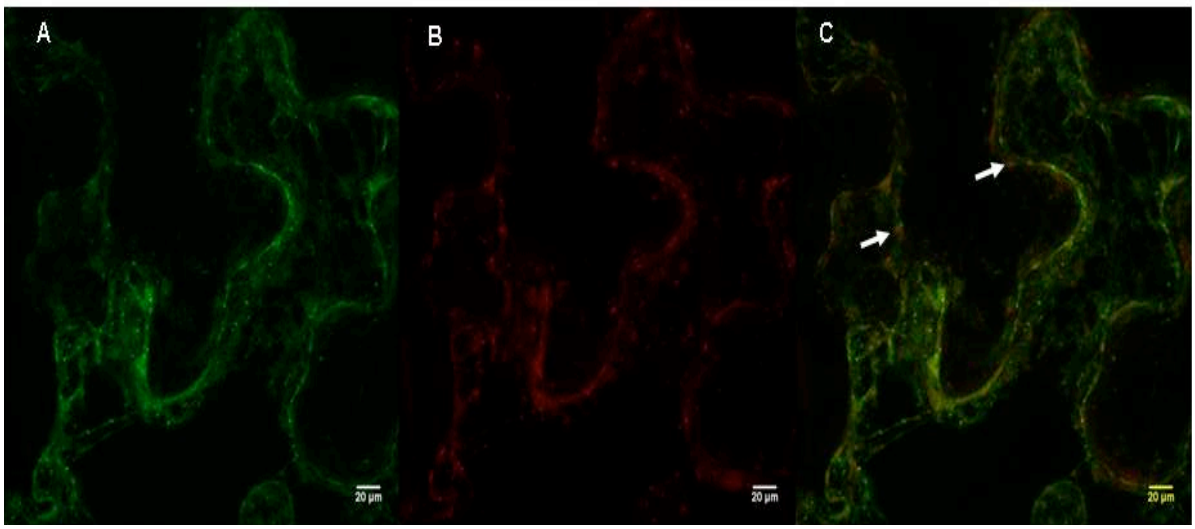

Figure 4-5: GFP-Chi does not colocalize with Gonst1-RFP
Nicotiana benthamiana agroinfiltrated leaves expressing A) GFP-Chi; B) Gonst1-RFP; C) merge. Arrows show Golgi labelled by Gonst1, which does not co-localize with GFP-Chi

Another widely used ct-VSD marker, RFP-AFVY (Hunter, et al., 2007) has been used in co-localization experiments with GFP-Chi. Both markers show an ER labelling (Figure 4-1),and small dots which have been described as a cortical ER (Zouhar, et al., 2009). Co-localization experiments performed with the ER luminal marker RFP-HDEL do not support this analysis as the fluorescence signal of these dots are perfectly separated from the ER labelling (Figure 4-6).

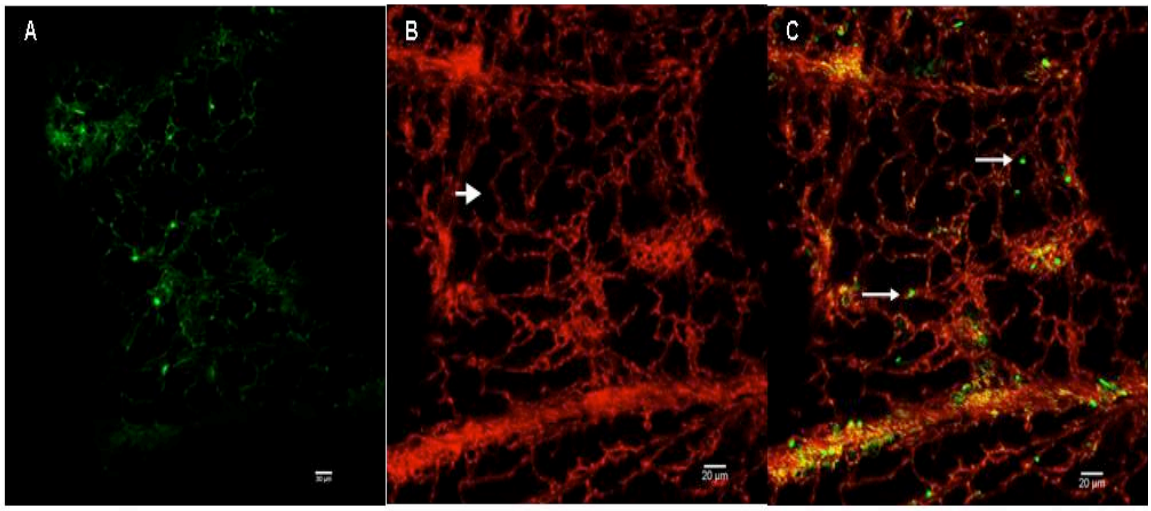

Figure 4-6: GFP-Chi does not colocalize with RFP-HDEL
Nicotiana benthamiana agroinfiltrated leaves expressing A) GFP-Chi; B) RFP-HDEL; C) merge. Arrow shows dots while arrowhead the typical ER labelling.

Also the hypothesis that they might be protein bodies can be rejected, as these structures do not tend to have continuity with the ER.

4.3 GFP-Chi aggregates and reaches the vacuole as a dimer

Aggregation was shown to be part of the sorting mechanism for the phaseolin (Castelli and Vitale, 2005). In order to test the hypothesis that GFP-Chi also aggregates in the ER and that its aggregates are effectively delivered to the vacuole, we fractionated extracts from agroinfiltrated N.benthamiana leaves coexpressing GFP-Chi, Gonst1-RFP (a Golgi marker) and with/without Sar1H74L to soluble and membrane fractions by ultra-centrifugation. We analysed the fractions by immunoblotting with antibodies for each marker. In Sar1H74L-treated samples we detected with the GFP antibodies a much increased ~60 KDa band, corresponding twice the molecular weight of GFP-Chi was detected in the membrane fraction, while the band corresponding to the monomeric form almost disappeared (Figure 4-7).

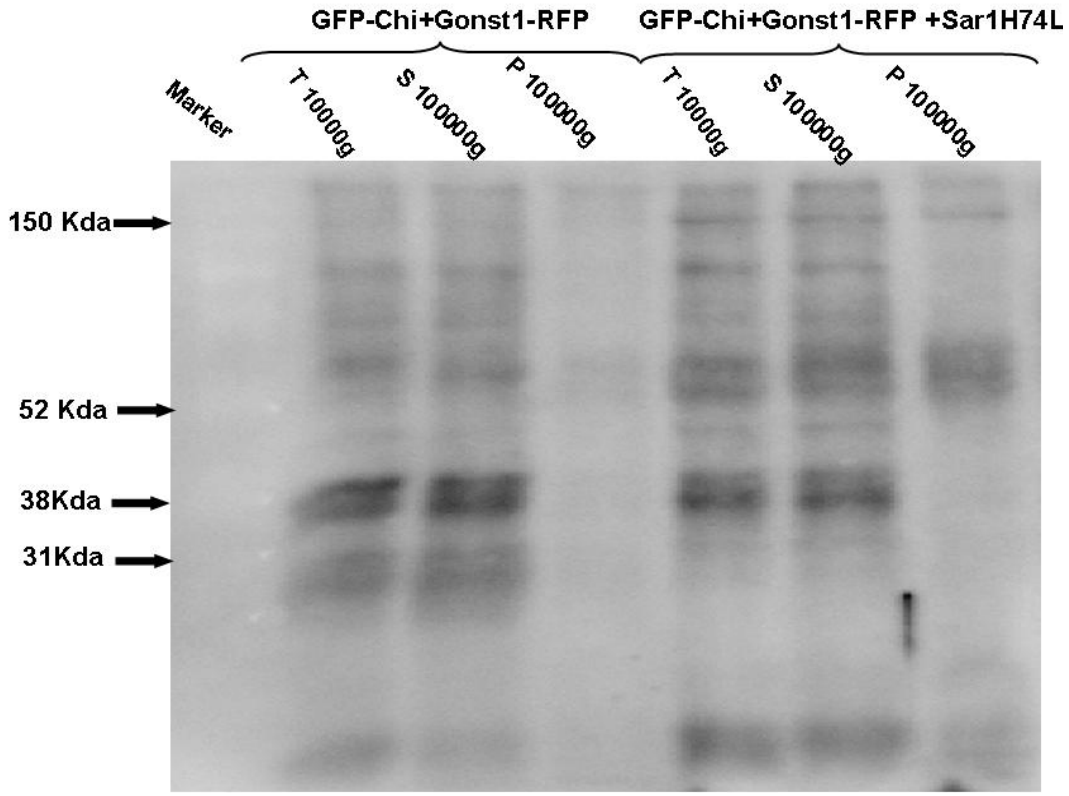

Figure 4-7: GFP-Chi aggregates in presence of Sar1H74L
N.benthamiana leaf extract after agroinfiltration to express GFP-Chi and Gonst1-RFP +/- Sar1H74L was fractionated by ultracentrifugation. T: 200µg of total proteins S: corresponding to the soluble proteins, P: corresponding membrane fraction. Detection with GFP antibodies.

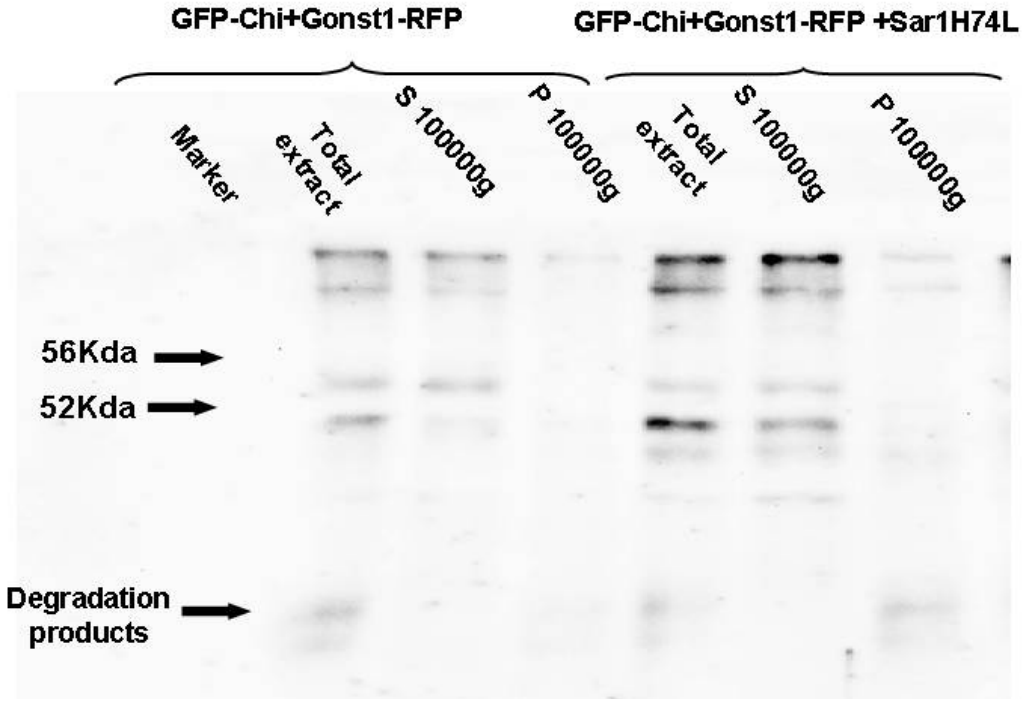

Figure 4-8: Gonst1RFP does not aggregate in presence of Sar1H74L
Approximately 200µg of total proteins were loaded onto the two lanes of total extract. S100000g lanes represent the proteins after ultracentrifugation at 100000g. P100000 lanes represent the corresponding membrane fraction. Anti RFP.

Bands were also detected at very high molecular weights, possibly corresponding to a pentamer. However the pattern detected by these antibodies is rather complex including a band at 38 KDa in treated and untreated samples. No reasonable explanation was found for this band, expect a possible ubiquitination or sumoylation modification.

Gonst1 RFP, used as control for the effect of the Sar1 mutant, does not show any aggregation in the pellet fraction except for some very high molecular weight bands, presents in the treated sample as in the untreated.

4.4 Immunogold labelling in GFP-Chi expressing plants

In order to identify the GFP-Chi accumulating structures, we further analysed stable plants expressing GFP-Chi (Fluckiger, et al., 2003) by immunoelectron microscopy. Unfortunately their nature remains elusive. In fact, we observed a clear ER labelling (Figure 4-9 A) and also a weak labelling in the central vacuole (arrows, Figure 4-9 B). Moreover, we also detected the labelling of a non-electron dense structure, which might be cytoplasm (arrowhead, Figure 4.9)

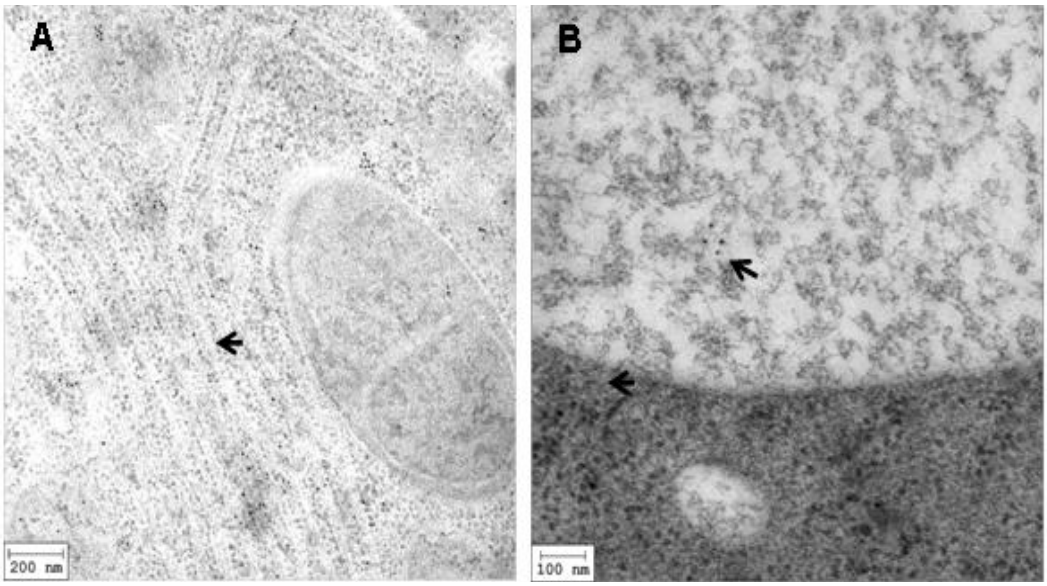

Figure 4 9: GFP-Chi accumulates in the ER, in the central vacuole and in non-identified organelles.
Two ultrathin sections of *A. thaliana* roots observed by TEM upon high-pressure freezing-freeze substitution fixation. A, ER labelling (arrow). B, vacuolar labelling (arrow) and a non-identified compartment (arrowhead).

4.5 Discussion

The existence of a Golgi-independent ER-vacuole pathway has been demonstrated in maturing pumpkin seeds (Hara-Nishimura, et al., 1998). This pathway includes large 200-400 nm dense vesicles (Precursor Accumulating vesicles, PAC) filled with vacuolar storage proteins, mainly 2S and 7S globulins. The production of storage proteins is very active in seeds and this pathway seems to ensure their efficient delivery to the PSV. Storage proteins are present at high concentrations in the ER lumen, where they tend to aggregate, even as soluble proteins. These aggregates are incorporated into PAC vesicles and transported to the PSV.

Although the presence of a PSV has also been demonstrated in green tissues (Park, et al., 2004a), no evidence for a Golgi-independent pathway has been provided so far. This may be due to a lack (or too low amounts) of storage proteins in green tissues and therefore to a reduction or suppression of this pathway.

GFP-Chi is a vacuolar reporter labelling the central vacuole in mature leaves and small dots in small Arabidopsis roots. These small dots were suggested to be small protein storage vacuoles (Fluckiger, et al., 2003), although no electron microscopic image is available for protein storage vacuoles in vegetative tissues. The present work also wanted to verify the existence of

PSV in vegetative tissues e.g. young roots of Arabidopsis stably expressing the fluorescent reporter. Unfortunately, in our high-pressure freezing-freeze substitution experiments, it was only possible to detect labelling of ER and unspecified compartments with the same electron-density as cytoplasm (Figure 4-10). This could be due to the absence of storage proteins in vegetative tissues and in consequence the loss of electron density so typical of PAC vesicles or dense vesicles, which made the identification of this compartment in vegetative tissues elusive. Another widely used vacuolar marker, RFP-AFVY was shown to be targeted to the central vacuole by its C-terminal tetrapeptide (the Ct-VSD of phaseolin (Greenwood and Chrispeels, 1985; Frigerio, et al., 1998; Frigerio, et al., 2001)). Like GFP-Chi, phaseolin labels intermediate compartments along the route to the central vacuole, defined as PSV (Park, et al., 2004b). Phaseolin passes through the Golgi, and its transport (and ultimately its labelling of the central vacuole) is inhibited by the overexpression of AtSa1H74L. Although both GFP-Chi and RFP-AFVY markers have a Ct-VSD, it is clear from confocal images that they label the vacuole at different times, as it is shown in Figure 4-3. Our results confirms a first description of a possible Golgi-bypassing route to the vacuole but overlapping for between the anthocyanins and GFP-Chi transport (Poustka, et al., 2007). The paper also showed in *A. thaliana* roots stably expressing GFP-Chi that a BFA treatment did not alter its typical punctuate pattern.

In two different papers (Sanmartin, et al., 2007; Zouhar, et al., 2009), Enrique Rojo's group used mutant lines of two different TGN syntaxins (a VTI12 KO line and VPS45 silenced line respectively), which both missorted the vacuolar reporter GFP-Chi to the extracellular space. In both cases they also noted a faint fluorescence in the lumen of the central vacuole, indicating a residual vacuolar targeting.

Hypothesizing that this "weak fluorescence" was due to an accumulation of the fluorescent reporter in the vacuolar lumen by a direct ER-to-Vacuole pathway bypassing the Golgi, we blocked the traffic between ER and Golgi by the transient expression of a Sar1 dominant-negative mutant. Sar1 belongs to the Ras protein super-family (Vernoud, et al., 2003) and acts between ER and Golgi by controlling the formation of COPII vesicles.. As widely demonstrated in yeast (Oka and Nakano, 1994), locking this protein in the active GTP- form with GTPγS (a non-hydrolysable analogue of GTP) resulted in the accumulation of functional ER-Golgi intermediate vesicles. Subsequently plants Sar1 mutants were developed, *Nt*Sar1H74L (Andreeva, et al., 2000) or *At*Sar1H74L (Takeuchi, et al., 2000), which are also GTP-locked and also prevents the fusion with the Golgi. These mutants turned out to be very useful tools to investigate the presence of alternative pathways to the canonical ER-Golgi

pathway. Although these mutants have been widely used, there is no description of the formation and accumulation of intermediate COPII vesicles in plants. This new element clarifies and unifies the mechanism of action of Sar1 in the formation of plant COPII vesicles with the yeast and human COPII vesicles.

The experiment performed with the vacuolar reporter GFP-Chi has also showed an association of the marker with the membrane of COPII vesicles (Figure 4-4). This could have different interpretations: 1) the cargo is captured in ER, confirming recent observations (Niemes, et al., 2010a) and therefore we observe a cargo-receptor (membrane bound) fluorescence; 2) an over-accumulation of the protein in the ER leads to an aggregation and then its association with the nascent COPII membrane, as already demonstrated for the vacuolar reporter phaseolin (Castelli and Vitale, 2005); 3) or it might be an equilibrium of this two mechanisms: a part of the proteins exits from the ER following the classical route (association with COPII membrane) while another part aggregates and is then delivered to the vacuole as a dimer. In fact, the hydrophobic tail of phaseolin is able to transiently associate to membranes and help phaseolin to be delivered as an aggregate to the vacuole, where it becomes soluble again. How a soluble protein like GFP-Chi could be made to aggregate (and remain so even under strong reducing conditions) by a short C-terminal peptide, which is also expected to be soluble remains to be explained only. Such an aggregation of soluble proteins resembles the aggregation of β-amyloid oligomers caused by the formation of intermolecular β-sheets. These insoluble oligomers are SDS-resistant (Haass and Selkoe, 2007b), as observed in this work for the GFP-Chi dimer.

5. Material &Methods

5.0 Bacterial strains

Escherichia coli XL-1 Blue: *rec*A1, *end*A1, *gyr*A96, *thi*-1 *hsd*R17 (rk-, mk+), *sup*E44, *rel*A1, λ-, *lac*-.
Agrobacterium tumefaciens strain GV3101.
E.coli and *A.tumefaciens* were grown in LB medium [0.5% NaCl; 0.5% (w/v) yeast extract; 1% (w/v) bacto-tryptone in H_2O] for liquid culture. *E.coli* was grown at 37°C shaking at 200 rpm whereas *A.tumefaciens* was grown at 28°C shaking at 150 rpm. For culture on solid medium, LB agar [LB medium plus 6% Agar] was used. Specific antibiotics were added in the medium in order to select bacteria carrying specific plasmids.

5.0.1 Preparation of heat-shock competent E.coli cells

5 ml selective LB medium (25 µg/ml tetracycline) was inoculated with a single *E.coli* colony and then incubated at 37 °C overnight under shaking. The day after this preculture was diluted in 500 ml of fresh liquid LB medium and incubated at 37 °C under shaking. The culture was grown until the OD_{600} reached 0.5, which represents the exponential phase of bacterial growth. Cells were then put on ice and recuperated by centrifugation at 5000 g for 15 minutes at 4 °C. From this step on the cells were kept cold throughout the preparation. The bacterial pellet was resuspended in 32 ml RF1 buffer (100 mM KCl; 30 mM $MnCl_2$; 30 mM K-acetate pH 7.5; 10 mM $CaCl_2$; 15% glycerol; pH 5.8 adjusted with acetic acid) and then left for 20 minutes on ice. Cells were recuperated by centrifugation at 5000 g for 15 minutes at 4 °C and the resulting pellet was resuspended in 8 ml RF2 buffer (10 mM MOPS pH 6.8; 10 mM KCl; 50 mM $CaCl_2$; 15% glycerol; pH 6.8 adjusted with NaOH). The suspension of competent bacteria was incubated for 20 minutes on ice. Finally, 100 µl aliquots were pipetted and then frozen in liquid nitrogen. Tubes were stored at -80 °C.

5.0.2 Transformation of E.coli by heat-shock

Competent *E.coli* cells were thawed on ice and then placed on pre-cooled 1.5 ml Eppendorf

tube containing 1 ng purified plasmid or 10 µl ligation mixture (approx. 200ng). Cells were incubated for 15-20 minutes on ice. They were then incubated for 90 seconds at 42 °C and immediately back on ice for 2 minutes. 1 ml liquid LB-medium without antibiotics was added and bacteria were then incubated for 1 hour at 37 °C under shaking. Finally, the bacterial culture was plated on a petri dish containing selective LB-medium and grown at 37 °C overnight.

5.0.3 Preparation of electroporation competent A.tumefaciens cells

500 ml selective LB medium (50 µg/ml rifampicin) was inoculated with 5 ml fresh overnight culture of *A.tumefaciens*. Cells were grown at 28 °C to an OD_{600} ~ 0.6 which represents the exponential phase of bacterial growing. The bacteria culture was then centrifuged at 4000 g for 15 minutes at 4 °C. From this step on the cells were kept cold on ice throughout all steps of the preparation. Cells were washed three times in glycerol solution (10% glycerol in water). After the last washing step the cells were resuspended in 1 ml glycerol solution for 100 ml start volume. Aliquots of 60 µl were pipetted and then frozen on dry ice. The aliquots were stored at -80 °C.

5.0.4 Transformation of A.tumefaciens by electroporation

Competent *A.tumefaciens* cells were thawed on ice and then transferred into pre-cooled 1.5 ml Eppendorf tubes containing 100 ng plasmid. Bacterial cells were then transferred to a chilled electroporation cuvette on ice (1 mm electroporation cuvette Eurogentec) and then transformed using an electroporator (Bio-Rad). The electroporation machine was set at 2 kV charging voltage. A 5 ms pulse obtained an efficient transformation. 500µl fresh LB medium (without antibiotics) was then added and cells were incubated for 1-2 hour at 28 °C. Finally 1/10 of transformed cells were plated on a petri dish containing selective LB agar and incubated at 28 °C for 2 days.

5.1 Plant Material and Plant Transformation Techniques

5.1.1 Growth conditions

A.thaliana and *N.benthamiana* plants were grown in the same growth chamber (Mobylux GroBanks) under the same growth conditions. The light intensity was 120 μE/m^2 · s with a photoperiod of 16 hours light and 8 hours darkness for long-day and 8 hours light and 16 hours darkness for short-day conditions. The relative humidity (RH) was 65% and the temperature was 22 °C for the day and 18 °C for the night.

5.1.2 Soils and mediums for growth

In vitro A.thaliana plants were grown on solid Murashige & Skoog (MS) medium [Murashige & Skoog (DUCHEFA) 4.47 g/l; sucrose 20 g/l; Phytagel (SIGMA) or Agar (Merck) 8 g/l; pH 5.6]. For liquid cultures (Arabidopsis roots incubation with 2BP), we used MS medium without phytagel or agar.
Non-sterile *A.thaliana* and *N.benthamiana* plants were grown on normal soil (RICOTER) containing 45% sand, 10% perlite, 25% compost and 20% peat.

5.1.3 Seed sterilization

An appropriate volume of seeds (~ 100 μl) was put into a 1.5 ml Eppendorf tube and warmed at 37 °C for 3-4 days. Seeds were incubated with 1 ml sterilization solution (2% bleach and 0.005% Triton X-100 (up to 0.01%) in 100% ethanol). Seeds were then agitated for 30 minutes using a bench top shaker. The solution was removed and seeds were washed several times with 100% ethanol. Finally seeds were dried under the sterile hood and then plated on sterile petri dishes containing solid MS medium.

5.1.4 Preparation of A.thaliana leaf protoplasts and PEG-mediated transformation

3-4 weeks old *A.thaliana* plants grown in sterile petri dishes under long-day conditions were used. Leaf rosettes were cut and put into sterile petri dishes containing 12 ml digestion solution [mannitol 400 mM; MES 5 mM; $CaCl_2$ 8 mM; cellulase Onozuka R-10 (SERVA) 1% w/v; macerozyme R-10 (SERVA) 0,25% w/v; pH 5.6] per plate. Leaves were incubated overnight in the dark at room temperature. The day after protoplasts were released by careful

shaking. The macerate was then filtered through a 100 μm mesh filter in order to eliminate leaf debris. The filtrate was transferred into 15 ml falcon tubes using a plastic Pasteur pipette and protoplasts were recuperated by centrifugation for 5 minutes at 50 g (brake off) at room temperature. Protoplasts precipitated in a pellet whereas debris stayed in the supernatant. After removing the supernatant protoplasts were washed three times with W5 solution (NaCl 154 mM; $CaCl_2$ 125 mM; KCl 5 mM; glucose 5 mM; MES 1.5 mM; pH 5.6). 2-3 ml protoplasts were layered on top of 6 ml 21% sucrose and then centrifuged for 10 minutes at 50 g (brake off) at room temperature. At this step live protoplasts accumulated in the interface between sucrose and W5 whereas broken protoplast precipitated to the bottom of the tube. Live protoplasts were harvested from the interface and then recuperated by centrifugation for 5 minutes at 50 g (brake off) at room temperature. Protoplasts were then washed three times in W5 and then incubated for 30 minutes on ice. Intact round-shaped protoplasts were counted using a Burker chamber. Finally, protoplasts were recuperated by centrifugation and resuspended in an appropriate volume of MaMg (mannitol 0.4 M; $MgCl_2$ 15 mM; MES 0.5 M; pH 5.6) in order to obtain 1.5 x 10^6 protoplast per 300 μl solution.

For PEG-mediated transformation 25 μg plasmid and 50 μg carrier DNA were added to 300 μl protoplasts and gently mixed. Immediately 325 μl PEG solution [PEG 4000 (Fluka) 40% w/v; mannitol 0.4 M; $Ca(NO_3)_2$ 0.1 M; pH 7-8] were gently added and mixed. Protoplasts were then incubated for 30 minutes at room temperature. 10 ml W5 solution were gently added mixing the tube from time to time. Protoplasts were then recuperated by centrifugation as previously and the supernatant was discarded. Finally, protoplasts were resuspended in 5 ml W5 solution and incubated overnight in darkness at room temperature.

5.2 Agro-infiltration of N.benthamiana leaves

A.tumefaciens carrying the construct of interest was plated on petri dishes containing selective LB medium-agar (50 μg/ml kanamycin; 50 μg/ml rifampicin). A single bacterial colony was inoculated in 5 ml selective LB liquid medium and incubated at 28°C overnight with shaking. The day after the culture was centrifuged at 5000 g for 10 minutes at room temperature and the bacterial pellet was washed three times with 10 ml agro-infiltration buffer (50 mM MES; 2 mM Na_3PO_4; 0.5% glucose; pH 5.6). After the last washing the bacterial pellet was resuspended in agro-infiltration buffer containing 100 μM acetosyringone to an optical density (OD_{600}) of 1. The bacterial cells were incubated for 1 hour at room temperature in darkness and then infiltrated into 2-4 week-old *N.benthamiana* leaves. Finally the infiltrated

plants were put in a growth chamber and left in darkness overnight.

5.3 Physcomitrella patens growth conditions

The standard conditions for *P. patens* in the lab are as follows: Cultures are grown in the culture room at 26 ± 2 ºC in discontinuous white light (16 hours / day). Light is provided by fluorescent tubes Sylvania GRO-LUX WS at quantum irradiance of 50 to 80 $\mu mol \cdot m^{-2} \cdot s^{-1}$, and with a red-far-red ratio of 1.2. Protonemal cultures are made in 9 cm Petri dishes containing solid culture medium and overlaid with cellophane disks (W.E. Cannings, Bristol, UK). The cellophane disk is not necessary but facilitates subsequent observations and collection of material.

Sporogenesis is performed in Magenta boxes, or in culture glass tubes on minimal medium (PP-NO_3 without glucose). Cultures with well differentiated gametophores are irrigated with sterile water and transferred at 17ºC in illuminated temperature-controlled growth chambers (Polytron, Weiss Technik AG) for three weeks to induce gametogenesis. Sporophyte development is further completed under standard conditions and the maturation is followed visually.

5.3.1 Strain conservation

Strains are conserved as fragmented protonemal suspension in sterile water in the refrigerator. These suspensions remain viable for several years. For short-term storage, collect a 6 day old protonemal culture in sterile water (1 plate in 5-10 mL) and fragment it with an Ultratorrax (Polytron, 30 sec. at position 4). Inoculate plates with freshly fragmented suspension. For long term storage, filter the suspension after fragmentation on a 100-500 µm stainless steel filter. Collect the fragments of protonema that are retained on the filter with a forceps and resuspend them in sterile water.

Spores provide another very convenient mean for long-term storage of moss strains. Collect one single spore capsule (resulting from a single fertilisation event) in 1 mL sterile water in an Eppendorf tube and store in the refrigerator. Spore germination has been obtained from 10-years-old spore suspensions.

Strains can also be stored for several months in the refrigerator as colonies on a Petri dish sealed with parafilm. This provides a convenient way for medium term storage of strains without fragmentation (i.e. directly from the culture room). In this case, simply take a piece of the colony and directly inoculate a PP NH_4 plate.

5.3.2 Culture media

PP NO_3

This is the minimal medium used for phenotypical analysis and for the production of spores.

Macro elements:

$CaNO_3 \cdot 4H_2O$	0.8 g/l
$MgSO_4 \cdot 7H_2O$	0.25 g/l
$FeSO_4 \cdot 7H_2O$	0.0125 g/l

These elements are weighted and directly added to the medium

Micro elements

$CuSO_4 \cdot 5H_2O$	0.055 mg/l
$ZnSO_4 \cdot 7H_2O$	0.055 mg/l
H_3BO_3	0.614 mg/l
$MnCl_2 \cdot 4H_2O$	0.389 mg/l
$CoCl_2 \cdot 6H_2O$	0.055 mg/l
KI	0.028 mg/l
$Na_2MoO_4 \cdot 2H_2O$	0.025 mg/l

Prepare a 1000 x stock solution, autoclave, store in the refrigerator and add 1 mL / L medium

Phosphate buffer

Dissolve 25 g KH_2PO_4 in 100 mL water and titrate to pH 7 with 4M KOH to make a 1000x stock. Autoclave and add 1 ml per litre of medium.

PP NH4

This medium is used for the production of chloronema-enriched protonema used to isolate protoplasts and for rapid large-scale amplification. The ammonium tartrate in the medium increases the yield of secondary chloronema, but does not allow the completion of the life cycle and must be absent for the production of spores.

Add to the minimal medium

NH_4 tartrate	500 mg/l
Glucose	5 g/l

Agar

Add 7 g/l Agar (Merck) and sterilise by autoclaving (20 min, 120°C). A precipitate forms during autoclaving (probably calcium phosphate). Pour the plates after sterilisation and avoid keeping molten medium since the precipitate will be more abundant. Solid plates can be stored for at least one month at room temperature.

Supplements

Supplements for auxotrophs

Thiamine HCl	500 µg/l
Para-aminobenzoic acid	250 µg/l
Nicotinic acid	1 mg/l

Supplements are added to the culture medium prior to sterilisation

Antibiotic supplements

For neomycin resistance, supplement the medium with 40 mg/L G-418 or paramomycin sulphate.

For hygromycin resistance, supplement the medium with 25 mg/L Hygromycin B.

For sulfadiazine resistance, supplement the medium with 150 mg/l sulfadiazine.

Antibiotics are added from a 1000x stock solution after autoclaving the medium.

Glucose

5g/L glucose is routinely added to the media to facilitate early detection of putative contaminations. But it MUST be absent from sporogenesis cultures. Protonema and

gametophores will turn brown and eventually die much earlier on glucose-containing medium. It must therefore be omitted for long term cultures and for the production of spores.

5.4 Protoplasts media

5.4.1 Protoplast solid culture medium.

Supplement PP NH_4 solid culture medium with 66 g/l mannitol and check osmolarity (around 480 mOsmol). Sterilise by autoclaving.

5.4.2 Protoplast liquid culture medium.

Supplement PP NH_4 culture medium without agar with 66 g/l mannitol and check osmolarity (around 480 mOsmol). Sterilise by autoclaving. A precipitate forms during autoclaving (probably calcium phosphate). Sediment the precipitate and use the clear supernatant.

5.4.3 Protoplast top layer

Mannitol 8.5 % or protoplasts liquid culture medium with 1.4 % agar

5.4.4 Protoplast isolation and regeneration

Collect protonema from 5 cultures grown for 5- 6 days on PP NH_4 and transfer to a 9 cm Petri dish containing 10 ml 0.48M mannitol.

Add 10 ml sterile 2% (w/v) non-purified Driselase (Fluka 44585, Sigma D-9515) and incubate at room temperature for 30 min. with occasional gentle mixing. (Driselase is dissolved in 0.48M mannitol, centrifuged at 10000 rpm for 10 min. to remove debris, buffered to pH 5.6 and sterilised by passage through a 0.45 µm filter).

Filter the preparation through a 100 µm stainless steel sieve and leave for an additional 15 min. to complete digestion.

Filter through a 50 µm stainless steel sieve and transfer to sterile 10 ml glass tubes. Harvest the protoplasts by low speed centrifugation (600 rpm for 5 min.) and gently resuspend the pellet in mannitol 0.48M.

Repeat centrifugation and resuspend the cells in 0.48M mannitol. Take a aliquot of the suspension (or of a 10X dilution in 0.48M mannitol) and count protoplasts with an

haemocytometer. The yield is usually about 10^6 viable protoplasts per initial culture plate. Viable protoplasts are identified by their intact shape, but only approx. 50% of these will regenerate. Vital staining at his stage is not required.

Repeat centrifugation and resuspend in 0.48M mannitol at the desired concentration. Mix one volume of protoplasts with one volume of molten top layer and aliquot 2 ml per 9 cm Petri dish containing solid protoplast culture medium overlaid with a cellophane disk. The ideal concentration for good regeneration is 10'000-30'000 protoplasts per Petri dish. Regeneration will be seriously delayed if there are less than 5000 protoplasts / Petri. Leave the protoplasts in darkness one night after isolation and then regenerate in the light in the culture room.

5.4.5 Transformation of Physcomitrella patens

-Isolate protoplasts from 5-6 days old protonemal culture digest with 1% Driselase for 30 minutes and then filter (100 µm sieve).

- Continue digestion for further 15 minutes and then filter (50 µm sieve).

- Transfer the suspension to sterile glass tubes and sediment the protoplasts by low speed centrifugation for 5 minutes at 600 g.

- Gently resuspend the pellet in 10 ml 8.5% mannitol and repeat centrifugation.

- Resuspend pellet in mannitol and count. Leave the protoplasts in mannitol before initiating transformation (1).

- Recentrifuge and then resuspend the protoplasts at a concentration of 1.2×10^6 / ml in MMM solution (2, 3).

- Dispense 10-15 µg of DNA into 14 ml Falcon tubes (in maximum 30 µl, the final concentration should be between 30-50 µg/ml, see note 4).

- Add 300 µl protoplast suspension and mix gently.

- Add 300 µl PEG solution and mix gently (see note 5).

- Heat shock 5 minutes at 45^o C.

- Bring back to room temperature and leave for an additional 10 minutes with occasional gentle mixing (see note 6).

- Progressively dilute the sample with moss liquid medium (5 x 300 µl and then 5 x 1 ml added sequentially every minute).

- Keep the transformed protoplasts overnight in darkness

-The next day, protoplasts may be further cultured in liquid medium for transient gene expression assays or embedded in protoplast top layer and plated on protoplast solid medium for further selection. For the selection of transformants, each transformation sample should be plated on 3-4 Petri dishes.

Notes

(1) Maintaining the protoplasts in MMM solution reduces cell viability.

(2) The MMM solution is required to achieve high transformation efficiency.

(3) Protoplast concentrations of 1 to 1.5 x 10^6 / ml are optimal for transformation efficiency and cell survival.

(4) A large precipitate containing DNA + cellular material will form upon PEG addition if the DNA concentration is high (< 70 µg / ml). This has been observed for PEG purified plasmid DNA, but may not be true for Qiagen column purified DNA. DNA concentrations lower than 20 µg / ml will reduce the efficiency of transformation.

(5) Mix immediately to avoid the separation of PEG and protoplasts.

(6) Longer incubation in PEG decreases cell survival and specific activity for further enzymatic assays (e.g.: GUS assay).

(7) Do not use the MMM solution for long time since it will decrease cell survival. The same is true if you wash and resuspend the cells before starting cultivation. Moreover, it seems that the cells, which have been permeabilised, will be preferentially killed by the washing step (as monitored by a decrease in specific activity).

Solutions.

Mannitol
Mannitol: 0.48 M (8.5%)

MMM
Mannitol: 0.48 M (8.5%)

Magnesium chloride: 15mM

MES: 0.1%, pH 5.6 with KOH

PEG
Mannitol 0.38 M (7 %)

Calcium nitrate 0.1M

PEG 4000 (Serva) 33 % (w.v.)

pH 8.0 with 10 mM Tris

Dissolve 4 g PEG in a final volume of 10 ml 0.38M mannitol, 0.1 M calcium nitrate. Heat the solution at 45°C to assist PEG dissolution. Buffer the solution with 10 mM Tris pH 7.2 and sterilise by autoclaving or by filtrating through a 0.20 µm filter. The PEG solution can be kept for up to 1 month without significant loss of efficiency. Longer storage will result in PEG hydrolysis, which induces a strong drop of pH and a low survival of protoplast. PEG 6000 can be used instead of PEG 4000, but the specific activity will be reduced. Different batches of PEG may have different properties so this should be checked.

5.5 MOLECULAR BIOLOGY

5.5.1 PCR

PCR reactions were performed combining the following components in a nuclease-free micro-centrifuge tube: buffer (final concentration 1X); 0.2 mM for each dNTP; 0.1-1 µM forward primer; 0.1-1 µM reverse primer; 1.25 U DNA polymerase (Promega); 100-500 ng DNA template; H_2O to a final volume of 50 µl. The reaction was performed in a thermal cycling machine respecting the following condition.

5.5.2 DNA digestion

Restriction enzyme digestions were performed mixing the following components in a 1.5 ml sterile Eppendorf tube: 0.2-1.5 µg substrate DNA; restriction buffer (final concentration 1X); BSA (final concentration 0.1 µg/µl); 5 u of restriction enzyme (usually Promega); H_2O to a final volume of 20 µl. The restrictions were performed for 1-4 hours at 37°C.

5.5.3 DNA ligase

DNA ligase reactions were performed mixing the following components in a 1.5 ml sterile Eppendorf tube: 100 ng vector DNA; 17 ng insert DNA; 10X ligation buffer (final concentration 1X); 0.1-1 U T4 DNA ligase (Promega); and H_2O to a final volume of 10 µl. The reactions were performed overnight at 4°C or for few hours at 14°C.

5.5.4 Total RNA extraction from A.thaliana leaves

0.25 g of *A.thaliana* leaves were collected and immediately frozen in liquid nitrogen. The tissue was then ground in liquid nitrogen using pre-cooled mortal and pestle. The tissue was transferred to a 2 ml Eppendorf tube (RNase free) pre-cooled in liquid nitrogen. 500 µl plant RNA purification reagent (Invitrogen) were immediately added. The tissue was resuspended by mixing using a vortex and then incubated for 5 minutes at room temperature. The tube was centrifuged for 2 minutes at 15'000 g in order to eliminate cell debris. The supernatant was then transferred in a new Eppendorf tube (RNase free). 100 µl 5M NaCl was added and then the tube was gently mixed. 300 µl chloroform was added and the tube was mixed 3 – 4 times by inversion. The tube was centrifuged at 15'000 g for 10 minutes at 4°C. The aqueous phase was transferred to a new Eppendorf tube (RNase free) and one volume of isopropanol was then added. The tube was incubated for 10 minutes at room temperature and then centrifuged at 15'000 g for 30 minutes at 4°C. The supernatant was discarded and the pellet was washed once with ethanol 75%. The pellet was then resuspended in an appropriate volume of RNase free H_2O. Finally the total RNA was treated with DNase (Promega) in order to eliminate contaminant genomic DNA and then quantified using a Nano-Drop spectrophotometer.

5.5.5 cDNA synthesis

1 µg total RNA extract was transferred to a 1.5 ml Eppendorf tube (RNase free). Then, 1 µl oligo-dT primer and 1 µl 10 mM dNTP were added. The volume was adjusted to 11 µl using an adequate volume of RNase free H_2O. The tube was incubated at 70°C for 5 minutes and then for 1 minute on ice. 12 µl mix [5 µl 5X transcriptase buffer; 1 µl 0.1 M DTT; 0.5 µl SuperScript III RT (Promega); 5.5 µl RNase free H_2O] was added to the tube. The reverse transcriptase reaction was performed at 50°C for 1 hour. Finally the tube was incubated for 15 minutes at 70°C in order to inactivate the reverse transcriptase and transferred on ice. The single strand cDNA was used to amplify AtRMR gene using specific pairs of primers.

5.5.6 Genomic DNA extraction from A.thaliana leaves

The top of an Eppendorf tube was used to collect *A.thaliana* leaf tissue. The tissue was powdered using a small pestle and then 400 µl extraction buffer (200 mM Tris-HCl pH 7.5; 250 mM NaCl; 25 mM EDTA; 0.5% SDS) were added. The tube was mixed for 5 minutes using a vortex and then centrifuged for 5 minutes at 15'000 g in order to eliminate cell debris. 300 µl supernatant were mixed with an equal volume of isopropanol. The tube was incubated at room temperature for 10 minutes and then centrifuged for 30 minutes at 15.000 g. The DNA pellet was washed once with 75% ethanol. Finally the DNA was resuspended in an adequate volume of sterile H_2O and then quantified using a Nano-Drop spectrophotometer.

5.5.7 DNA precipitation

1/10 the volume sodium acetate (NaAc) 3M and 2 volumes ethanol were added to the DNA samples. The samples were incubated at – 80°C for a few minutes in order to precipitate the DNA. They were centrifuged for 30 minutes at 4°C and DNA pellets were then washed once with 70% ethanol. Finally, samples were dried and then resuspended in an adequate volume of sterile H_2O.

5.5.8 DNA extraction from agarose gel

The DNA extraction was performed using the Wizard SV Gel and PCR Clean-Up system (Promega) as indicated in the provider's protocol.

5.5.9 Isolation of plasmid DNA from E.coli in a small-scale

A single bacterial colony was inoculated into 5 ml of LB medium containing the adequate antibiotic. The culture was then incubated overnight at 37°C with shaking (250 rpm). The day after 1.5 ml culture was centrifuged at 20000 g in order to pull down bacterial cells. The pellet was resuspended in 150 µl resuspension buffer P1 (50 mM Tris-HCl pH 8; 10 mM EDTA; 100 mg/ml RNase). 150 µl of lysis buffer P2 (200 mM NaOH; 1% SDS) were then added and the sample was gently mixed a few times. The sample was incubated for 5 minutes at room temperature and 150 µl equilibration buffer P3 (3M NaOAc pH 5.5) were then added. The

sample was gently mixed and incubated for a few minutes on ice. The samples were then centrifuged for 15 minutes at 20000 g in order to precipitate the bacterial lysate. The supernatant containing plasmid DNA was transferred into a new Eppendorf tube and 0.7 volumes of isopropanol were added. The tube was centrifuged at 20000 g for 30 minutes. The DNA pellet was then washed once with 70% ethanol. Finally the pellet was dried and resuspended in an adequate volume sterile H_2O.

Isolation of plasmid DNA for sequencing was performed using the NucleoSpin plasmid kit (MACHEREY-NAGEL) as indicated in the provider's protocol.

5.5.10 Isolation of plasmid DNA from E.coli in a big-scale

Isolation of plasmid DNA was performed using the NucleoBond Xtra Midi Plus kit (MACHEREY-NAGEL) as indicated in manufacturer's instructions.

5.5.11 DNA electrophoresis

DNA electrophoresis was performed using a Bio-Rad apparatus. Agarose gels were prepared with 0.7-2.5% of agarose (depending on the size of DNA fragments) in 0.5X TBE and using ethidium bromide as a DNA colorant. In a small gel the DNA samples, were separated at 90-95V whereas they were separated at 120 V in a big gel. The DNA was visualized under UV light using a GEL-DOC system from Bio-Rad.

5.6 PROTEIN TECHNIQUES

5.6.1 Chloroform/methanol precipitation

Protein precipitation was performed according to the following table:

Sample Volume	100 µl	125 µl	200 µl	250 µl	800 µl	1,5 ml
MeOH	240 µl	300 µl	480 µl	600 µl	1920 µl	3,6 ml
$CHCl_3$	80 µl	100 µl	160 µl	200 µl	640 µl	1,2 ml
Vortex						
H_20	320 µl	400 µl	640 µl	800 µl	2156 µl	4,8 ml

Discard the upper phase (MeOH+ H_20) and then protein precipitation adding excess MeOH as it follows:

MeOH	240µl	300 µl	480 µl	600 µl	1920 µl	3,6 ml

Samples are vortex mixed, centrifuged at 20000g 14 °C for 30 minutes. Pellets were air dried and resuspended in 1 volume of sample buffer and then heated at 100 °C for 5 minutes.

5.6.2 Protein extraction for solubilisation assay

Proteins were extracted from adult *Arabidopsis thaliana* rosettes. After grinding in liquid nitrogen, samples were resuspended in TNE Buffer (25mM Tris-HCl pH 7.5, 125 mM NaCl, 5 mM EDTA) as described in (Borner, et al., 2005). 1mg total protein was then incubated 1h at 4 °C with different detergents at the concentrations indicated in Results and ultracentrifuged at 35000rpm in a SW55Ti rotor (~ 110000g). 100 µl soluble fractions were purified by chloroform/methanol method and loaded onto a SDS-PAGE. 5x concentrated membrane fractions were loaded onto a SDS-PAGE (when I loaded equal volumes, no band was detectable in the membrane fraction). Detection was performed by western blotting using anti-RMR1 antibodies at 1:5000 dilution.

5.6.3 Sucrose gradient fractionation

Formation of the gradient:

1. Layer the dense 55 %sucrose solution (2ml) in a 5 ml centrifuge tube.

2. Overlay the dense sucrose carefully with the same volume of 12 % sucrose solution . Do not disturb the interface at this point.

3. Close the tube with a silicon rubber stopper.

4. Gently lay down the tube rack on its side, and allow diffusion for 1 to 3 hr.

5. Slowly put the tube rack back to the upright position, and the gradients are now ready to use.

Samples preparation:

Pellet protoplasts. With a 200 µl tip, pipette the suspension up and down about twenty times to break the protoplasts. Do not let the material warm up.

With a micro-pipette load 600 µl on top of the gradient. Keep everything on ice. Remember to load each gradient with homogenate made in the same buffer (magnesium or EDTA).

Centrifuge at 35.000 rpm (~110 000g), 4°C for 2 h in a Beckman SW55Ti rotor

Collect 200 µl fractions. Store at -20°C. Add 650 µl denaturation buffer for SDS-PAGE to the bottom of the tube and collect what you solubilise: this will be the last fraction, containing material that was denser than 55% sucrose.

BUFFER A (to homogenise tissues):

100 mM Tris-HCl, pH 7.8

10 mM KCl

With either 2 mM of $MgCl_2$ or 1mM EDTA (to observe an ER shift)

5.6.4 SDS-PAGE

The SDS-PAGE was made using a Mini Protean III apparatus (Bio-Rad). A discontinuous gel was used, composed of a stacking (4.5% acrylamide/bisacrylamide) and running (15%) gels (see below). The gels were then immerged in 1X Tris-glycine electrophoresis buffer. Before loading, samples were boiled for 5 minutes at 100°C in order to denature proteins For each lane 100 µg total protein extract in 1X sample buffer were loaded. Finally the electrophoresis was performed at constant voltage (100 V) until the blue dye reached the bottom of the gel. Loading of sucrose gradient fractions were performed using PerfectBlue Doppelgelsystem Twin ExW S system (PEQLAB) because suitable for a higher number of fractions.

Running gel (15%)

H_2O	3.4 ml
30% acrylamide/bisacrylamide mix	4 ml
1.5 M Tris-HCl pH 8.8	2.5 ml
10% ammonium persulfate (APS)	100 µl
TEMED	4 µl

Stacking gel (4.5%)

H_2O	3.15 ml
30% acrylamide/bisacrylamide mix	0.83 ml
0.5 M Tris-HCl pH 6.8	1.26 ml
10% ammonium persulfate (APS)	50 µl
TEMED	5 µl

Tris-glycine electrophoresis buffer

25 mM Tris; 250 mM glycine pH 8.3; 0.1% (w/v) SDS

Sample buffer

50 mM Tris-HCl pH 6.8; 100 mM dithiothreitol (DTT); 2% (w/v) SDS; 0.1% bromophenol blue; 10% (v/v) glycerol.

5.6.5 Western Blot

After SDS-PAGE the proteins were transferred to a membrane (Immobilon-PSQ 0.2 μm MILLIPORE) using a Mini Protean III system (Bio-Rad). Before blotting, the membrane was activated by soaking in 95% ethanol for 10 minutes. Then the sandwich was assembled (sponge, filter paper, gel, membrane, filter paper, sponge) starting from the black side of cassette (anode) to the white side (cathode). Finally the sandwich was immerged in the cassette containing 1X blotting buffer (25 mM Tris; 192 mM glycine). The transfer was performed at constant voltage, 20 V, for 4 – 5 hours at 4°C or at 10V ON.

The transfer membrane was then incubated for 1 hour at room temperature in blocking buffer (1X PBS; 5% skimmed milk). This step is necessary to block unspecific antibody-binding sites. The membrane was incubated for 1 hour at room temperature in buffer containing a specific primary antibody (1X PBS; 5% skimmed milk; 0.2% Tween-20; primary antibody diluted 1:5.000). The membrane was then washed 3 times for 15 minutes in washing solution (1X PBS; 0.2% Tween-20). After the last wash the membrane was incubated for 1 hour at room temperature in buffer containing a secondary antibody (1X PBS; 5% skimmed milk; 0.2% Tween-20; secondary antibody diluted 1:10.000). Then the membrane was washed 3 times in washing solution for 15 minutes. Finally the secondary antibody was revealed using the ECL plus detection kit (GE Healthcare). The chemiluminescent reaction product by HRP-coupled secondary antibody was detected by a Chemidoc XRS System (Bio-Rad).

For transfer proteins run through PerfectBlue Doppelgelsystem Twin ExW S system and perform a western blotting, it was used PerfectBlue Tank-Electro Blotter Web M and transferred at 200V constantly. Both systems are supplied by PEQLAB.

For detection of RMR1 palmitoylated form of RMR1 the slightly different solutions have been used: anti-RMR1 antibody 1:1000, secondary antibody 1:5000. The other solutions were used as indicated above.

5.6.6 Membrane Stripping

In order to dissociate the complex primary antibody/investigated protein, a Western blot membrane was incubated with 50 ml of stripping buffer (50 mM Tris-HCl pH 6.8; 2% SDS; 100 mM β-mercaptoethanol). The incubation was performed in a water bath heated at 59°C for 1h. Then the membrane was washed several times with 1X PBS until all β-mercaptoethanol residues were removed. Finally, the membrane was ready for another cycle

of immune-blotting.

5.6.7 BSA (Biotin Switch assay)

As starting material we will use protoplasts (PPS) from *Arabidopsis thaliana* leaves or *Arabidopsis* tissues (1-2 mg of tissue depending on the quantity of protein. We will use at least 1 mg of proteins).

We Collect PPS and Re-suspend cell pellets in 500 µl of ice-cold lysis Buffer with 30 mM NEM (*N*-Ethylmaleimide) +Protease inhibitor, and break the cells by pipetting. NEM will block all the free cysteines). Proteins extract is then incubated for 1 hour at 4 °C on a roller table and centrifuged at 4 °C, 500 x g for 10 minutes to remove insoluble material. Then protein concentration using Nanodrop, set at 280nm, is determined. Classic method to determine protein concentrations are not recommended as TX-100 interacts with Bradford and Lowry chemicals (According to Wan et al. 2007). After, combine one milligram of protein with lysis buffer to a total volume of 1ml and incubate overnight at 4 °C on a roller table. In some cases addition of saponin to 0.5 % can increase blocking efficiency and S-acylated protein extraction. Then, precipitate proteins at room temperature using methanol/chloroform; mixing thoroughly and centrifuge at 15'000 x g for 30 minutes at 14 °C; you remove and discard the upper phase without disturbing the interface and add 4 volumes of methanol, mix and incubate at -20°C for 20 minutes for four times.

Then, centrifuge for 20 minutes at 5'000 x g at 4 °C, pour off the supernatant and air-dry the pellet for 10 minutes at room temperature.

Resuspend the pellet in 200 µl of resuspension buffer by sonicating in a water bath for 10 minutes and gentle agitation on a roller table at room temperature until solubilised. Gentle mixing at 37 °C for 10 minutes can improve solubilisation of proteins.

We then divide the solution into two equal aliquots and combine one with 800 µl fresh 1 M hydroxylamine buffer, 1 mM EDTA, protease inhibitors and 100 µl fresh 4.4 mM biotin-BMCC (HA solution) (Thermo scientific) dissolved in DMF or DMSO and gently mix for 2-3h at RT. Treat the remaining aliquot identically but replace hydroxylamine with 50 mM Tris pH 7 (cleavage of all modified cysteines).

Precipitate proteins at room temperature using methanol/chloroform (1x) as described previously and wash in methanol (3x) to remove traces of non reacted-BMCC-biotin and resuspend each sample in 100 µl resuspension buffer and add 900 µl PBS containing 0.2% Triton X-100.

Remove 50-100 µl to act as a loading control, chloroform/methanol precipitate as described previously and resuspend in 3 x SDS-PAGE sample buffer.

Equilibrate the streptavidin columns with the binding buffer according to the manufacturer's instruction and load the remaining sample with Streptavidin HP spin trap (GE Healthcare) for 2 hour at room temperature on a roller table.

Wash columns three times with the washing buffer by centrifugation at 150 x g.

Elute proteins are by the elution buffer (400ul), then precipitate proteins by chloroform/methanol and resuspended in 30 µl of 2Xsample buffer. Analyse samples by SDS/PAGE and Western blotting.

General solutions for BSA

Lysis buffer

1 x PBS pH 7.4

Protease inhibitors

1 mM EDTA

1 % (up to 2%) Triton X-100

1% Brij-96

0.3% Saponin

25 mM N-ethylmaleimide

Resuspension buffer

1 x PBS pH 7.4

8 M Urea

2 % SDS

1M Hydroxylamine (HA buffer)

1 M Hydroxylamine in water (pH to 7.4 with NaOH) freshly prepared

Wash buffer

1 x PBS pH 7.4

NaCl to 500 mM

0.1 % SDS

10x Elution Buffer

1 M glycine-HCl, pH 2.9

Binding buffer
TBS (50 mM Tris, 150 mM NaCl, pH 7.5)

5.6.8 Membrane fractionation from N.benthamiana leaves

N.benthamiana leaves expressing fluorescent constructs were grinded in liquid nitrogen in presence of PVPP and sand and Buffer A. Total extract was quickly centrifuged at 1000g to get rid of all cellular debris, sand and PVPP. The supernatant was collected and further centrifuged at 15'000xg for 15 minutes to get rid of nuclei and plastids, obtaining a microsomal fraction. The supernatant was ultracentrifuged in SW55Ti rotor for 2h at 110'000xg. Pellet was resuspended in resuspension buffer (TBS 1M pH7.5, Urea 9M, Triton X100 1%). Equal volumes of the soluble and membrane fractions were purified by chloroform/ methanol precipitation, resuspended in sample buffer and analysed by SDS-PAGE.

5.7 MICROSCOPY

5.7.1 Transmission electro microscopy (TEM)

We used a JEM 1400 transmission electron microscope (JEOL) operating at 80 kV at the Heidelberg Institute of Plant Sciences (Prof. D.G. Robinson)

5.7.2 Preparation of the samples

Six days-old *A.thaliana* plantlets grown in sterile conditions were used. Root tips were excised using a scalpel. Five to six root tips were placed in a planchette (1 mm of thickness) containing Tris-buffer pH 6.6. A second planchette was used to cover the first one. The planchette was frozen in a high-pressure freezer (HPF010; Bal-Tec). After this step the planchette was maintained in liquid nitrogen in order to preserve the quality of the tissue.
The second step of freeze substitution was performed in Leica AFS unit (for the freeze substitution). The planchette containing root tips was submerged in the pre-cooled substitution solution at -85°C (dry acetone supplemented with 10% methanol and 0.3% uranyl

acetate). The substitution was performed at -85°C for 16 hours and then the temperature was gradually increased to -50°C within about 5 hours. This procedure allows substituting the cellular aqueous phase with the substitution solution. The substitution solution was then removed and the sample was infiltrated in resin Lowicryl HM20 resin (Polysciences). This resin works at an optimal temperature of -50°C. For this step, the root tips were incubated at increasing concentration of HM20 (30%, 50%, 75%, 100%) in 100% ethanol. Each incubation was performed for 1 hour at -50°C which is the optimal temperature for this kind of resin. After the last incubation step the roots tips were placed in small containers containing 100% resin. Finally the polymerization was performed for two days using an UV lamp. The polymerization was proceeding until the temperature arrived above 0°C. An additional polymerization at room temperature is necessary to increase the hardness of the resin.

5.7.3 Immunogold labelling

Resin-included root tip samples were used to prepare thin sections with a microtome. Sections were then placed on a particular grind covered with a plastic film (formavar) and dried for few minutes at room temperature. The grid was then incubated for 1 hour at room temperature in blocking solution (3% BSA in PBS) in order to block all unspecific antibody-binding sites. The grid was then incubated for 1 hour at room temperature in washing buffer containing a specific primary antibody (1% BSA in PBS containing primary antibody). Several dilutions of primary anti-GFP antibody were tested, finding an optimal dilution of 1:700. The grid was washed three times with washing buffer (1% BSA in PBS) for 10 minutes at room temperature. The grid was then incubated for 1 hour at room temperature in buffer containing a specific anti-Goat secondary antibody (1% BSA in PBS containing secondary antibody). The secondary antibody conjugated with gold particles of 10 nm (BioCell GAR10) was used at a dilution of 1:50. The grind was washed two times with washing solution (1% BSA in PBS) for 5 minutes at room temperature. Then the grind was washed three times with bi-distilled water for 5 minutes at room temperature. Finally the grid was dried using a filter paper.

5.7.4 Post-staining with uranyl acetate/lead citrate

The post-staining is necessary to improve the contrast of sections for an adequate observation of ultrastructural structures with the TEM. The grid was incubated one minute in uranyl

acetate solution [2% (w/v) uranyl acetate in bi-distilled water]. The grid was washed 3 times in bi-distilled water in order to eliminate all residues of uranyl acetate solution. The grid was then incubated for 1 minute in lead citrate solution (0.1-0.4% w/v). The grid was washed 2 times in bi-distilled water. The last wash was done flushing vigorously with a pipette. Finally the grid was dried using filter paper and was ready for the transmission electron microscope.

5.8 Scanning Electron microscopy

5.8.1 METHOD

Specimens were fixed in a mix of 2% paraformaldehyde (PFA) and 2.5% glutaraldehyde (GA) in 0.1M sodium cacodylate (pH 7.4) for 1-2 hours at room temperature and then washed three times in buffer. They were postfixed in 1% OsO_4 in the same buffer for an hour and washed three times in the buffer. For small specimens centrifugation is necessary at all steps
They were dehydrated in a graded acetone series and air-dried. The dried samples were mounted on stubs on double carbon tape (Leit Tabs, Plano) and carbon glue (Leit C, Plano), coated with a thin gold layer by a Sputter Coater (SCD 005, Baltec) and examined in a PHILIPS ESEM XL 30 Scanning Electron Microscope

Cacodylate Buffer

For a stock solution of 0.2M:

- Sodium cacodylate trihydrate 4,28g in 50 ml H_2O
- adjust to pH 7.4 with HCl 0.2N
- complete to 100 ml with H_2O

Fixation with paraformaldehyde

20% paraformaldehyde (PFA)

- 20g of PFA in 8ml distilled H_2O
- Incubate 5 minutes in a water bath at 60-70°C
- Let cool down to room temperature and add 1-3 drops 1N NaOH
- Complete to 10 ml with distilled water
- If necessary incubate in the water bath to dissolve completely

For 10ml of fixative:	final concentration
1 ml PFA 20%	2%
1 ml GA 25%	2.5%
5 ml 0.2M cacodylate buffer	0.1M
3 ml H_2O	

If necessary adjust the molarity with sucrose

Fixation with OsO_4

For 4 ml:	
1 ml OsO_4 4%	1%
2 ml 0.2M cacodylate buffer	0.1M
H_2O	1 ml

5.9 Confocal Microscopy

Images were collected with a TCS SP5 II confocal laser scanning microscope (Leica). Digital images were acquired using LAS AF (version: 2.0.0 build 1934) and processed using ImageJ 1.41o (National Institute of Health, USA).

5.10 PLASMIDS AND CONSTRUCTS

The binary vector pGREEN0229/pSOUP was used for plant transformation via *Agrobacterium tumefaciens*.

5.10.1 pGREEN0229 contains:

pSa-ORI: *Agrobacterium* origin of replication

ColEl-ori: *E.coli* origin of replication

NptI: neomycin phosphotransferase gene, which provides kanamycin resistance

LB: Left border

RB: Right border

Nos-bar: Gene, which provides BASTA resistance

LacZ: Gene, which encodes the β-galactosidase α fragment and includes the MCS

MCS: Multi cloning site

5.10.2 pSOUP contains:

ColEl-ori: *E.coli* origin of replication

oriV: Origin of replication compatible with pSa-ORI in *Agrobacterium*

RepA: Gene encoding the replicase RepA, needed in *trans* by the pSa-ORI

trfA: Replication gene

Tet-r: Gene, which provides tetracycline-resistance

5.10.3 List of Constructs and stable expressing plant lines

For the sequences of the primers, see the table X at the end of the methods section

5.10.4 pGREEN_35S

pGREEN0229 with the 35S promoter and terminator cloned into the XhoI/SacI sites of the MCS.

5.10.5 pGREEN_YFP

A multi cloning site (MCS), the sequence encoding a polyglycine linker (Gly-Gly-Gly-Gly-Gly-Gly) and a HA tag were fused at the 5' sequence of YFP (yellow fluorescent protein) by sequential PCR. The following primers were used: linker_HA_YFP_n fw/c_YFP rev for the first PCR; MCS_linker fw/c_YFP rev for the second PCR. The PCR product was digested with BamHI/SalI and then cloned between the 35S promoter and terminator of pGREEN_35S digested with the same restriction enzymes.

5.10.6 pGREEN_SpYFP

Specific pairs of primers were used in sequential PCR to amplify the YFP gene fused at 5' end with the sequence encoding for the AtRMR1 signal peptide and at 3' end with the sequence encoding for a polyglycine linker (Gly-Gly-Gly-Gly-Gly-Gly), a Myc tag and multi cloning site (MCS). The following primers were used: prim1_SpYFP fw/prim1_linker_Myc rev for the first PCR; prim2_SpYFP fw/prim2_linker_Myc rev for the second PCR. The generated sequence was produced as BamHI/SalI fragment. The fragment was then cloned between the 35S promoter and terminator present in pGREEN_35S using the same restriction enzymes.

5.10.7 pGREEN_RFP

A multi cloning site (MCS), the sequence encoding a polyglycine linker (Gly-Gly-Gly-Gly-Gly-Gly) and a Myc tag were fused at the 5' sequence of RFP (monomeric red fluorescent protein) by sequential PCR. The following primers were used: linker_Myc_RFP fw/RFP rev for the first PCR; linker fw/RFP rev for the second PCR. The PCR product was digested with BamHI/SalI fragment and cloned between the 35S promoter and terminator of pGREEN_35S

digested with the same restriction enzymes.

5.10.8 pGREEN SpYFP_RMR1

The cDNA of *At*RMR1 without the sequence encoding the signal peptide was amplified as an EcoRI/SpeI fragment using the following primers: EcoRI_delRMR1 fw and delRMR1_SpeI rev. The resulting fragment was then cloned into pGREEN_SpYFP digested with the same restriction enzymes.

5.10.9 pGREEN RMR1_YFP

The AtRMR1 full length cDNA was amplified as an EcoRI/SpeI fragment using the following primers: EcoRI_RMR1 fw and RMR1_SpeI rev. The resulting fragment was digested with EcoRI/SpeI and cloned into pGREEN_SpYFP digested with the same restriction enzymes.

5.10.10 pGREEN RMR1_RFP

The *At*RMR1 full length cDNA was amplified as an EcoRI/SpeI fragment using the following primers: EcoRI_RMR1 fw and RMR1_SpeI rev. The resulting fragment was digested with EcoRI/SpeI and cloned into pGREEN_SpYFP digested with the same restriction enzymes

5.10.11 pGREEN p6_RFP

The p6 full length CDS from BYV (Beet Yellow Virus) (Peremyslov, et al., 2004) was amplified using the following primers: EcoRI_p6 fw / p6_SpeI rev. The resulting fragment was digested with EcoRI/SpeI and cloned into pGREEN_RFP digested with same restriction enzymes.

5.10.12 pGREEN GONST1-RFP

The AtGONST1 full length CDS (Baldwin, et al., 2001) was amplified using the following primers: EcoRI_GONST1 fw and GONST1_SpeI rev. The resulting fragment was digested with EcoRI/SpeI and cloned into pGREEN_RFP digested with the same restriction enzymes.

5.10.13 pGREEN GFP-Chi

GFP-Chi was subcloned into pGREEN as a XhoI/HindIII fragment from pGY1: GFP-Chi (Di Sansebastiano, et al., 1998)

5.10.14 pGREEN Venus SYP61

Venus SYP61 CDS, cloned in pGY1, was kindly provided by Dr. Uemura (Uemura, et al., 2004)

5.10.15 pGREEN GFP-Talin

The GFP-Talin was subcloned into pGREEN 35S-Ter as an EcoRV/SpeI fragment from pYSC14 (kindly provided by Dr. D. Schaefer) (Finka, et al., 2007)

5.10.16 MBD-RFP

It was kindly provided by Dr. Martine Pastuglia (plasmid pH7WGR2) (Crowell, et al., 2009).

5.10.17 pCAMBIA EGFP-Rac8

It was kindly provided by Yalovsky (Lavy, et al., 2002)

5.10.18 pGREEN p6RFP

The p6 full length cDNA from BYV (Beet Yellow Virus) (Peremyslov, et al., 2004) was cloned as fragment EcoRI/SpeI in pGREEN RFP

5.10.19 Sar1H74L

Sar1H74L was kindly provided by Dr. Chris Hawes (Andreeva, et al., 2000)

5.10.20 Constructs to generate point mutants

All the point mutants were generated by using the Phusion protocol (New England Biolabs) with some modifications: 5' phosphorylated primers were designed according to the manufacturer's instructions, but using 200 ng of DNA as template instead of 10 ng. PCR was carried out as follows: 1 min 98°C as initial denaturation step, 30 sec 98°C, 30 sec in a touchdown PCR starting from the highest TM of the couple of primers and descending 0.3°C at each cycle, 72°C according to the length of the vector (1min/1kb), 20 min at 72°C. This standard program was repeated for 20-25 cycles. The PCR product was then incubated for 1h at 37°C with DpnI (an enzyme that cuts methylated DNA and therefore will digest the parental DNA, pGREEN RMR1YFP). DNA was precipitated with 1/10 volume 3M NaAc pH 5.6 and 2 volumes of ethanol, incubated at -20 °C for 1-2h and then centrifuged at 20000g for 30 minutes. The pellet was washed three times in 70% ethanol and then air dried. The pellet

was resuspended in 15µl water for 1h at room temperature; ligase buffer and ligase were added to a final volume in 20µl and incubated overnight at 14°C. The following day the ligation product was transformed into *E.coli* and plated on a selective medium.

The mutation C1A (cysteine 182 mutated in alanine) was generated using the primers:
C182Afw/C182Arev

The mutation C3A (cysteine 250 mutated in alanine) was generated using the primers:
C250Afw/C251Arev

The mutation C4A (cysteine 251 mutated in alanine) was generated using the primers:
C251Afw/C251Arev

5.11 Use of Drugs and Dyes

2Bromo-palmitate (2BR, SIGMA) was dissolved in DMSO at stock concentration of 1M and stored at -20 °C for long period. The working concentration was 1mM (1:1000).

FM4-64 (INVITROGEN) was dissolved in DMSO at the concentration of 3mM and used at working concentration of 3µM for both pollen tubes and *A. thaliana* roots as described in (Zonia and Munnik, 2008; Geldner, et al., 2009). For short time observation with FM4-64 incubation time and then observation was 10-15 minutes. For longer time observation, incubation was 30 minutes (in this case the dye was washed out by three consecutive centrifugations at 60g for washing out the probe).

5.11.1 N.benthamiana pollen germination medium

Pollen was harvested were germinated in the following medium:

Quantities for 100 ml of solution:

$MgSO_4x7H_20$	0.8 µM	1,97mg (100x)
H_3BO_3	1.6 µM	100 mg (100000x)
$Ca(NO_3)_2$	3 mM	70 mg
KNO_3	1 mM	10,111 mg
MES	10 mM	195,2 mg
Sucrose	8%	

pH 6 with KOH

Pollen tubes were germinated for two hours as the polar growth was faster and therefore easier to observe possible variations in pollen tubes elongation. 2BP was added at the final concentration of 1mM and incubated for 2h. Pollen tubes were counted using a Nikon inverse microscope. We considered as germinated pollen tubes for which the tube was longer than the grain diameter as described in (Wang, et al., 2005). The length of the pollen tubes was

determined with the ImageJ software. The known distance in a cytometer was used as reference length.

5.11.2 Physcomitrella patens transgenic lines

5.11.2.1Pp αTub-GFP

P patens stably expressing αTub-GFP was kindly provided by Dr. Hiwatashi (Hiwatashi, et al., 2008).

5.11.2.2Pp GFP-Talin

P patens stably expressing GFP-talin was kindly provided by Dr. Schaefer (Finka, et al., 2007).

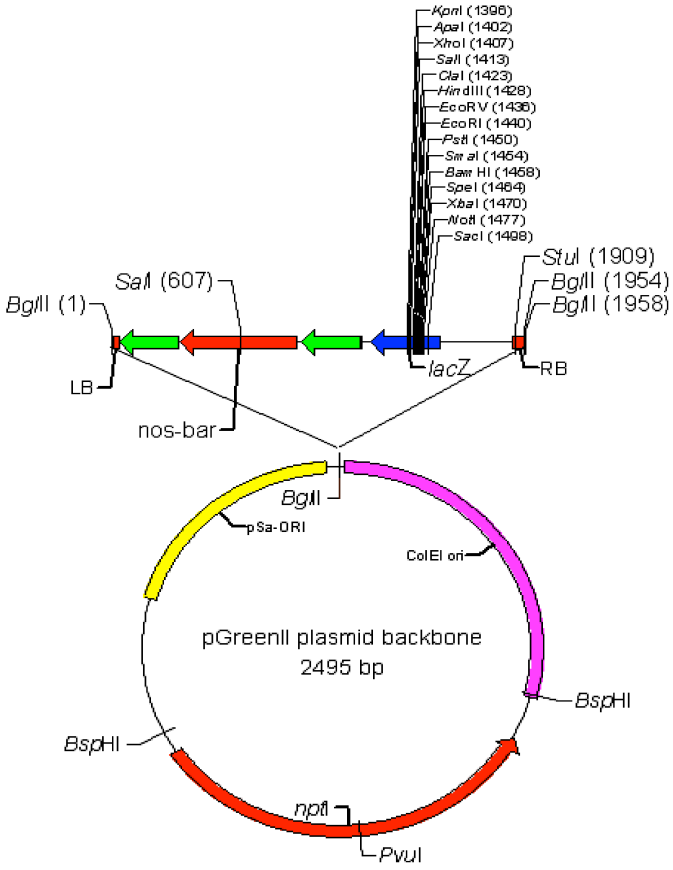

Figure 5. 1: pGreen
Representation of the main Vector used in this study

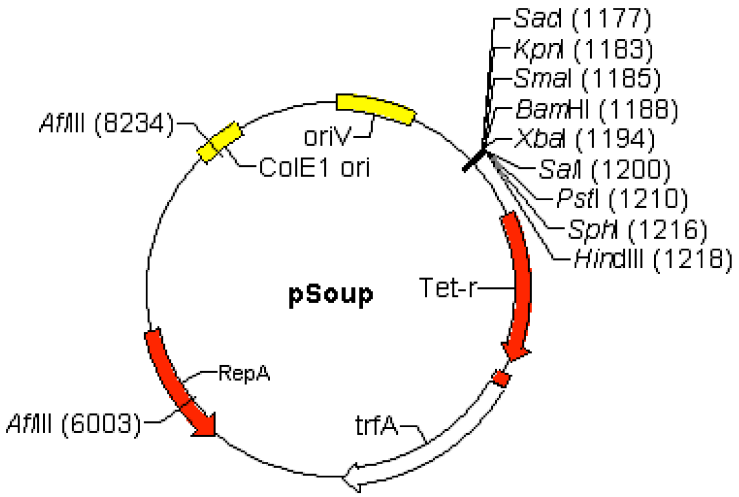

Figure 5. 2: pSOUP

Figure 5. 3: pGREEN: RMR1C1C2C3CYFP
Sequence of the triple cysteine mutant

Primer	Sequence
linker_HA_YFP_n fw	GGAGGAGGAGGAGGAGGATACCCATACGACGTCCCAGACTACGCTG TGAGCAAGGGCGAGGAGCTG
c_YFP rev	GCGCGCGTCGACTTACTTGTACAGCTCGTC
MCS_linker fw	GCGCGCGGATCCGAATTCTCTAGAAAGCTTACTAGTCATATGGGAGGAG GAGGAGGAGGA
Linker_Myc_YFP_c fw	GGAGGAGGAGGAGGAGGAGAACAACAAAAACTTATTTCTGAAGAAGAT CTGGACAAGCAGAAGAACGGCATC
linker_Myc_RFP fw	GGAGGAGGAGGAGGAGGAGAACAACAAAAACTTATTTCTGAAGAAGAT CTGGCCTCCTCCGAGGACGTCATCA
linker fw	GGCCGGGGATCCGAATTCTCTAGAAAGCTTACTAGTCATATGGGAGGAG GAGGAGGAGGAGAACAAC
RFP rev	CCGGCCGTCGACTTATGCTCCAGTACTGTGGCGGCCC
EcoRI_delRMR1 fw	GGCCGGGAATTCAAAGTTATTTTGATGAGGAATAACATCA
delRMR1_SpeI rev	CCGGCCACTAGTCTAACAGTCTGGAAGCGAG
EcoRI_RMR1 fw	GCGCGCGAATTCATGAATCGTGCTTTGGTCC
RMR1_SpeI rev	GCGCGCACTAGTACAGTCTGGAAGCGAGTTTGC
prim1_SpYFP fw	CTGTTTCTTGTTTAGCTTCAAGCGTGAGCAAGGGCGAGGAGCTGT
prim1_linker_Myc rev	TCTTCAGAAATAAGTTTTTGTTGTTCTCCTCCTCCTCCTCCTCCCTTGTACA GCTCGTCCATGCCG
prim2_linker_Myc rev	CCGGCCGTCGACACTAGTAAGCTTTCTAGAGAATTCCAGATCTTCTTCAG AAATAAGTTTTTGTTG
prim2_SpYFP fw	GGCCGGGGATCCATGAATCGTGCTTTGGTCCTACTTTTATATGTTTGTACT GTTTCTTGTTTAGCTTCAAG
EcoRI_GONST1 fw	GGCCGGGAATTCATGAAATTGTACGAACACGATG
GONST1_SpeI rev	GGCCGGACTAGTGGACTTCTCCCTCATTTTGG
EcoRI_p6 fw	GCGCGCGAATTCATGGACTGTGTACTCCGCTC
p6_SpeI rev	GCGCGCACTAGTCACGACCGTGGAACGGTTGA
C182Afw	CGGCTGTTCTCGCTACTGCTTTCTTTGTGCG
C182Arev	ACATTGCAAGCAGCGAGATAAACGAAACCGCC
C250Afw	GCTCAGGCTCTTACCTGCCGCTCACAAGTTTCATGC
C251Arev	TTGTCTCCAACAGTGTAGTCTTCAAGGC
C251Afw	GCTCAGGCTCTTACCTTGCGCTCACAAGTTTCATGC
120 fw	TGACGCACAATCCCACTATCCTTCGCA
121 rev	TGTAGAGAGAGACTGGTGATTTC

Table 5. 1: List of the primers used in this work

6. Outlooks

This study aimed to study an important eukaryotic post-translational modification, the S-palmitoylation. Until now, there was no study of palmitoylation in plant cell biology. In the first part of this study (chapter 2), we wanted to study the palmitoylation of the vacuolar receptor AtRMR1, as predicted *in silico*. We used a very innovative technique, the Biotin Switch Assay, which does not use radioactive palmitate, is much less time-consuming as it is possible to obtain results after three to four days (Hemsley, et al., 2008). Another advantage for cell biology is that it allows the characterization of entire palmitoyl-proteomes. Yeast and neuronal palmitoyl-proteomes (Kang, et al., 2008a)have indeed been recently characterized. The study of RMR1's palmitoylation revealed the first palmitoylated plant transmembrane protein. The palmitoylation of a small fraction of RMR1 at a higher molecular weight deserves further discussion. It would be very interesting indeed to see how a homodimer (or a protein complex) can be associated even in denaturing conditions. Therefore, the isolation of the protein (e.g. by immunoprecipitation) could answer this question. In this regard, the production of an antibody raised against the cytosolic domains would greatly assist in understanding the nature of post-translational modification of RMR1.

Different aspects remain to be clarified for RMR1. The protein can be detected both by western (Park, et al., 2007; Zava, 2007) blotting and by immunoelectron microscopy (Hinz, et al., 2007). However expression of its fluorescent-protein tagged versions is so low, even when driven by a strong promoter, that it was only possible to observe them in the presence of the silencing inhibitor p19. This suggests that the amount of protein in the cell is tightly regulated. In this regard, the RING-H2 domain might be a good candidate for the instability of the protein, and therefore for its low accumulation. A RING-H2 domain is present in many E3 ubiquitin ligases, and the mammalian homolog of RMR RNF13 is itself an ubiquitin ligase. Thus ubiquitination assays, as well as *in vitro* incubation of fusion proteins in presence of an inhibitor of proteasomal degradation, e.g. MG132, could provide some hints to the mechanism of RMR1 instability. Another aspect that deserves more thorough attention is surely the association of RMR1 with lipid rafts and the role of palmitoylation in this association. Preliminary results already suggest such a function (Hinz, personal communication).

In the second part of this thesis (chapter 3), I addressed the more general role of

palmitoylation in the secretory pathway through the use of a potent palmitoylation inhibitor: 2BP. This study showed a specific action of the drug in TGN/post-TGN compartments. The drug affected the structural maintenance of macrovesicles of secretion (Zonia and Munnik, 2008). The macrovesicles of secretion have recently been characterized by cryo-fixation and by electron tomography(Toyooka, et al., 2009a) (Kang, et al., 2011). They are structures reminiscent of a bunch of grapes, where each grape is a secretory vesicle. They are associated with the building with TGN-rich secretory vesicles with a diameter of few tens of nanometres. These vesicles are particularly visible in tissues with a high growth rate, such as pollen tubes. 2BP drastically changed the state of aggregation of macrovesicles of secretion. In an imaged way, each grape was released and a diffuse fluorescence was observed. Palmitoylation is therefore important in the formation or stability of this important secretory structure. A possible extension of this work would be the isolation of palmitoylated proteins involved in this stabilization.

In addition, palmitoylated Rabs were detected for the first time in a plant. Their presence in animal cells had already been established during the characterization of the palmitoyl-proteome of neurons (Kang, et al., 2008a), but no result was obtained on their role. The three plant Rabs for which I detected the effect of 2BP are located in post-Golgi compartments. This makes their involvement in secretion processes very likely. This working hypothesis could be demonstrated with mutants of the three Rabs lacking their putative palmitoylation sites, in combination with markers of secretion, such as secGFP, which is normally secreted into the apoplast). Certainly the role of palmitoylation in Rabs remains an extremely attractive research filed considering how little we know about it.

In a last part of the thesis (chapter 4) I decided to investigate the route of secretion of GFP-Chi, a vacuolar marker widely used in the lab that can be followed along the route of secretion. Two articles reported the trafficking of this marker by the Golgi-TGN-PVC pathway (Sanmartin, et al., 2007, Zouhar, et al., 2009). Instead Poutska et al., (2008) demonstrated that the marker managed to get out of the ER and into small compartments even in the presence of BFA, which inhibits this pathway. The nature of these small compartments is not entirely clear, although they could be the recently described storage PVC (Shen, 2011). Electron microscopy studies on cryo-fixed Arabidopsis thaliana root tips expressing the fluorescent reporter did not clarify this point. Unexpectedly, when GFP-Chi was co-expressed with NtSar1H74L (a dominant-negative mutant also blocking the ER-Golgi trafficking by preventing the formation of COPII vesicles, (Oka and Nakano, 1994; Andreeva, et al., 2000; Sparkes, et al., 2005)) the reporter arrived at the vacuole even faster then in the controls since

labelled vacuoles could be observed at earlier expression times. This suggests that the alternative pathway bypassing the Golgi can take over a higher proportion of cargo when the main pathway is blocked and is also faster to bring GFP-Chi to the vacuole.

I also detected the presence of a possible GFP-Chi dimer associated with the membrane fraction upon ultracentrifugation. The nature of this dimer of a soluble protein remains to be investigated although several cases of aggregation of soluble proteins have been reported in the literature (like β-amyloids presents in the of Alzheimer disease, (Haass and Selkoe, 2007a). Another matter of great interest is whether the dimer reaches the vacuole or is only transient intermediate during the transport to the vacuole. Western blot analysis of isolated vacuoles from leaves expressing the reporter in presence of the dominant-negative mutant would answer this question.

Finally, the use of biochemical techniques such as confocal microscopy could answer the log-time question of the receptor responsible for the transport of GFP-Chi to the vacuole and whether the same receptor is involved in the two pathways. From a biological point of view this remains one of the few examples of an alternative pathway to the vacuole in leaves, previously only known in seeds.

References

Adjobo-Hermans, M. J., Goedhart, J., and Gadella, T. W. (2006) Plant G protein heterotrimers require dual lipidation motifs of Galpha and Ggamma and do not dissociate upon activation. J. Cell Sci. 119(Pt 24):5087 - 5097.

Ahmed, S. U., Bar-Peled, M., and Raikhel, N. V. (1997) Cloning and Subcellular Location of an Arabidopsis Receptor-like Protein that shares Common Features with Protein-Sorting Receptors of Eukaryotic Cells. Plant Physiol. 114:325-336.

Ahmed, S. U., Rojo, E., Kovaleva, V., Venkataraman, S., Dombrowski, J. E., Matsuoka, K., and Raikhel, N. V. (2000) The plant vacuolar sorting receptor AtELP is involved in transport of NH(2)-terminal propeptide-containing vacuolar proteins in Arabidopsis thaliana. J. Cell Biol. 149(7):1335-44.

Andreeva, A. V., Zheng, H., Saint-Jore, C. M., Kutuzov, M. A., Evans, D. E., and Hawes, C. R. (2000) Organization of transport from endoplasmic reticulum to Golgi in higher plants. Biochem. Scty. Trans. 28(Part 4):505-512.

Arcaro, A., and Wymann, M. P. (1993) Wortmannin is a potent phosphatidylinositol 3-kinase inhibitor: the role of phosphatidylinositol 3,4,5-trisphosphate in neutrophil responses. Biochemical J. 296 (Pt 2):297-301.

Arellano, M., Coll, P. M., and Perez, P. (1999) RHO GTPases in the control of cell morphology, cell polarity, and actin localization in fission yeast. Microsc Res Tech 47(1):51-60.

Arighi, C. N., Hartnell, L. M., Aguilar, R. C., Haft, C. R., and Bonifacino, J. S. (2004) Role of the mammalian retromer in sorting of the cation-independent mannose 6-phosphate receptor. J. Cell Biol. 165(1):123-133.

Austin, C. D., and Shields, D. (1996) Formation of nascent secretory vesicles from the trans-Golgi network of endocrine cells is inhibited by tyrosine kinase and phosphatase inhibitors. J. Cell Biol. 135(6 Pt 1):1471-83.

Avila, E. L., Brown, M., Pan, S., Desikan, R., Neill, S. J., Girke, T., Surpin, M., and Raikhel, N. V. (2008) Expression analysis of Arabidopsis vacuolar sorting receptor 3 reveals a putative function in guard cells. J Exp Bot 59(6):1149-61.

Babst, M. (2005) A protein's final ESCRT. Traffic 6(1):2-9.

Babst, M. (2006) A close-up of the ESCRTs. Dev Cell 10(5):547-8.

Babu, P., Deschenes, R. J., and Robinson, L. C. (2004) Akr1p-dependent palmitoylation of Yck2p yeast casein kinase 1 is necessary and sufficient for plasma membrane targeting. J. Biol. Chem. 279(26):27138-47.

Baggiolini, M., Dewald, B., Schnyder, J., Ruch, W., Cooper, P. H., and Payne, T. G. (1987) Inhibition of the phagocytosis-induced respiratory burst by the fungal metabolite wortmannin and some analogues. Exp Cell Res 169(2):408-18.

Baldwin, T. C., Handford, M. G., Yuseff, M. I., Orellana, A., and Dupree, P. (2001) Identification and characterization of GONST1, a golgi-localized GDP-mannose transporter in Arabidopsis. Plant Cell 13(10):2283-95.

Baluska, F., Hlavacka, A., Samaj, J., Palme, K., Robinson, D. G., Matoh, T., McCurdy, D. W., Menzel, D., and Volkmann, D. (2002) F-actin-dependent endocytosis of cell wall pectins in meristematic root cells. Insights from brefeldin A-induced compartments. Plant Physiol. 130(1):422-31.

Bannykh, S. I., Nishimura, N., and Balch, W. E. (1998) Getting into the Golgi. Trends Cell Biol. 8(1):21-25.

Bano, M. C., Jackson, C. S., and Magee, A. I. (1998) Pseudo-enzymatic S-acylation of a myristoylated yes protein tyrosine kinase peptide in vitro may reflect non-enzymatic S-acylation in vivo. Biochemical J. 330 (Pt 2):723-31.
Barlowe, C., D'Enfert, C., and Schekman, R. (1993) Purification and characterization of SAR1p, a small GTP-binding protein required for transport vesicle formation from the endoplasmic reticulum. J. Biol. Chem. 268(2):873-79.
Bassham Diane, C., Brandizzi, F., Otegui Marisa, S., and Sanderfoot Anton, A.
2009 The Secretory System of Arabidopsis. *In* The Arabidopsis Book. Pp. 1-29. The Arabidopsis Book, Vol. null: The American Society of Plant Biologists.
Bastie, C., Luquet, S., Holst, D., Jehl-Pietri, C., and Grimaldi, P. A. (2000) Alterations of peroxisome proliferator-activated receptor delta activity affect fatty acid-controlled adipose differentiation. J. Biol. Chem. 275(49):38768-73.
Baxter-Burrell, A., Yang, Z., Springer, P. S., and Bailey-Serres, J. (2002) RopGAP4-Dependent Rop GTPase Rheostat Control of Arabidopsis Oxygen Deprivation Tolerance. Science 296(5575):2026-2028.
Behnia, R., and Munro, S. (2005) Organelle identity and the signposts for membrane traffic. Nature 438(7068):597-604.
Bharadwaj, M., and Bizzozero, O. A. (1995) Myelin P0 glycoprotein and a synthetic peptide containing the palmitoylation site are both autoacylated. J Neurochem 65(4):1805-15.
Biel, M., Deck, P., Giannis, A., and Waldmann, H. (2006) Synthesis and Evaluation of Acyl Protein Thioesterase 1 (APT1) Inhibitors. Chemistry - A European Journal 12(15):4121-4143.
Biermann, B., Randall, S. K., and Crowell, D. N. (1996) Identification and isoprenylation of plant GTP-binding proteins. Plant Mol. Biol. 31(5):1021-8.
Bijlmakers, M. J., and Marsh, M. (2003) The on-off story of protein palmitoylation. Trends Cell Biol 13(1):32-42.
Bischoff, F., Vahlkamp, L., Molendijk, A., and Palme, K. (2000) Localization of AtROP4 and AtROP6 and interaction with the guanine nucleotide dissociation inhibitor AtRhoGDI1 from Arabidopsis. Plant Mol. Biol. 42(3):515-530.
Bizzozero, O. A., Bixler, H. A., and Pastuszyn, A. (2001) Structural determinants influencing the reaction of cysteine-containing peptides with palmitoyl-coenzyme A and other thioesters. Biochim. Biophys. Acta 1545(1-2):278-88.
Blobel, G., and Dobberstein, B. (1975) Transfer of proteins across membranes. I. Presence of proteolytically processed and unprocessed nascent immunoglobulin light chains on membrane-bound ribosomes of murine myeloma. J. Cell Biol. 67:835-851.
Bocock, J. P., Carmicle, S., Chhotani, S., Ruffolo, M. R., Chu, H., and Erickson, A. H. (2009) The PA-TM-RING protein RING finger protein 13 is an endosomal integral membrane E3 ubiquitin ligase whose RING finger domain is released to the cytoplasm by proteolysis. Febs J 276(7):1860-77.
Bogdanove, A. J., and Martin, G. B. (2000) AvrPto-dependent Pto-interacting proteins and AvrPto-interacting proteins in tomato. Proc. Natl. Acad. Sci. USA 97(16):8836-+.
Boisson, B., Giglione, C., and Meinnel, T. (2003) Unexpected protein families including cell defense components feature in the N-myristoylome of a higher eukaryote. J. Biol. Chem. 278(44):43418-29.
Boman, A. L., Zhang, C., Zhu, X., and Kahn, R. A. (2000) A family of ADP-ribosylation factor effectors that can alter membrane transport through the trans-Golgi. Mol Biol Cell 11(4):1241-55.
Bonifacino, J. S., and Rojas, R. (2006) Retrograde transport from endosomes to the trans-Golgi network. Nat Rev Mol Cell Biol 7(8):568-79.
Boonsirichai, K., Sedbrook, J. C., Chen, R., Gilroy, S., and Masson, P. H. (2003) ALTERED RESPONSE TO GRAVITY is a peripheral membrane protein that modulates gravity-

induced cytoplasmic alkalinization and lateral auxin transport in plant statocytes. Plant Cell 15(11):2612-25.
Borden, K. L. (2000) RING domains: master builders of molecular scaffolds? J. Mol. Biol. 295(5):1103-12.
Borner, G. H. H., Sherrier, D. J., Weimar, T., Michaelson, L. V., Hawkins, N. D., MacAskill, A., Napier, J. A., Beale, M. H., Lilley, K. S., and Dupree, P. (2005) Analysis of Detergent-Resistant Membranes in Arabidopsis. Evidence for Plasma Membrane Lipid Rafts. Plant Physiol. 137(1):104-116.
Bowman, E. J., Siebers, A., and Altendorf, K. (1988) Bafilomycins: a class of inhibitors of membrane ATPases from microorganisms, animal cells, and plant cells. Proc Natl Acad Sci U S A 85(21):7972-6.
Boyd, M. R., Farina, C., Belfiore, P., Gagliardi, S., Kim, J. W., Hayakawa, Y., Beutler, J. A., McKee, T. C., Bowman, B. J., and Bowman, E. J. (2001) Discovery of a novel antitumor benzolactone enamide class that selectively inhibits mammalian vacuolar-type (H+)-atpases. J Pharmacol Exp Ther 297(1):114-20.
Brandes, R., Arad, R., and Bar-Tana, J. (1995a) Inducers of adipose conversion activate transcription promoted by a peroxisome proliferators response element in 3T3-L1 cells. Biochemical Pharmacology 50(11):1949-1951.
Brandes, R., Arad, R., and Bar-Tana, J. (1995b) Inducers of adipose conversion activate transcription promoted by a peroxisome proliferators response element in 3T3-L1 cells. Biochem Pharmacol 50(11):1949-51.
Brandizzi, F., Frangne, N., Marc-Martin, S., Hawes, C., Neuhaus, J. M., and Paris, N. (2002) The destination for single-pass membrane proteins is influenced markedly by the length of the hydrophobic domain. Plant Cell 14(5):1077-92.
Briknarova, K., Nasertorabi, F., Havert, M. L., Eggleston, E., Hoyt, D. W., Li, C., Olson, A. J., Vuori, K., and Ely, K. R. (2005) The serine-rich domain from Crk-associated substrate (p130cas) is a four-helix bundle. J. Biol. Chem. 280(23):21908-14.
Briknarová, K., Nasertorabi, F., Havert, M. L., Eggleston, E., Hoyt, D. W., Li, C., Olson, A. J., Vuori, K., and Ely, K. R. (2005) The Serine-rich Domain from Crk-associated Substrate (p130cas) Is a Four-helix Bundle. J. Biol. Chem. 280(23):21908-21914.
Cai, G., Moscatelli, A., and Cresti, M. (1997) Cytoskeletal organization and pollen tube growth. Trends Plant Sci 2(3):86-91.
Cai, G., Romagnoli, S., Moscatelli, A., Ovidi, E., Gambellini, G., Tiezzi, A., and Cresti, M. (2000) Identification and characterization of a novel microtubule-based motor associated with membranous organelles in tobacco pollen tubes. Plant Cell 12(9):1719-1736.
Calhoun, B. C., Lapierre, L. A., Chew, C. S., and Goldenring, J. R. (1998) Rab11a redistributes to apical secretory canaliculus during stimulation of gastric parietal cells. Am J Physiol 275(1 Pt 1):C163-70.
Camacho, L., and Malho, R. (2003) Endo/exocytosis in the pollen tube apex is differentially regulated by Ca2+ and GTPases. J Exp Bot 54(380):83-92.
Camacho, L., Smertenko, A. P., Perez-Gomez, J., Hussey, P. J., and Moore, I. (2009) Arabidopsis Rab-E GTPases exhibit a novel interaction with a plasma-membrane phosphatidylinositol-4-phosphate 5-kinase. J. Cell Sci. 122(23):4383-4392.
Camp, L. A., and Hofmann, S. L. (1993) Purification and properties of a palmitoyl-protein thioesterase that cleaves palmitate from H-Ras. J. Biol. Chem. 268(30):22566 - 22574.
Camp, L. A., Verkruyse, L. A., Afendis, S. J., Slaughter, C. A., and Hofmann, S. L. (1994) Molecular cloning and expression of palmitoyl-protein thioesterase. J. Biol. Chem. 269(37):23212-9.
Cao, X., Rogers, S. W., Butler, J., Beevers, L., and Rogers, J. C. (2000) Structural requirements for ligand binding by a probable plant vacuolar sorting receptor. Plant Cell 12(4):493-506.

Caron, J. (1997) Posttranslational modification of tubulin by palmitoylation: I. In vivo and cell-free studies. Mol. Biol. Cell 8(4):621-636.
Castelli, S., and Vitale, A. (2005) The phaseolin vacuolar sorting signal promotes transient, strong membrane association and aggregation of the bean storage protein in transgenic tobacco. J Exp Bot.
Castle, A., Huang, A., and Castle, J. (1997) Passive sorting in maturing granules of AtT-20 Cells: The entry and exit of salivary amylase and proline-rich protein. J. Cell Biol. 138:45-54.
Chabin-Brion, K., Marceiller, J., Perez, F., Settegrana, C., Drechou, A., Durand, G., and Pous, C. (2001) The Golgi Complex Is a Microtubule-organizing Organelle. Mol. Biol. Cell 12(7):2047-2060.
Chase, J. F., and Tubbs, P. K. (1972) Specific inhibition of mitochondrial fatty acid oxidation by 2-bromopalmitate and its coenzyme A and carnitine esters. Biochemical J. 129(1):55-65.
Chen, A., Wu, K., Fuchs, S. Y., Tan, P., Gomez, C., and Pan, Z.-Q. (2000) The Conserved RING-H2 Finger of ROC1 Is Required for Ubiquitin Ligation. J. Biol. Chem. 275(20):15432-15439.
Chen, H. Q., Tannous, M., Veluthakal, R., Amin, R., and Kowluru, A. (2003) Novel roles for palmitoylation of Ras in IL-1 beta-induced nitric oxide release and caspase 3 activation in insulin-secreting beta cells. Biochem Pharmacol 66(9):1681-94.
Chenette, E. J., Abo, A., and Der, C. J. (2005) Critical and distinct roles of amino- and carboxyl-terminal sequences in regulation of the biological activity of the Chp atypical Rho GTPase. J. Biol. Chem. 280(14):13784-92.
Chow, C.-M., Neto, H., Foucart, C., and Moore, I. (2008) Rab-A2 and Rab-A3 GTPases Define a trans-Golgi Endosomal Membrane Domain in Arabidopsis That Contributes Substantially to the Cell Plate. Plant Cell 20(1):101-123.
Chrispeels, M. J., Crawford, N. M., and Schroeder, J. I. (1999) Proteins for Transport of Water and Mineral Nutrients across the Membranes of Plant Cells. Plant Cell 11:661-675.
Chrispeels, M. J., and Raikhel, N. V. (1992) Short peptide domains target proteins to plant vacuoles. Cell 68(4):613-6.
Cole, R. A., and Fowler, J. E. (2006) Polarized growth: maintaining focus on the tip. Curr Opin Plant Biol 9(6):579-88.
Coleman, R. A., Rao, P., Fogelsong, R. J., and Bardes, E. S. (1992) 2-Bromopalmitoyl-CoA and 2-bromopalmitate: promiscuous inhibitors of membrane-bound enzymes. Biochim. Biophys. Acta 1125(2):203-9.
Collins, B. M. (2008) The structure and function of the retromer protein complex. Traffic 9(11):1811-22.
Collins, B. M., Norwood, S. J., Kerr, M. C., Mahony, D., Seaman, M. N., Teasdale, R. D., and Owen, D. J. (2008) Structure of Vps26B and mapping of its interaction with the retromer protein complex. Traffic 9(3):366-79.
Conibear, E., and Davis, N. G. (2010) Palmitoylation and depalmitoylation dynamics at a glance. J. Cell Sci. 123(23):4007-4010.
Conibear, E., and Stevens, T. H. (1998) Multiple sorting pathways between the late Golgi and the vacuole in yeast. Biochim. Biophys. Acta 1404(1-2):211-30.
Corvera, S., D'Arrigo, A., and Stenmark, H. (1999) Phosphoinositides in membrane traffic. Curr Opin Cell Biol 11(4):460-5.
Coury, L. A., Hiller, M., Mathai, J. C., Jones, E. W., Zeidel, M. L., and Brodsky, J. L. (1999) Water transport across yeast vacuolar and plasma membrane-targeted secretory vesicles occurs by passive diffusion. J. Bacteriol. 181(14):4437-40.
Crowell, E. F., Bischoff, V., Desprez, T., Rolland, A., Stierhof, Y.-D., Schumacher, K., Gonneau, M., Hofte, H., and Vernhettes, S. (2009) Pausing of Golgi Bodies on Microtubules Regulates Secretion of Cellulose Synthase Complexes in Arabidopsis. Plant Cell

21(4):1141-1154.
Crowley, K. S., Reinhart, G. D., and Johnson, A. E. (1993) The signal sequence moves through a ribosomal tunnel into a noncytoplasmic aqueous environment at the ER membrane early in translocation. Cell 73(6):1101-1115.
Cunha, D. A., Hekerman, P., Ladriere, L., Bazarra-Castro, A., Ortis, F., Wakeham, M. C., Moore, F., Rasschaert, J., Cardozo, A. K., Bellomo, E., Overbergh, L., Mathieu, C., Lupi, R., Hai, T., Herchuelz, A., Marchetti, P., Rutter, G. A., Eizirik, D. L., and Cnop, M. (2008) Initiation and execution of lipotoxic ER stress in pancreatic beta-cells. J. Cell Sci. 121(Pt 14):2308-18.
Das, S., Hussain, A., Bock, C., Keller, W. A., and Georges, F. (2005) Cloning of Brassica napus phospholipase C2 (BnPLC2), phosphatidylinositol 3-kinase (BnVPS34) and phosphatidylinositol synthase1 (BnPtdIns S1)--comparative analysis of the effect of abiotic stresses on the expression of phosphatidylinositol signal transduction-related genes in B. napus. Planta 220(5):777-84.
daSilva, L. L., Foresti, O., and Denecke, J. (2006) Targeting of the plant vacuolar sorting receptor BP80 is dependent on multiple sorting signals in the cytosolic tail. Plant Cell 18(6):1477-97.
Dasilva, L. L., Taylor, J. P., Hadlington, J. L., Hanton, S. L., Snowden, C. J., Fox, S. J., Foresti, O., Brandizzi, F., and Denecke, J. (2005) Receptor salvage from the prevacuolar compartment is essential for efficient vacuolar protein targeting. Plant Cell 17(1):132-48.
Davis, K. L., Martin, E., Turko, I. V., and Murad, F. (2001) Novel effects of nitric oxide. Annu Rev Pharmacol Toxicol 41:203-36.
Deck, P., Pendzialek, D., Biel, M., Wagner, M., Popkirova, B., Ludolph, B., Kragol, G., Kuhlmann, J., Giannis, A., and Waldmann, H. (2005) Development and biological evaluation of acyl protein thioesterase 1 (APT1) inhibitors. Angew Chem Int Ed Engl 44(31):4975-80.
DeJesus, G., and Bizzozero, O. A. (2002) Effect of 2-fluoropalmitate, cerulenin and tunicamycin on the palmitoylation and intracellular translocation of myelin proteolipid protein. Neurochem Res 27(12):1669-75.
Delhaize, E., Gruber, B. D., Pittman, J. K., White, R. G., Leung, H., Miao, Y., Jiang, L., Ryan, P. R., and Richardson, A. E. (2007) A role for the AtMTP11 gene of Arabidopsis in manganese transport and tolerance. Plant J. 51(2):198-210.
Dell'Angelica, E. C., Puertollano, R., Mullins, C., Aguilar, R. C., Vargas, J. D., Hartnell, L. M., and Bonifacino, J. S. (2000) GGAs: A family of ADP ribosylation factor-binding proteins related to adaptors and associated with the Golgi complex. J. Cell Biol. 149(1):81-93.
Denecke, J., Goldman, M., Demolder, J., Seurinck, J., and Botterman, J. (1991) The Tobacco Luminal Binding Protein Is Encoded by a Multigene Family. Plant Cell 3(9):1025-1035.
Derksen, J., Rutten, T., Lichtscheidl, I. K., de Win, A. H. N., Pierson, E. S., and Rongen, G. (1995) Quantitative analysis of the distribution of organelles in tobacco pollen tubes: implications for exocytosis and endocytosis. Protopl. 188(3):267-276.
Dettmer, J., Hong-Hermesdorf, A., Stierhof, Y. D., and Schumacher, K. (2006) Vacuolar H+-ATPase activity is required for endocytic and secretory trafficking in Arabidopsis. Plant Cell 18(3):715-730.
Dettmer, J., Schubert, D., Calvo-Weimar, O., Stierhof, Y. D., Schmidt, R., and Schumacher, K. (2005) Essential role of the V-ATPase in male gametophyte development. Plant J. 41(1):117-24.
Dhonukshe, P., Aniento, F., Hwang, I., Robinson, D. G., Mravec, J., Stierhof, Y. D., and Friml, J. (2007) Clathrin-Mediated Constitutive Endocytosis of PIN Auxin Efflux Carriers in Arabidopsis. Curr Biol.
Di Sansebastiano, G. P., Paris, N., Marc-Martin, S., and Neuhaus, J.-M. (1998) Specific

accumulation of GFP in a non-acidic vacuolar compartment via a C-terminal propeptide-mediated sorting pathway. Plant J. 15(4):449-457.
Di Sansebastiano, G. P., Paris, N., Marc-Martin, S., and Neuhaus, J.-M. (2001) Regeneration of a lytic central vacuole and of neutral peripheral vacuoles can be visualized by green fluorescent proteins targeted to either type of vacuoles. Plant Physiol. 126(1):78-86.
Dietrich, L. E., and Ungermann, C. (2004) On the mechanism of protein palmitoylation. EMBO Rep 5(11):1053-7.
Dighe, S. A., and Kozminski, K. G. (2008) Swf1p, a member of the DHHC-CRD family of palmitoyltransferases, regulates the actin cytoskeleton and polarized secretion independently of its DHHC motif. Mol Biol Cell 19(10):4454-68.
Dixon, N., Pali, T., Kee, T. P., Ball, S., Harrison, M. A., Findlay, J. B., Nyman, J., Vaananen, K., Finbow, M. E., and Marsh, D. (2008) Interaction of spin-labeled inhibitors of the vacuolar H+-ATPase with the transmembrane Vo-sector. Biophys J 94(2):506-14.
Dombrovski, J. E., Schroeder, M. R., Bednarek, S. Y., and Raikhel, N. V. (1993) Determination of the functional elements within the vacuolar targeting signal of barley lectin. Plant Cell 5:587-596.
Dombrowski, J. E., Schroeder, M. R., Bednarek, S. Y., and Raikhel, N. V. (1993) Determination of the functional elements within the vacuolar targeting signal of barley lectin. Plant Cell 5(5):587-96.
Donohoe, B. S., Kang, B.-H., and Staehelin, L. A. (2007) Identification and characterization of COPIa- and COPIb-type vesicle classes associated with plant and algal Golgi. Proc. Natl. Acad. Sci. USA 104(1):163-168.
Driouich, A., Zhang, G. F., and Staehelin, L. A. (1993) Effect of Brefeldin A on the Structure of the Golgi Apparatus and on the Synthesis and Secretion of Proteins and Polysaccharides in Sycamore Maple (Acer pseudoplatanus) Suspension-Cultured Cells. Plant Physiol. 101(4):1363-1373.
Drisdel, R. C., Alexander, J. K., Sayeed, A., and Green, W. N. (2006) Assays of protein palmitoylation. Methods 40(2):127-134.
Drisdel, R. C., and Green, W. N. (2004) Labeling and quantifying sites of protein palmitoylation. Biotechniques 36(2):276-85.
Drisdel, R. C., Manzana, E., and Green, W. N. (2004) The role of palmitoylation in functional expression of nicotinic alpha7 receptors. J Neurosci 24(46):10502-10.
Drose, S., and Altendorf, K. (1997) Bafilomycins and concanamycins as inhibitors of V-ATPases and P-ATPases. J Exp Biol 200(Pt 1):1-8.
Duman, J. G., Tyagarajan, K., Kolsi, M. S., Moore, H. P., and Forte, J. G. (1999) Expression of rab11a N124I in gastric parietal cells inhibits stimulatory recruitment of the H+-K+-ATPase. Am J Physiol 277(3 Pt 1):C361-72.
Duncan, J. A., and Gilman, A. G. (1996) Autoacylation of G protein alpha subunits. J. Biol. Chem. 271(38):23594-600.
Duncan, J. A., and Gilman, A. G. (1998) A cytoplasmic acyl-protein thioesterase that removes palmitate from G protein alpha subunits and p21(RAS). J. Biol. Chem. 273(25):15830-7.
Duncan, J. A., and Gilman, A. G. (2002) Characterization of Saccharomyces cerevisiae acyl-protein thioesterase 1, the enzyme responsible for G protein alpha subunit deacylation in vivo. J. Biol. Chem. 277(35):31740-52.
Eisenhaber, B., Wildpaner, M., Schultz, C. J., Borner, G. H. H., Dupree, P., and Eisenhaber, F. (2003) Glycosylphosphatidylinositol Lipid Anchoring of Plant Proteins. Sensitive Prediction from Sequence- and Genome-Wide Studies for Arabidopsis and Rice. Plant Physiol. 133(4):1691-1701.
Eizirik, D. L., Cardozo, A. K., and Cnop, M. (2008) The role for endoplasmic reticulum stress in diabetes mellitus. Endocr Rev 29(1):42-61.
El-Husseini, A. E.-D., Schnell, E., Dakoji, S., Sweeney, N., Zhou, Q., Prange, O., Gauthier-

Campbell, C., Aguilera-Moreno, A., Nicoll, R. A., and Bredt, D. S. (2002) Synaptic Strength Regulated by Palmitate Cycling on PSD-95. 108(6):849-863.
Ellis, R. J. (1997) Molecular chaperones: avoiding the crowd. Curr. Biol. 7:R531-R533.
Englund, P. T. (1993) The structure and biosynthesis of glycosyl phosphatidylinositol protein anchors. Annu Rev Biochem 62:121-38.
Erickson, H. P. (1997) Stretching Single Protein Molecules: Titin is a Weird Spring. Science 276:1090-1092.
Essen, L. O., Perisic, O., Cheung, R., Katan, M., and Williams, R. L. (1996) Crystal structure of a mammalian phosphoinositide-specific phospholipase C delta. Nature 380(6575):595-602.
Faergeman, N. J., and Knudsen, J. (1997) Role of long-chain fatty acyl-CoA esters in the regulation of metabolism and in cell signalling. Biochemical J. 323 (Pt 1):1-12.
Farazi, T. A., Waksman, G., and Gordon, J. I. (2001) Structures of Saccharomyces cerevisiae N-myristoyltransferase with bound myristoylCoA and peptide provide insights about substrate recognition and catalysis. Biochem. 40(21):6335-43.
Fedorov, A. N., and Baldwin, T. O. (1997) Cotranslational protein folding. J. Biol. Chem. 272(52):32715-8.
Feng, Y., and Davis, N. G. (2000) Akr1p and the type I casein kinases act prior to the ubiquitination step of yeast endocytosis: Akr1p is required for kinase localization to the plasma membrane. Mol. Cell. Biol. 20(14):5350-9.
Finka, A., Schaefer, D. G., Saidi, Y., Goloubinoff, P., and Zryd, J. P. (2007) In vivo visualization of F-actin structures during the development of the moss Physcomitrella patens. New Phytol 174(1):63-76.
Fluckiger, R., De Caroli, M., Piro, G., Dalessandro, G., Neuhaus, J. M., and Di Sansebastiano, G. P. (2003) Vacuolar system distribution in Arabidopsis tissues, visualized using GFP fusion proteins. J Exp Bot 54(387):1577-84.
Franco, M., Chardin, P., Chabre, M., and Paris, S. (1995) Myristoylation of ADP-ribosylation factor 1 facilitates nucleotide exchange at physiological Mg2+ levels. J. Biol. Chem. 270(3):1337-41.
Freemont, P. S. (2000) RING for destruction? Curr Biol 10(2):R84-7.
Frigerio, L., De Virgilio, M., Prada, A., Faoro, F., and Vitale, A. (1998) Sorting of phaseolin to the vacuole is saturable and requires a short C-terminal peptide. Plant Cell 10(6):1031-1042.
Frigerio, L., Foresti, O., Hernández Felipe, D., Paris, N., Neuhaus, J.-M., and Vitale, A. (2001) The C-terminal tetrapeptide of phaseolin is sufficient to target green fluorescent protein to the vacuole. J. Plant Physiol. 158:499-503.
Fu, Y., Wu, G., and Yang, Z. (2001) Rop GTPase-dependent dynamics of tip-localized F-actin controls tip growth in pollen tubes. J. Cell Biol. 152(5):1019-32.
Fukasawa, T., Hara-Nishimura, I., and Nishimura, M. (1988) Biosynthesis, Intracellular Transport and In Vitro Processing of 11S Globulin Precursor Proteins of Developing Castor Bean Endosperm. Plant Cell Physiol. 29(2):339-345.
Fukata, Y., and Fukata, M. (2010) Protein palmitoylation in neuronal development and synaptic plasticity. Nat Rev Neurosci 11(3):161-175.
Fullekrug, J., and Simons, K. (2004) Lipid rafts and apical membrane traffic. Ann N Y Acad Sci 1014:164-9.
Gagliardi, S., Nadler, G., Consolandi, E., Parini, C., Morvan, M., Legave, M. N., Belfiore, P., Zocchetti, A., Clarke, G. D., James, I., Nambi, P., Gowen, M., and Farina, C. (1998) 5-(5,6-Dichloro-2-indolyl)-2-methoxy-2,4-pentadienamides: novel and selective inhibitors of the vacuolar H+-ATPase of osteoclasts with bone antiresorptive activity. J Med Chem 41(10):1568-73.
Gazit, A., Osherov, N., Posner, I., Bar-Sinai, A., Gilon, C., and Levitzki, A. (1993)

Tyrphostins. 3. Structure-activity relationship studies of alpha-substituted benzylidenemalononitrile 5-S-aryltyrphostins. J Med Chem 36(23):3556-64.
Gazit, A., Yaish, P., Gilon, C., and Levitzki, A. (1989) Tyrphostins I: synthesis and biological activity of protein tyrosine kinase inhibitors. J Med Chem 32(10):2344-52.
Geldner, N. (2004) The plant endosomal system-its structure and role in signal transduction and plant development. Planta.
Geldner, N., Anders, N., Wolters, H., Keicher, J., Kornberger, W., Müller, P., Delbarre, A., Ueda, T., Nakano, A., and Jürgens, G. (2003) The Arabidopsis GNOM ARF-GEF mediates endosomal recycling, auxin transport, and auxin-dependent plant growth. Cell 112(2):219-30.
Geldner, N., Dénervaud-Tendon, V., Hyman, D. L., Mayer, U., Stierhof, Y.-D., and Chory, J. (2009) Rapid, combinatorial analysis of membrane compartments in intact plants with a multicolor marker set. Plant J. 59(1):169-178.
Geldner, N., Friml, J., Stierhof, Y. D., Jürgens, G., and Palme, K. (2001) Auxin transport inhibitors block PIN1 cycling and vesicle trafficking. Nature 413(6854):425-8.
Geldner, N., Hyman, D. L., Wang, X., Schumacher, K., and Chory, J. (2007) Endosomal signaling of plant steroid receptor kinase BRI1. Genes Dev 21(13):1598-602.
Gething, M. J. (1997) Protein folding. The difference with prokaryotes [news; comment]. Nature 388(6640):329, 331.
Ghosh, P., Dahms, N. M., and Kornfeld, S. (2003a) Mannose 6-phosphate receptors: New twists in the tale. Nature Rev. Mol. Cell Biol. 4(3):202-212.
Ghosh, P., Griffith, J., Geuze, H. J., and Kornfeld, S. (2003b) Mammalian GGAs act together to sort mannose 6-phosphate receptors. J. Cell Biol. 163(4):755-766.
Ghosh, P., and Kornfeld, S. (2003) AP-1 binding to sorting signals and release from clathrin-coated vesicles is regulated by phosphorylation. J. Cell Biol. 160(5):699-708.
Ghosh, R. N., Mallet, W. G., Soe, T. T., McGraw, T. E., and Maxfield, F. R. (1998) An endocytosed TGN38 chimeric protein is delivered to the TGN after trafficking through the endocytic recycling compartment in CHO cells. J. Cell Biol. 142(4):923-36.
Gibson, M. C., and Perrimon, N. (2003) Apicobasal polarization: epithelial form and function. Curr Opin Cell Biol 15(6):747-52.
Glickman, M. H., and Ciechanover, A. (2002) The ubiquitin-proteasome proteolytic pathway: destruction for the sake of construction. Physiol Rev 82(2):373-428.
Glomset, J. A., Gelb, M. H., and Farnsworth, C. C. (1990) Prenyl proteins in eukaryotic cells: a new type of membrane anchor. Trends Biochem. Sci. 15(4):139-42.
Gniadek, T. J., and Warren, G. (2007) WatershedCounting3D: A New Method for Segmenting and Counting Punctate Structures from Confocal Image Data. Traffic 8(4):339-346.
Goud, B., Salminen, A., Walworth, N. C., and Novick, P. J. (1988) A GTP-binding protein required for secretion rapidly associates with secretory vesicles and the plasma membrane in yeast. Cell 53(5):753-68.
Greaves, J., and Chamberlain, L. H. (2007) Palmitoylation-dependent protein sorting. J. Cell Biol.
Grebe, M., Friml, J., Swarup, R., Ljung, K., Sandberg, G., Terlou, M., Palme, K., Bennett, M. J., and Scheres, B. (2002) Cell polarity signaling in Arabidopsis involves a BFA-sensitive auxin influx pathway. Curr Biol 12(4):329-34.
Grebe, M., Xu, J., Mobius, W., Ueda, T., Nakano, A., Geuze, H. J., Rook, M. B., and Scheres, B. (2003) Arabidopsis sterol endocytosis involves actin-mediated trafficking via ARA6-positive early endosomes. Curr Biol 13(16):1378-87.
Greenwood, J. S., and Chrispeels, M. J. (1985) Correct targeting of the bean storage protein phaseolin in the seeds of transformed tobacco. Plant Physiol. 79:65-71.
Gu, Y., Fu, Y., Dowd, P., Li, S., Vernoud, V., Gilroy, S., and Yang, Z. (2005) A Rho family

GTPase controls actin dynamics and tip growth via two counteracting downstream pathways in pollen tubes. The Journal of Cell Biology 169(1):127-138.
Gu, Y., Wang, Z., and Yang, Z. (2004) ROP/RAC GTPase: an old new master regulator for plant signaling. Curr. Opin. Plant Biol. 7(5):527-536.
Gwiazda, K. S., Yang, T. L., Lin, Y., and Johnson, J. D. (2009) Effects of palmitate on ER and cytosolic Ca2+ homeostasis in beta-cells. Am J Physiol Endocrinol Metab 296(4):E690-701.
Haas, T. J., Sliwinski, M. K., Martinez, D. E., Preuss, M., Ebine, K., Ueda, T., Nielsen, E., Odorizzi, G., and Otegui, M. S. (2007) The Arabidopsis AAA ATPase SKD1 Is Involved in Multivesicular Endosome Function and Interacts with Its Positive Regulator LYST-INTERACTING PROTEIN5. Plant Cell 19 1295-1312.
Haass, C., and Selkoe, D. J. (2007a) Soluble protein oligomers in neurodegeneration: lessons from the Alzheimer's amyloid [beta]-peptide. Nat Rev Mol Cell Biol 8(2):101-112.
Haass, C., and Selkoe, D. J. (2007b) Soluble protein oligomers in neurodegeneration: lessons from the Alzheimer's amyloid beta-peptide. Nat Rev Mol Cell Biol 8(2):101-12.
Hadlington, J. L., and Denecke, J. (2000) Sorting of soluble proteins in the secretory pathway of plants. Curr Opin Plant Biol 3(6):461-8.
Haft, C. R., de la Luz Sierra, M., Barr, V. A., Haft, D. H., and Taylor, S. I. (1998) Identification of a family of sorting nexin molecules and characterization of their association with receptors. Mol. Cell. Biol. 18(12):7278-87.
Haft, C. R., Sierra, M. L., Bafford, R., Lesniak, M. A., Barr, V. A., and Taylor, S. I. (2000) Human orthologs of yeast vacuolar protein sorting proteins vps26, 29, and 35: assembly into multimeric complexes. Mol Biol Cell 11(12):4105-16.
Hamman, B. D., Hendershot, L. M., and Johnson, A. E. (1998) BiP maintains the permeability barrier of the ER membrane by sealing the lumenal end of the translocon pore before and early in translocation. Cell 92(6):747-58.
Happel, N., Höning, S., Neuhaus, J.-M., Paris, N., Robinson, D. G., and Holstein, S. E. (2004) Arabidopsis mu A-adaptin interacts with the tyrosine motif of the vacuolar sorting receptor VSR-PS1. Plant J. 37(5):678-93.
Hara-Nishimura, I., Inoue, K., and Nishimura, M. (1991) A unique vacuolar processing enzyme responsible for conversion of several proprotein precursors into the mature forms. FEBS Letters 294(1-2):89-93.
Hara-Nishimura, I., Nishimura, M., and Akazawa, T. (1985) Biosynthesis and Intracellular Transport of 11S Globulin in Developing Pumpkin Cotyledons. Plant Physiol. 77(3):747-752.
Hara-Nishimura, I., Shimada, T., Hatano, K., Takeuchi, Y., and Nishimura, M. (1998) Transport of Storage Proteins to Protein Storage Vacuoles Is Mediated by Large Precursor-Accumulating Vesicles. Plant Cell 10(5):825-836.
Hemsley, P., Taylor, L., and Grierson, C. (2008) Assaying protein palmitoylation in plants. Plant Methods 4(1):2.
Hemsley, P. A. (2009) Protein S-acylation in plants (Review). Mol Membr Biol 26(1):114-25.
Hemsley, P. A., and Grierson, C. S. (2008) Multiple roles for protein palmitoylation in plants. Trends Plant Sci 13(6):295-302.
Hemsley, P. A., Kemp, A. C., and Grierson, C. S. (2005) The TIP GROWTH DEFECTIVE1 S-acyl transferase regulates plant cell growth in Arabidopsis. Plant Cell 17(9):2554-63.
Hess, D. T., Slater, T. M., Wilson, M. C., and Skene, J. H. (1992) The 25 kDa synaptosomal-associated protein SNAP-25 is the major methionine-rich polypeptide in rapid axonal transport and a major substrate for palmitoylation in adult CNS. J Neurosci 12(12):4634-41.
Higgins, C. F. (1992) ABC transporters: from microorganisms to man. Annu Rev Cell Biol 8:67-113.
Higgins, T. J. V., Chandler, P. M., Randall, P. J., Spencer, D., Beach, L. R., Blagrove, R. J.,

Kortt, A. A., and Inglis, A. S. (1986) Gene Structure, Protein Structure, and Regulation of the Synthesis of a Sulfur-rich Protein in Pea Seeds*. J. Biol. Chem. 261:11124-111130.
Hillmer, S., Movafeghi, A., Robinson, D. G., and Hinz, G. (2001) Vacuolar storage proteins are sorted in the cis-cisternae of the pea cotyledon Golgi apparatus. J. Cell Biol. 152:41-50.
Hinz, G., Colanesi, S., Hillmer, S., Rogers, J. C., and Robinson, D. G. (2007) Localization of vacuolar transport receptors and cargo proteins in the Golgi apparatus of developing Arabidopsis embryos. Traffic 8(10):1452-64.
Hinz, G., Hillmer, S., Bäumer, M., and Hohl, I. (1999) Vacuolar storage proteins and the putative vacuolar sorting receptor BP-80 exit the Golgi apparatus of developing pea cotyledons in different transport vesicles. Plant Cell 11:1509-1524.
Hinz, G., Menze, A., Hohl, I., and Vaux, D. (1997) Isolation of prolegumin from developing pea seeds - its binding to endomembranes and assembly into prolegumin hexamers in the protein storage vacuole. J. Exp. Bot. 48(306):139-149.
Hirst, J., Futter, C. E., and Hopkins, C. R. (1998a) The kinetics of mannose 6-phosphate receptor trafficking in the endocytic pathway in hep-2 cells - the receptor enters and rapidly leaves multivesicular endosomes without accumulating in a prelysosomal compartment. Mol. Biol. Cell 9(4):809-816.
Hirst, J., Futter, C. E., and Hopkins, C. R. (1998b) The kinetics of mannose 6-phosphate receptor trafficking in the endocytic pathway in HEp-2 cells: the receptor enters and rapidly leaves multivesicular endosomes without accumulating in a prelysosomal compartment. Mol Biol Cell 9(4):809-16.
Hirst, J., Lui, W. W., Bright, N. A., Totty, N., Seaman, M. N., and Robinson, M. S. (2000) A family of proteins with gamma-adaptin and VHS domains that facilitate trafficking between the trans-Golgi network and the vacuole/lysosome. J. Cell Biol. 149(1):67-80.
Hiwatashi, Y., Obara, M., Sato, Y., Fujita, T., Murata, T., and Hasebe, M. (2008) Kinesins are indispensable for interdigitation of phragmoplast microtubules in the moss Physcomitrella patens. Plant Cell 20(11):3094-106.
Hohl, I., Robinson, D. G., Chrispeels, M. J., and Hinz, G. (1996) Transport of storage proteins to the vacuole is mediated by vesicles without a clathrin coat. J. Cell Sci. 109(Part 10):2539-2550.
Holen, I., Stromhaug, P. E., Gordon, P. B., Fengsrud, M., Berg, T. O., and Seglen, P. O. (1995) Inhibition of autophagy and multiple steps in asialoglycoprotein endocytosis by inhibitors of tyrosine protein kinases (tyrphostins). J. Biol. Chem. 270(21):12823-31.
Holwerda, B. C., Galvin, N. J., Baranski, T. J., and Rogers, J. C. (1990) In Vitro Processing of Aleurain, a Barley Vacuolar Thiol Protease. Plant Cell 2(11):1091-1106.
Holwerda, B. C., Padgett, H. S., and Rogers, J. C. (1992) Proaleurain vacuolar targeting is mediated by short contiguous peptide interactions. Plant Cell 4(3):307-318.
Hou, H., John Peter, A. T., Meiringer, C., Subramanian, K., and Ungermann, C. (2009) Analysis of DHHC acyltransferases implies overlapping substrate specificity and a two-step reaction mechanism. Traffic 10(8):1061-73.
Huang, K., Yanai, A., Kang, R., Arstikaitis, P., Singaraja, R. R., Metzler, M., Mullard, A., Haigh, B., Gauthier-Campbell, C., Gutekunst, C. A., Hayden, M. R., and El-Husseini, A. (2004) Huntingtin-interacting protein HIP14 is a palmitoyl transferase involved in palmitoylation and trafficking of multiple neuronal proteins. Neuron 44(6):977-86.
Huang, K. M., D'Hondt, K., Riezman, H., and Lemmon, S. K. (1999) Clathrin functions in the absence of heterotetrameric adaptors and AP180-related proteins in yeast. EMBO J. 18(14):3897-908.
Huber, L. A., de Hoop, M. J., Dupree, P., Zerial, M., Simons, K., and Dotti, C. (1993) Protein transport to the dendritic plasma membrane of cultured neurons is regulated by rab8p. The Journal of Cell Biology 123(1):47-55.
Hunter, P. R., Craddock, C. P., Di Benedetto, S., Roberts, L. M., and Frigerio, L. (2007)

Fluorescent Reporter Proteins for the Tonoplast and the Vacuolar Lumen Identify a Single Vacuolar Compartment in Arabidopsis Cells. Plant Physiol.:pp.107.103945.
Hurtley, S. M., and Helenius, A. (1989) Protein oligomerization in the endoplasmic reticulum. Annu Rev Cell Biol 5:277-307.
Huss, M., Sasse, F., Kunze, B., Jansen, R., Steinmetz, H., Ingenhorst, G., Zeeck, A., and Wieczorek, H. (2005) Archazolid and apicularen: novel specific V-ATPase inhibitors. BMC Biochem 6:13.
Huss, M., and Wieczorek, H. (2009) Inhibitors of V-ATPases: old and new players. J Exp Biol 212(Pt 3):341-6.
Hwang, J. U., Wu, G., Yan, A., Lee, Y. J., Grierson, C. S., and Yang, Z. (2010) Pollen-tube tip growth requires a balance of lateral propagation and global inhibition of Rho-family GTPase activity. J. Cell Sci. 123(Pt 3):340-50.
Inaba, T., Nagano, Y., Nagasaki, T., and Sasaki, Y. (2002) Distinct localization of two closely related Ypt3/Rab11 proteins on the trafficking pathway in higher plants. J. Biol. Chem. 277(11):9183-8.
Ishikawa, F., Suga, S., Uemura, T., Sato, M. H., and Maeshima, M. (2005) Novel type aquaporin SIPs are mainly localized to the ER membrane and show cell-specific expression in Arabidopsis thaliana. FEBS Lett. 579(25):5814-20.
Jackson, C. L., and Casanova, J. E. (2000) Turning on ARF: the Sec7 family of guanine-nucleotide-exchange factors. Trends Cell Biol 10(2):60-7.
Jackson, P. K., Eldridge, A. G., Freed, E., Furstenthal, L., Hsu, J. Y., Kaiser, B. K., and Reimann, J. D. (2000) The lore of the RINGs: substrate recognition and catalysis by ubiquitin ligases. Trends Cell Biol 10(10):429-39.
Jackson, R. C., and Blobel, G. (1980) Post-translational processing of full-length presecretory proteins with canine pancreatic signal peptidase. Ann N Y Acad Sci 343:391-404.
Jaffe, A. B., and Hall, A. (2005) Rho GTPases: biochemistry and biology. Annu Rev Cell Dev Biol 21:247-69.
Jaillais, Y., Fobis-Loisy, I., Miege, C., and Gaude, T. (2008) Evidence for a sorting endosome in Arabidopsis root cells. Plant J. 53(2):237-247.
Jaillais, Y., Fobis-Loisy, I., Miege, C., Rollin, C., and Gaude, T. (2006) AtSNX1 defines an endosome for auxin-carrier trafficking in Arabidopsis. Nature.
Jaillais, Y., Santambrogio, M., Rozier, F., Fobis-Loisy, I., Miege, C., and Gaude, T. (2007) The Retromer Protein VPS29 Links Cell Polarity and Organ Initiation in Plants. Cell 130(6):1057-1070.
Jakobs, S. (2006) High resolution imaging of live mitochondria. Biochimica et Biophysica Acta (BBA) - Molecular Cell Research 1763(5-6):561-575.
Jiang, L., Phillips, T. E., Rogers, S. W., and Rogers, J. C. (2000) Biogenesis of the protein storage vacuole crystalloid. J. Cell Biol. 150(4):755-770.
Joazeiro, C. A. P., and Weissman, A. M. (2000) RING Finger Proteins: Mediators of Ubiquitin Ligase Activity. Cell 102:549-552.
Joazeiro, C. A. P., Wing, S. S., Huang, H.-k., Leverson, J. D., Hunter, T., and Liu, Y.-C. (1999) The Tyrosine Kinase Negative Regulator c-Cbl as a RING-Type, E2-Dependent Ubiquitin-Protein Ligase. Science 286(5438):309-312.
Johansen, J. N., Chow, C.-M., Moore, I., and Hawes, C. (2009) AtRAB-H1b and AtRAB-H1c GTPases, homologues of the yeast Ypt6, target reporter proteins to the Golgi when expressed in Nicotiana tabacum and Arabidopsis thaliana. J. Exp. Bot. 60(11):3179-3193.
Johanson, U., Karlsson, M., Johansson, I., Gustavsson, S., Sjövall, S., Fraysse, L., A., W., and Kjelbom, P. (2001) The Complete Set of Genes Encoding Major Intrinsic Proteins in Arabidopsis Provides a Fremework for a New Nomenclature for Major Intrinsic Proteins in Plants. Plant Physiol. 126:1358-1369.
Johnson, D. R., Bhatnagar, R. S., Knoll, L. J., and Gordon, J. I. (1994) Genetic and

biochemical studies of protein N-myristoylation. Annu Rev Biochem 63:869-914.
Johnson, K. D., Herman, E. M., and Chrispeels, M. J. (1989) An abundant, highly conserved tonoplast protein in seeds. Plant Physiol. 91(3):1006-1013.
Joseph, M., and Nagaraj, R. (1995) Interaction of peptides corresponding to fatty acylation sites in proteins with model membranes. J. Biol. Chem. 270(28):16749-55.
Jürgens, G. (2004) Membrane trafficking in plants. Annu Rev Cell Dev Biol 20:481-504.
Jürgens, G. (2005) Cytokinesis in higher plants. Annu Rev Plant Biol 56:281-99.
Kahn, R. A., Der, C. J., and Bokoch, G. M. (1992) The ras superfamily of GTP-binding proteins: guidelines on nomenclature. FASEB J 6(8):2512-3.
Kandasamy, S. K., and Larson, R. G. (2006) Molecular dynamics simulations of model trans-membrane peptides in lipid bilayers: a systematic investigation of hydrophobic mismatch. Biophys J 90(7):2326-43.
Kang, B.-H., Nielsen, E., Preuss, M. L., Mastronarde, D., and Staehelin, L. A. (2011) Electron Tomography of RabA4b- and PI-4Kβ1-Labeled Trans Golgi Network Compartments in Arabidopsis. Traffic 12(3):313-329.
Kang, R., Wan, J., Arstikaitis, P., Takahashi, H., Huang, K., Bailey, A. O., Thompson, J. X., Roth, A. F., Drisdel, R. C., Mastro, R., Green, W. N., Yates Iii, J. R., Davis, N. G., and El-Husseini, A. (2008a) Neural palmitoyl-proteomics reveals dynamic synaptic palmitoylation. Nature 456(7224):904-909.
Kang, R., Wan, J., Arstikaitis, P., Takahashi, H., Huang, K., Bailey, A. O., Thompson, J. X., Roth, A. F., Drisdel, R. C., Mastro, R., Green, W. N., Yates, J. R., 3rd, Davis, N. G., and El-Husseini, A. (2008b) Neural palmitoyl-proteomics reveals dynamic synaptic palmitoylation. Nature 456(7224):904-9.
Karaskov, E., Scott, C., Zhang, L., Teodoro, T., Ravazzola, M., and Volchuk, A. (2006) Chronic palmitate but not oleate exposure induces endoplasmic reticulum stress, which may contribute to INS-1 pancreatic beta-cell apoptosis. Endocrinology 147(7):3398-407.
Kato, N., He, H., and Steger, A. P. (2010) A Systems Model of Vesicle Trafficking in Arabidopsis Pollen Tubes. Plant Physiol. 152(2):590-601.
Keen, J. H. (1990) Clathrin and associated assembly and disassembly proteins. Annu Rev Biochem 59:415-38.
Keller, C. A., Yuan, X., Panzanelli, P., Martin, M. L., Alldred, M., Sassoe-Pognetto, M., and Luscher, B. (2004) The gamma2 subunit of GABA(A) receptors is a substrate for palmitoylation by GODZ. J Neurosci 24(26):5881-91.
Keller, P., and Simons, K. (1997) Post-Golgi biosynthetic trafficking. J. Cell Sci. 110(24):3001-3009.
Kim, H., Kang, H., Jang, M., Chang, J. H., Miao, Y., Jiang, L., and Hwang, I. (2010) Homomeric Interaction of AtVSR1 Is Essential for Its Function as a Vacuolar Sorting Receptor. Plant Physiol. 154(1):134-148.
Kim, J. W., Shin-Ya, K., Furihata, K., Hayakawa, Y., and Seto, H. (1999) Oximidines I and II: Novel Antitumor Macrolides from Pseudomonas sp. J Org Chem 64(1):153-155.
Kirchhausen, T., Harrison, S. C., and Heuser, J. (1986) Configuration of clathrin trimers: evidence from electron microscopy. J Ultrastruct Mol Struct Res 94(3):199-208.
Kirsch, T., Paris, N., Butler, J. M., Beevers, L., and Rogers, J. C. (1994) Purification and initial characterization of a potential plant vacuolar targeting receptor. Proc Natl Acad Sci U S A 91(8):3403-7.
Kirsch, T., Saalbach, G., Raikhel, N. V., and Beevers, L. (1996) Interaction of a potential vacuolar targeting receptor with amino- and carboxyl-terminal targeting determinants. Plant Physiol. 111(2):469-474.
Kjellbom, P., Larsson, C., Johansson, I. I., Karlsson, M., and Johanson, U. (1999) Aquaporins and water homeostasis in plants. Trends Plant Sci 4(8):308-314.
Kleine-Vehn, J., Leitner, J., Zwiewka, M., Sauer, M., Abas, L., Luschnig, C., and Friml, J.

(2008) Differential degradation of PIN2 auxin efflux carrier by retromer-dependent vacuolar targeting. Proc. Natl. Acad. Sci. USA 105(46):17812-17817.
Knight, Z. A., Gonzalez, B., Feldman, M. E., Zunder, E. R., Goldenberg, D. D., Williams, O., Loewith, R., Stokoe, D., Balla, A., Toth, B., Balla, T., Weiss, W. A., Williams, R. L., and Shokat, K. M. (2006) A pharmacological map of the PI3-K family defines a role for p110alpha in insulin signaling. Cell 125(4):733-47.
Knight, Z. A., and Shokat, K. M. (2007) Chemically targeting the PI3K family. Biochem Soc Trans 35(Pt 2):245-9.
Koide, Y., Hirano, H., Matsuoka, K., and Nakamura, K. (1997) The N-terminal propeptide of the precursor to sporamin acts as a vacuole-targeting signal even at the C terminus of the mature part in tobacco cells. Plant Physiol. 114(3):863-70.
Kornfeld, S. (1992) Structure and function of the mannose 6-phosphate/insulinlike growth factor II receptors. Annu Rev Biochem 61:307-30.
Kost, B., Spielhofer, P., and Chua, N. H. (1998) A GFP-mouse talin fusion protein labels plant actin filaments in vivo and visualizes the actin cytoskeleton in growing pollen tubes. Plant J. 16(3):393-401.
Kovalenko, M., Gazit, A., Bohmer, A., Rorsman, C., Ronnstrand, L., Heldin, C. H., Waltenberger, J., Bohmer, F. D., and Levitzki, A. (1994) Selective platelet-derived growth factor receptor kinase blockers reverse sis-transformation. Cancer Res 54(23):6106-14.
Kunze, B., Jansen, R., Sasse, F., Hofle, G., and Reichenbach, H. (1998) Apicularens A and B, new cytostatic macrolides from Chondromyces species (myxobacteria): production, physico-chemical and biological properties. J Antibiot (Tokyo) 51(12):1075-80.
Kurten, R. C., Cadena, D. L., and Gill, G. N. (1996) Enhanced degradation of EGF receptors by a sorting nexin, SNX1. Science 272(5264):1008-10.
Lam, K. K., Davey, M., Sun, B., Roth, A. F., Davis, N. G., and Conibear, E. (2006) Palmitoylation by the DHHC protein Pfa4 regulates the ER exit of Chs3. J. Cell Biol. 174(1):19-25.
Lam, S. K., Siu, C. L., Hillmer, S., Jang, S., An, G., Robinson, D. G., and Jiang, L. (2007) Rice SCAMP1 Defines Clathrin-Coated, trans-Golgi-Located Tubular-Vesicular Structures as an Early Endosome in Tobacco BY-2 Cells. Plant Cell.
Lata, S., Schoehn, G., Jain, A., Pires, R., Piehler, J., Gottlinger, H. G., and Weissenhorn, W. (2008) Helical Structures of ESCRT-III Are Disassembled by VPS4. Science.
Lavy, M., Bracha-Drori, K., Sternberg, H., and Yalovsky, S. (2002) A cell-specific, prenylation-independent mechanism regulates targeting of type II RACs. Plant Cell 14(10):2431-50.
Lawrence, C. M., Ray, S., Babyonyshev, M., Galluser, R., Borhani, D. W., and Harrison, S. C. (1999) Crystal structure of the ectodomain of human transferrin receptor. Science 286(5440):779-82.
Laybutt, D. R., Preston, A. M., Akerfeldt, M. C., Kench, J. G., Busch, A. K., Biankin, A. V., and Biden, T. J. (2007) Endoplasmic reticulum stress contributes to beta cell apoptosis in type 2 diabetes. Diabetologia 50(4):752-63.
Lee, M. C., Miller, E. A., Goldberg, J., Orci, L., and Schekman, R. (2004) Bi-directional protein transport between the ER and Golgi. Annu Rev Cell Dev Biol 20:87-123.
Lemmon, M. A., Ferguson, K. M., and Abrams, C. S. (2002) Pleckstrin homology domains and the cytoskeleton. FEBS Lett. 513(1):71-6.
Lemmon, S. K., and Traub, L. M. (2000) Sorting in the endosomal system in yeast and animal cells. Curr Opin Cell Biol 12(4):457-66.
Levanony, H., Rubin, R., Altschuler, Y., and Galili, G. (1992) Evidence for a novel route of wheat storage proteins to vacuoles. J. Cell Biol. 119(5):1117-1128.
Levental, I., Grzybek, M., and Simons, K. (2010a) Greasing their way: lipid modifications determine protein association with membrane rafts. Biochem. 49(30):6305-16.

Levental, I., Lingwood, D., Grzybek, M., Coskun, U., and Simons, K. (2010b) Palmitoylation regulates raft affinity for the majority of integral raft proteins. Proc Natl Acad Sci U S A.
Leventis, R., Juel, G., Knudsen, J. K., and Silvius, J. R. (1997) Acyl-CoA binding proteins inhibit the nonenzymic S-acylation of cysteinyl-containing peptide sequences by long-chain acyl-CoAs. Biochem. 36(18):5546-53.
Leverson, J. D., Joazeiro, C. A. P., Page, A. M., Huang, H.-k., Hieter, P., and Hunter, T. (2000) The APC11 RING-H2 Finger Mediates E2-Dependent Ubiquitination. Mol. Biol. Cell 11(7):2315-2325.
Levitzki, A., and Mishani, E. (2006) Tyrphostins and other tyrosine kinase inhibitors. Annu Rev Biochem 75:93-109.
Li, H., Lin, Y., Heath, R. M., Zhu, M. X., and Yang, Z. (1999) Control of pollen tube tip growth by a Rop GTPase-dependent pathway that leads to tip-localized calcium influx. Plant Cell 11(9):1731-42.
Liberek, K., Lewandowska, A., and Zietkiewicz, S. (2008) Chaperones in control of protein disaggregation. EMBO J. 27(2):328-35.
Linder, M. E., and Deschenes, R. J. (2007) Palmitoylation: policing protein stability and traffic. Nat Rev Mol Cell Biol 8(1):74-84.
Lobo, S., Greentree, W. K., Linder, M. E., and Deschenes, R. J. (2002) Identification of a Ras palmitoyltransferase in Saccharomyces cerevisiae. J. Biol. Chem. 277(43):41268-73.
Luo, X., and Hofmann, K. (2001) The protease-associated domain: a homology domain associated with multiple classes of proteases. Trends Biochem. Sci. 26(3):147-8.
Lycett, G. (2008) The role of Rab GTPases in cell wall metabolism. J Exp Bot.
Maeshima, M. (1992) Characterization of the Major Integral Protein of Vacuolar Membrane. Plant Physiol. 98(4):1248-1254.
Maeshima, M., Mimura, T., and Sato, T. (1994) Distribution of vacuolar H+-pyrophosphatase and a membrane integral protein in a variety of green plants. Plant Cell Physiol 35(2):323-328.
Maeshima, M., Sasaki, T., and Asahi, T. (1985) Characterization of major proteins in sweet potato tuberous roots. Phytochemistry 24(9):1899-1902.
Mallard, F., Antony, C., Tenza, D., Salamero, J., Goud, B., and Johannes, L. (1998) Direct pathway from early/recycling endosomes to the Golgi apparatus revealed through the study of shiga toxin B-fragment transport. J. Cell Biol. 143(4):973-90.
Mallet, W. G., and Maxfield, F. R. (1999) Chimeric forms of furin and TGN38 are transported with the plasma membrane in the trans-Golgi network via distinct endosomal pathways. J. Cell Biol. 146(2):345-59.
Marc, J. (1997) Microtubule-organizing centres in plants. 2(6):223-230.
Martin, S. G., and Chang, F. (2006) Dynamics of the formin for3p in actin cable assembly. Curr Biol 16(12):1161-70.
Marty-Mazars, D., Clemencet, M. C., Dozolme, P., and Marty, F. (1995) Antibodies to the tonoplast from the storage parenchyma cells of beetroot recognize a major intrinsic protein related to TIPs. Eur J Cell Biol 66(1):106-18.
Marty, F., and Branton, D. (1980) Analytical characterization of beetroot vacuole membrane. The Journal of Cell Biology 87(1):72-83.
Mathur, J., and Hulskamp, M. (2002) Microtubules and microfilaments in cell morphogenesis in higher plants. Curr Biol 12(19):R669-76.
Matsuoka, K., Higuchi, T., Maeshima, M., and Nakamura, K. (1997) A vacuolar-type H^+-ATPase in a nonvacuolar organelle is required for the sorting of soluble vacuolar protein precursors in tobacco cells. Plant Cell 9(4):533-546.
Matsuoka, K., and Nakamura, K. (1991) Propeptide of a precursor to a plant vacuolar protein required for vacuolar targeting. Proc. Natl. Acad. Sci. USA 88(3):834-838.
Matsuoka, K., and Nakamura, K. (1992) Transport of a sweet potato storage protein,

sporamin, to the vacuole in yeast cells. Plant. Cell. Physiol. 33(4):453-462.
Maurel, C. (1997) Aquaporins and water permeability of plant membranes. Annual Review of Plant Physiology & Plant Molecular Biology 48:399-429.
Maurel, C., Reizer, J., Schroeder, J. I., and Chrispeels, M. J. (1993) The vacuolar membrane protein g-TIP creates water specific channels in Xenopus oocytes. EMBO J. 12(6):2241-2247.
Maurel, C., Verdoucq, L., Luu, D. T., and Santoni, V. (2008) Plant aquaporins: membrane channels with multiple integrated functions. Annu Rev Plant Biol 59:595-624.
Mayer, U., Ruiz, R. A. T., Berleth, T., Miseera, S., and Juurgens, G. (1991) Mutations affecting body organization in the Arabidopsis embryo. Nature 353(6343):402-407.
Mayor, S., and Riezman, H. (2004) Sorting GPI-anchored proteins. Nat Rev Mol Cell Biol 5(2):110-20.
Mayorga, L. S., and Campoy, E. M. (2010) Modeling Fusion/Fission-Dependent Intracellular Transport of Fluid Phase Markers. Traffic 11(7):1001-1015.
McElver, J., Patton, D., Rumbaugh, M., Liu, C. M., Yang, L. J., and Meinke, D. (2000) The TITAN5 gene of arabidopsis encodes a protein related to the ADP ribosylation factor family of GTP binding proteins. Plant Cell 12(8):1379-1392.
McKee, T. C., Galinis, D. L., Pannell, L. K., Cardellina, J. H., Laakso, J., Ireland, C. M., Murray, L., Capon, R. J., and Boyd, M. R. (1998) The Lobatamides, Novel Cytotoxic Macrolides from Southwestern Pacific Tunicates†. The Journal of Organic Chemistry 63(22):7805-7810.
McLaughlin, S., and Aderem, A. (1995) The myristoyl-electrostatic switch: a modulator of reversible protein-membrane interactions. Trends Biochem. Sci. 20(7):272-6.
Meinnel, T., and Giglione, C. (2008) Tools for analyzing and predicting N-terminal protein modifications. Proteomics 8(4):626-49.
Melchers, L. S., Sela-Buurlage, M. B., Vloemans, S. A., Woloshuk, C. P., van Roekel, J. S. C., Pen, J., van den Elzen, P. J. M., and Cornelissen, B. J. C. (1993) Extracellular targeting of the vacuolar tobacco proteins-AP24, chitinase and β-1,3-glucanase in transgenic plants. Plant Mol. Biol. 21(4):583-593.
Menche, D., Hassfeld, J., Steinmetz, H., Huss, M., Wieczorek, H., and Sasse, F. (2007) The first hydroxylated archazolid from the myxobacterium Cystobacter violaceus: isolation, structural elucidation and V-ATPase inhibition. J Antibiot (Tokyo) 60(5):328-31.
Meyer, U., Benghezal, M., Imhof, I., and Conzelmann, A. (2000) Active site determination of Gpi8p, a caspase-related enzyme required for glycosylphosphatidylinositol anchor addition to proteins. Biochem. 39(12):3461-71.
Miao, Y., Li, K. Y., Li, H. Y., Yao, X., and Jiang, L. (2008) The vacuolar transport of aleurain-GFP and 2S albumin-GFP fusions is mediated by the same pre-vacuolar compartments in tobacco BY-2 and Arabidopsis suspension cultured cells. Plant J. 56:824-839.
Miao, Y., Yan, P. K., Kim, H., Hwang, I., and Jiang, L. (2006) Localization of Green Fluorescent Protein Fusions with the Seven Arabidopsis Vacuolar Sorting Receptors to Prevacuolar Compartments in Tobacco BY-2 Cells. Plant Physiol. 142(3):945-962.
Miller, J. J., Summers, M. K., Hansen, D. V., Nachury, M. V., Lehman, N. L., Loktev, A., and Jackson, P. K. (2006) Emi1 stably binds and inhibits the anaphase-promoting complex/cyclosome as a pseudosubstrate inhibitor. Genes Dev 20(17):2410-20.
Miyake, S., Lupher, M. L., Druker, B., and Band, H. (1998) The tyrosine kinase regulator Cbl enhances the ubiquitination and degradation of the platelet-derived growth factor receptor α. Proc. Natl. Acad. Sci. USA 95(14):7927-7932.
Molenaar, C. M., Prange, R., and Gallwitz, D. (1988) A carboxyl-terminal cysteine residue is required for palmitic acid binding and biological activity of the ras-related yeast YPT1 protein. EMBO J. 7(4):971-6.

Moscatelli, A., Cai, G., Ciampolini, F., and Cresti, M. (1998) Dynein heavy chain-related polypeptides are associated with organelles in pollen tubes of <i>Nicotiana tabacum</i&gt. Sexual Plant Reproduction 11(1):31-40.
Moscatelli, A., Ciampolini, F., Rodighiero, S., Onelli, E., Cresti, M., Santo, N., and Idilli, A. (2007) Distinct endocytic pathways identified in tobacco pollen tubes using charged nanogold. J. Cell Sci. 120(21):3804-3819.
Moss, J., and Vaughan, M. (1998) Molecules in the ARF orbit. J. Biol. Chem. 273(34):21431-4.
Mossner, E., Iwai, H., and Glockshuber, R. (2000) Influence of the pK(a) value of the buried, active-site cysteine on the redox properties of thioredoxin-like oxidoreductases. FEBS Lett. 477(1-2):21-6.
Musch, A. (2004) Microtubule organization and function in epithelial cells. Traffic 5(1):1-9.
Nadler, G., Morvan, M., Delimoge, I., Belfiore, P., Zocchetti, A., James, I., Zembryki, D., Lee-Rycakzewski, E., Parini, C., Consolandi, E., Gagliardi, S., and Farina, C. (1998) (2Z,4E)-5-(5,6-dichloro-2-indolyl)-2-methoxy-N-(1,2,2,6,6- pentamethylpiperidin-4-yl)-2,4-pentadienamide, a novel, potent and selective inhibitor of the osteoclast V-ATPase. Bioorg Med Chem Lett 8(24):3621-6.
Nagano, Y., Okada, Y., Narita, H., Asaka, Y., and Sasaki, Y. (1995) Location of light-repressible, small GTP-binding protein of the YPT/rab family in the growing zone of etiolated pea stems. Proc Natl Acad Sci U S A 92(14):6314-8.
Nakamura, S., and Hayashi, T. (1993) Purification and properties of an extracellular Endo-1,4-beta-Glucanase from Suspension-Cultured poplar cells. Plant Cell Physiol 34(7):1009-1013.
Nakano, A., Brada, D., and Schekman, R. (1988) A membrane glycoprotein, Sec12p, required for protein transport from the endoplasmic reticulum to the Golgi apparatus in yeast. J. Cell Biol. 107(3):851-63.
Nakata, T., Terada, S., and Hirokawa, N. (1998) Visualization of the dynamics of synaptic vesicle and plasma membrane proteins in living axons. J. Cell Biol. 140(3):659-74.
Nalivaeva, N. N., and Turner, A. J. (2001) Post-translational modifications of proteins: acetylcholinesterase as a model system. Proteomics 1(6):735-47.
Nebenfuhr, A., Ritzenthaler, C., and Robinson, D. G. (2002) Brefeldin A: deciphering an enigmatic inhibitor of secretion. Plant Physiol. 130(3):1102-8.
Neuhaus, J.-M., and Paris, N.
2005 Plant vacuoles. from biogenesis to function. *In* Plant Endocytosis. Samaj, J., Baluska, F., and Menzel, D., eds. Pp. 63-82. Plant Cell Monograph.
Neuhaus, J. M., and Rogers, J. C. (1998) Sorting of proteins to vacuoles in plant cells. Plant Mol. Biol. 38(1-2):127-44.
Neuhaus, J. M., Sticher, L., Meins, F., and Boller, T. (1991) A short C-terminal sequence is necessary and sufficient for the targeting of chitinases to the plant vacuole. Proc. Natl. Acad. Sci. USA 88(22):10362-10366.
Niemes, S., Labs, M., Scheuring, D., Krueger, F., Langhans, M., Jesenofsky, B., Robinson, D. G., and Pimpl, P. (2010a) Sorting of plant vacuolar proteins is initiated in the ER. Plant J. 62(4):601-14.
Niemes, S., Langhans, M., Viotti, C., Scheuring, D., San Wan Yan, M., Jiang, L., Hillmer, S., Robinson, D. G., and Pimpl, P. (2010b) Retromer recycles vacuolar sorting receptors from the trans-Golgi network. Plant J. 61(1):107-21.
Noritake, J., Fukata, Y., Iwanaga, T., Hosomi, N., Tsutsumi, R., Matsuda, N., Tani, H., Iwanari, H., Mochizuki, Y., Kodama, T., Matsuura, Y., Bredt, D. S., Hamakubo, T., and Fukata, M. (2009) Mobile DHHC palmitoylating enzyme mediates activity-sensitive synaptic targeting of PSD-95. J. Cell Biol. 186(1):147-60.
Nothwehr, S. F., Ha, S. A., and Bruinsma, P. (2000) Sorting of yeast membrane proteins into

an endosome-to-Golgi pathway involves direct interaction of their cytosolic domains with Vps35p. J. Cell Biol. 151(2):297-309.
O'Brien, M., and Colwell, R. R. (1987) A Rapid Test for Chitinase Activity That Uses 4-Methylumbelliferyl-N-Acetyl-β-D-Glucosaminide. Appl Environ Microbiol. 53(7):1718-1720.
Ohno, Y., Kihara, A., Sano, T., and Igarashi, Y. (2006) Intracellular localization and tissue-specific distribution of human and yeast DHHC cysteine-rich domain-containing proteins. Biochim. Biophys. Acta 1761(4):474-83.
Oka, T., and Nakano, A. (1994) Inhibition of GTP hydrolysis by Sar1p causes accumulation of vesicles that are a functional intermediate of the ER-to-Golgi transport in yeast. J. Cell Biol. 124(4):425-34.
Oliviusson, P., Heinzerling, O., Hillmer, S., Hinz, G., Tse, Y. C., Jiang, L., and Robinson, D. G. (2006) Plant retromer, localized to the prevacuolar compartment and microvesicles in Arabidopsis, may interact with vacuolar sorting receptors. Plant Cell 18(5):1239-52.
Omura, S., and H. Tanaka (1984) Macrolide antibiotics: chemistry, biology and practice. Academic Press, Inc., Orlando, Fla.
Ortiz-Zapater, E., Soriano-Ortega, E., Marcote, M. J., Ortiz-Masia, D., and Aniento, F. (2006) Trafficking of the human transferrin receptor in plant cells: effects of tyrphostin A23 and brefeldin A. Plant J.
Osherov, N., Gazit, A., Gilon, C., and Levitzki, A. (1993) Selective inhibition of the epidermal growth factor and HER2/neu receptors by tyrphostins. J. Biol. Chem. 268(15):11134-42.
Otegui, M. S., Noh, Y. S., Martinez, D. E., Vila Petroff, M. G., Staehelin, L. A., Amasino, R. M., and Guiamet, J. J. (2005) Senescence-associated vacuoles with intense proteolytic activity develop in leaves of Arabidopsis and soybean. Plant J. 41(6):831-44.
Pali, T., Whyteside, G., Dixon, N., Kee, T. P., Ball, S., Harrison, M. A., Findlay, J. B., Finbow, M. E., and Marsh, D. (2004) Interaction of inhibitors of the vacuolar H(+)-ATPase with the transmembrane Vo-sector. Biochem. 43(38):12297-305.
Paris, N., Rogers, S. W., Jiang, L., Kirsch, T., Beevers, L., Phillips, T. E., and Rogers, J. C. (1997) Molecular cloning and further characterization of a probable plant vacuolar sorting receptor. Plant Physiol. 115:29-39.
Park, J. H., Oufattole, M., and Rogers, J. C. (2007) Golgi-mediated vacuolar sorting in plant cells: RMR proteins are sorting receptors for the protein aggregation/membrane internalization pathway. Plant Science 172(4):728-745.
Park, M., Kim, S. J., Vitale, A., and Hwang, I. (2004a) Identification of the protein storage vacuole and protein targeting to the vacuole in leaf cells of three plant species. Plant Physiol. 134(2):625-39.
Park, M., Kim, S. J., Vitale, A., and Hwang, I. (2004b) Identification of the Protein Storage Vacuole and Protein Targeting to the Vacuole in Leaf Cells of Three Plant Species. Plant Physiol. 134(2):625-639.
Pedersen, P. L., and Carafoli, E. (1987) Ion motive ATPases. I. Ubiquity, properties, and significance to cell function. Trends Biochem. Sci. 12:146-150.
Pepinsky, R. B., Zeng, C., Wen, D., Rayhorn, P., Baker, D. P., Williams, K. P., Bixler, S. A., Ambrose, C. M., Garber, E. A., Miatkowski, K., Taylor, F. R., Wang, E. A., and Galdes, A. (1998) Identification of a palmitic acid-modified form of human Sonic hedgehog. J. Biol. Chem. 273(22):14037-45.
Percherancier, Y., Planchenault, T., Valenzuela-Fernandez, A., Virelizier, J. L., Arenzana-Seisdedos, F., and Bachelerie, F. (2001) Palmitoylation-dependent control of degradation, life span, and membrane expression of the CCR5 receptor. J. Biol. Chem. 276(34):31936-44.
Pereira-Leal, J. B., Hume, A. N., and Seabra, M. C. (2001) Prenylation of Rab GTPases:

molecular mechanisms and involvement in genetic disease. FEBS Lett. 498(2-3):197-200.
Peremyslov, V. V., Pan, Y. W., and Dolja, V. V. (2004) Movement protein of a closterovirus is a type III integral transmembrane protein localized to the endoplasmic reticulum. J Virol 78(7):3704-9.
Pfeffer, S. (2003) Membrane domains in the secretory and endocytic pathways. Cell 112(4):507-17.
Phan, N. Q., Kim, S. J., and Bassham, D. C. (2008) Overexpression of Arabidopsis sorting nexin AtSNX2b inhibits endocytic trafficking to the vacuole. Mol Plant 1(6):961-76.
Pickart, C. M. (2001) Mechanisms underlying ubiquitination. Annu Rev Biochem 70:503-33.
Pierre, M., Traverso, J. A., Boisson, B., Domenichini, S., Bouchez, D., Giglione, C., and Meinnel, T. (2007) N-myristoylation regulates the SnRK1 pathway in Arabidopsis. Plant Cell 19(9):2804-21.
Pinheiro, H., Samalova, M., Geldner, N., Chory, J., Martinez, A., and Moore, I. (2009) Genetic evidence that the higher plant Rab-D1 and Rab-D2 GTPases exhibit distinct but overlapping interactions in the early secretory pathway. J. Cell Sci. 122(Pt 20):3749-58.
Posner, I., Engel, M., Gazit, A., and Levitzki, A. (1994) Kinetics of inhibition by tyrphostins of the tyrosine kinase activity of the epidermal growth factor receptor and analysis by a new computer program. Mol Pharmacol 45(4):673-83.
Poustka, F., Irani, N. G., Feller, A., Lu, Y., Pourcel, L., Frame, K., and Grotewold, E. (2007) A Trafficking Pathway for Anthocyanins Overlaps with the Endoplasmic Reticulum-to-Vacuole Protein-Sorting Route in Arabidopsis and Contributes to the Formation of Vacuolar Inclusions. Plant Physiol. 145(4):1323-1335.
Prescott, G. R., Gorleku, O. A., Greaves, J., and Chamberlain, L. H. (2009) Palmitoylation of the synaptic vesicle fusion machinery. J Neurochem 110(4):1135-49.
Press, B., Feng, Y., Hoflack, B., and Wandinger-Ness, A. (1998) Mutant Rab7 causes the accumulation of cathepsin D and cation-independent mannose 6-phosphate receptor in an early endocytic compartment. J. Cell Biol. 140(5):1075-89.
Quesnel, S., and Silvius, J. R. (1994) Cysteine-containing peptide sequences exhibit facile uncatalyzed transacylation and acyl-CoA-dependent acylation at the lipid bilayer interface. Biochem. 33(45):13340-8.
Quigley, F., Rosenberg, J. M., Shachar-Hill, Y., and Bohnert, H. J. (2002) From genome to function: the Arabidopsis aquaporins. Genome Biol 3(1):RESEARCH0001.
Rehman, R. U., Stigliano, E., Lycett, G. W., Sticher, L., Sbano, F., Faraco, M., Dalessandro, G., and Di Sansebastiano, G. P. (2008) Tomato Rab11a characterization evidenced a difference between SYP121-dependent and SYP122-dependent exocytosis. Plant Cell Physiol 49(5):751-66.
Reichardt, I., Stierhof, Y. D., Mayer, U., Richter, S., Schwarz, H., Schumacher, K., and Jürgens, G. (2007) Plant Cytokinesis Requires De Novo Secretory Trafficking but Not Endocytosis. Curr Biol.
Remizov, O., Jakubov, R., Dufer, M., Krippeit Drews, P., Drews, G., Waring, M., Brabant, G., Wienbergen, A., Rustenbeck, I., and Schofl, C. (2003) Palmitate-induced Ca2+-signaling in pancreatic beta-cells. Mol Cell Endocrinol 212(1-2):1-9.
Resh, M. D. (1999) Fatty acylation of proteins: new insights into membrane targeting of myristoylated and palmitoylated proteins. Biochim. Biophys. Acta 1451(1):1-16.
Resh, M. D. (2006a) Palmitoylation of Ligands, Receptors, and Intracellular Signaling Molecules. Sci. STKE 2006(359):re14-.
Resh, M. D. (2006b) Use of analogs and inhibitors to study the functional significance of protein palmitoylation. Methods 40(2):191-7.
Richter, S., Geldner, N., Schrader, J., Wolters, H., Stierhof, Y.-D., Rios, G., Koncz, C., Robinson, D. G., and Jurgens, G. (2007) Functional diversification of closely related ARF-GEFs in protein secretion and recycling. Nature 448(7152):488-492.

Richter, S., Voss, U., and Jürgens, G. (2009) Post-Golgi Traffic in Plants. Traffic.
Rivero, F., and Somesh, B. P. (2002) Signal transduction pathways regulated by Rho GTPases in <i>Dictyostelium</i>. Journal of Muscle Research and Cell Motility 23(7):737-749.
Robinson, D. G., Albrecht, S., and Moriysu, Y. (2004) The V-ATPase inhibitors concanamycin A and bafilomycin A lead to Golgi swelling in tobacco BY-2 cells. Protopl. 224(3-4):255-60.
Robinson, D. G., Jiang, L., and Schumacher, K. (2008a) The endosomal system of plants: charting new and familiar territories. Plant Physiol. 147(4):1482-92.
Robinson, D. G., Langhans, M., Saint-Jore-Dupas, C., and Hawes, C. (2008b) BFA effects are tissue and not just plant specific. Trends Plant Sci 13(8):405-408.
Rocks, O., Gerauer, M., Vartak, N., Koch, S., Huang, Z. P., Pechlivanis, M., Kuhlmann, J., Brunsveld, L., Chandra, A., Ellinger, B., Waldmann, H., and Bastiaens, P. I. (2010) The palmitoylation machinery is a spatially organizing system for peripheral membrane proteins. Cell 141(3):458-71.
Rocks, O., Peyker, A., Kahms, M., Verveer, P. J., Koerner, C., Lumbierres, M., Kuhlmann, J., Waldmann, H., Wittinghofer, A., and Bastiaens, P. I. H. (2005) An Acylation Cycle Regulates Localization and Activity of Palmitoylated Ras Isoforms. Science 307(5716):1746-1752.
Rojo, E., Sharma, V. K., Kovaleva, V., Raikhel, N. V., and Fletcher, J. C. (2002) CLV3 is localized to the extracellular space, where it activates the Arabidopsis CLAVATA stem cell signaling pathway. Plant Cell 14(5):969-977.
Romagnoli, S., Cai, G., and Cresti, M. (2003) In Vitro Assays Demonstrate That Pollen Tube Organelles Use Kinesin-Related Motor Proteins to Move along Microtubules. Plant Cell 15(1):251-269.
Rose, J. K. C., and Lee, S.-J. (2010) Straying off the Highway: Trafficking of Secreted Plant Proteins and Complexity in the Plant Cell Wall Proteome. Plant Physiol. 153(2):433-436.
Rosenbaum, J. (2000) Cytoskeleton: Functions for tubulin modifications at last. Curr. Biol. 10(21):R801-R803.
Roskoski, R., Jr. (2003) Protein prenylation: a pivotal posttranslational process. Biochem Biophys Res Commun 303(1):1-7.
Roth, A. F., Feng, Y., Chen, L., and Davis, N. G. (2002) The yeast DHHC cysteine-rich domain protein Akr1p is a palmitoyl transferase. J. Cell Biol. 159(1):23-8.
Roth, A. F., Wan, J., Bailey, A. O., Sun, B., Kuchar, J. A., Green, W. N., Phinney, B. S., Yates, J. R., and Davis, N. G. (2006) Global analysis of protein palmitoylation in yeast. Cell 125(5):1003 - 1013.
Rudd, P. M., Endo, T., Colominas, C., Groth, D., Wheeler, S. F., Harvey, D. J., Wormald, M. R., Serban, H., Prusiner, S. B., Kobata, A., and Dwek, R. A. (1999) Glycosylation differences between the normal and pathogenic prion protein isoforms. Proc Natl Acad Sci U S A 96(23):13044-9.
Ryan, E., Grierson, C. S., Cavell, A., Steer, M., and Dolan, L. (1998) TIP1 is required for both tip growth and non-tip growth in Arabidopsis. New Phytologist 138(1):49-58.
Saalbach, G., Jung, R., Kunze, G., Saalbach, I., Adler, K., and Muntz, K. (1991) Different legumin protein domains act as vacuolar targeting signals. Plant Cell 3(7):695-708.
Sadhu, C., Masinovsky, B., Dick, K., Sowell, C. G., and Staunton, D. E. (2003) Essential role of phosphoinositide 3-kinase delta in neutrophil directional movement. J Immunol 170(5):2647-54.
Saint-Jean, B., Seveno-Carpentier, E., Alcon, C., Neuhaus, J. M., and Paris, N. (2010) The cytosolic tail dipeptide Ile-Met of the pea receptor BP80 is required for recycling from the prevacuole and for endocytosis. Plant Cell 22(8):2825-37.
Sakurai, J., Ishikawa, F., Yamaguchi, T., Uemura, M., and Maeshima, M. (2005)

Identification of 33 rice aquaporin genes and analysis of their expression and function. Plant Cell Physiol 46(9):1568-77.
Salminen, A., and Novick, P. J. (1987) A ras-like protein is required for a post-Golgi event in yeast secretion. Cell 49(4):527-38.
Sanmartin, M., Ordonez, A., Sohn, E. J., Robert, S., Sanchez-Serrano, J. J., Surpin, M. A., Raikhel, N. V., and Rojo, E. (2007) Divergent functions of VTI12 and VTI11 in trafficking to storage and lytic vacuoles in Arabidopsis. Proc. Natl. Acad. Sci. USA 104(9):3645-3650.
Sansebastiano, G.-P. D., Paris, N., Marc-Martin, S., and Neuhaus, J.-M. (1998) Specific accumulation of GFP in a non-acidic vacuolar compartment via a C-terminal propeptide-mediated sorting pathway. Plant J. 15(4):449-457.
Sansebastiano, G. P. D., Rehman, R. U., and Neuhaus, J.-M. (2007) Rat β-glucuronidase as a reporter protein for the analysis of the plant secretory pathway. Plant Biosystems - An International Journal Dealing with all Aspects of Plant Biology: Official Journal of the Societa Botanica Italiana 141(3):329 - 336.
Sasse, F., Steinmetz, H., Hofle, G., and Reichenbach, H. (2003) Archazolids, new cytotoxic macrolactones from Archangium gephyra (Myxobacteria). Production, isolation, physico-chemical and biological properties. J Antibiot (Tokyo) 56(6):520-5.
Satiat-Jeunemaitre, B., and Hawes, C. (1992) Redistribution of a Golgi glycoprotein in plant cells treated with Brefeldin A. J. Cell Sci. 103(4):1153-1166.
Schellmann, S., and Pimpl, P. (2009) Coats of endosomal protein sorting: retromer and ESCRT. Curr Opin Plant Biol.
Schiefelbein, J., Galway, M., Masucci, J., and Ford, S. (1993) Pollen tube and root-hair tip growth is disrupted in a mutant of Arabidopsis thaliana. Plant Physiol. 103(3):979-85.
Schmid, S. L. (1997) Clathrin-coated vesicle formation and protein sorting - an integrated process. Annu. Rev. Biochem. 66:511-548.
Schnell, S., Schaefer, M., and Schofl, C. (2007) Free fatty acids increase cytosolic free calcium and stimulate insulin secretion from beta-cells through activation of GPR40. Mol Cell Endocrinol 263(1-2):173-80.
Schroeder, H., Leventis, R., Rex, S., Schelhaas, M., Nagele, E., Waldmann, H., and Silvius, J. R. (1997) S-Acylation and plasma membrane targeting of the farnesylated carboxyl-terminal peptide of N-ras in mammalian fibroblasts. Biochem. 36(42):13102-9.
Schroeder, H., Leventis, R., Shahinian, S., Walton, P. A., and Silvius, J. R. (1996) Lipid-modified, cysteinyl-containing peptides of diverse structures are efficiently S-acylated at the plasma membrane of mammalian cells. J. Cell Biol. 134(3):647-60.
Schwamborn, J. C., and Puschel, A. W. (2004) The sequential activity of the GTPases Rap1B and Cdc42 determines neuronal polarity. Nat Neurosci 7(9):923-9.
Seaman, M. N., McCaffery, J. M., and Emr, S. D. (1998) A membrane coat complex essential for endosome-to-Golgi retrograde transport in yeast. J. Cell Biol. 142(3):665-81.
Shao, X., Li, C., Fernandez, I., Zhang, X., Sudhof, T. C., and Rizo, J. (1997) Synaptotagmin-syntaxin interaction: the C2 domain as a Ca2+-dependent electrostatic switch. Neuron 18(1):133-42.
Shechter, Y., Yaish, P., Chorev, M., Gilon, C., Braun, S., and Levitzki, A. (1989) Inhibition of insulin-dependent lipogenesis and anti-lipolysis by protein tyrosine kinase inhibitors. EMBO J. 8(6):1671-6.
Shibata, Y., Voeltz, G. K., and Rapoport, T. A. (2006) Rough sheets and smooth tubules. Cell 126(3):435-9.
Shimada, T., Fuji, K., Tamura, K., Kondo, M., Nishimura, M., and Hara-Nishimura, I. (2003a) Vacuolar sorting receptor for seed storage proteins in Arabidopsis thaliana. Proc. Natl. Acad. Sci. USA 100(26):16095-16100.
Shimada, T., Koumoto, Y., Li, L., Yamazaki, M., Kondo, M., Nishimura, M., and Hara-Nishimura, I. (2006) AtVPS29, a Putative Component of a Retromer Complex, is Required

for the Efficient Sorting of Seed Storage Proteins. Plant Cell Physiol 47(9):1187-1194.
Shimada, T., Watanabe, E., Tamura, K., Hayashi, Y., Nishimura, M., and Hara-Nishimura, I. (2002) A vacuolar sorting receptor PV72 on the membrane of vesicles that accumulate precursors of seed storage proteins (PAC vesicles). Plant Cell Physiol 43(10):1086-95.
Shimada, T., Yamada, K., Kataoka, M., Nakaune, S., Koumoto, Y., Kuroyanagi, M., Tabata, S., Kato, T., Shinozaki, K., Seki, M., Kobayashi, M., Kondo, M., Nishimura, M., and Hara-Nishimura, I. (2003b) Vacuolar processing enzymes are essential for proper processing of seed storage proteins in Arabidopsis thaliana. J. Biol. Chem. 278(34):32292-9.
Silady, R. A., Ehrhardt, D. W., Jackson, K., Faulkner, C., Oparka, K., and Somerville, C. R. (2008) The GRV2/RME-8 protein of Arabidopsis functions in the late endocytic pathway and is required for vacuolar membrane flow. Plant J. 53(1):29-41.
Smotrys, J. E., and Linder, M. E. (2004) Palmitoylation of intracellular signaling proteins: regulation and function. Annu Rev Biochem 73:559-87.
Solimena, M., Dirkx, R., Jr., Radzynski, M., Mundigl, O., and De Camilli, P. (1994) A signal located within amino acids 1-27 of GAD65 is required for its targeting to the Golgi complex region. J. Cell Biol. 126(2):331-41.
Sorek, N., Poraty, L., Sternberg, H., Bar, E., Lewinsohn, E., and Yalovsky, S. (2007) Activation Status-Coupled Transient S Acylation Determines Membrane Partitioning of a Plant Rho-Related GTPase. Mol. Cell. Biol. 27(6):2144-2154.
Sorek, N., Segev, O., Gutman, O., Bar, E., Richter, S., Poraty, L., Hirsch, J. A., Henis, Y. I., Lewinsohn, E., Jurgens, G., and Yalovsky, S. (2010) An S-acylation switch of conserved G domain cysteines is required for polarity signaling by ROP GTPases. Curr Biol 20(10):914-20.
Soyombo, A. A., and Hofmann, S. L. (1997) Molecular cloning and expression of palmitoyl-protein thioesterase 2 (PPT2), a homolog of lysosomal palmitoyl-protein thioesterase with a distinct substrate specificity. J. Biol. Chem. 272(43):27456-63.
Sparkes, I. A., Hawes, C., and Baker, A. (2005) AtPEX2 and AtPEX10 are targeted to peroxisomes independently of known endoplasmic reticulum trafficking routes. Plant Physiol. 139(2):690-700.
Stagg, S. M., Gurkan, C., Fowler, D. M., LaPointe, P., Foss, T. R., Potter, C. S., Carragher, B., and Balch, W. E. (2006) Structure of the Sec13/31 COPII coat cage. Nature 439(7073):234-8.
Stagg, S. M., LaPointe, P., and Balch, W. E. (2007) Structural design of cage and coat scaffolds that direct membrane traffic. Curr Opin Struct Biol 17(2):221-8.
Stagg, S. M., LaPointe, P., Razvi, A., Gurkan, C., Potter, C. S., Carragher, B., and Balch, W. E. (2008) Structural basis for cargo regulation of COPII coat assembly. Cell 134(3):474-84.
Steinmann, T., Geldner, N., Grebe, M., Mangold, S., Jackson, C. L., Paris, S., Galweiler, L., Palme, K., and Jurgens, G. (1999) Coordinated polar localization of auxin efflux carrier PIN1 by GNOM ARF GEF. Science 286(5438):316-8.
Stenmark, H., and Olkkonen, V. M. (2001) The Rab GTPase family. Genome Biol 2(5):REVIEWS3007.
Sticher, L., Hinz, U., Meyer, A. D., and Meins, F. (1992) Intracellular transport and processing of a tobacco vacuolar β-1,3-glucanase. Planta 188(4):559-565.
Subramanian, K., Dietrich, L. E., Hou, H., Lagrassa, T. J., Meiringer, C. T., and Ungermann, C. (2006) Palmitoylation determines the function of Vac8 at the yeast vacuole. J. Cell Sci. 119(Pt 12):2477-85.
Sutton, R. B., Davletov, B. A., Berghuis, A. M., Sudhof, T. C., and Sprang, S. R. (1995) Structure of the first C2 domain of synaptotagmin I: a novel Ca2+/phospholipid-binding fold. Cell 80(6):929-38.
Swarthout, J. T., Lobo, S., Farh, L., Croke, M. R., Greentree, W. K., Deschenes, R. J., and Linder, M. E. (2005) DHHC9 and GCP16 constitute a human protein fatty acyltransferase

with specificity for H- and N-Ras. J. Biol. Chem. 280(35):31141-8.
Szumlanski, A. L., and Nielsen, E. (2009) The Rab GTPase RabA4d Regulates Pollen Tube Tip Growth in Arabidopsis thaliana. Plant Cell 21(2):526-544.
Takano, J., Miwa, K., Yuan, L., von Wiren, N., and Fujiwara, T. (2005) Endocytosis and degradation of BOR1, a boron transporter of Arabidopsis thaliana, regulated by boron availability. Proc. Natl. Acad. Sci. USA 102(34):12276-12281.
Takeuchi, M., Tada, M., Saito, C., Yashiroda, H., and Nakano, A. (1998) Isolation of a tobacco cDNA encoding Sar1 GTPase and analysis of its dominant mutations in vesicular traffic using a yeast complementation system. Plant Cell Physiol 39(6):590-9.
Takeuchi, M., Ueda, T., Sato, K., Abe, H., Nagata, T., and Nakano, A. (2000) A dominant negative mutant of Sar1 GTPase inhibits protein transport from the endoplasmic reticulum to the Golgi apparatus in tobacco and Arabidopsis cultured cells. Plant Journal 23(4):517-525.
Tapper, H., and Sundler, R. (1995) Bafilomycin A1 inhibits lysosomal, phagosomal, and plasma membrane H(+)-ATPase and induces lysosomal enzyme secretion in macrophages. J Cell Physiol 163(1):137-44.
Tavernier, E., Le Quoc, D., and Le Quoc, K. (1993) Lipid composition of the vacuolar membrane of Acer pseudoplatanus cultured cells. Biochim. Biophys. Acta 1167(3):242-7.
Teh, O.-k., and Moore, I. (2007) An ARF-GEF acting at the Golgi and in selective endocytosis in polarized plant cells. Nature 448(7152):493-496.
Thomas, C., Tholl, S., Moes, D., Dieterle, M., Papuga, J., Moreau, F., and Steinmetz, A. (2009) Actin bundling in plants. Cell Motil Cytoskeleton 66(11):940-57.
Topinka, J. R., and Bredt, D. S. (1998) N-terminal palmitoylation of PSD-95 regulates association with cell membranes and interaction with K+ channel Kv1.4. Neuron 20(1):125-34.
Toyooka, K., Goto, Y., Asatsuma, S., Koizumi, M., Mitsui, T., and Matsuoka, K. (2009a) A mobile secretory vesicle cluster involved in mass transport from the Golgi to the plant cell exterior. Plant Cell 21(4):1212-29.
Toyooka, K., Goto, Y., Asatsuma, S., Koizumi, M., Mitsui, T., and Matsuoka, K. (2009b) A Mobile Secretory Vesicle Cluster Involved in Mass Transport from the Golgi to the Plant Cell Exterior. The Plant Cell Online 21(4):1212-1229.
Traub, L. M., and Kornfeld, S. (1997) The trans-Golgi network: a late secretory sorting station. Curr Opin Cell Biol 9(4):527-33.
Tse, Y. C., Lo, S. W., Hillmer, S., Dupree, P., and Jiang, L. (2006) Dynamic Response of Prevacuolar Compartments to Brefeldin A in Plant Cells. Plant Physiol. 142(4):1442-1459.
Tse, Y. C., Mo, B., Hillmer, S., Zhao, M., Lo, S. W., Robinson, D. G., and Jiang, L. (2004) Identification of multivesicular bodies as prevacuolar compartments in Nicotiana tabacum BY-2 cells. Plant Cell 16(3):672-93.
Tyerman, S., Bohnert, H., Maurel, C., Steudle, E., and Smith, J. (1999) Plant acuaporins: their molecular biology, biophysics and significance for plant water relations. J. Exp. Bot. 50(suppl_1):1055-1071.
Udenfriend, S., and Kodukula, K. (1995) How glycosylphosphatidylinositol-anchored membrane proteins are made. Annu Rev Biochem 64:563-91.
Ueda, T., Yamaguchi, M., Uchimiya, H., and Nakano, A. (2001) Ara6, a plant-unique novel type Rab GTPase, functions in the endocytic pathway of Arabidopsis thaliana. EMBO J. 20(17):4730-41.
Uemura, T., Ueda, T., Ohniwa, R. L., Nakano, A., Takeyasu, K., and Sato, M. H. (2004) Systematic analysis of SNARE molecules in Arabidopsis: dissection of the post-Golgi network in plant cells. Cell Struct Funct 29(2):49-65.
Umata, T., Moriyama, Y., Futai, M., and Mekada, E. (1990) The cytotoxic action of diphtheria toxin and its degradation in intact Vero cells are inhibited by bafilomycin A1, a

specific inhibitor of vacuolar-type H(+)-ATPase. J. Biol. Chem. 265(35):21940-5.
Umezawa, H., Imoto, M., Sawa, T., Isshiki, K., Matsuda, N., Uchida, T., Iinuma, H., Hamada, M., and Takeuchi, T. (1986) Studies on a new epidermal growth factor-receptor kinase inhibitor, erbstatin, produced by MH435-hF3. J Antibiot (Tokyo) 39(1):170-3.
Ungewickell, E., and Branton, D. (1981) Assembly units of clathrin coats. Nature 289(5796):420-2.
Valdez-Taubas, J., and Pelham, H. (2005) Swf1-dependent palmitoylation of the SNARE Tlg1 prevents its ubiquitination and degradation. EMBO J. 24(14):2524-32.
Vanhaesebroeck, B., Leevers, S. J., Ahmadi, K., Timms, J., Katso, R., Driscoll, P. C., Woscholski, R., Parker, P. J., and Waterfield, M. D. (2001) Synthesis and function of 3-phosphorylated inositol lipids. Annu Rev Biochem 70:535-602.
Vanoosthuyse, V., Tichtinsky, G., Dumas, C., Gaude, T., and Cock, J. M. (2003) Interaction of calmodulin, a sorting nexin and kinase-associated protein phosphatase with the Brassica oleracea S locus receptor kinase. Plant Physiol. 133(2):919-29.
Veit, M. (2000) Palmitoylation of the 25-kDa synaptosomal protein (SNAP-25) in vitro occurs in the absence of an enzyme, but is stimulated by binding to syntaxin. Biochemical J. 345(Part 1):145-151.
Veit, M., Sachs, K., Heckelmann, M., Maretzki, D., Hofmann, K. P., and Schmidt, M. F. (1998) Palmitoylation of rhodopsin with S-protein acyltransferase: enzyme catalyzed reaction versus autocatalytic acylation. Biochim. Biophys. Acta 1394(1):90-8.
Verkruyse, L. A., and Hofmann, S. L. (1996) Lysosomal targeting of palmitoyl-protein thioesterase. J. Biol. Chem. 271(26):15831-15836.
Vermeer, J. E. M., van Leeuwen, W., Tobena-Santamaria, R., Laxalt, A. M., Jones, D. R., Divecha, N., Gadella, T. W. J., and Munnik, T. (2006) Visualization of PtdIns3P dynamics in living plant cells. Plant J. 47(5):687-700.
Vernoud, V., Horton, A. C., Yang, Z., and Nielsen, E. (2003) Analysis of the small GTPase gene superfamily of Arabidopsis. Plant Physiol. 131(3):1191-208.
Vidali, L., Rounds, C. M., Hepler, P. K., and Bezanilla, M. (2009) Lifeact-mEGFP reveals a dynamic apical F-actin network in tip growing plant cells. PLoS One 4(5):e5744.
Villarejo, A., Buren, S., Larsson, S., Dejardin, A., Monne, M., Rudhe, C., Karlsson, J., Jansson, S., Lerouge, P., Rolland, N., von Heijne, G., Grebe, M., Bako, L., and Samuelsson, G. (2005) Evidence for a protein transported through the secretory pathway en route to the higher plant chloroplast. Nat Cell Biol 7(12):1124-31.
Viotti, C., Bubeck, J., Stierhof, Y.-D., Krebs, M., Langhans, M., van den Berg, W., van Dongen, W., Richter, S., Geldner, N., Takano, J., Jurgens, G., de Vries, S. C., Robinson, D. G., and Schumacher, K. (2010) Endocytic and Secretory Traffic in Arabidopsis Merge in the Trans-Golgi Network/Early Endosome, an Independent and Highly Dynamic Organelle. Plant Cell 22(4):1344-1357.
Vitale, A., Ceriotti, A., and Denecke, J. (1993) The Role of the Endoplasmic-Reticulum in Protein-Synthesis, Modification and Intracellular-Transport. J. Exp. Bot. 44(266):1417-1444.
Vitale, A., and Chrispeels, M. J. (1992) Sorting of Proteins to the Vacuoles of Plant Cells. BioEss 14(3):151-160.
Vitale, A., and Denecke, J. (1999) The endoplasmic reticulum - Gateway of the secretory pathway. Plant Cell 11(4):615-628.
Vitale, A., and Raikhel, N. V. (1999) What do proteins need to reach different vacuoles? Trends Plant Sci 4(4):149-155.
Vitha, S., Baluska, F., Braun, M., Samaj, J., Volkmann, D., and Barlow, P. W. (2000) Comparison of cryofixation and aldehyde fixation for plant actin immunocytochemistry: aldehydes do not destroy F-actin. Histochem J 32(8):457-66.
Vlahos, C. J., Matter, W. F., Hui, K. Y., and Brown, R. F. (1994) A specific inhibitor of

phosphatidylinositol 3-kinase, 2-(4-morpholinyl)-8-phenyl-4H-1-benzopyran-4-one (LY294002). J. Biol. Chem. 269(7):5241-8.
Waheed, A. A., and Jones, T. L. (2002) Hsp90 interactions and acylation target the G protein Galpha 12 but not Galpha 13 to lipid rafts. J. Biol. Chem. 277(36):32409-12.
Wallace, I. S., Choi, W. G., and Roberts, D. M. (2006) The structure, function and regulation of the nodulin 26-like intrinsic protein family of plant aquaglyceroporins. Biochim. Biophys. Acta 1758(8):1165-75.
Walsh, C. (2006) Posttranslational modification of proteins: expanding nature's inventory. Roberts and Company Publishers:1-490.
Wang, J., Cai, Y., Miao, Y., Lam, S. K., and Jiang, L. (2009) Wortmannin induces homotypic fusion of plant prevacuolar compartments. J. Exp. Bot.:erp136.
Wang, J., Li, Y., Lo, S. W., Hillmer, S., Sun, S. S. M., Robinson, D. G., and Jiang, L. (2007) Protein Mobilization in Germinating Mung Bean Seeds Involves Vacuolar Sorting Receptors and Multivesicular Bodies. Plant Physiol.:pp.107.096263.
Wang, Q., Kong, L., Hao, H., Wang, X., Lin, J., Samaj, J., and Baluska, F. (2005) Effects of Brefeldin A on Pollen Germination and Tube Growth. Antagonistic Effects on Endocytosis and Secretion. Plant Physiol. 139(4):1692-1703.
Watanabe, E., Shimada, T., Kuroyanagi, M., Nishimura, M., and Hara-Nishimura, I. (2002) Calcium-mediated association of a putative vacuolar sorting receptor PV72 with a propeptide of 2S albumin. J. Biol. Chem. 277(10):8708-15.
Watanabe, E., Shimada, T., Tamura, K., Matsushima, R., Koumoto, Y., Nishimura, M., and Hara-Nishimura, I. (2004) An ER-localized form of PV72, a seed-specific vacuolar sorting receptor, interferes the transport of an NPIR-containing proteinase in Arabidopsis leaves. Plant Cell Physiol 45(1):9-17.
Waters, M. G., and Pfeffer, S. R. (1999) Membrane tethering in intracellular transport. Curr Opin Cell Biol 11(4):453-9.
Webb, Y., Hermida-Matsumoto, L., and Resh, M. D. (2000) Inhibition of Protein Palmitoylation, Raft Localization, and T Cell Signaling by 2-Bromopalmitate and Polyunsaturated Fatty Acids. J. Biol. Chem. 275(1):261-270.
Weig, A., Deswarte, C., and Chrispeels, M. J. (1997) The major intrinsic protein family of arabidopsis has 23 members that form three distinct groups with functional aquaporins in each group. Plant Physiol. 114(4):1347-1357.
Welters, P., Takegawa, K., Emr, S. D., and Chrispeels, M. J. (1994) AtVPS34, a phosphatidylinositol 3-kinase of Arabidopsis thaliana, is an essential protein with homology to a calcium-dependent lipid binding domain. Proc Natl Acad Sci U S A 91(24):11398-402.
Westermann, S., and Weber, K. (2003) Post-translational modifications regulate microtubule function. Nat Rev Mol Cell Biol 4(12):938-948.
Williams, R. L., and Urbe, S. (2007) The emerging shape of the ESCRT machinery. Nat Rev Mol Cell Biol 8(5):355-368.
Wurmser, A. E., Gary, J. D., and Emr, S. D. (1999) Phosphoinositide 3-kinases and their FYVE domain-containing effectors as regulators of vacuolar/lysosomal membrane trafficking pathways. J. Biol. Chem. 274(14):9129-32.
Wymann, M. P., Bulgarellileva, G., Zvelebil, M. J., Pirola, L., Vanhaesebroeck, B., Waterfield, M. D., and Panayotou, G. (1996) Wortmannin inactivates phosphoinositide 3-kinase by covalent modification of lys-802, a residue involved in the phosphate transfer reaction. Mol. Cell. Biol. 16(4):1722-1733.
Yaish, P., Gazit, A., Gilon, C., and Levitzki, A. (1988) Blocking of EGF-dependent cell proliferation by EGF receptor kinase inhibitors. Science 242(4880):933-5.
Yamazaki, M., Shimada, T., Takahashi, H., Tamura, K., Kondo, M., Nishimura, M., and Hara-Nishimura, I. (2008) Arabidopsis VPS35, a Retromer Component, Is Required for Vacuolar Protein Sorting and Involved in Plant Growth and Leaf Senescence. Plant Cell

Physiol.
Yeung, B. G., Phan, H. L., and Payne, G. S. (1999) Adaptor complex-independent clathrin function in yeast. Mol Biol Cell 10(11):3643-59.
Yoshida, S., Kawata, T., Uemura, M., and Niki, T. (1986) Isolation and Characterization of Tonoplast from Chilling-Sensitive Etiolated Seedlings of Vigna radiata L. Plant Physiol. 80(1):161-166.
Zava, O. (2007) Functional characterization of AtRMR proteins in Arabidopsis thaliana Institut de Biologie, Université de Neuchâtel.
Zeng, Q., Wang, X., and Running, M. P. (2007) Dual Lipid Modification of Arabidopsis Gamma Subunits Is Required for Efficient Plasma Membrane Targeting. Plant Physiol.:pp.106.093583.
Zerial, M., and McBride, H. (2001) Rab proteins as membrane organizers. Nat Rev Mol Cell Biol 2(2):107-17.
Zhang, F. L., and Casey, P. J. (1996) Protein prenylation: molecular mechanisms and functional consequences. Annu Rev Biochem 65:241-69.
Zhao, L., Lobo, S., Dong, X., Ault, A. D., and Deschenes, R. J. (2002) Erf4p and Erf2p form an endoplasmic reticulum-associated complex involved in the plasma membrane localization of yeast Ras proteins. J. Biol. Chem. 277(51):49352-9.
Zheng, H., Camacho, L., Wee, E., Batoko, H., Legen, J., Leaver, C. J., Malho, R., Hussey, P. J., and Moore, I. (2005) A Rab-E GTPase mutant acts downstream of the Rab-D subclass in biosynthetic membrane traffic to the plasma membrane in tobacco leaf epidermis. Plant Cell 17(7):2020-36.
Zheng, Z. L., and Yang, Z. B. (2000) The Rop GTPase switch turns on polar growth in pollen. Trends Plant Sci 5(7):298-303.
Zonia, L., and Munnik, T. (2008) Vesicle trafficking dynamics and visualization of zones of exocytosis and endocytosis in tobacco pollen tubes. J Exp Bot 59(4):861-73.
Zonia, L., and Munnik, T. (2009) Uncovering hidden treasures in pollen tube growth mechanics. Trends Plant Sci 14(6):318-327.
Zouhar, J., Muñoz, A., and Rojo, E. (2010) Functional specialization within the vacuolar sorting receptor family: VSR1, VSR3 and VSR4 sort vacuolar storage cargo in seeds and vegetative tissues. Plant J. 64(4):577-588.
Zouhar, J., Rojo, E., and Bassham, D. C. (2009) AtVPS45 is a positive regulator of the SYP41/SYP61/VTI12 SNARE complex involved in trafficking of vacuolar cargo. Plant Physiol.:pp.108.134361.